PURIFICATION OF BIODIESEL USING DEEP EUTECTIC SOLVENTS IN LIQUID MEMBRANE SEPARATOR WITH ACTIVATED CARBON AND GRAPHENE

KHALID MOHSIN ABED

FACULTY OF ENGINEERING
UNIVERSITI MALAYA
KUALA LUMPUR

2024

PURIFICATION OF BIODIESEL USING DEEP EUTECTIC SOLVENTS IN LIQUID MEMBRANE SEPARATOR WITH ACTIVATED CARBON AND GRAPHENE

KHALID MOHSIN ABED

THESIS SUBMITTED IN FULFILMENT OF THE REQUIREMENTS FOR THE DEGREE OF DOCTOR OF PHILOSOPHY

FACULTY OF ENGINEERING

UNIVERSITI MALAYA

KUALA LUMPUR

2024

UNIVERSITI MALAYA

ORIGINAL LITERARY WORK DECLARATION

Name of Candidate: **KHALID MOHSIN ABED**

Matric No: **17222270/1**

Name of Degree: **Doctor of Philosophy**

Title of Thesis: **Purification of Biodiesel Using Deep Eutectic Solvents in Liquid Membrane Separator with Activated Carbon and Graphene**

Field of Study: **Engineering and Engineering Trades (Chemical and Process)/ Bioprocess Engineering**

I do solemnly and sincerely declare that:

(1) I am the sole author/writer of this Work;
(2) This Work is original;
(3) Any use of any work in which copyright exists was done by way of fair dealing and for permitted purposes and any excerpt or extract from, or reference to or reproduction of any copyright work has been disclosed expressly and sufficiently and the title of the Work and its authorship have been acknowledged in this Work;
(4) I do not have any actual knowledge nor do I ought reasonably to know that the making of this work constitutes an infringement of any copyright work;
(5) I hereby assign all and every rights in the copyright to this Work to the Universiti Malaya ("UM"), who henceforth shall be owner of the copyright in this Work and that any reproduction or use in any form or by any means whatsoever is prohibited without the written consent of UM having been first had and obtained;
(6) I am fully aware that if in the course of making this Work I have infringed any copyright whether intentionally or otherwise, I may be subject to legal action or any other action as may be determined by UM.

Candidate's Signature Date: December 05, 2024

Subscribed and solemnly declared before,

Witness's Signature Date: December 05, 2024

ABSTRACT

The biodiesel industry is an essential aspect of renewable energy, but it has limitations due to contaminants, in particular the soap content. The present study focuses on the development of a water-free downstream process to remove the soap from crude biodiesel. Emulsion liquid membrane (ELM) technique has been employed, and it has been used for purifying different contaminants. Green solvents such as deep eutectic solvents (DESs) is used as a stripping phase, and carbon materials (activated carbon and graphene) are integrated to enhance the DES for soap removal. Activated carbon (AC) was synthesized from palm raceme-derived biomass due to its plentiful supply and environmental sustainability. Lipase activity was utilized as an indicator to assess the optimal AC under different parameters as well as to investigate the biocompatibility of AC and DES. The results showed that the optimum conditions of AC's synthesis were 0.5 impregnation ratio, 150 minutes, and 400 °C. DES prepared from alanine/sodium hydroxide exhibited good biocompatibility with AC. AC was integrated with two different techniques which are DES-based liquid-liquid extraction and novel DES-based ELM for soap removal from biodiesel. Additionally, computational screening of different DESs via COSMO-RS was used in the ELM system for soap removal. This particular study highlights the potential of COSMO-RS in predicting the best DES candidate as a stripping phase in the ELM system based on solvent capacity. The DESs were prepared from two salts, namely tetramethylammonium chloride (TMAC) and choline chloride (ChCl), with different hydrogen bond donors (HBD) such as lactic acid (LA), glycerol (Gly), ethylene glycol (EG), diethylene glycol (DEG) and triethylene glycol (TEG). ELM results illustrated a superior soap removal efficiency of 1.87 ppm in comparison to liquid-liquid extraction results which was 23.23 ppm. The highest removal efficiency of 99.75% was achieved for TMAC:LA under the following conditions: 2 wt.% of the surfactant, 0.5 wt.% of AC, 1:4 DES molar ratio, 1:1 DES: BD ratio, 400 rpm mixing speed, and 6

min extraction time. LA-based DES as natural DES also showed high removal efficiency (99.6%) under the following conditions: 2 wt.% of the surfactant, 0.3 g of graphene, 1:4 DES molar ratio, 1:1 DES: BD ratio, 400 rpm mixing speed, and 6 min extraction time. Novel DESs were successfully prepared from TEG as hydrogen bond donors with TMAC and ChCl as ammonium salts. These two DESs were combined with AC for soap removal and the efficiency were 99.1% and 97.5% for TMAC:TEG and ChCl:TEG, respectively, with a salt:HBD molar ratio of 1:4, DES:biodiesel ratio of 1:1, 2 wt% surfactant, 10 min, 400 rpm, 0.5 treatment ratio and 0.5 wt% AC dosage. The kinetics of sodium ion transport during ELM system adheres to the first-order kinetic model. The overall mass transfer coefficient, mass transfer coefficient of the external phase in an agitated reactor, and the interfacial reaction rate constant of 5.188×10^{-9},1.373×10^{-7} , and 5.392×10^{-9} m/s, respectively. Overall, the integration of DES and carbon materials in the ELM system provides a new cleaner, more effective, and simpler route for biodiesel downstream processing.

Keywords: Emulsion Liquid Membrane, Biodiesel, Deep Eutectic Solvents, COSMO-RS, Purification.

ABSTRAK

Industri biodiesel merupakan aspek penting bagi tenaga boleh diperbaharui, tetapi ia mempunyai had akibat bahan cemar, khususnya kandungan sabun. Kajian ini memberi tumpuan kepada pembangunan proses hiliran bebas air untuk mengeluarkan sabun daripada biodiesel mentah. Teknik membran cecair emulsi (ELM) telah digunakan, dan ia telah digunakan untuk membersihkan bahan cemar yang berbeza. Pelarut hijau seperti pelarut eutektik dalam (DES) digunakan sebagai fasa pelucutan, dan bahan karbon (karbon teraktif dan graphene) disepadukan untuk meningkatkan DES bagi penyingkiran sabun. Karbon teraktif (AC) telah disintesis daripada biojisim terbitan raseme sawit kerana bekalannya yang banyak dan kelestarian alam sekitar. Aktiviti lipase digunakan sebagai penunjuk untuk menilai AC optimum di bawah parameter yang berbeza, termasuk suhu pengkarbonan, nisbah impregnasi, dan masa pengkarbonan untuk menyiasat biokompatibiliti AC dan DES. Keputusan menunjukkan bahawa keadaan optimum sintesis AC ialah nisbah impregnasi 0.5, 150 minit, dan suhu pengkarbonan 400 °C. DES yang disediakan daripada alanin/natrium hidroksida mempamerkan biokeserasian yang baik dengan AC. AC telah disepadukan dengan dua teknik berbeza iaitu pengekstrakan cecair-cecair berasaskan DES dan ELM berasaskan DES untuk penyingkiran sabun daripada biodiesel. Tambahan pula, pemeriksaan pengiraan DES yang berbeza melalui COSMO-RS telah digunakan dalam sistem ELM untuk penyingkiran sabun. Kajian khusus ini menyerlahkan potensi COSMO-RS dalam meramalkan calon DES terbaik sebagai fasa pelucutan dalam sistem ELM berdasarkan kapasiti pelarut. DES disediakan daripada dua garam, iaitu tetramethylammonium chloride (TMAC) dan choline chloride (ChCl), dengan penderma ikatan hidrogen (HBD) berbeza seperti asid laktik (LA), gliserol (Gly), etilena glikol (EG), dietilena glikol. (DEG) dan trietilena glikol (TEG). σ-profil dan σ-potential ialah alat khusus yang digunakan untuk menyiasat interaksi molekul antara molekul sabun dalam setiap fasa.

Keputusan ELM menggambarkan kecekapan penyingkiran sabun yang unggul sebanyak 1.87 ppm berbanding keputusan pengekstrakan cecair-cecair iaitu 23.23 ppm. Kecekapan penyingkiran tertinggi sebanyak 99.75% telah dicapai untuk TMAC: LA di bawah keadaan berikut: 2 wt.% surfaktan, 0.5 wt.% AC, nisbah molar 1:4 DES sebagai fasa pelucutan, 1:1 DES: nisbah BD , 400 rpm kelajuan pencampuran, dan 6 minit masa pengekstrakan. DES berasaskan LA sebagai DES semula jadi juga menunjukkan kecekapan penyingkiran yang tinggi (99.6 %) di bawah keadaan berikut: 2% berat surfaktan, 0.3 g graphene, nisbah molar 1:4 DES sebagai fasa pelucutan, 1:1 DES: nisbah BD , 400 rpm kelajuan pencampuran, dan masa pengekstrakan 6 minit. Novel DES telah berjaya disediakan daripada TEG sebagai penderma ikatan hidrogen dengan TMAC dan ChCl sebagai garam ammonium. Kedua-dua DES ini digabungkan dengan AC untuk penyingkiran sabun dan kecekapan adalah 99.1% dan 97.5% untuk TMAC:TEG(DES3) dan ChCl:TEG(DES6), masing-masing, dengan garam: nisbah molar HBD 1:4, DES: nisbah biodiesel 1:1, kepekatan surfaktan 2% berat, tempoh pengekstrakan 10 minit, kelajuan pencampuran 400 rpm, nisbah rawatan 0.5 dan dos AC 0.5% berat. Kinetik mekanisma pengangkutan ion natrium semasa sistem ELM mematuhi model kinetik tertib pertama. Pekali pemindahan jisim keseluruhan, pekali pemindahan jisim fasa luaran dalam reaktor bergolak, dan pemalar kadar tindak balas antara muka ialah 5.188×10^{-9} , 1.373×10^{-7} , dan 5.392×10^{-9} m/s, masing-masing. Secara keseluruhannya, penyepaduan DES dan bahan karbon dalam sistem ELM menyediakan laluan baharu yang lebih bersih, berkesan dan mudah untuk pemprosesan hiliran biodiesel.

Kata kunci: membran cecair emulsi, biodiesel, pelarut eutektik dalam, COSMO-RS, Pemurnian.

ACKNOWLEDGEMENTS

The research presented in this thesis could only become real with the help and support of people whom I would like to appreciate herewith.

First and foremost, I would like to express my most sincere gratitude to my supervisors; Dr. Hanee Farzana Hizaddin for her encourgement and trust in me; Dr. Adeeb Hayyan for his guidance and never-ending support; and Prof. Ir. Dr. Mohd Ali Hashim for his expertise and constructive advice.

I would like to thank all the staff of the Department of Chemical Engineering at the Universiti Malaya for their cooperation and generous help. I would also like to acknowledge the scholarship that I was granted by the Department of Chemical Engineering at the University of Baghdad, Iraq.

My eternal gratitude goes to my parents for their immense love; my mother's prayers, patience, and support; my father's lifetime guiding light. My heartfelt thanks also go to my beloved family members, with a special appreciation to my eldest brother and life mentor, Ali, for his unconditional love and support.

TABLE OF CONTENTS

List of Figures

List of Tables

List of Symbols and Abbreviations

Symbols

A_g	:	Surface area of the emulsion globules
$C\infty$	:	Capacity
C_o	:	Initial concentration
C_t	:	Concentration at any time
D	:	Diffusion coefficient
D_g	:	Average globule size
%E	:	Extraction efficiency
E_s	:	Activation energy for conductivity
E_μ	:	Activation energy for viscosity
J_{Na+}	:	Molar flux of sodium
J_{Soap}	:	Molar flux of soap
K_{cat}	:	Catalytic measures of the turnover number
K_F	:	Interfacial reaction rate constant
K_m	:	Michaelis–Menten constant
K_M	:	Mass transfer coefficient of the external phase
K_o	:	Overall mass transfer coefficient
K_{obs}	:	Reaction rate constant
N	:	Mixing speed
R	:	Gas constant
S	:	Conductivity
S_g	:	Globule's surface area
S_o	:	Pre-exponential factor for conductivity
T	:	Temperature
V	:	Volume
V_f	:	Volumes of the emulsion after extraction
V_g	:	Globule's volume
V_{max}	:	Maximum velocity
V_o	:	Volumes of the emulsion before extraction
V_T	:	Total volume of emulsion
β	:	Percentage of breakage
$\gamma\infty$	:	Activity coefficient

μ	:	Viscosity
μ_o	:	Pre-exponential factor for viscosity
ρ	:	Density

Abbreviations

AC	:	Activated carbon
ACPO	:	Acidic crude palm oil
AML	:	Amano lipase from Burkholderia cepacia
AOCS	:	American oil chemists' society
ASTM	:	American Society for Testing and Materials
BET	:	Brunner Emmet and Teller
BLM	:	Bulk liquid membrane
BTPC	:	Benzyltriphenylphosphonium chloride
ChCl	:	Choline chloride
COSMO-RS	:	Conductor-like Screening Model for Real Solvents
CTRL	:	Control
DAC	:	N,N-diethylenethanolammonium chloride
DEG	:	Diethylene glycol
DESs	:	Deep eutectic solvents
DFT	:	Density Functional Theory
DG	:	Diglycerides
DSC	:	Differential scanning calorimeter
EG	:	Ethylene glycol
ELM	:	Emulsion liquid membrane
EN 14214	:	European Committee for Standardization that describes the requirements and test methods for FAME
FAME	:	Fatty acid methyl ester
FFAs	:	Free fatty acids
GELM	:	Green emulsion liquid membrane
Gly	:	Glycerol
HBA	:	Hydrogen bond acceptor
HBD	:	Hydrogen bond donor

ICP-OES	:	Inductively coupled plasma-optical emission
IL	:	Ionic liquids
IR	:	Impregnation ratio
LA	:	Lactic acid
LM	:	Liquid membrane
MBR	:	Membrane bioreactors
MG	:	Monoglycerides
MTPB	:	Methyltriphenylphosphonium bromide
NADES	:	Natural deep eutectic solvent
*p*NP	:	*p*-nitrophenol
*p*NPP	:	*p*-nitrophenyl palmitate
PPL	:	Lipase from the porcine pancreas
RPO	:	Refined palm oil
SEM	:	Scanning electron microscopy
SSE	:	Sum square errors
TBP	:	Tributylphosphate
TEG	:	Triethylene glycol
TG	:	Triglycerides
TGA	:	Thermogravimetric analysis
TMAC	:	Tetramethylammonium chloride
TZVP	:	Triple-zeta valence potential
VFT	:	Vogel-fulcher-tamman

List of Appendices

CHAPTER 1: INTRODUCTION

1.1. Background

Fossil fuels, which account for 88% of global energy use, are mostly derived from non-renewable energy sources and hence pose a significant threat to the environment (Thangaraj et al., 2019). This motivates the perpetual quest for a viable replacement. It seems that biofuels made from sustainable energy sources are the way to go. When compared to other biofuels (bio alcohols and biodiesel) has seen the most widespread adoption, renewable, non-toxic, environmentally friendly, biodegradable, and having a good combustion emission profile are some of how it is described (Jahirul et al., 2013; Thangaraj et al., 2019). Transesterification of ample vegetable oil or animal fat catalyzed by alkali is the most prevalent process used to produce biodiesel (Borges & Díaz, 2012). Even if chemical approaches have been shown to work, enzymatic methods for biodiesel generation offer many benefits (Akoh et al., 2007; Franjo et al., 2018). To name a few advantages, (Budžaki et al., 2015) mild reaction conditions, little waste, low energy requirement, the ability to select or even create substrate-specific enzymes, low water usage, etc.

However, during the transesterification process, the side effects of the catalysts, such as soap and glycerol production, pose challenges regardless of which catalyst is utilised. One of the main reasons biodiesel is still not competitive with diesel fuel is because its downstream processing is complicated and expensive. Atadashi et al. (2011) report that purification procedures account for 60-80% of total process expenses in biodiesel production. A decanter is used to separate the glycerol and crude biodiesel, and then an evaporator is used to get rid of the alcohol. Because it still contains free glycerol, soap (if biodiesel is made via chemical catalysis), traces of the catalyst, methanol, metals, water,

oil, and glycerides, crude biodiesel is still unsuitable for use in engines even after these processes are carried out. This contamination must be eliminated before the biodiesel can meet industry requirements (such as ASTM D6751 (Astm, 2012) and EN 14214 (Casas et al., 2010)).

Biodiesel can be cleaned using a variety of techniques, including wet washing, dry washing, and membrane separation. The most popular technique is called liquid extraction, which involves the use of water in various cleaning operations. Large volumes of polluted wastewater are generated due to water use, posing serious disposal issues (Atadashi et al. 2011). To clean 1 dm^3 of biodiesel to standard, it takes 10 dm^3 of water, as stated by Karaosmanolu et al. (1996). To slang this problem, it is suggested to use environmentally friendly solvents like inexpensive ionic liquids (IL) substitutes known as deep eutectic solvents (DESs) (Hayyan et al., 2010; Ho et al., 2015). Solid organic salts, such as choline chloride, are combined with a hydrogen bond donor molecule, like ethylene glycol or glycerol, to create DESs (Abbott et al., 2003, 2004, and 2006). Because of their low toxicity and high biodegradability, they are considered environmentally friendly. DESs have been used effectively for biodiesel purification (Abbott et al., 2004; M. Hayyan et al., 2010; Ho et al., 2015; Homan et al., 2017; Shahbaz et al., 2011a, 2013) but typically in discontinuous extractors/separators where shakers are used to improve mass transfer. Next, batch operations would be replaced with continuous processes to make the process more cost-effective. The efficiency of extraction and separation operations can be improved by reducing the length of the diffusion channels between phases. Liquid membrane techniques have several technical benefits (high surface area, high diffusivity of molecules, high solute transfer rate, may be operating continuously and flexibly, extraction and stripping in one operation, internal phase volume is smaller than the feed phase, recyclability of solvents, etc.) This has attracted considerable attention in several diverse fields (Chakraborty et al., 2006). The efficiency of extraction

and purification operations in liquid membranes can also be improved by using absorbent materials because of their rough and large surface area. Furthermore, the absorbent can be recycled and reused.

In this work, biodiesel was synthesized by transesterification of fresh vigitable oil and waste cooking oil. Activated carbon is also synthesized from palm raceme using chemical activation. After biodiesel production, purification (soap removal) with different DESs and carbon materials was integrated with the emulsion liquid membrane (ELM) technique. The obtained results were compared with biodiesel purification performed by liquid-liquid extraction.

1.2. Problem Statement

A variety of methods, including wet washing, dry washing, washing with solid adsorbents, ion exchangers, and membrane separation, are available for soap removal from biodiesel. However, many of these purification methods involve the use of water in various cleaning operations. Furthermore, many of these approaches are expensive and complex, do not lead to the complete decontamination of biodiesel, and produce a lot of wastewater.

Consequently, there is a growing need to develop alternative methods to clean up contaminated biodiesel. In this work, natural adsorbents like activated carbon made from palm raceme and green solvents like DES will be used instead of water to remove soap from biodiesel in a way that works well. In addition, uncomplicated methods with high performance, such as liquid membrane techniques, should be used by integrating them with natural absorbents and green solvents.

The information on membrane technology is vital and significant, but there are still gaps and shortcomings, especially in the liquid membrane technique. These are; therefore, emphasized, and relevant research directions are needed. This study will provide a new

branch of deep eutectic solvents-based emulsion liquid membranes and activated carbon. This research will contribute to the understanding of the relationships between deep eutectic solvent properties and activated carbon, as well as the mechanism of soap removal via an emulsion liquid membrane. This could potentially lead to the development of a solution for reducing environmental pollution that is produced by the water washing technique.

1.3. Research Questions

The following research questions have been provided to address the aforementioned research gap:

1. What are the optimal operating conditions and characterization of AC preparation for soap removal?
2. What are the suitable sustainable and green solvents for the purification of biodiesel?
3. Which DESs demonstrate the highest potential for effective soap removal?
4. What are the optimal operating conditions for maximizing soap removal efficiency using AC and DESs in a liquid-liquid extraction?
5. What are the optimal parameters and reaction kinetics for soap removal from biodiesel using DES and AC in an ELM system?

1.4. Research Aim and Objectives

Liquid membrane purification techniques have received considerable attention because of their potential advantages over other separation techniques. The main objective of this study is to develop an ELM technique for the purification of soap dispersed in crude biodiesel. The product that is cleaned up by the ELM technique should meet the standards for soap in biodiesel, and therefore the objectives of the study are to:

1. Investigate the effect of varying operation conditions parameters on activated carbon production from palm raceme.
2. Study the physicochemical properties (density, viscosity, conductivity, and thermal stability) of new DESs at different temperatures.
3. Screen different DESs using computation software (COSMO-RS) for the selection of the potential DESs for soap removal.
4. Optimize the operating conditions for soap removal using the activated carbon and DESs in the liquid-liquid extraction technique.
5. Perform optimization and kinetic studies for soap removal from crude biodiesel using DES and activated carbon in an emulsion liquid membrane system.

1.5. Scope of the Study

This study focuses on developing and optimizing methods for soap removal from crude biodiesel, leaving novel approaches such as integrating deep eutectic solvents and carbon materials. Figure 1.1 represents the framework methodology of this research and includes:

1. Production of activated carbon: Activated carbon will be produced from palm raceme and characterized for its potential as an adsorbent for soap removal.
2. Preparation and characterization of DES: The physicochemical properties of selected DES (density, viscosity, conductivity, and thermal stability) will be analyzed at various temperatures.
3. Computational screening: Computational tools like the Conductor-like Screening Model for Real Solvents (COSMO-RS) will be used to select the best candidates DESs for soap removal in different techniques which are liquid-liquid separation and emulsion liquid membrane.

4. Liquid-liquid extraction technique: The liquid-liquid extraction technique will be explored to optimize the operating conditions for soap removal using activated carbon and deep eutectic solvents.

5. Emulsion liquid membrane study: Kinetic and optimization studies will be conducted to evaluate the efficacy of DES and activated carbon in an emulsion liquid membrane (ELM) system for soap removal.

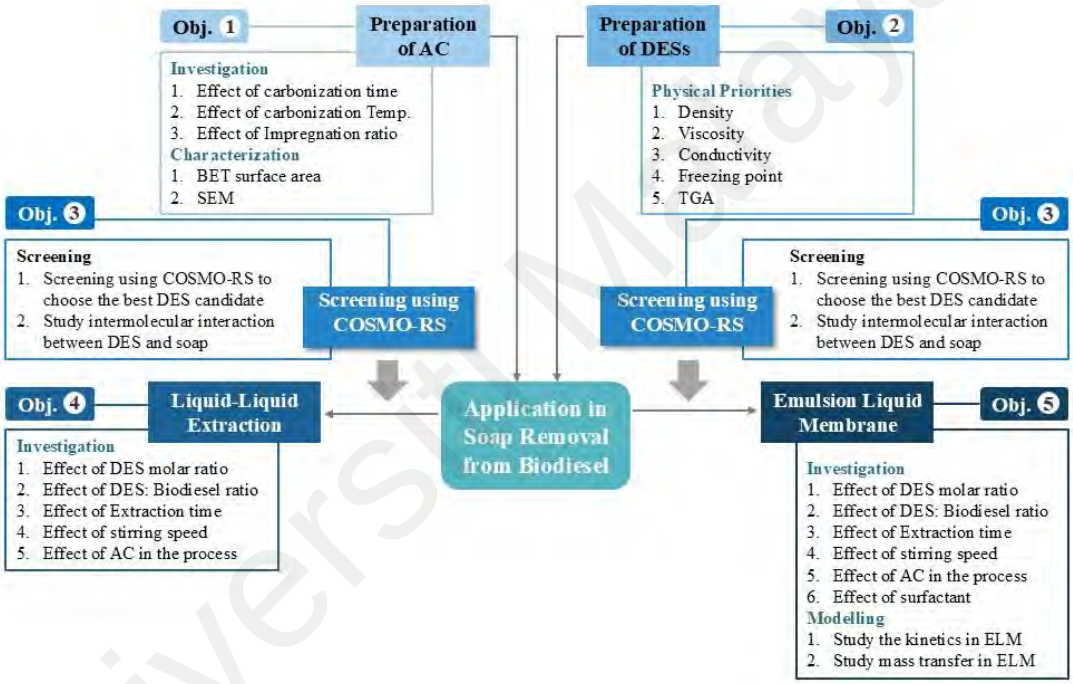

Figure 1.1: Framework methodology of research

1.6. Limitations of Study

Emulsion liquid membranes (ELM) can be employed in both extraction and stripping processes, offering high separation capacity and selectivity at a lower cost. These techniques are effective in reducing contaminants, such as glycerol and soap, to less than 2 ppm. Their potential for contaminant removal is significant due to the large mass transfer area and the reduced solvent usage, all in the absence of water.

Despite the successful purification of biodiesel with desirable physicochemical properties through ELM processes, challenges remain, including emulsion instability and limitations in applications requiring extreme temperatures due to emulsion stability. Further research is necessary to explore emulsion stability, breakdown, emulsification time, and the proper selection of the stripping phase during the refining process. These aspects warrant more attention in the field of biodiesel refining.

1.7. Outline of Study

This thesis consists of eight chapters. Chapter 2 (Theoretical Background) presents a literature review of impurities in crude biodiesel. The chapter also includes an overview of various biodiesel purification techniques, a general overview of liquid membrane-based separation technology, and the principle of operation for the separation technique used in this compatibility of study research. Chapters 3 to 7 consist of several manuscripts that were sent to scientific journals for publication. This format required the duplication of several common concepts (e.g., experimental sections) in these chapters. Chapter 8 contains a general conclusion that relates to Chapters 3 to 7 and provides various recommendations for future research. References and appendices (where applicable) are supplied for each chapter of the thesis.

CHAPTER 2: LITERATURE REVIEW

2.1. Introduction

Constant challenges to the environment are due to the cumulative effects of decades-long negative influences of industrialization. The growing global population has intensified the demand for cleaner energy sources to ensure societal sustainability. Fossil fuels, which account for 88% of global energy consumption are mostly derived from non-renewable energy sources which poses a significant threat to the environment (Paola et al., 2021; Thangaraj et al., 2019). This motivates the perpetual quest for a viable replacement for fossil fuels. Biofuels derived from sustainable energy sources could be the answer to this problem. When compared to other biofuels (bio-alcohols and biogas), biodiesel has witnessed the most widespread application. It possesses a lower emission profile upon combustion, in addition its renewability, affordability, non-toxicity, environmental friendliness and biodegradability (Melo et al., 2024; Jahirul et al., 2013; Ramos et al., 2019). The transesterification of alkali-catalyzed animal fats and vegetable (edible) oils is the most prevalent method to produce biodiesel (Borges & Díaz, 2012). The enzymatic methods for biodiesel generation still offer many benefits though the chemical conversion into biodiesel is still more viable (Akoh et al., 2007; Franjo et al., 2018). Among the advantages of enzymatic methods are mild reaction conditions, low waste generation, low energy consumption, the selection of substrate-specific enzymes, low water consumption, etc. (Budžaki et al., 2015).

Biodiesel is a type of renewable diesel fuel that shares many of the same characteristics as diesel refined from petroleum. A transition to biodiesel is a step toward "sustainable energy," as the fuel is renewable and produces lower hazardous exhaust pollutants when burned compared to petroleum diesel (Al-Humairi et al., 2022; Hayyan et al., 2021).

Biodiesel can be derived from different sources, such as animal fats, vegetable oils, or even microorganisms such as microalgae and cyanobacteria through a chemical reaction with short-chain alcohols called transesterification (Osorio-González et al., 2020).

Nevertheless, irrespective of the catalyst type, few concerns pertain to the by-products generated by the catalysts, such as glycerol and soap that are liberated during the transesterification process. The primary reason why biodiesel is still inefficient compared to petroleum diesel is that it requires intricate and costly purification steps (Atadashi, Aroua, & Aziz, 2011). Tai-Shung (2007) mentioned that 60–80% of the total cost of biodiesel is incurred by the purification process. A decanter is used to separate the glycerin from biodiesel, followed by the elimination of unreacted alcohol by an evaporator. Even after these procedures, biodiesel is often incompatible with engines as it contains contaminants such as soap, free glycerol, residual catalyst, free fatty acid, alcohol, water, and partial glyceride. These contaminants must be eliminated before the quality of the biodiesel conforms to the industrial specifications (ASTM D6751 (Astm, 2012) and EN 14214 (Casas et al., 2010)).

Different techniques can be used for biodiesel purification, such as dry washing, wet washing, and membrane purification. The most popular technique is the liquid extraction method, which involves the use of water in the cleaning process. The utilization of water in the cleaning process forms large volumes of polluted wastewater which poses serious disposal problems (Atadashi et al., 2011). The volume of water required for the washing process is ten times that of the unpurified biodiesel, as stated by Karaosmanolu et al. (1996). Alternatively, it is suggested to utilize environmentally friendly solvents such as deep eutectic solvents (DESs) which are economically viable and applicable for integration into the washing process (Hayyan et al., 2010), (Ho et al., 2015). The preparation of DESs involves the mixing of a hydrogen bond acceptor (HBA) and a hydrogen bond donor (HBD) (Abbott et al., 2003, 2004, 2006). They are considered eco-

friendly solvents as they are biodegradable and non-toxic. DESs have been used effectively for the purification of biodiesel, but usually in batch mode for liquid extraction processes with shakers to enhance the diffusion (Abbott et al., 2004, 2006; Hayyan et al., 2010; Ho et al., 2015).

The wet and dry washing technique could be replaced by a liquid membrane (LM) process to make the process more cost-effective. The efficiency of extraction and separation operations could be improved by minimizing the diffusion path between the phases. The LM techniques offer various benefits such as high surface area, thin membrane layer, high solute mass transfer, and flexibility, combined extraction and stripping processes, low receiving phase volume than the source phase, solvents recyclability, etc. These advantages via the LM technique of separation have gained considerable attention in several diverse fields (Chakraborty & Bart, 2006), including the biodiesel industry and vegetable oil refinery (Hayyan et al., 2022).

In a different strategy, solid particles in the emulsion liquid membrane (ELM) enhance the stability of the emulsion globules and prevent the globules from impact and agglomeration (Al-Obaidi et al., 2021; Lin et al., 2015). Activated carbon (AC) possesses a rough surface with a high surface area, in addition to the numerous void spaces that lead to stronger bonding between the oxygen groups of the contaminants and the surface of the AC. It is well known that the adsorbate interacts with the surface of the adsorbent either chemically or physically, via chemisorption or physisorption, respectively (Fadhil & Abdulahad, 2014). Although methods such as wet and dry washing eliminate the contaminants, they frequently form a significant amount of wastewater. The various contaminants found in biodiesel, such as glycerol, methanol, soap, water, and catalyst residues, require thorough purification techniques which are necessary for both environmental sustainability and peak engine efficiency. Recently, there are very few investigations on BLM and ELM techniques for the removal of contaminants from crude

biodiesel. Therefore, this review describes the contamination in biodiesel and processing technologies based on their practical nature, encompassing equilibrium-driven, affinity-centered, membrane-facilitated, solid-liquid, and reactive purification processes. In addition, special emphasis is devoted on the liquid membrane-based purification processes for crude biodiesel. The efficient and advanced purification methods in biodiesel production are essential for a high-quality biodiesel and for meeting the EN14214 and ASTM D6517. This review chapter fills a gap in the literature by highlighting the novel research using ELM and BLM approaches for the purification of crude biodiesel.

2.2. Contaminations in Biodiesel

The biodiesel layer must be separated from the glycerin after the transesterification reaction, where an additional purification process is required (Bateni & Karimi, 2016). Due to the significant difference in the densities of glycerol and biodiesel, as well as their poor mutual solubility, simple and straightforward separation processes such as centrifugation and gravity settlement can be employed (Atadashi, Aroua, & Aziz, 2011). The most significant impurities in biodiesel, which restrict its application beyond that of biofuel, are presented in this paragraph. Unsaponifiable matter, bounded glycerin, free glycerin, water, alcohols, soaps, free fatty acids (FFAs), catalysts, and oxidation products are examples of the different types of contaminants. The elimination of these contaminants is necessary to produce biodiesel that complies with worldwide standards such as the American Society for Testing Materials (ASTM D6751) and European standards (EN 14214) (Table 2.1).

Table 2.1:International standards of biodiesel based on ASTM D6751 and EN14214 specifications.

Property	EN 14214		ASTM D6751		Units
	Min.	Max.	Min.	Max.	
Density (15 ^{O}C)	860	900	-	-	kg/m^3
Kinematic viscosity (40 ^{O}C)	3.5	5	1.9	6	mm^2/s
Flash point	120	-	93	-	^{O} C
Cloud point	-	-	Report		^{O} C
Distillation- atmospheric equivalent temperature, 90% recovered	-	-	-	360	^{O} C
Cetane number	51	-	47	-	-
Copper strip corrosion	-	1(class)	-	3 (-)	rating
Oxidative stability	6	-	-	3	hours
Acid value	-	0.5		0.5	mg KOH/g
Iodine value	-	120		-	g I/100g
Earth alkali metals (Ca +/ Mg)	-	5	-	5 (combined)	ppm
Alkali metals (Na +/ K +)	-	5		5 (combined)	ppm
Sulfur content	-	10	-	15(S15grade) 500(S500grade)	ppm
Phosphorus content	-	0.001	-	0.001	mass %
Carbon residue	-	0.3	-	0.05	% m/m
Sulfated ash	-	0.02	-	0.02	% m/m
Ester content	96.5	-		-	% m/m
FAME content with ≥4 double bond	-	1	-	-	% m/m
Linolic acid content	-	12		-	% m/m
Methanol content	-	0.2	-	0.2	% m/m
Water content	-	0.05	-	0.05	% Vol
Total contaminants	-	24	-	-	mg/Kg
Monoglyceride	-	0.8	-	-	% m/m
Diglyceride	-	0.2	-	-	% m/m
Triglyceride	-	0.2	-	0.2	% m/m
Free glycerin	-	0.02	-	0.02	% m/m
Total glycerin	-	0.25	-	0.24	% m/m

Impurities in crude biodiesel produce unwanted effects during the processing and storage steps. The FFA, water, alcohol, free glycerin, glycerides, soap, and catalyst residues are some of the contaminants found in crude biodiesel. Unpurified biodiesel may cause

serious engine problems such as filter blockage, coking on injectors, excessive engine wear, high carbon deposits, engine knocking, thickening, and gelling of lubricant oil, and instability of the engine system (Dunn, 2011). The effects of the contaminants on the biodiesel and combustion engines as well as the standard specifications based on ASTM and EN are listed in Table 2.2.

Table 2.2:Impurities on biodiesel and engine their impact as well as standard specification based on ASTM D6751 and EN 14214.

Contamination	Impact
FFA	Low oxidative stability and corrosion
Water	FFA formation, corrosion, pitting in the pistons, reducing heat combustion, ice crystal formation resulting in gelling of residual fuel, reduc engine's useful life, deterioration of biodiesel quality, reduce the calorific value of the fuel, and bacterial proliferation (filter blockage)
Alcohol	Having a low flash point, low viscosity and density, natural rubber seals and gaskets deteriorate over time and a high susceptibility to corrosion
Glycerides: Monoglyceride Diglyceride Triglyceride	Problems with crystallization, high viscosity, turbidity, and deposit format on injectors, valves and pistons.
Alkali metals (soap and catalyst) Na^+ / K^+	Abrasive engine deposits, filter blockage due to highly sulfated ash, engine corrosion problems and deposits on the injectors.
Free glycerol	Increased exhaust emissions of aldehydes and acrolein and difficulties settling down

2.2.1. Acid value and FFA

Acid value (mg/g) is the quantity of KOH in milligrams required to neutralize the acidic components in one gram of biodiesel. The amount of acidic groups in biodiesel can be measured using acid value assessment method. The standard protocol according to the American Oil Chemists' Society (AOCS) involves the titration of a known volume of

sample dissolved in an organic solvent with KOH solution with known molarity and phenolphthalein as the indicator (de Oliveira et al., 2010). Residual mineral acids from the manufacturing process, remnants of FFA from the hydrolysis process of esters, and the oxidized byproducts in the form of organic acids are examples of acidic compounds that present in biodiesel (Perera et al., 2022). The acid value directly represents the amount of FFA present in the biodiesel, which in turn indicates the corrosiveness, blockage of the filter, and water content in the biodiesel. In addition, the freshness of the biodiesel can be determined using this parameter. The acid value of biodiesel is likely to increase after prolonged storage due to oxidation. Fangrui et al. (Ma & Hanna, 1999) explain how a trace amount of FFA and water could be present in even refined fats and oils. Triglycerides hydrolyze rapidly in the presence of water, which raises the FFA's amount in vegetable oils (Tomasevic & Siler-Marinkovic, 2003). FFA and water have a detrimental impact on the alkali-catalyzed transesterification process due to the consumption of the catalyst, production of soap, and lowering of the catalytic activity producing lower conversion and yield (Ma et al., 1998; Tomasevic & Siler-Marinkovic, 2003). Ma et al. (1998) reported that 0.9 % of FFAs was present in the reaction feed during the transesterification of beef tallow using an alkali catalyst, and the observed yield of biodiesel reached the lowest value of less than 5%. Accordingly, they mentioned that the amount of FFAs should not exceed 0.5%. This indicates that the leftovers of fats and vegetable oils, especially crude and used oils- must be purified to eliminate the FFAs. Kusdiana and Saka (2004) investigated the impact of water on the production of methyl esters using the supercritical method (43 MPa, 350 °C, 4 min of reaction time with 42:1 molar ratio of methanol: oil) in comparison to the acidic and alkaline-catalyzed methods. In the supercritical technique, the mixing of water into the reaction mixture did not significantly influence the conversion process (Kusdiana & Saka, 2004). This study (Kusdiana & Saka, 2004) shows a constant conversion of triglycerides independent of the

FFA content present in the acidic and alkaline-catalyzed and supercritical methods. Additionally, Vávra et al. (2017) investigated FFA removal from the ester phase using calcium hydroxide. Specifically, the influence of calcium hydroxide on the FFA ratio, acid number, and water content was investigated due to their effect on the kinetics and thermodynamics of the process. The addition of a small amount of water initiates a reaction between the calcium ions and FFA to produce the calcium soap. The centrifugation process was used to remove the solidified calcium soap. Moreover, an established simulation model allows for the calculation of the ideal FFA removal parameters, which are as follows: 3.33:1 molar ratio of calcium to FFAs, 0.14 wt.% of water in the feed phase, and three hours reaction duration, in order to verify that the biodiesel meets the EN 14214 specialization.

2.2.2. Water

The pollution of biodiesel in water resources is widespread. It is a common knowledge that water inhibits the biodiesel transesterification reaction, hence water-free vegetable oils and fats are preferred as raw materials (Kusdiana & Saka, 2004). Water deactivates and even destroys the catalysts. Moreover, water is a serious contaminant in biodiesel fuel, producing corrosion in the fuel system of the engine. Rust or known as ferric oxide is the most common product of steel corrosion, but the storage tanks could be also damaged by the formation of corrosive acids from the oxidization of water (Wirawan et al., 2024). Based on EN 14214 and ASTM D 6751 criteria for biodiesel, the content of water, glycerol, FFAs, and alcohol must be at a minimum value (Table 1). Thus, the presence of water is far more detrimental compared to the deleterious impact of FFAs. The presence of water reduces the catalyst's activity, whereas FFA interacts with the catalyst to release the fatty acid salt molecule (Balat & Balat, 2010). An excess of water could lower the fuel's calorific value and deteriorate the engine's parts (Praveena et al., 2024). Therefore, the water content should be maintained at or lower than 0.06% (F. Ma

et al., 1998), which is significantly below than the maximum permitted FFA level. Waste vegetable oils and crude oils pose challenges that prevent their optimal use due to their inherent water presence together with the FFAs (Tomasevic & Siler-Marinkovic, 2003). Burton (Burton, 2008) stated that petrol could only absorb about 50 ppm of humidity, while biodiesel could absorb 150 ppm of humidity. Demirbas (Demirbas, 2009) observed that the heat of combustion decreases with the water content in the biodiesel. Furthermore, water crystallizes into ice as it gets closer to the freezing point (Demirbas, 2009). These crystals promote nucleation spots and accelerate the leftover fuel's gelling process. The majority of micro-organisms utilize water as a part of their respiratory system (Atadashi et al., 2012). However, water accelerates the hydrolysis reaction and the growth of bacterial colonies could block the fuel system (Predojević, 2008). The presence of water may lead to unwanted side reactions such as saponification reaction, especially in high concentrations of the alkaline catalyst and FFA (Predojević, 2008). The saponification reaction significantly affects the conversion of biodiesel, reduces the quality of biofuel, and consequently affects the nozzles and engine lifetime (Atadashi et al., 2012). However, the water content has no effect on the biodiesel yields, as the complete conversion can be completed independently of the water content.

2.2.3. Free glycerol

Free glycerol, which is a byproduct of the transesterification reactions is not present when esters are thoroughly cleaned with water. Glycerol may remain in the biodiesel if the glycerin phase is not properly separated from the biodiesel or if the biodiesel is not thoroughly washed with water after the separation process (Miyuranga et al., 2022). Glycerin is also present when the distillation process is used for the removal of glycerin. It is believed that the free glycerin in the biodiesel facilitates the formation of deposits in the engine. Free glycerin settles at the bottom of the storage tanks due to the poorly solubility of glycerol in methyl esters. The low solubility of free glycerol in biodiesel is

due to the polarity differences, viscosity, and densities. It was reported that the density of biodiesel is 860 - 885 kg/m^3, while the density of glycerol is approximately 1260 kg/m^3 (McNutt & Yang, 2017). Water and monoglycerides possess strong affinities towards free glycerin. It is speculated that the presence of glycerin increases the concentration of these compounds in the tank's sediments in the presence of the ester (Avagyan et al., 2019).

Abbot et al. (2007) employed a glycerol-based DES for the separation of glycerol from biodiesel produced via ethanolysis of rapeseed and soybean oils with KOH as a catalyst. The HBA:HBD ratio of 1:1 (choline chloride: glycerol) was the best efficient ratio for glycerol elimination. The concentration of glycerol remaining in the rapeseed and soybean biodiesels were 0.02 and 0.06%, respectively 09:05 PM.

Wang et al. (2009) used three ceramic membranes with different sizes of 0.6, 0.2, and 0.1 μm to eliminate the glycerol from crude biodiesel produced via an alkali-catalyzed transesterification. The 0.1 μm membrane size gave the best result in the elimination of free glycerol at a temperature and pressure of 60 ^{O} C and 0.15 MPa, respectively. Under the same working conditions, the flow through the membrane was 83.3% of the original flux when the volumetric concentration ratio reached 4. The amount of free glycerol was reduced to 0.0108% which complies with the worldwide standards of the ASTM D6751 and EN 14214 specifications (Wang et al., 2009).

Suppalakpanya et al. (2010) used bleaching earth and pure glycerol for the removal of free glycerol from biodiesel produced via an alkaline-catalyzed ethanolysis of palm oil. The product was heated in a microwave at 70 Watts for one minute. Following gravity-based separation, the biodiesel layer was treated with bleaching earth, mixed for five minutes, and centrifuged after heated to 80 ^{O}C to eliminate the remaining ethanol. The optimum conditions were 1.2 % of bleaching earth and 1.2 % of pure glycerol, where the residual glycerol concentration was lowered from the recommended level. The final purified biodiesel complied with the ASTM D6751 specification.

Wall et al. (2011) employed an ion exchange approach in the form of a fixed bed reactor for glycerol and soap removal from crude biodiesel. Three ion exchange resins, T45BDMP, T45BD, and BD 10Dry were used in this investigation. The potassium-based soap was unaffected by the particle size of the resins, while the extraction efficiency of sodium-based soap improved as the particle size decreased. When the processed biodiesel was placed in 200 and 550 bed volumes, the ion exchange resins decreased the glycerol content from 0.08% to less than 0.02% and the soap content from 1200 mg/kg to less than 50 mg/kg, respectively.

Shahbaz et al. (2012) designed an artificial network model to predict glycerol removal from crude biodiesel using experimental data and application of DESs as the extractant solvent. Methyl triphenyl phosphonium bromide and choline chloride were the hydrogen bond acceptors and various hydrogen bond donors in the synthesis of the DESs. The model's input was the composition of DESs and the DES: biodiesel mole fractions. The Levenberg-Marquardt optimization approach was used for the training of a feed-forward neural network with four hidden neurons. The predicted model agrees well with the measured results with a standard deviation of 4.64% (Shahbaz et al., 2012).

Hayyan et al. (2022) used a natural deep eutectic solvent (DES) via a novel BLM technique to purify the crude biodiesel from glycerol. The quaternary ammonium salt-glycerol-based DES was used as the membrane phase, while diethyl ether was used as the stripping phase. The different parameters (mixing speed, duration time, DES molar ratio, and DES: biodiesel ratio) were investigated to determine the extraction and stripping efficiency of the system. The results show that the proposed technique successfully eliminated glycerol according to the EN 14214 and ASTM D6751 criteria.

2.2.4. Bounded glyceride

Transesterification produces varying amounts of monoglycerides (MG), diglycerides (DG), and triglycerides (TG). These substances are referred to as "bounded glycerin"

herein (Freedman et al., 1984). In theory, there shouldn't be remnants of TGs when alcohol is utilized at a rate of 2.0 times the theoretical amount (or 100% excess) (Jan C. J. Bart, 2010). However, the MG and DG could be present in trace amounts. These partially reacted and polarized the glycerides, hence are expected to be drawn into the glycerin phase and eliminated during the phase separation step. The results may overestimate the relative quantities of bounded glycerol in the ester.

Shahbaz et al. (Shahbaz et al., 2010, 2011b) showed that DES-based glycols are effective for the elimination of bounded glycerol, free, and total glycerol from biodiesel. The DES-based choline chloride: ethylene glycol at HBA:HBD ratio of 1:2.5 and the DES-based 2,2,2-trifluoroacetamide at HBA:HBD ratio 1:1.75, effectively eliminated the glycerol from the crude biodiesel (Shahbaz et al., 2010). The DES based on methyltriphenylphosphunium bromide and triethylene glycol or ethylene glycol eliminated all the free glycerol, where the total glycerol concentration was lowered below the specification (Shahbaz et al., 2011b). Furthermore, at the DES: biodiesel molar ratio of 3:1 and 0.75:1, mono and diglycerides were eliminated by DES-based triethylene glycol (1:4 molar ratio) for 37.9% and 53.4%, respectively (Shahbaz et al., 2011b). In comparison to the DESs prepared from ethylene glycol, triethylene glycol, or 2,2,2-trifluoroacetamide, the DES prepared from glycerol as the HBD gave lower removal efficiencies. Conversely, glycerol was more effectively removed by the phosphonium-based DESs than the ammonium-based DESs.

2.2.5. Alcohols

Biodiesel may consist of more than 4% of methanol after the separation of glycerol. The elimination of alcohol from biodiesel and glycerol is one of the most utilized purification techniques in the production of biodiesel. To reduce the biodiesel production cost, the excess methanol utilized in the transesterification reaction can be reused. Furthermore,

since methanol is toxic and combustible, it is important to decrease the emissions into the environment. However, the purification techniques could be utilized to meet alcohol concentration specifications for biodiesel, such as the ASTM D6751 and EN 14214 (Tabatabaei et al., 2015). The acceptable alcohol concentration in biodiesel, based on the EN 14214 standard, is 0.2 mol%, since the alcohol concentration has a large impact on the biodiesel flash point (Boog et al., 2011). The compression-ignition engines are particularly vulnerable to explosions caused by excessive methanol in the fuel. A fuel's flash point can be affected by the methanol content in the fuel (Rodriguez, 2016). A study (Rodriguez, 2016) has shown that the presence of methanol and ethanol decreases the flash point of fatty acid methyl ester biodiesel. The presence of alcohol can be lowered to appropriate levels by washing with water or using a vacuum distillation (Amelio et al., 2016), both of which are in accordance with the ASTM and EN standards. Moreover, alcohol is one of the most important contaminants to be removed for securing safe storage and transportation.

2.2.6. Soap and residual of alkali catalyst

Most of the production process of biodiesel is performed with the aid of an alkaline catalyst such as NaOH, CH_3ONa, or KOH. The transesterification process is difficult without the presence of a catalyst, consequently, the by-products of a reaction (alky esters) are typically polluted with other substances. The Na and K ions are the most strictly regulated since sodium hydroxide and potassium hydroxide are employed as catalysts. These substances may clog the vehicle's mechanical units; they are present in the form of soaps (fatty acid salts) or as solid abrasives (Chaves et al., 2008; de Jesus et al., 2008; Pohl et al., 2010). Furthermore, due to the plant's (raw material) adsorption of metals from the soil, additional inorganic pollutants (such as Ni, Cu, Cd, Pb, Zn, etc.) could be detected in biodiesel or may be included throughout the production, as well as in the storage step (Lobo et al., 2011). The FFA, soap, and catalysts are removed together

with other impurities. The remaining FFA reacts with the catalyst to produce soap (Miyuranga et al., 2022) as presented in Eq. 2.1. The removal of soaps occurs during the water-washing process where this procedure also eliminates remnants of the catalysts. The water content reduces the catalyst's activity, whereas FFA interacts with the catalyst to release the soap molecule (Balat & Balat, 2010). The release of fatty acid salt decreases the biodiesel product and significantly complicates the final product isolation and refinement. Moreover, the soap molecules increases the viscosity leading to the formation of hydrogels and emulsions, making the glycerol harder to separate (Demirbas, 2005), (Demirbas, 2009). The main issue associated with these pollutants is the degradation of the soap or catalyst residues into ash upon the combustion of the fuel in the engine. The present specification of the ash concentration of biodiesel of 0.02% in biodiesel is considered as a limitation as it cannot exceed 0.01%, as specified by ASTM D975.

Baroutian et al. (2012) successfully used water washing and adsorption techniques in a two-step purification process to eliminate the residual potassium hydroxide catalyst from the crude biodiesel. The first stage involves washing and mixing the crude biodiesel in acidified hot water (60 ^{O} C and 0.1% tannic acid) at a volume ratio of acidified water: biodiesel of 2:1. The process was carried out until the biodiesel layer became clear. The residual catalyst content decreases from 44.32 mg KOH/kg to 5.74 mg KOH/kg after the first step. The second step utilizes activated carbon (AC) from palm shells in the adsorption process. The AC was suspended in prewashed biodiesel and then shaken at a regular temperature. Different parameters such as the temperature, adsorbent dosage, and duration were investigated with respect to the residual catalyst elimination. The removal of the catalyst reaches 24% under the optimum conditions (0.9 g of AC / 25 mL of biodiesel, 20 hr, and 40 ^{O}C). The study demonstrates the viability of adsorption methods for the elimination of water and enhance the specification of biodiesel fuel in diesel engine applications (Baroutian et al., 2012).

From an economic viewpoint, the quantitative monitoring of metallic elements in fuel samples is critical to the fuel industries and also to other service industries. Determining the overall amount of a particular metallic and semi-metallic component or tracking the changes in the content over time is becoming an important step in biodiesel purification. This kind of analysis is essential for the high quality control of biodiesel purification (Chaves et al., 2010; de Jesus et al., 2010). The corrosion of the fuel tank in automobile engines, which depends on the properties of fuels, is one of the most important factors to be considered (de Amorim et al., 2006; de Jesus et al., 2008; Haseeb et al., 2010).

$$HO-\overset{\overset{O}{\|}}{C}-R_1 + NaOH \rightarrow Na^+ - O - \overset{\overset{O}{\|}}{C}-R_1 + H_2O \quad (2.1)$$

2.2.7. Unsaponifiable Matter

The organic compounds that do not combine with alkali to produce soap are known as unsaponifiable matter. Compounds of this type include sterols, alcohols of greater molecular weight, pigments, waxes, and hydrocarbons. Wax contaminants in biodiesel cause filter blockages, decrease the heating value, increase viscosity and density, and negatively impact the engine efficiency. Controlling these contaminants is essential for the best engine performance utilizing biodiesel (Barabás & Todoruţ, 2011). As these are non-polar substances, they are found in the biodiesel phase even after the transesterification process. Unsaponifiable materials contains various groups of unsaturated compounds, such as open-chain aliphatic and cyclic aliphatic functional groups, as well as the aromatic functional groups (Gunstone, 2009). The polarity of the sterols may alter the temperature of crystallization but the unsaponifiable materials may not influence the performance of the engine in other ways.

The quality requirements for biodiesel are set by standards of ASTM D6715 and EN 14214, which aim to prevent or minimize the negative impacts of contaminants. The purification techniques must be used to eliminate the contaminants contained in the crude biodiesel in order for it to meet the standards' purity requirements.

2.3. Biodiesel Purification Techniques

Different impurities are present in the product of biodiesel after the transesterification reaction is finished. A large amount of these contaminants must be eliminated in order to meet the international standard specification for biodiesel as a fuel. The biodiesel can be purified using different approaches, some of which have been proposed in the literature (Atadashi et al., 2011b, 2011a). Twenty to thirty percent (v/v) of the purified biodiesel is generated from the polluted wastewater. The purification expenses for biodiesel account for 60-80% of the overall processing costs (Atadashi et al., 2011a). Many purification processes have been researched and utilized to lower the cost of biodiesel purification. Generally speaking, these techniques can be classified as either innovative or traditional. The wet and dry washing are examples of the standard techniques, whereas membranes-based separation processes are examples of innovative techniques (Veljković et al., 2015). Figure 2.1 presents the schematic diagram of biodiesel purification techniques. Researchers have tried washing the solution with water, filtering it via a membrane, using adsorbents and employing ion exchange resins to eliminate contaminants like soap and glycerin (Berrios & Skelton, 2008; He et al., 2006; Kucek et al., 2007; Predojević, 2008; Yori et al., 2007). The outcomes of these investigations towards biodiesel purification are discussed in the following sections.

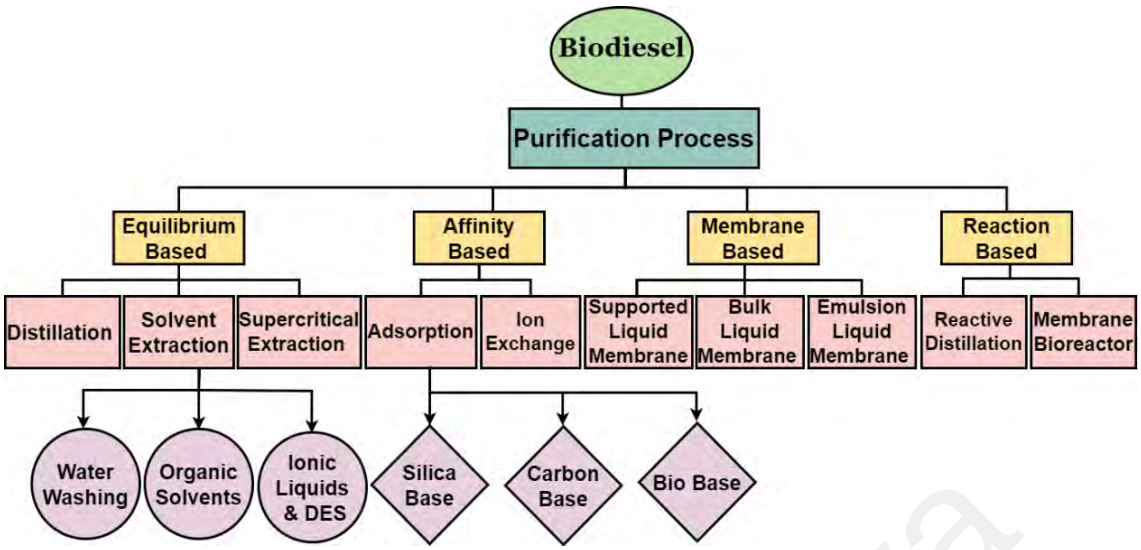

Figure 2.1: Schematic diagram explaining techniques for biodiesel purification.

2.3.1. Equilibrium-Based Separation Technique

Equilibrium-based separation techniques can be classified as distillation and solvent extraction. They are the most widely known equilibrium-based separation techniques (Huang & Ramaswamy, 2013). Furthermore, Wei et al. (Wei et al., 2014) reported the effective utilization of the supercritical extraction technique by employing carbon dioxide at 40 °C and 30 MPa, resulting in a 99.94% biodiesel separation efficiency.

2.3.1.1. Distillation

Distillation is one of the most common methods for the separate volatile compounds from heavy substances in liquid mixtures (Kockmann, 2014; Nag, 2015). There are various distillation methods such as traditional, reactive, azeotropic, and molecular distillations (Doherty et al., 2008). The traditional methods of distillation are widely used techniques in the purification of biodiesel for the removal of impurities such as water and alcohols (Atadashi, Aroua, & Aziz, 2011; Atadashi et al., 2011b; Stojković et al., 2014). High-vacuum molecular distillation is another technique for the purification of biodiesel, where the volatile molecules could be easily evaporated under vacuum conditions on a condensed surface. In reality, the condensed surface is closer to the molecules than the

mean free path of the molecule, thus there is very few collisions of the molecules from the surrounding gases (Erich, 1982). Wang et al. (2010) employed molecular distillation for biodiesel purification from cooking oil waste at 120 °C and achieved a 98% separation yield (Wang et al., 2010). Rodriguez and Martinello (2021) employed a two-molecular stage approach (Figure 2.2) for the reduction of glycerol and glycerides in the biodiesel produced from soyabean oil, with ethanol and NaOH as the catalyst (Rodriguez & Martinello, 2021). Esters and residues of ethanol, glycerol, and glycerides (TG, DG, and MG) that did not react during the transesterification are present in the crude biodiesel. The boiling temperature also differs: biodiesel at 355 °C, glycerol at 290 °C, TG approximately at 400 °C, ethanol at 78.8 °C, while MG and DG boiling points are in the middle range. A vacuum rotary evaporator is used to separate the ethanol, and two molecular distillation processes are performed to isolate the GL and MG, DG, and TG. A falling film vaporizer, an inner condenser, and a vacuum system with a mechanical pump are the components of the molecular distillation apparatus. The ideal parameters (70°C and 240 rpm) for the second stage of distillation are established in the first stage. The required, semi-purified biodiesel was then obtained by repeating these steps. The lighter components such as glycerol and biodiesel are distilled at 150°C and 240 rpm, while the heavier contaminants (MG, DG, and TG) are present as the residue, which was distilled in the second stage. The purified biodiesel achieved international standards with high yield (98% and 82% in the first and second step respectively) and greatly reducing the glycerol (around 72-100%) (Rodriguez & Martinello, 2021). The other contamination present are 0.018 wt.% of MG, 0.026 wt.% of DG, 0.000 wt.% of TG, and 0.024 wt.% of GT (Rodriguez & Martinello, 2021).

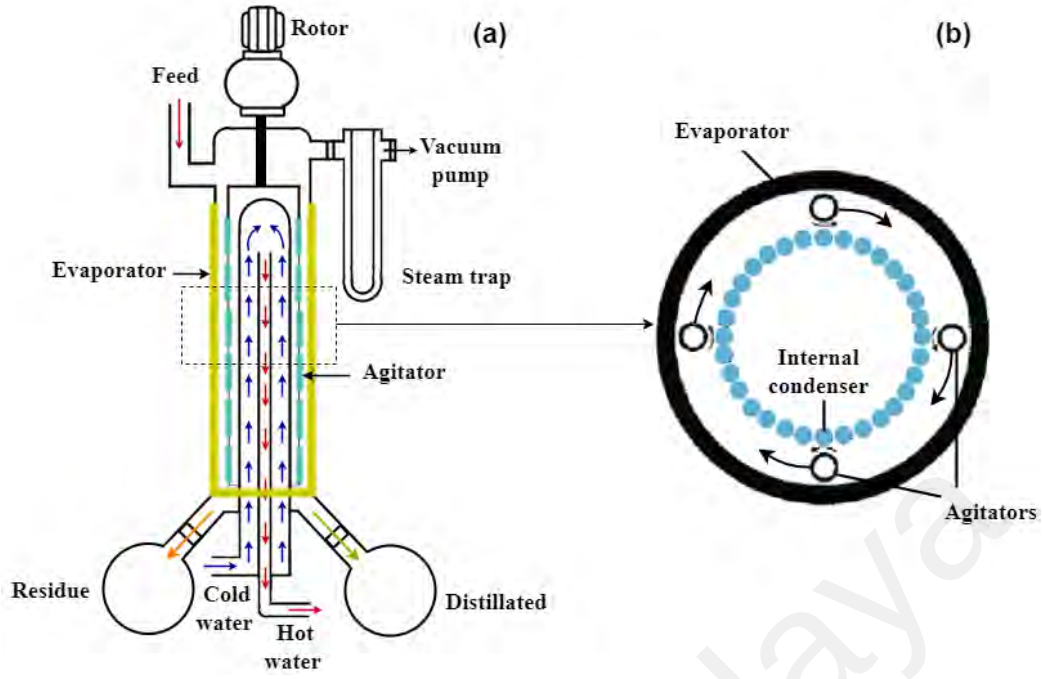

Figure 2.2: Experimental setup of molecular distillation scheme for biodiesel purification. (a) side view and (b) transversal view (Rodriguez & Martinello, 2021).

2.3.1.2. Solvent Extraction

Solvent extraction techniques can be classified as water washing, organic solvents, ionic liquids (IL), and DESs. The following subsections summarise each technique.

- **Water Washing Technique**

Biodiesel could be purified using various wet washing methods, where the most popular is the liquid-liquid extraction or often called the solvent extraction technique (Veljković et al., 2015). In this method, a suitable solvent is utilized for the extraction of the desired components from the liquid source (Huang & Ramaswamy, 2013). Water washing and acidified water are used to eliminate contaminants such as glycerol and soap (Atadashi et al., 2011b; Veljković et al., 2015). The acidity, volume and temperature of the water are the key variables that improve the biodiesel purification (Stojković et al., 2014). The volumetric mass transfer coefficient increases with the volume of water, allowing for more diffusion of glycerol from the biodiesel into the water phase. Therefore, the

enhancement of the mass transfer coefficient of glycerol improves the purification process (Atadashi et al., 2011b; Muniyappa et al., 1996). Additionally, the solubility of water in biodiesel is enhanced as the temperatures increase, which leads to a large water content in the final biodiesel (Stojković et al., 2014). It appears that water cleaning is ineffective for the elimination of calcium oxide. Additionally, stirring during the water washing process enhances the mass transfer phenomena, but it also leads to emulsion formation and loss of yield (Atadashi et al., 2011b). The water consumption in the water washing step is the major concern in the biodiesel purification process. It is estimated that 3-4 liters of water are needed for the purification of 1 liter of biodiesel, which incurs expenses in the purification step, owing to the substantial volume of the wastewater released (Veljković et al., 2015). Moreover, the presence of water in biodiesel could promote corrosion of the steel parts of the fuel system in the engine. Rust or ferric oxide (Fe_2O_3) is the most common product of corrosion, but the release of the corrosive acid upon the oxidation of water also damages the storage tanks.

It is important to note that the purity of the source of oil and the reaction circumstances such as the presence of a catalyst and methanol concentration determines the amount of water needed in the purification of biodiesel (Saifuddin & Chua, 2004). Huge efforts have been devoted to finding better purification procedures or suitable solvents to solve problems of high water usage. To recycle the water stream, Jaber et al. (Jaber et al., 2015) presented an innovative purification technique that focuses on the recycling of effluent through microfiltration and AC as the adsorbent. Such a procedure could reduce the water usage by 15% overall (Jaber et al., 2015).

- **Organic Solvents**

Organic solvents are also utilized in solvent extraction or liquid-liquid extraction methods for biodiesel purification. Organic solvents such as n-hexane and petroleum ether are used in biodiesel purification. In this technique, biodiesel is dissolved in organic solvents prior

to the additional purification steps (Atadashi et al., 2011b; Karaosmanoğlu et al., 1996). After this method, biodiesel is usually washed with water to eliminate the remnants of soap or catalysts. Ma et al. (1998) used petroleum ether to wash the methyl ester and acetic acid to neutralize the alkali. The utilization of acetic acid limits the use of water in the washing methods and prevents emulsion formation. Karaosmanoğlu et al. (1996) reported that crude biodiesel could be refined using petroleum ether. This method was applied following the decantation of biodiesel and glycerol. The solid catalyst was separated from the reaction vessel while the methanol was removed using a rotary evaporator. Petroleum ether and water were introduced into the separating funnel after the addition of the biodiesel, while the pH of the solution was adjusted using acetic acid (Karaosmanoğlu et al., 1996). After three times washing with water, the final biodiesel was separated by heating overnight with Na_2SO_4 to remove the remaining impurities (Karaosmanoğlu et al., 1996).

Wange et al. (2007) used petroleum ether to purify fatty acid methyl ester (FAME) and washed it with hot water until the pH of the wash became neutral. N-hexane was also utilized for biodiesel separation at room temperature with a ratio of 1:1. The final mixture was 93 wt.% after washing three times with water (Wang et al., 2007). Furthermore, Soriano Jr et al. (Soriano Jr et al., 2009) used tetrahydrofuran as a co-solvent with methanol for the transesterification process. The tetrahydrofuran and alcohol were removed after the transesterification process by distillation under vacuum, followed by cleaning using petroleum ether. The tetrahydrofuran used in the heterogeneous system eliminates the mass transfer effects (Soriano Jr et al., 2009).

- **Ionic Liquids and Deep Eutectic Solvents**

IL have gathered increasing attention as environmentally friendly solvents as they are recyclable, non-volatile and non-flammable. This makes them a good and safer choice for

the extraction processes. Ionic liquids have a wide range of applications due to their ability to dissolve a wide variety of inorganic, organic and organometallic compounds; however, their high cost places obstacles for large scale applications (Shahbaz et al., 2010).

DESs are similar to ionic liquids. DESs are prospective solvents for biodiesel separations as they are easy to prepare, lower cost, with favorable solvent properties such as biodegradability, non-toxicity and inertness to water (Shahbaz et al., 2010, 2011a). The physicochemical attributes of DESs such as adjustable freezing points, enhanced viscosity, improved solvation capacity, heightened thermal stability, and elevated freezing points are suitable for industrial applications (Hayyan et al., 2021). The formation of DESs involves the mixing of hydrogen bond acceptors (HBAs) like ammonium or phosphonium salts with hydrogen bond donors (HBDs) such as urea and ethylene glycol (Hayyan et al., 2013; Juneidi et al., 2015) Furthermore, the prepared DESs exhibit notable eutectic advantages such as the formation of a stable product mixture and robust network of hydrogen bonds, thereby contributing to their intrinsic stability (Yadav & Pandey, 2014).

Abbott et al. (2007) reported some promising results on the ability of DES-based glycerol and quaternary ammonium salts to eliminate free glycerol from biodiesel. The impact of DES molar ratio and duration to reach equilibrium, as well as the recyclability, were examined. The results showed that 1:1 DES molar ratio was the best for the elimination of free glycerol from biodiesel (Abbott et al., 2007). A recrystallization process was used to recycle choline chloride at 1:2 DES molar ratio (Abbott et al., 2007). Hayyan et al. (Hayyan et al., 2010) prepared several DESs from choline chloride and methyltriphenylphosphonium bromide salts and used them as solvents to remove remnants of KOH in biodiesel. Figure 2.3 shows the schematic diagram for biodiesel purification using DES.

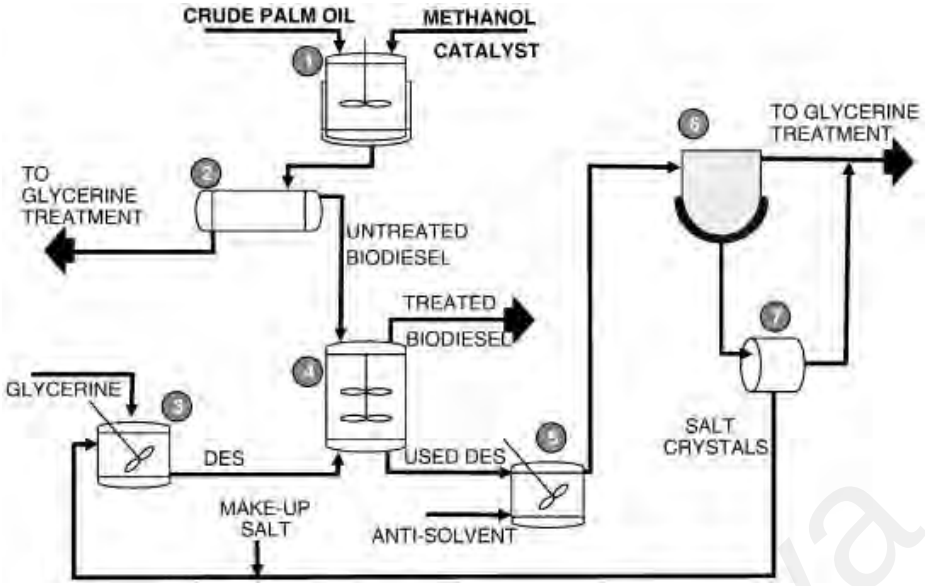

Figure 2.3: Schematic diagram of an integrated process for the production and purification of biodiesel using DES (Hayyan et al., 2010).

Shahbaz et al. (2010) used choline chloride, 2,2,2-trifluoroacetamide, and ether ethylene glycol to prepare two series of DES, which were used for biodiesel purification. Glycerol was effectively removed from palm oil-based biodiesel using DES/biodiesel ratios of 2.5:1 and 3:1, where ChCl/ethylene glycol (molar ratio 1:2.5) and ChCl/2,2,2-trifluracetamide (molar ratio 1:1.75) were used as the DES, respectively (Shahbaz et al., 2010). Shahbaz et al. (2011a) found that glycerol, mono-glycerides, diglycerides, and KOH from the biodiesel could be efficiently removed using the DES prepared from methyl triphenyl phosphonium bromide and ethylene glycol (Shahbaz et al., 2011a). Ba˘ci´et al. (2021) used choline chloride-based DES as the reaction media in an integrated process of biodiesel production and purification. In this study, the transesterification of oil, catalyzed by an enzyme, with concurrent glycerin removal from the reaction was optimized. The optimum conditions such as DES molar ratio, water content, phases mass ratio were evaluated. The results showed that higher biodiesel yield (43.54%) and higher removal efficiency of glycerol (less than 0.0019%) were achieved at the following conditions: 1:3.5 DES molar ratio, 6.6% water content and phases mass ratio of 1:1. The

integration system using a micro-extractor is a good choice for future simultaneous production and refinery of biodiesel (Bačić et al., 2021).

Hayyan et al. (2022) investigate ten types of ionic liquids for the esterification of FFA in acidic crude oil as shown in Figure 2.4. The FFA content was efficiently decreased to less than 1% when using 1-butyl-3-methylimidazolium hydrogen sulfate as the catalyst for the pre-treatment of acidic crude palm oil (Hayyan et al., 2022). The results showed that 1 wt.% of [BMIM][HSO4] could lower the FFA concentration from 10.77% to 1.87%, indicating that the Ils is a strong active catalyst for the treatment of highly acidic crude palm oil (ACPO) (Hayyan et al., 2022).

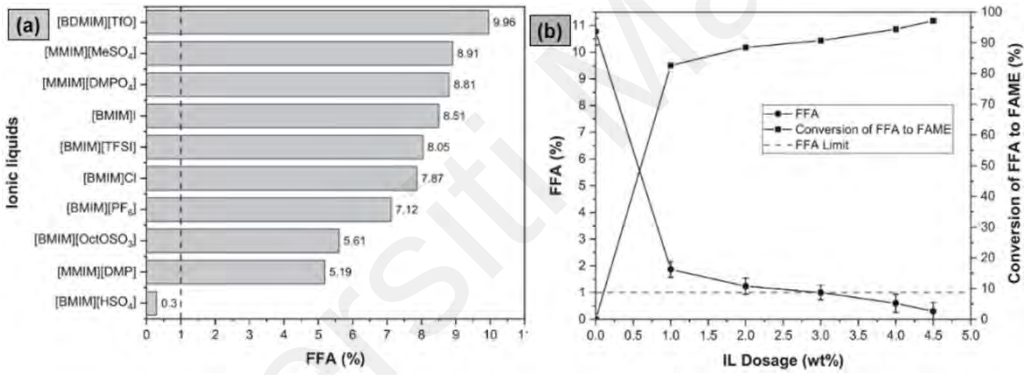

Figure 2.4: Ability of different IL to reduce the FFA concentration and (b) The impact of IL dosage on both FFA concentration elimination and FAME conversion (Hayyan et al., 2022).

2.3.1.3. Supercritical extraction technique

The term supercritical fluid extraction utilizes the mass transfer that takes place at operating conditions above the solvent's critical point. The supercritical CO_2 is the preferred solvent in biomass processing due to its low environmental impact (Mantell et al., 2013; Steytler, 1996). Wei et al. (2014) employed supercritical CO_2 for biodiesel separation. Figure 2.5 shows the schematic diagram of the supercritical extraction

technique. The yield of biodiesel separation was 99.94 % at 40 °C and 30 Mpa, with 7 ml/min of CO_2 and a 90-min reaction time (Wei et al., 2014).

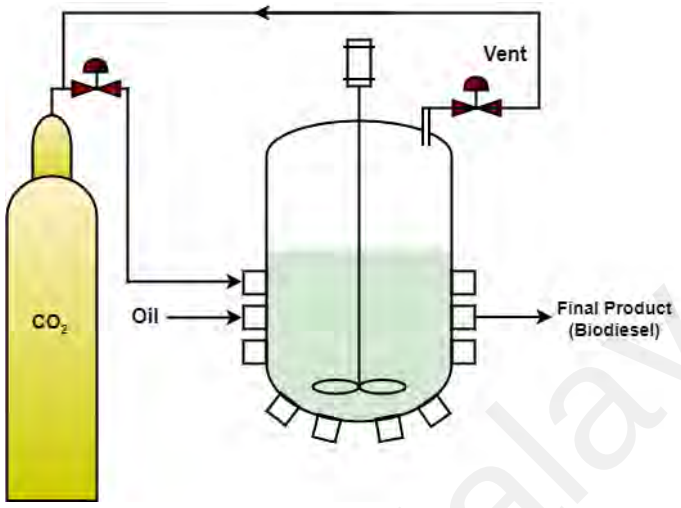

Figure 2.5: Supercritical extraction technique

Demirbas (2002) studied the supercritical methanol technique for biodiesel production and refinery. The supercritical method was carried out in a stainless steel tubular autoclave, where the temperature and pressure were continuously tracked to 850 K and 100 Mpa, respectively. The autoclave is normally filled with a certain volume of oil and liquid methanol in various molar ratios during a run. Following every experiment, the gas is ventilated and the product is transferred into the storage tank for further analysis (Demirbas, 2005). Supercritical methanol technology is less energy-intensive, non-catalytic, has a shorter reaction duration, is environmentally friendly, and produces a simpler purification technique for the product (Demirbas, 2005; Demirbaş, 2002).

Kusdia and Saka (2004) used a supercritical methanol approach for biodiesel production and treatment. This approach involves the processing of vegetable oil, especially water in an oil mixture and supercritical methanol in the absence of the catalyst. Triglyceride transesterification and hydrolysis, and methyl esterification of fatty acids take place simultaneously under these circumstances. A significant quantity of methyl esters

appropriate for the synthesis of biodiesel is produced as the outcome of this process (Kusdiana & Saka, 2004). This eco-friendly process allows the facile preparation of biodiesel from crude vegetable oil and its byproducts, especially when working with feedstocks that include water (Kusdiana & Saka, 2004). The catalytic supercritical methanol transesterification is performed at 520 K in an autoclave with a catalyst mixture of 1%–5% NaOH, CaO, and MgO. The conversion increases to 60–90% within the first minute of the catalytic supercritical methanol transesterification process (Demirbas, 2009). The soap production was decreased in the transesterification reaction of rapeseed crude oil with supercritical/subcritical methanol with the addition of a comparatively small amount (1%) of NaOH (Wang et al., 2007).

Madras et al. (2004) reported the esterification of vegetable oil using a supercritical mixture of alcohols (methanol and ethanol) at 200-400 °C and 200 bar. Additionally, the biodiesel was produced enzymatically using the supercritical CO_2. The results showed that only 30% of the conversions were achieved in the enzyme-catalyzed reactions in supercritical carbon dioxide, whereas practically 100% of the conversions were achieved using supercritical methanol and ethanol (Madras et al., 2004).

2.3.2. Affinity-Based Separation Techniques

Affinity-based separation techniques refer to processes that utilize adsorbents and resins for ion exchange in biodiesel purification. These techniques are also known as “dry washing techniques.” In these methods, suitable adsorbents are utilized to selectively remove contaminants from the liquid phase by binding them to their surface (Atadashi et al., 2015; Huang & Ramaswamy, 2013). Affinity-based separation techniques have various benefits over wet washing techniques, among them are decreased purification time, small and simple unit structures, with the absence of water hence no wastewater formation (Atadashi et al., 2011b). The following sections will provide a brief overview of the most widely prevalent affinity-based separation processes in biodiesel purification.

2.3.2.1. Adsorption Process

The Adsorption techniques refer to the binding of adsorbates from a fluid to a solid surface, or known as the adsorbent (Wall et al., 2011). The adsorption technique has shown great promise for the purification of biodiesel due to the low cost, ease of design and operation, and adsorbent selectivity (de Castro Vasques et al., 2013). Adsorption and absorption are not interchangeable, yet the term "sorption" applies to both techniques. During adsorption, the adsorbates are adhered to the surface of the adsorbent (Venkatesan, 2013). Adsorption methods for the purification of biodiesel can be categorized based on the type of absorbents used. Silica-based absorbents such as Magnesol, bio-based absorbents such as cellulosic substrates and carbon-based adsorbents are among the most common adsorbents for these techniques. These absorbents have great attraction for polar contaminants such as glycerol, glycerides, methanol, pigments, alkali metals, and soap (Atadashi, 2015). High-quality biodiesel could be produced by using adsorption techniques, and since it is water-free it meets the ASTM D6751's requirement of less than 500 ppm water content (Atadashi, 2015). Nevertheless, the biodiesel's water concentration is typically higher than 1000 parts per million during water washing, making its removal challenging, expensive, and longer time consumption (Atadashi, Aroua, Aziz, et al., 2011b). Figure 2.6 presents the schematic diagram of the adsorption purification technique for contaminations from crude biodiesel.

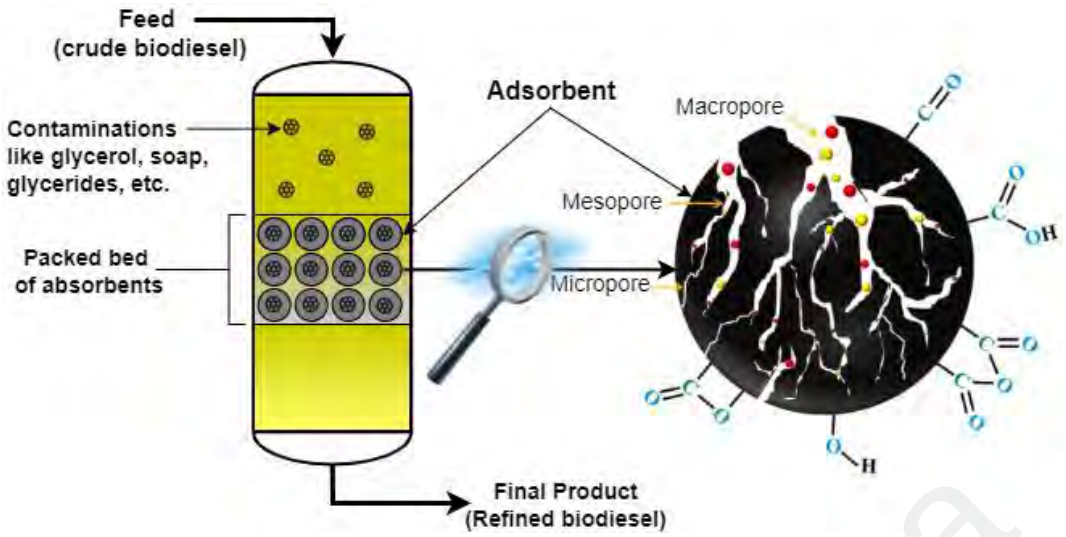

Figure 2.6: Schematic diagram of the adsorption purification technique for contaminants from crude biodiesel.

Berrios and Skelton (2008) experimented the use of magnesol at different amounts in a batch reactor at 60 °C with a sample equipped with an adjustable speed mixer and submerged in a water bath. The Büchner funnel and water extractor were used in vacuum conditions for the separation of the final sample. Additionally, the immediate product was eliminated by centrifugation. Biodiesel with the presence of 0.03% glycerol and 0.51% methanol were present as the contaminants in the final product (Berrios & Skelton, 2008). Nevertheless, the primary constraint on the application of magnesol is the paucity of knowledge regarding this procedure, its catalytic effectiveness, and the nuances of its efficacy (Atadashi et al., 2011b). Table 2.3 presents the most common absorbents and applications for the removal of impurities for biodiesel purification.

Bertman et al. (2009) examined the use of magnesol to neutralize contaminants such as soap in crude biodiesel, which is a result of alkali catalysis. The purification of biodiesel with magnesol requires 1.5-3 wt.% of biodiesel followed by mixing, then filtration by a 5 μm cloth filter, and finally the biodiesel is passed through a 0.45 or 0.55 μm filter. The magnesol-based biodiesel treatment was in agreement with the ASTM D6751 and EN14214 specifications (Bertram et al., 2009). Faccini et al. (Faccini et al., 2011)

investigated the purification of biodiesel using silica and magnesol. The results showed the effective performance of the absorbents (2% silica and 1% magnesol), the outcomes are 61 ppm soap, 0.17 $mgKOHg^{-1}$ for acid number, 500 mg/kg of water, 0.03% of glycerol and 0.22% of methanol. The glycerol content was greater than the minimal limit of ASTM D6751 specifications (Faccini et al., 2011).

Table 2.3: Most common adsorbent materials and contaminants are presented in adsorption techniques for biodiesel purification.

Adsorption Technique	Targeted Impurity	Experimental conditions	Key findings/ remarks/ observations	References
Silica-based absorbents	Free glycerol, methanol, and monoglycerides	-60 Å mesoporous of adsorbent silica, 0.5-3.0 g of silica was added to biodiesel and was stirred for at 2h room temperature.	-The Langmuir adsorption constant and the saturation capacity constants were found to be equal to 2.22 cm^3/µmol and 0.239 g/g, respectively.	Mazzieri et al., 2008
	Glycerol	-Fixed silica beds (sg=280 m^2 /g crushed and sieved to 10-40 meshes), glycerol feed (0.1-0.25%) and velocities (5-10 cm/min),	-Reduced the glycerol lower than ASTM specification, saturation capacity: 0.13-0.15 g glycerol/g silica, and Processing capacity was 0.01-0.02 m^3 biodiesel /kg silica	Yori et al., 2007

Adsorption Technique	Targeted Impurity	Experimental conditions	Key findings/ remarks/ observations	References
	Trace acids and glycerides.	-Non-catalytic one-step reaction with adsorption, 280°C temperature, methanol: ratios of 15-20, waterless	-Silica gel was effective at removing trace acids and glycerides.	Manuale et al., 2011
	FFAs, glycerol, soap	-HCl: sodium silicate ratio 3:1, drying time 2hr, temperature of 70 ºC and 150 ºC, 3% silica aerogel (surface area of 371 m2/g and average pore size of 3.75 nm).	-Glycerol content reduced from 4% to 0.1%. Second-order pseudo model with k = 0.0036 g/mg min.	Silviana et al., 2021

Adsorption Technique	Targeted Impurity	Experimental conditions	Key findings/ remarks/ observations	References
	Calcium soap and leached calcium	-Silica as adsorbent under vacuum (0.2 bar) and mild temperature (65–90 °C).	-Removal of unreacted oil species, glycerol, and calcium soap from biodiesel.	Catarino et al., 2020
	Water	-Silica gel desiccant in fuel tanks with varying biodiesel concentrations.	-Reduction of biodiesel degradation rate and bacterial growth.	Azhad & Fathallah, 2023
	Methanol and glycerol	-0.75% (w/w) magnesium silicate particles, 60 °C, 10 min of reaction.	-magnesium silicate removed glycerol to specification levels.	Berrios & Skelton, 2008
	FFAs	-Silica gel (surface area 2319 m^2/g), sieved to 106-212 μm diameter particles. -Temperature: 25°C, time: 30 min mixing at 10% FAME concentration and 4 g adsorbent dosage.	-The maximum FFA adsorption capacity was not reached, so the full saturation capacities were not determined. -Reduced FFAs from 1.96% to 1.19%.	Özgül-Yücel & Türkay, 2003
	Steryl glucosides and glycerides	-Magnesium silicate and bleaching earth as adsorbents. -Adsorbent levels (<1 wt%), duration 5-10 min, and temperature 70-75°C.	-Magnesium silicate reduced Steryl glucosides to ~20 mg/kg, while bleaching earth only reached ~50 mg/kg. -Removed some mono-, di-, and triglycerides.	Na-Ranong et al., 2015

Adsorption Technique	Targeted Impurity	Experimental conditions	Key findings/ remarks/ observations	References
	Moisture content and total glycerol	-Treatments using different adsorbents, such as natural silicate, diatomaceous earth, neutral bleaching earth, and acid-activated. Using 5 wt.% of absorbent, 10 min and 25°C.	-Moisture content and total glycerol content were both dramatically reduced.	Plata et al., 2015
	Methanol, glycerol and other impurities	-Olive cake as a bioadsorbent, 2% adsorbent with a particle size of ≤ 900 μm at 40 min contact time.	99.7% of the free glycerol and 29.8% of the FFA was removed. Soap and Catalyst= 0 ppm Free glycerol= 0 mg/kg Acid value=0.23 mg KOH/g Peroxide value= 29.0 meq/Kg. Iodine value= 19.6 g I_2/100g Saponification value= 151 mg KOH/g.	Alnaief et al., 2020
	FFAs and glycerides	-Silica gel and diatomaceous earth used as adsorbents were stirred with biodiesel at 90 °C in a vacuum (0.21 bar) for 90 min.	-Elimination of FFAs and glycerides from biodiesel and compliance with EN 14214. -FFA adsorption capacity was 140% for Silica gel and 10% for diatomaceous earth.	Manuale et al., 2011

Adsorption Technique	Targeted Impurity	Experimental conditions	Key findings/ remarks/ observations	References
	Soap, methanol, glycerol, glycerides, and content	-Batch reactor with 100 mL sample size, magnesium silicate and bentonites as adsorbents, 15-minute contact time, room temperature, three adsorbent concentrations (0.50%, 0.75%, and 1.00% wt.), and varying agitation speeds (200, 400, and 600 rpm), centrifugation at 4000 rpm for 10 minutes.	-purification method effectively removed methanol, soap, and glycerol, while none influenced glyceride content, and they were as follows: Soap content= 2.639×10^{-4} g soap/g oil (4.4×10^{-4} initial) Water content= 741 mg/kg (771 initial). Methanol content= 0.27 wt.% (15.16 initial) Free glycerol content =0.008 wt.% (0.01 initial) Triglyceride content= 0.05 wt.% (0.04 initial) Diglyceride content= 0.43 wt.% (0.35 initial) Monoglyceride content =0.51wt.% (0.5 initial)	Berrios et al., 2011

Adsorption Technique	Targeted Impurity	Experimental conditions	Key findings/ remarks/ observations	References
	Contaminations in biodiesel like acid value, metals, soap, water, methanol, glycerol, glycerides.	-Biodiesel was heated and stirred until reaching 65 °C. At this point, 1% or 2% (m/m) of each adsorbent related to the weight of biodiesel, was presented, mixing for 20 min and 65 °C. Th absorbents include: silica, Magnesol®, Purolite PD 206® and Amberlite BD10 DRY®).	-The main results found for Magnesol® 1% and silica 2% were values below 0.17 mg KOH/g for acid number, 1 mg/kg of K, 61 ppm of soap, 500 mg/kg of water, 0.22% of methanol and 0.03% of free glycerol	Faccini et al., 2011
Activated carbon-based absorbents	FFAs	-Rice hull ash (surface area 5.9 m^2/g), sieved to 106-212 μm diameter particles. Temperature: 25°C, time: 30 min mixing at 10% FAME concentration and 4 g adsorbent dosage.	-The maximum FFA adsorption capacity was not reached, so the full saturation capacities were not determined. FFAs reduced from 2.06% to 1.67%.	Özgül-Yücel & Türkay, 2003
	flash point, pour point, acid value, higher heating value, and refractive index	Activated carbon (AC) and surface-modified AC with the following iodine number: $AC_{Authentic}$ (iodine number =1,123 mg I_2/g AC) AC_{H2SO4} (iodine number =897.3 mg I_2/g AC) AC_{HCl} (iodine number =590 mg I_2/g AC) A column with AC bed at a rate of 15 drop/min.	-The properties of biodiesel were within the ASTM specifications.	Fadhil & Dheyab, 2015
	glycerin and glycerides, catalyst, water content, and alcohol	50 gm of biodiesel in batch mode under heating at 65 °C and stirring. 4% of rice husk ash (RHA), in the same magnitude of acid solution and Magnesol® 1%, and time of purification was 20 min.	-An efficient removal of glycerine and glycerides, catalyst and water content and alcohol were obtained with the use of RHA.	Manique et al., 2012

Adsorption Technique	Targeted Impurity	Experimental conditions	Key findings/ remarks/ observations	References
	FFAs and glycerides	-AC and Impregnated AC as adsorbents Refining time: 200 and 720 min and adsorbed dosage = 5 g/100g	-Elimination of FFAs and glycerides from biodiesel and compliance with EN 14214. FFA adsorption capacity as follows: AC= 4.6% (200 min). AC= 6% (720 min). Impregnated AC= 4% (200 min). Impregnated AC= 5% (720 min).	Manuale et al., 2011
	Glycerol, monoglycerides, and diglycerides	-AC and modified AC by HNO3 as absorbent with a surface area of 945.93 and 848.50 m^2/g, respectively. 20 mL of biodiesel solution was placed into a 125 mL conical flask with 0.300 g of adsorbent at 30◦C for 24 h and a constant speed of 150 rpm.	-AC had a low adsorption capacity for glycerol, while modified AC increased the adsorption capacity from 53% to 86%, and after 30 h the glycerol content in biodiesel was 0.02 wt.%. -The pseudo-first-order kinetic model fit well with monoglycerides, whereas the pseudo-second-order model was more suitable for glycerol and diglycerides.	Castro Vasques et al., 2013

Adsorption Technique	Targeted Impurity	Experimental conditions	Key findings/ remarks/ observations	References
Bio-based absorbents	Free glycerin, combined alkalinity, acidity index, and turbidity	-Adsorbents Average pore diameter: Select 450®= 10.2971 nm cellulose= 7.0601 nm corn starch= 7.0758 nm potato starch= 7.0037 nm cassava starch= 7.6795 nm rice starch= 7.2950 nm, adding 1%, 2%, 5%, and 10% (w/v) of adsorbents to the biodiesel, and constant stirring of 150 rpm for 10 min at 25°C.	-All adsorbents presented good efficiency in the impurities removal and showed similar behaviour independent of the kind or amount of adsorbent employed.	Gomes et al., 2015
	Methanol, free glycerol, water content, and metals ($Na+$, $K+$, Ca_2+, and Mg_2+)	-Eucalyptus pulp as absorbent, optimal condition:1.0 g of cellulose in a column of 1.3 cm in diameter under pressure of 18 psi.	- Methanol, free glycerol, and water content in the permeate were 0.268 ± 0.009, 0.0081 ± 0.0001% w/w and 636 mg/kg, respectively.	Squissato et al., 2015
	FFA, peroxides value, moisture, bulk density, cloud point, flash point, free and total glycerin, and color.	-Mixing 100 g of biodiesel with 10 g of activated earth in a 250-mL amber bottle, heated to 30 C, and stirred at 21.959 xg for 60 min. The purified biodiesel was removed from the activated earth by centrifuging at 15,3009 xg for 20 min at 4 C.	-The product met the ASTM and D6751 specifications for moisture, bulk density, cloud point, flash point, FFAs, free and total glycerin, Na, P, and S.	Solval & Sathivel, 2012

Adsorption Technique	Targeted Impurity	Experimental conditions	Key findings/ remarks/ observations	References
	Purification of biodiesel from waste cooking oil, like glycerol and water content	-Sawdust, coconut fiber, nutshell, rice husk, and water hyacinth fiber were used as bio adsorbents; these were compared with commercial adsorbents (Amberlite BD10DRY and Magnesol).	-Sawdust reduced the acid value and free glycerol by 31.3% and 54.8%, respectively, and was more effective than Amberlite BD10DRY. The water content after sawdust filtration was superior to Magnesol and equivalent to Amberlite BD10DRY.	Manique et al., 2012
	Glycerol, and water content	-Sugarcane bagasse as an adsorbent. Adsorbent loading was from 0.1 to 3 wt% and stirred at 120 rpm at 30 ◦C for 2 hr.	3 wt.% of sugarcane bagasse adsorbents were able to remove 40% of glycerin from crude biodiesel, thus yielding 87% with less than 0.02 wt.% of glycerin. Increased the water content, this increase is associated with adsorption of water from the atmosphere.	Alves et al., 2016; Yori et al., 2007

2.3.2.2. Ion Exchange

Purification of biodiesel using ion-exchange resin is an industrial method similar to adsorption (Berrios et al., 2011; Berrios & Skelton, 2008). Ion exchange falls within the category of electrostatic adsorption. Ion exchange is a process where the ions are transferred from a solution to the exchanger due to the electrostatic attraction between the individual ions of a given species and the surface functional groups (Berrios et al., 2013). Ion exchangers are composed of a matrix with charged groups on the surface (Berrios et al., 2013). Ion exchange resins are one of the most widely used types of ion exchange material. The structure of the material affects its ion-exchange capacity. They are usually produced by surface functionalization of styrene and divinylbenzene polymer mixture which is the main constituent of the exchanger material. These ion exchangers possess acidic and alkaline binding sites and thus have great affinity towards polar impurities like alcohol, glycerol, glycerides, alkali metals, and soap. This method is followed by the utilization of a filter to make the method more efficient and effective. Figure 2.7 presents the purification technique steps of biodiesel with an ion-exchange resin. Impurities in biodiesel such as glycerol and FFA can be effectively extracted via the ion-exchange procedure (Berrios & Skelton, 2008). In addition, the ion-exchange resin was employed to purify spent cooking oil into biodiesel. The use of an ion exchanger in dry washing step offers many benefits due to the high affinity towards polar impurities in biodiesel, without the need for water washing, has high efficiency and facile compared to wet washing, could be adapted to a variety of industrial setups, low cost, minimal impact on the environment, and with the possibility of recycling of the waste product (Atadashi, Aroua, Aziz, et al., 2011b).

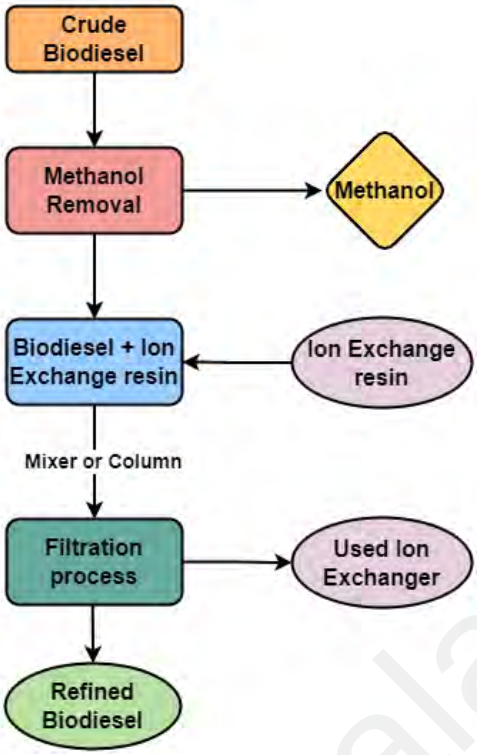

Figure 2.7: Schematic diagram of ion exchange technique steps for biodiesel purification.

Berrios and Skelton (2008) investigated the performance of an ion exchange resin for the purification of biodiesel. The biodiesel was pumped into the column embedded by ion exchange resin at a controlled flow rate. The results showed that PD10 and PD206 resins could not extract the methanol, whereas they successfully eliminated the soap and reduced the glycerol content to 0.01 wt.% while the methanol concentration was 1.14% which significantly exceeded the EN14214 specifications (Berrios & Skelton, 2008).

The used cooking oil biodiesel could be purified by utilizing an ion-exchange resin (Lewatit® GF202). The removal efficiency of glycerol, methanol, and soap are 20%, 98.8%, and 52.2%, respectively. Lewatit® GF202 offers the benefit of being renewable, in contrast to the non-renewability of other resins (Berrios et al., 2011). Furthermore, the resins of ion exchange offer cost-effective solutions for the elimination of water and glycerol, as well as soaps, salts, and catalyst residues. Table 2.4 presents the ion exchange resins and conditions that are commonly utilized in the adsorption techniques for the purification of biodiesel.

Table 2.4: Most common ion exchange resin that is presented in adsorption techniques for biodiesel purification.

Adsorption Technique	Targeted Impurity	Experimental conditions	Key findings/ remarks/ observations	References
Ion Exchange	Soap, methanol, glycerol, and glyceride content	- Lewatit® GF 202 was used as Ion exchange resin. biodiesel passes through a resin column (1.5 cm diameter). The flow was 1.5–2 BV/h (BV: bed volumes) and space velocity at 2.01 1/h at 22°C. The fresh ion exchange resin (Lewatit® GF202) was first preconditioned by washing with 3–4 BV of methanol at 2 BV h^{-1} for drying.	-The results show that the purification method effectively removed soap, methanol, and glycerol, while none influenced glyceride content, and they were as follows: Soap content= $3.25x10^{-4}$ g soap/g oil ($4.4x10^{-4}$ initial). Water content= 741 mg/kg (771 initial). Methanol content= 0.14 wt.% (15.16 initial). Free glycerol content=0.008 wt.% (0.01 initial). Triglyceride content= 0.03 wt.% (0.04 initial) Diglyceride content= 0.35 wt.% (0.35 initial) Monoglyceride content =0.51wt.% (0.5 initial)	Berrios et al., 2011

Adsorption Technique	Targeted Impurity	Experimental conditions	Key findings/ remarks/ observations	References
	Soap and glycerin	-T45BD, T45BDMP, PD206, DR-G8, and BD10 were used as ion exchange reasons. -Involved a glass column with packed resin beds (2.5 to 7.6 cm in diameter) and controlled flow rates.	-The soap levels reduced from 1200 ppm to below 50 ppm (at 550 BV) and glycerin levels reduced from 0.08% to below 0.02% (at 200 BV).	Wall et al., 2011
	Glycerol	-Sulfonated polystyrene-divinylbenzene resins (1180H and1180Na) as adsorbents. biodiesel /glycerol solution was placed into a 100 mL flask, then dry resins (0.15 g) were added followed by shaking at 200 rpm for 8 hr at 303 K.	-Sulfonic groups significantly influenced glycerol uptake from BD. 1180H had a greater affinity for glycerol in the temperature range of 303−323 K compared to 1180Na. 1180H: Non-ideal, physical, and endothermic, while1180Na: Exothermic and both spontaneous with increased randomness	Chen, Wang, Ma, et al., 2012
	Glycerol	-Amberlite XAD1180 as adsorbent. -The experiment involved introducing dry 1180Na (exchange capacity of 3.7 mmol g−1) into 100 mL conical flasks containing a 50 g biodiesel /glycerol (glycerol content= 0.44 mg/g, and water content= 861 ppm). The sample was conducted in an orbital shaker at 200 rpm for 20 hours.	-Glycerol content was reduced through effective adsorption, and the process was completed successfully in 8 hours at 303 K.	Chen et al., 2012

Adsorption Technique	Targeted Impurity	Experimental conditions	Key findings/ remarks/ observations	References
	Glycerol	-The experimental involved washing tilizings resins with acid and base solutions, obtaining specific resin types (H-type and OH-type), adding 0.10 g of these resins to biodiesel /glycerol solutions, and shaking them at 30 °C for 24 hr.	-Excellent adsorption properties observed. Maximum adsorption capacity up to 439.31 mg/g dry resin. -Strongly basic anion exchange resins showed better glycerol adsorption.	Li et al., 2018
	Calcium oxide, glycerol, and glyceride	- Biodiesel passing through a column packed with Cation-exchange resin (15DRY, IRC76, 31WET, 200CTNA) as adsorbent. 0.5 g of resins was stirred into 25 ml of biodiesel (80 vol%)–methanol (20 vol%) mixture in a glass vessel for 1 h.	-The removal using 15DRY in the presence (20%) and absence of methanol, as follows: Free glycerol content (wt.%) = <0.01 and 0.12 (20%methanol) Triglyceride content (wt.%) = 0.2 and 0.1 (20%methanol) Diglyceride content (wt.%) = 0.1 and 0.2 (20%methanol) Monoglyceride content (wt.%) = 0.8 and 0.9 (20%methanol)	

Adsorption Technique	Targeted Impurity	Experimental conditions	Key findings/ remarks/ observations	References
	FFAs, water, glycerol, and dark brown pigment	600 g of resin packed in the expanded-bed reactor (inner diameter of 5.0 cm and length of 50 cm) with an anion-exchange resin (PA306S), at 50°C. Mixed waste cooking oil and methanol (3.5:1 or 3:1 molar ratio) were supplied to the column at a constant flow rate of 120 cm^3/h.	The impurities like FFA, water, glycerol, and dark brown pigment, were removed from the product by the adsorption on the resin. In addition, the product met the EN14214 and ASTM D6751 specifications.	Shibasaki-Kitakawa et al., 2011
	Contaminations in biodiesel	-The process involved loading 1.2 kg of cation-exchange resin (PK208LH) into the first column (i.d., ϕ 5.0 cm × 100 cm) and 1.1 kg of anion-exchange resin (PA306S) into the second and third columns (i.d., ϕ 5.0 cm × 50 cm). A 1:11 molar ratio of oil and methanol feed mixture was supplied to the column at 50°C	-The effluent fully met the international biodiesel standard specifications without any downstream purification processes except for removing methanol.	Shibasaki-Kitakawa et al., 2013
	Contaminations in biodiesel like acid value, metals, soap water, glycerol, glycerides, and methanol.	- Biodiesel was heated and stirred slowly until reaching 65 °C. At this point, 1% or 2% (m/m) of each adsorbent (Magnesol®, silica, Amberlite BD10 DRY® and Purolite PD 206®), related to the mass of biodiesel, was added and maintained at 65 °C and stirring for 20 min.	-The results obtained using inorganic matrices (Magnesol® and silica) showed better adsorption properties than using organic resins (BD10 DRY® and Purolite PD 206®).	Faccini et al., 2011

Adsorption Technique	Targeted Impurity	Experimental conditions	Key findings/ remarks/ observations	References
	Contaminations in biodiesel like acid value, iodine number, and water content.	-Cation-exchange resin was used, and biodiesel was treated with 2–40 wt.% (to biodiesel mass) of resin at 500 rpm, for 1 h at room temperature. Regarding the ceramic membrane (0.1 μm) system, 250 mL of crude biodiesel was poured into a feed vessel and cross-filtered once by the membrane ceramic tube using a peristaltic pump at 6.25 L h^{-1}.	-The 0.1 μm ceramic membrane was more effective than the cation-exchange resin, but it was not possible to obtain a good quality product using both methods.	Dias et al., 2014
	Contaminations in biodiesel like acid value, iodine number, water content, and metals (Na + K).	- Biodiesel was passed through a column (5 cm in diameter and 30 cm in length) packed with a 15 cm length of ion-exchange R (Lewatit GF 202) that retained the impurities (water, ions of K, and glycerol), at a mean flow rate of 2 bed volumes/h (or about 236 cm3/h). The R beads are uniform, 0.65 mm in diameter, with a density of 1.24 g/mL and a bulk density of 0.740 g/mL.	-Results also show that the resin purification reduced biodiesel acidity and kinematic viscosity, while did not comply with the standard limit for the metals (Na + K).	Mata et al., 2011
	Contaminations in biodiesel like fatty acid value, iodine number, and water content.	-Biodiesel passed through the ion-exchange resins (Purolite-PD 206) at room temperature, and biodiesel corresponding to one and a half times the amount of resin was passed through the ion-exchange resins at 1 h.	-Biodiesel produced from waste frying oil with an FFA value of 4.6% using two-step acid-base reactions and purification by Purolite-PD 206 met the requirements of EN 14214.	Sabudak & Yildiz, 2010

Adsorption Technique	Targeted Impurity	Experimental conditions	Key findings/ remarks/ observations	References
	Contaminations in biodiesel FFA and glycerides.	-The process involved loading cation-exchange resin (PK208LH) into the first column (i.d. 10 cm, length 100 cm) and anion-exchange resin (PA306S) into the second column (i.d. 5 cm, length 50 cm), amount of resin in the range of 0.63–5.3 kg. biodiesel passed through the column at a regulated flow rate.	-A high-quality biodiesel that was obtained satisfied worldwide criteria except for oxidation stability.	Shibasaki-Kitakawa et al., 2015
	Production of high-quality biodiesel and reducing the contaminants in biodiesel	87.5 g of cation-exchange resin (NKC-9) packed in the first column (i.d. 25 mm, height 450 mm) and 80 g of anion-exchange resin (D261) into the second columns, 0.6 ml/min feed flow rate at 323 K.	-The main parameters of the product met the EN 14214 and Chinese standard of biodiesel. The free glycerol, total glycerine, water content, sulfur content, and acid values were 0.0189wt%, 0.192wt%, 0.03wt%, 0.001wt%, and 0.25 mg KOH/g, respectively.	He et al., 2015
	Sodium and chloride ions	-Amberlite 252 and Amberlite IRA-420 resins with particle sizes of 0.494 and 0.49 mm respectively, were used as absorbent. The Na+ removal was studied at a water content of 10, 30, 50, and 100 %, while the chloride removal was studied at 303, 318, and 333K.	-Amberlite 252 was a good choice to remove Na+ from glycerol/water solutions with a high salt concentration and Amberlite IRA-420 was used for chloride removal.	Carmona et al., 2009; Carmona, et al., 2009

Adsorption Technique	Targeted Impurity	Experimental conditions	Key findings/ remarks/ observations	References
	Acidity value and total glycerin	-Biodiesel reacts with methanol in the presence of 30% Amberlyst-15 resin as a catalyst in the oil bath at 80 o C.	-The process decreased the total glycerin from 0.063 to 0.005 wt.%, and the acid value from 4.07 to 3.17 mg KOH/g of biodiesel produced from soap stock.	Park et al., 2008

2.3.3. Reaction-based separation process

The common reaction-based separation techniques include techniques such as membrane bioreactors, reactive distillation and absorptive distillation techniques (Huang & Ramaswamy, 2013).

2.3.3.1. Membrane bioreactor-based purification process

Membrane bioreactors (MBR) are a promising example of integrated techniques by combining biocatalytic (enzyme, microorganism, plant/animal cell) with the separation processes. MBR can be utilized in biodiesel production and refineries. Dubé et al. (Dubé et al., 2007) designed the MBR for the removal of residual vegetable oil from fatty acid methyl esters (FAME) products after the transesterification process. The experiments were carried out in the semi-batch reactor with variations in temperatures, catalyst dosages, and feedstocks. The oil-to- biodiesel conversion was greatly enhanced by the temperature and catalyst dosage with an increase in the methanol/oil flow rate. The MBR was effective in eliminating unreacted oil from the prepared biodiesel producing high-quality biodiesel (Dubé et al., 2007). The concentration of the catalyst (Baroutian et al., 2011; Tremblay et al., 2008), the optimal conversion time (Cao et al., 2008a, 2008b) and the alcohol-to-oil ratio (Cao et al., 2008a, 2008b) were investigated to improve the inorganic membrane in the bioreactor technology. It is essential to maximize the conversion efficiency in order to reduce the accumulation of unreacted oil in the bioreactor (Baroutian et al., 2011; Tremblay et al., 2008).

Tremblay et al. (Tremblay et al., 2008) tested the loading of sodium hydroxide into the TiO_2 membrane in the methanol-oil system. After 2 hours of operation time, 100% conversion was achieved with a loading of 0.03 wt.% NaOH. A loading of 0.05 wt. of the catalyst was required to shorten the residence time to an hour (Tremblay et al., 2008). However, increasing the NaOH concentration (up to 1 wt.%) had a positive impact on the

oil conversion in the bioreactor, leading to a 98.2% conversion at a load of 1 wt.% catalyst (Tremblay et al., 2008). Baroutian et al. (2011) developed a novel continuous MBR that produces high-quality biodiesel from palm oil without the need for washing or purifying procedures. Figure 2.8 shows the developed MBR for the simultaneous heterogeneous alkali transesterification process and triglyceride separation. A microporous TiO_2/Al_2O_3 membrane was packed with potassium hydroxide catalyst and supported by AC to achieve this process. The dimensions of the membrane were 0.4 m in length, 0.016 m inner diameter, 0.0254 m in outer diameter, and 0.05 μm in pore size. Three digital peristaltic pumps were utilized to establish circulation within the system and feed the raw materials. The temperature adjustments for the reaction were achieved using a coiled heat exchanger in a hot water circulator bath. The authors (Baroutian et al., 2011) examined the KOH dosage as high as 250 mg/cm^3 at 323.15 and 343.15 K in a MBR with AC as shown in Figure 10. With a dosage of 37.5 mg/cm^3, the conversion achieved a maximum of 89.3% at 343.15 K; with a subsequent increment of 143.75 mg/cm^3 which resulted in the conversions as high as 93.5% at 343.15 K. In contrast, the conversion was reduced to 91.5% at 250 mg/cm^3 as a result of the fatty acid salt production (Baroutian et al., 2011).

Tremblay et al. Falahati and Tremblay (Falahati & Tremblay, 2012) used a TiO_2 membrane for ultrafiltration with a 30 nm pore diameter for the conversion of canola oil in the MRB for 35 min at 65 °C. This study utilized NaOH dosages of 0.5% and 1.4% by weight at 338.15 K. However, with a residence duration of 35 minutes, it was unable to acquire a membrane pressure in a steady-state condition, as it suddenly increased to above 350 kPa in less than 20 minutes. The membrane pressure could be stabilized for canola oil by enhancing the residence duration to 60 minutes (Falahati & Tremblay, 2012). The authors examined a wide range of fuel sources at this minimum operation duration and determined that higher operation durations were required for certain fuel sources to set the pressure at controlled levels (80 minutes for waste cooking oil and 65 minutes for

corn oil) (Falahati & Tremblay, 2012). Cao et al. (2008a) used 11:1 to 46:1 alcohol/oil molar ratios to produce high purity FAME from different lipids. Cao et al. (Cao et al., 2008b) suggested reusing the alcohol phase to achieve a lower molar ratio (6:1). Cao et al. (Cao et al., 2008a) used a TiO_2 membrane bioreactor with a 300 kDa molecular weight limit to recycle the alcohol and biodiesel. The FAME formation was unaffected by 100% recycling (without purge) and remained between 0.0355 and 0.0423 kg/min. As a result, the researchers (Cao et al., 2008a) recommend 50% reuse for the alcohol phase to avoid bioreactor pollution (Gomes et al., 2011; Saleh, Tremblay, et al., 2010). Further studies (Cao et al., 2008a) have utilized alcohol reprocessing to obtain a 10:1 molar ratio for palm, soybean, canola oils, and colored fats. All experiments were completed at 65 °C with a loading of 0.5 wt.% NaOH. This process outperformed a batch process at the same conditions for glycerol concentration with washing of both bioreactors, conforming to the ASTM requirements (below 0.24 wt.%). Canola and soybean products could achieve this requirement without any washing.

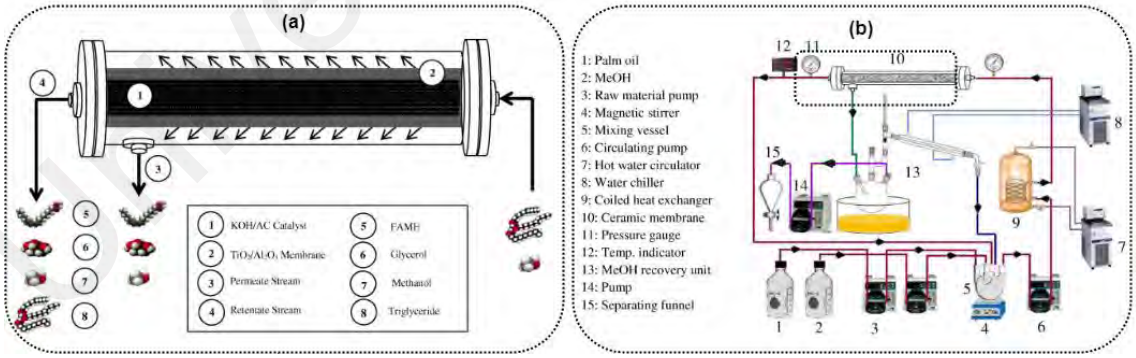

Figure 2.8: Experimental setup of MBR designed for the simultaneous production and purification of biodiesel (Baroutian et al., 2011)

2.3.3.2. Reactive distillation-based purification techniques

The reactive distillation technique combines two processes (reaction and distillation) in the same system. It is a system-driven technology that could be used to produce biodiesel (Kiss et al., 2008) and improve flash pyrolysis of the oil (Mahfud et al., 2007). Wang et al. (Wang et al., 2001) observed a 10% decrease in energy usage and a 50% enhancement in yield for the hydrolysis yield of methyl acetate via reactive distillation, matching the standard technique of a fixed-bed reactor followed by distillation. Furthermore, in the event of extremely slow reactions with extended contact times which requires huge column sizes, the reaction rate may also restrict the use of reactive distillation (Kiss, 2010; Kiss et al., 2006, 2008; Kolah et al., 2013).

Kiss et al. (2006) developed a sustainable approach for biodiesel synthesis and refinery based on the integration of catalysis by solid acid and reactive distillation. Different absorbents were utilized and investigated on their ability and stability in the fatty acid esterification with various alcohols such as methanol, ethanol and propanol, etc. Temperatures higher than 373 K were used for the process to remove water and change the equilibrium in favor of the ester synthesis. Reactive distillation was designed using a combination of detailed models and experimental data. The primary finding was the identification of sulfated zirconia as a suitable acid catalyst, demonstrating outstanding stability during the process, excellent activity and selectivity toward the intended ester result (Kiss et al., 2006). This continuous process offers benefits over the batch process such as greater efficiency, less sulfur content, and the absence of waste salt stream (Kiss et al., 2006).

Mahfud et al. (2007) investigated the improvement of flash pyrolysis of oil via reactive distillation utilizing butanol and homogeneous acidic catalyst at 49.85 – 79.85 °C and lower pressure (10 kPa). The data indicates that the amount of water from the pyrolysis

of oil decreases substantially. The improved pyrolysis of oils could be achieved by utilizing butanol and a homogeneous acidic catalyst, where the acidity and heating values are significantly enhanced (Mahfud et al., 2007).

Reactive distillation with an acid catalyst has the possibility of being employed for biodiesel processing or for the preprocessing of feedstocks with high FFA content (Kolah et al., 2013; Russbueldt & Hoelderich, 2009; Simasatitkul et al., 2011). However, numerous designs have been investigated in an effort to optimize the rate of reaction and biodiesel production (Kolah et al., 2013). It should be noted that the alcohol recovery stage could be omitted when the biodiesel is produced by reactive distillation (Qiu et al., 2010). In addition, reactive distillation can be utilized to produce triacetin, a biofuel additive, by the esterification of glycerol with acetic acid (Hasabnis & Mahajani, 2010) as presented in Figure 2.9.

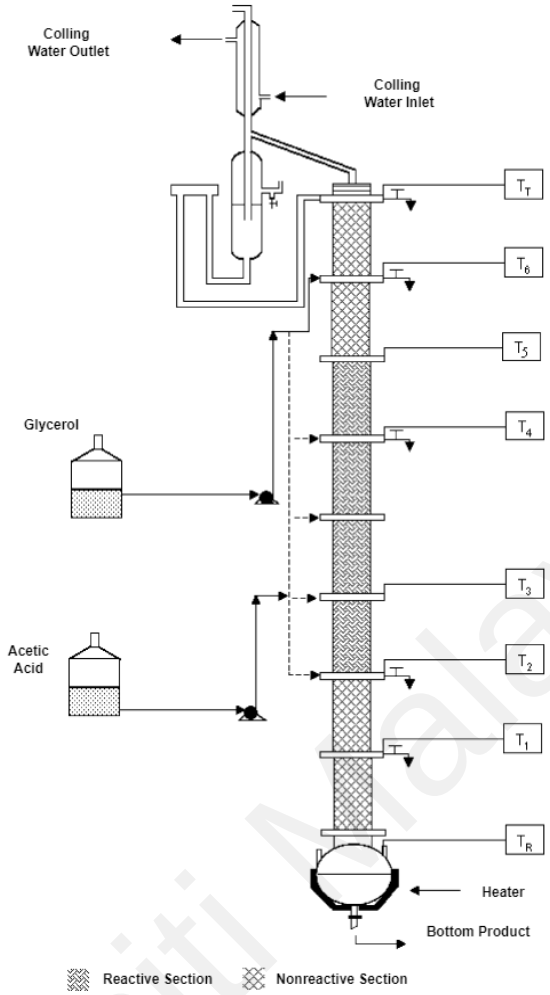

Figure 2.9: Reactive distillation technique combines two processes (reaction and distillation) in the same system.

It is a system-driven technology that could be used to produce biodiesel (Kiss et al., 2008) and improve flash pyrolysis of the oil (Mahfud et al., 2007). Wang et al. (Wang et al., 2001) observed a 10% decrease in energy usage and a 50% enhancement in yield for the hydrolysis yield of methyl acetate via reactive distillation, matching the standard technique of a fixed-bed reactor followed by distillation. Furthermore, in the event of extremely slow reactions with extended contact times which requires huge column sizes, the reaction rate may also restrict the use of reactive distillation (Kiss, 2010; Kiss et al., 2006, 2008; Kolah et al., 2013).

Kiss et al. (2006) developed a sustainable approach for biodiesel synthesis and refinery based on the integration of catalysis by solid acid and reactive distillation. Different absorbents were utilized and investigated on their ability and stability in the fatty acid esterification with various alcohols such as methanol, ethanol and propanol, etc. Temperatures higher than 373 K were used for the process to remove water and change the equilibrium in favor of the ester synthesis. Reactive distillation was designed using a combination of detailed models and experimental data. The primary finding was the identification of sulfated zirconia as a suitable acid catalyst, demonstrating outstanding stability during the process, excellent activity and selectivity toward the intended ester result (Kiss et al., 2006). This continuous process offers benefits over the batch process such as greater efficiency, less sulfur content, and the absence of waste salt stream (Kiss et al., 2006).

2.3.4. Membrane-Based Purification Techniques in Biodiesel Refinery

There are typically three categories of liquid membranes based on the configuration definition i.e. bulk liquid membrane (BLM), emulsion liquid membrane (ELM), and supported or immobilized liquid membrane. Polymeric-inclusion, dual-module hollow-fiber and gel membranes are also sometimes included in these definitions, although some authors argue that they are all just modifications of supported liquid membrane and BLM, respectively. Liquid Membrane techniques for biodiesel purification are the product of innovative techniques developed to circumvent the drawbacks of traditional techniques and to further enhance biodiesel purity (Abed et al., 2023). Membranes are used in these techniques because they are thought to be the most efficient means of purifying biodiesel and because they have benefits over traditional methods in terms of being both economically and environmentally friendly (Atadashi, Aroua, & Aziz, 2011; Atadashi et al., 2011b). The following sections contain in-depth discussions of these types of membranes.

2.3.4.1. Supported Liquid Membrane

Recently, various alternate "water-free" purification techniques have been utilized and developed, such as membrane filtration. The membrane filtration technique is utilized to eliminate large amounts of water needed in the biodiesel refining.

Wang et al. (2009) investigated the elimination of soap and glycerol from biodiesel using a ceramic membrane. In this study, the crude biodiesel was passed through the ceramic membrane with a pore size of 0.6, 0.2, and 0.1 μm. The biodiesel was pumped through the membrane at 333.15 K and 0.15 Mpa. The soap content and free glycerol were analyzed after 3 minutes and compared for each pore sizes (Wang et al., 2009). Table 2.5 compares the different membrane pore diameters and water-washing techniques for the purification of crude biodiesel.

Gomes et al. (2011) investigated the glycerol removal from biodiesel after the transesterification process using a 0.2 μm ceramic membrane at different pressures. The technique does not require previous settling for glycerol separation, nevertheless, the reaction mixture transforms into microfiltration after the addition of acidic water. The mechanism of glycerol removal via a supported ceramic membrane was suggested as presented in Figure 2.10. The glycerol removal from biodiesel via the micro-ceramic membrane was effective and gave a glycerol content lower than 0.02% from the upper international limit (Gomes et al., 2011).

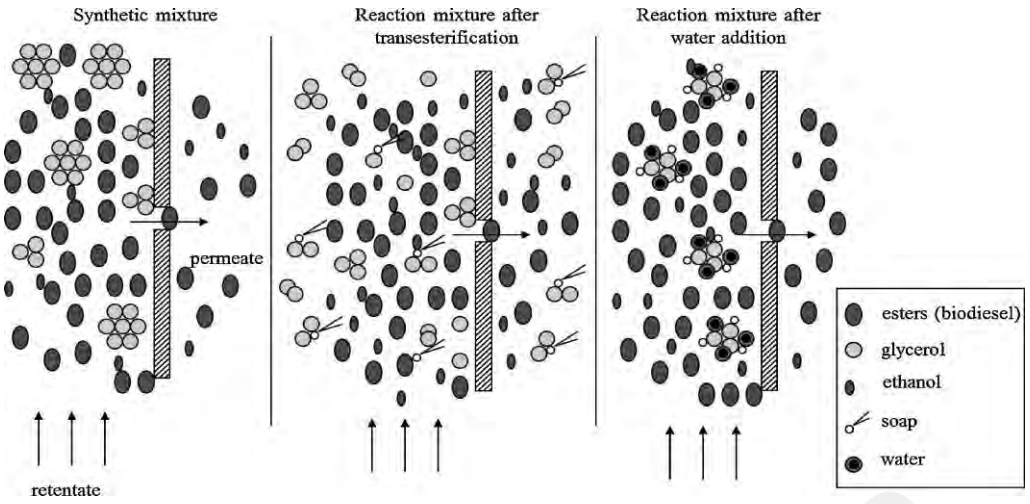

Figure 2.10: Suggested mechanism for the purification of biodiesel via microfiltration ceramic membrane (Gomes et al., 2011).

Atadashi et al. (Atadashi et al., 2015) studied the removal of catalyst and glycerin impurities in the biodiesel using the membrane filtration method. In this study, the raw biodiesel was passed through a multi-channeled tubular membrane with a pore size of 0.05 μm. The membrane system was investigated on the operating conditions such as temperature (°C), transmembrane pressure (bar), and flow rate ($L.min^{-1}$). According to their findings, the application of a ceramic membrane with a pore size of 0.05 μm allows the effective separation of biodiesel from free glycerol and soap. The optimal operating parameters are as follows: temperature of 40 °C, transmembrane pressure of 2 bar, flow rate of 105 $L.min^{-1}$ and a permeate flux of 22.17 $kg.m^{-2}$ hr^{-1}.

Amelio et al. (2016) investigated the ability to use a membrane contactor-based liquid-liquid extraction for biodiesel purification. Water as an extractant and a membrane reactor, were used to enhance the purification process and reduce the environmental effect. The results indicated that the utilization a membrane reactor-based liquid-liquid is an effective technique for the purification of biodiesel, providing advantages over traditional techniques in terms of efficacy, lower water usage, and environmental effects

(Amelio et al., 2016). Generally, this investigation advances the creation of more effective and environmentally friendly biodiesel purification methods.

Table 2.5: Comparison of membrane pore size and water washing for biodiesel purification (Wang et al., 2009).

	Metals ($mg.kg^{-1}$)				Free glycerol (%wt)
	K	Na	Ca	Mg	
Raw BD	160	8.98	1.45	0.33	0.261
0.01 μm pore size	1.7	1.36	0.95	0.15	0.0152
0.02 μm pore size	2.2	0.88	0.55	0.26	0.0257
0.06 μm pore size	4.25	0.68	0.7	0.25	0.0276
Water washing method	2.46	1.41	0.64	0.18	0.0179

2.3.4.2. Bulk Liquid Membrane

The BLM is a type of liquid membrane. The BLM technique is a liquid membrane with three phases as follows: the source phase which consists of the compounds to be removed; the membrane layer as the diffusion medium; and the receiving phase (Nabieyan et al., 2007). In a BLM, the source and receiving layers are separated by a relatively thick layer of an immiscible fluid (Yang et al., 2009). The BLM methods are often used for the elimination of metallic ions (Das et al., 2014; Kogelnig et al., 2010; Nezhadali et al., 2016; Singh et al., 2011), separation of anionic (Pirmoradi & Ashrafizadeh, 2017) and organic (Soniya & Muthuraman, 2015) contaminants, separation of bioactive compounds (Abed, 2014; Abed & Al-Hemiri, 2015; Al-Hemiri et al., 2012; Al-Shahwany et al., 2013), and biorefinery processes (Hayyan et al., 2022). The extraction of contaminant from the source layer and the stripping by the receiving phase occurs in the same process. The extraction and stripping efficiencies can be described by Eq.s (2) and (3) respectively. In most of these applications, the source and receiving layers are in aqueous solutions

while the transport medium is an organic phase. However, the reverse arrangement is also possible. The BLM technique is simple and affordable compared to other kinds of liquid membranes. Figure 2.11 shows the postulated diagram of impurity removal (like glycerol and soap, etc.) and transport during feed, membrane, and stripping phases via the BLM system. Due to the simplicity in construction and properties such as constant contact area, and flexibility of manipulation (Soniya & Muthuraman, 2015), the BLM is an advanced technique for the investigation of the kinetics and transport processes of numerous purification methods. Other advantages of BLM are the ease of processing, efficient separation, and high performance; hence BLM are considered for industrial applications (Chang, 2016). From the survey of the published works, a gap in previous works utilizing BLM technology for biodiesel purification was identified. Specifically, the study conducted by Hayyan et al. (2022) examined the removal of free glycerol from biodiesel. Consequently, researching this technology presents some challenges due to the inherent advantages it offers, as mentioned earlier.

$$\text{Extraction efficiency} = \frac{\text{initial concentration} - \text{contaminant's final concentration}}{\text{initial concentration}}$$ ficiency=initial concentration-contaminant's final concentration /initial concentration (2.2)

$$\text{Stripping efficiency} = \frac{\text{contaminant concentration in stripping phase}}{\text{initial concentration} - \text{contaminant's final concentration}}$$ iciency=contaminant concentration in stripping phase /initial concentration- contaminant's final concentration (2.3)

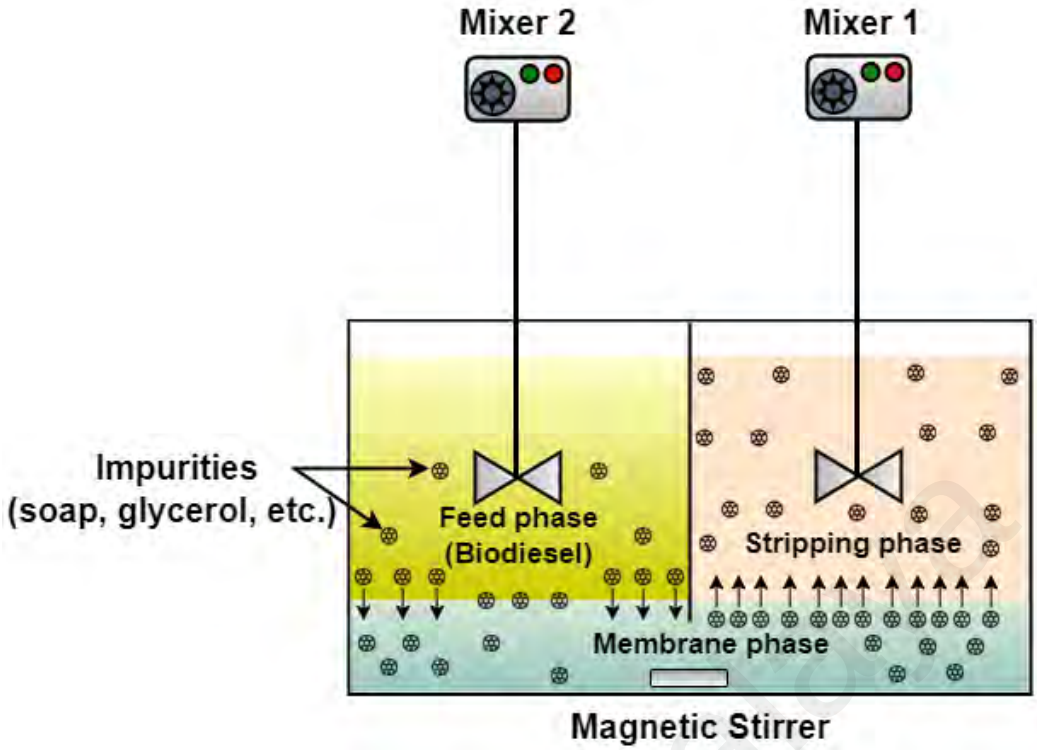

Figure 2.11: Schematic diagram of BLM explains the path of impurities removal (like glycerol and soap, etc.) and transport during feed, membrane, and stripping phases.

Hayyan et al. (2022) used a base-catalyzed transesterification process to produce crude biodiesel from palm oil. It had 0.33 wt.% of free glycerol which is lower compared to the limit set by international standard of biodiesel. In this study, the authors (Hayyan et al., 2022) developed a novel technique for the elimination of glycerol from crude biodiesel by using the BLM method, which was created from traditional solvent extraction techniques, where the crude biodiesel was added into the feed phase. The DES is the membrane phase while for the first time, diethyl ether is the stripping agent due to its immiscibility in DES and glycerol solubility. Combining the extraction and stripping procedures into a single system enables simultaneous solvent recovery using a DES based on glycerol and quaternary ammonium salts (choline chloride) as the membrane phase. The BLM system was investigated of the extraction and striping efficiencies, together with the impact of other variable conditions on the efficiency such as the HBA:HBD ratio,

DES to biodiesel ratio, stirring speed and duration. The kinetic parameters (k_1 and k_2) for glycerol diffusion were calculated by using the glycerol concentration in the source and the receiving phase. According to their findings, the application of BLM has allowed the effective glycerol separation from crude biodiesel when using DES as the liquid membrane and the glycerol content in biodiesel conforms to international standards such as EN 14214 and ASTM D6759. The optimal operating parameters for the BLM system are as follows: HBA:HBD ratio of 1:2, DES:biodiesel mass ratio of 1:1, mixing speed of 200 rpm, and operation duration of 240 min. Under these optimized parameters, the kinetic rate constant is 0.0037 min^{-1} and 0.0066 min^{-1}, for k_1 and k_2, respectively. The kinetic rate constant with two irreversible steps fitted well with the experimental results. In conclusion, this study demonstrated a new approach of environmentally friendly solvents for biodiesel purification vis the BLM technology. The proposed technique was effective in reducing the glycerol content in biodiesel to meet the standard limits.

- **Mechanism, Kinetic and Mass Transfer in BLM System**

Different investigations were conducted in the literature to describe the mechanism, kinetics and mass transfer of the solute in the BLM methods. An effective and green method of refining biodiesel is offered by BLM techniques, which guarantee premium fuel for renewable energy sources. BLM consists of an effective membrane phase between the feed and stripping phases. The active phase selectively interacts with and eliminates the polar contaminants from the biodiesel phase. Hayyan et al. (Hayyan et al., 2022) studied the transport mechanism of glycerol from crude biodiesel. The contaminants transported in the BLM techniques are hypothesized to occur through a reaction on the source side of the interface and a reaction in the receiving phase of the membrane interface (Abed, 2014). Figure 2.12 shows the mechanism of glycerol removal from biodiesel as suggested by Hayyan et. al. (2022). Generally, the contaminants' mass

transfer follows the first-order kinetic mechanism of two consecutive irreversible reactions:

$$F \xrightarrow{k_1} M \xrightarrow{k_2} S \tag{2.4}$$

Where F, M, and S represent the contaminant in the feed, membrane and stripping phases respectively, while k_1 and k_2 represent the extraction and stripping rate constant.

The solute mass balance was used to calculate the contaminant concentration in the membrane layer after measuring the contaminant concentration in the source and receiving phases (Hayyan et al., 2022). The concentration terms in the BLM phases are described in the Eq. (2.5):

$$G_f = \frac{C_f}{C_o} \qquad G_m = \frac{C_m}{C_o} \qquad G_s = \frac{C_s}{C_o} \tag{2.5}$$

Where C_o, C_f, C_m, and C_s is the contaminant initial concentration, contaminant concentration in the source, membrane and receiving phases, respectively. The materials balance can be expressed in Eq. (2.6) as follows:

$$G_f + G_m + G_s = 1 \tag{2.6}$$

Hayyan et. all (2022) studied the kinetics of glycerol removal from FAME based on the following Eq. described by the first order kinetic model:

$$\frac{d\,G_F}{dt} = K_1\,G_F = Q_F \tag{2.7}$$

$$\frac{d\,G_M}{dt} = K_1\,G_F - K_2\,G_M = Q_M \tag{2.8}$$

$$\frac{d\,G_S}{dt} = K_2\,G_M = Q_S \tag{2.9}$$

Where, Q_F , Q_M , and Q_S are the feed, membrane, and stripping fluxes respectively. The expression of $G_F, G_M,$ and G_S are derived by the integration of Eq. (2.7), (2.8), and (2.9):

$$G_F = \exp(-k_1 t) \tag{2.10}$$

$$G_M = \frac{k_1}{k_1 - k_2}[\exp(-k_1 t) - \exp(-k_2 t)] \quad (2.11)$$

$$G_S = 1 - \frac{k_1 k_2}{k_2 - k_1}[k_2 \exp(-k_1 t) - k_1 \exp(-k_2 t)] \quad (2.12)$$

Q_I is derived by Eq.s (2.10), (2.11), and (2.12) as follows:

$$Q_F = -k_1 \exp(-k_1\, t) \quad (2.13)$$

$$Q_M = \frac{k_1}{k_1 - k_2}[\exp(-k_1\, t) - \exp(-k_2\, t)] \quad (2.14)$$

$$Q_S = \frac{k_1 k_2}{k_2 - k_1}[k_2 \exp(-k_1\, t) - k_1 \exp(-k_2\, t)] \quad (2.15)$$

The contaminant maximum fluxes through the BLM are achieved when Q_M is zero:

$$Q_F^{max} = -k_1 \exp(-k_1\, t_{max}) \quad (2.16)$$

$$Q_M^{max} = \frac{k_1}{k_1 - k_2}[\exp(-k_1\, t_{max}) - \exp(-k_2\, t_{max})] = 0 \quad (2.17)$$

$$Q_S^{max} = \frac{k_1 k_2}{k_2 - k_1}[k_2 \exp(-k_1\, t_{max}) - k_1 \exp(-k_2\, t_{max})] \quad (2.18)$$

The maximum time (t_{max}) and $G_{M\,max}$ can be obtained from Eq. (2.17) and (2.11) respectively, as shown in Eq. (2.19):

$$t_{max} = \frac{\ln(\frac{k_1}{k_2})}{k_1 - k_2} \quad (2.19)$$

$$G_{M\,max} = (\frac{k_1}{k_2})^{-k_2/(k_1 - k_2)} \quad (2.20)$$

According to the mass transfer kinetic model, the temporal variance of Q_M and Q_S is bi-exponential, whereas t provides a decreasing mono-exponential curve. The experimental effects were interpreted using non-linear curve fitting method. Moreover, the model demonstrates the mechanism of contaminant mass transfer from the source phase to the membrane phase when stripped by the receiving phase and the driving force of the concentration gradient.

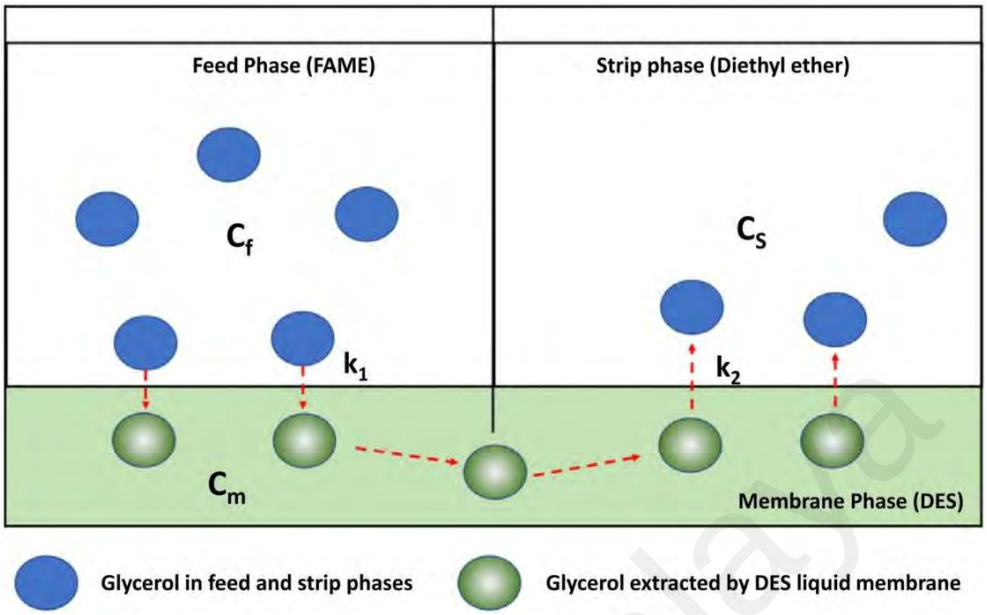

Figure 2.12: Transport mechanism of glycerol through DES to strip phase via BLM system (Hayyan et al., 2022).

2.3.4.3. ELM Technique

Li (1968) developed the ELM concept in 1968. An immiscible liquid membrane contains an emulsion of the stripping phase. After mixing with the source solution, the emulsion mass transport occurs from the source to the internal phase. There are two types of liquid membranes which are aqueous and organic, with the former more commonly described in literature. From the benefits and drawbacks of the suggested approach, it is clear that the ELM technique has a bright prospect to improve the purification procedures, beyond the use of environmentally friendly solvents. ELM offers a more economical option compared to the traditional liquid-liquid extraction processes by decreasing the amount of water, solvents, and total operating costs (Davoodi-Nasab et al., 2018).

Additionally, the use of ELM offers a variety of improved separation methods that maximize purification by utilizing the solubility, hydrophobicity, electrostatic charge, and

molecule size (Azarang et al., 2019). ELM represents a significant breakthrough in purification technology by facilitating enhanced separation effectiveness by minimizing the diffusion path between the phases. Moreover, the notable operational benefits provided by ELM are significant. ELM streamlines the extraction and stripping processes by providing continuous and flexible operation, a lower membrane thickness, high surface area, and improved solute transfer rates (Davoodi-Nasab et al., 2018). In keeping with the objectives of environmental sustainability, it also employs smaller stripping phase volumes than the external phase, which lowers the solvent consumption and encourages recyclability (Chakraborty & Bart, 2006). Table 2.6 demonstrates the key points and merits of ELM as a promising purification method for the biodiesel downstream industry.

But there are still some difficulties even with these benefits. The stability of the emulsion becomes a crucial issue since instability could reduce the extraction efficiency (Suliman et al., 2021). Two important phenomena that could lead to the emulsion's instability are the break-down and swelling (Ardehali et al., 2020). Emulsion break-down refers to the breakage of emulsion droplets caused by the inner droplets within the globule interface or by the coalescence between larger globules (Ficheux et al., 1998). The primary causes of this phenomenon include surfactant molecule hydration, micelle transport, and molecular diffusion (Colinart et al., 1984; Suliman et al., 2023). A number of adjusting variables have been studied in order to produce a stable ELM method. These include the different types and amounts of surfactants, agitation rate and duration, initial external phase concentration, carrier, and internal agent quantity, external to internal ratio, and treatment ratio (Imdad & Dohare, 2022; Rosly et al., 2020; Tahmasebizadeh et al., 2021).

Table 2.6: Key points for ELM as a promising technique in the biodiesel industry.

Key points	Description
Performance and effectiveness	The ELM approach offers high extraction efficiency, effectively removing contaminants from biodiesel while maintaining product quality.
Simplicity	ELM requires fewer pieces of equipment compared to traditional methods, streamlining the purification process and eliminating the need for additional treatment steps.
Recyclability	Both the liquid membrane phase and stripping phase in ELM are recyclable, reducing resource consumption and waste production, and thus enhancing sustainability.
Environmental Impact	ELM minimizes environmental impact by eliminating the need for large quantities of water and reducing solvent usage, thereby lowering operating expenses and environmental footprint.
Reduction in solvent usage	ELM employs fewer organic solvents, and eco-friendly alternatives like ionic liquids and DESs can be utilized, promoting sustainability without compromising efficacy.
Simple and advanced extraction technique	ELM offers a straightforward and advanced extraction process, facilitating ease of implementation and saving time and energy.
Mass transfer rate	The ELM method provides a high surface area for interaction between phases, leading to enhanced mass transfer rates and improved solute removal efficiency.

Chakraborty et al. (2006) reported the separation of toluene from n-heptane via the ELM techniques. In this study, a-cyclodextrin and b-cyclodextrin were used as the carrier oil/water/oil system. The separation performance and separation factors were investigated by varying the operating conditions such as the carrier concentration, operating time, amount of solvent and volume fraction of the membrane phase. According to their findings, the suitable surfactant concentration, volume fraction, and relative amount of solvent were 1%wt., 0.3 and 0.4, respectively. These results show that the emulsion was

stable and uniform, which provides a high rate of mass transfer coefficient for the toluene separation from heptane. To assess the ELM stability, the leakage % is calculated by the following Eq.:

$$\text{Lekage } \% = \frac{\text{Concentration (ext)}}{\text{Concentration (in,max)}} \times 100 \quad (2.21)$$

Where concentration (ext) is the contaminant content leakage from the stripping phase to the source feed phase, while the concentration (in, max) is the contaminant maximum content in the source layer.

Ng et al. (2010) investigated the performance of ELM for phenol removal at various operating parameters such as the emulsification speed, membrane feed phase ratio, membrane stripping phase ratio, emulsification duration, surfactant concentration, carrier content, and stripping phase concentration. The phenol removal efficiency was 89.33% under optimum conditions.

Kargari (2013) utilized the ELM method for the removal of 4-chlorophenol from wastewater in a water treatment system. The impacts of the external phase concentration, initial feed pH, stripping phase concentration, and stirring speed were investigated in this study. They reported that this method could eliminate 4-chlorophenol from the feed phase with 100 ppm of solute in just 5 minutes.

Jiao et al. (2013) investigated the removal of bisphenol from an aqueous solution by the ELM technique. The ELM system consists of kerosene and a PO^{-4} surfactant as a membrane phase, while sodium hydroxide was the stripping agent. The impact of the operating conditions was investigated using the response surface methodology. The operation variables are the PO^{-4} concentration, the external phase volume ratio to the emulsion phase, the concentration of the stripping phase, and the ratio of the membrane phase to the stripping phase. The experimental results showed that 97.52% extraction efficiency of bisphenol could be achieved (Jiao et al., 2013).

The removal of 4-nitrophenol from wastewater via the ELM technique was also studied by Chaouchi and Hamdaoui (2016). The ELM system consists of hexane as the membrane, span 80 as the surfactant, and Na_2CO_3 as the stripping phase. The external phase % vol and initial concentration on the 4-nitrophenol removal were investigated. The experimental results showed that >99% extraction efficiency of 4-nitrophenol was achieved at the optimum operating conditions (Chaouchi & Hamdaoui, 2016). Jusoh et al. (Jusoh et al., 2020) demonstrated the viability of ELM towards the separation of polyphenols from the palm oil mill sterilization condensate. The system consists of tributylphosphate (TBP) as the carrier, span 80 as the surfactant, kerosene as the diluent, and sodium as the receiving agent. The results showed that 83% of polyphenols were extracted at optimal conditions of 0.1 M TBP, 1 M NaOH, a treatment ratio of 1:5, pH of the external phase of 5, and 5% v/v octanol as the modifier (Chaouchi & Hamdaoui, 2016).

Recently, ionic liquids have been introduced in the ELM technique. The use of ionic liquids in this technique gave interesting results in the transport and purification processes. These ionic solvents were added into the membrane phase, as the transporter of contaminants from the outer phase to the extraction phase. This technique was used in various processes such as the removal of hydrocarbons from industrial and polluted water (Al-Obaidi et al., 2021). In another embodiment, ionic liquids have been replaced by a special kind of ionic liquid which is the deep eutectic solvent (DES) that is cheaper and more environmentally friendly. DESs have been introduced as phase extractions in liquid-membrane technology. This technique shows promising and interesting results compared to the water-washing methods for biodiesel purification. These solvents gave promising results in the purification of biodiesel from contaminants.

Soap removal from biodiesel via the DES-based ELM in the presence of AC was studied. The ELM system consists of silicon oil and sorbitan monolaurates as the membrane layer

and DES as the stripping agent in the presence of AC. In this investigation, there are three primary steps in the procedure (Figure 2.13); First, the formation of the emulsion membrane by combining 0.15 weight percent surfactant with 10 milli-liters of silicon oil and blending with 0.3 weight percent AC at 10,000 rpm for three minutes, then homogenising the emulsion membrane phase for another three minutes at 10,000 rpm after adding 10 mL of DES. Secondly, the emulsions were added into 30 mL of biodiesel phase containing 765 mg/kg of fatty acid salts. The mixture is then mixed for 10 minutes at 300 rpm. By using a DES-based ELM system, the soap molecules transfer from the feed phase (biodiesel) to the internal phase. Thirdly, the mixture was poured into a separation funnel to form three layers. Finally, the titration method of AOCS Technique Cc 1795 was utilized to assess the soap content. The HBA: HBD ratio, DES: biodiesel ratio, extraction time, surfactant content, and stirring speed were investigated.

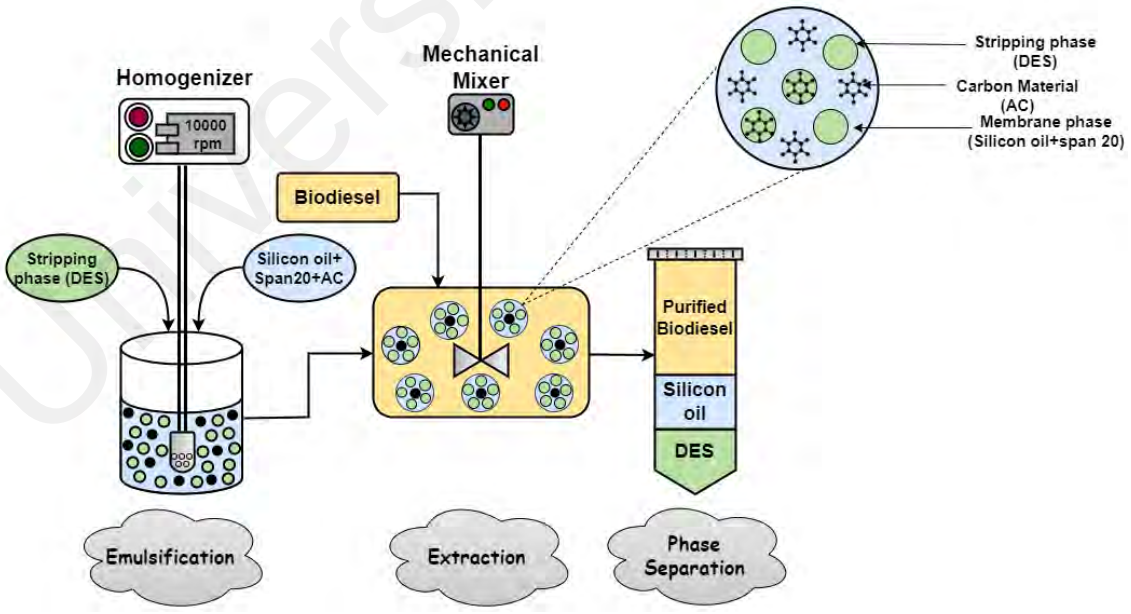

Figure 2.13: DES-based ELM technique for purification of biodiesel

The experimental results showed the highest soap removal of 99.75% at a 1:4 HBA:HBD ratio, 2 wt% of sorbitan monolaurates, 0.5 wt% of AC, a 1:1 DES: biodiesel ratio, a 400 rpm stirring speed, and a 6 min extraction time. The fatty acid salt elimination via the DES/ ELM follows the first-order kinetic model with a kinetic constant of 0.01 s^{-1}. It shows that the crude biodiesel can be effectively purified without using huge amounts of water in the washing step, making it a more environmentally friendly option than the traditional water washing method. As a result, this method has demonstrated promising results and warrants further study for the purification of biodiesel, particularly from the perspective of removing additional contaminants from biodiesel to meet international requirements. Understanding the complex correlation between the ELM characteristics and operational factors is crucial for realising the complete potential of the emulsion membrane-based purification processes and guaranteeing their sustainability and effectiveness in various uses.

- **Mechanism, Kinetic and Mass Transfer in ELM Techniqe**

The ELM technique is employed for the removal of contaminants from the biodiesel. In this technique, the emulsions are synthesized by dispersing the stripping phase in the membrane phase and then mixing the emulsion with the biodiesel. The stripping phase binds to the polar impurities such as glycerol, alkali metals, and fatty acid salts, etc.(Chatzifragkou & Papanikolaou, 2012). Figure 2.14 explains the mechanism of contaminants (such as soap) elimination from the biodiesel using the DES/ ELM technique. During interaction and diffusion, contaminants move from the biodiesel phase into the emulsion phase, which is then stripped by DES. The emulsion separates from the biodiesel after sufficient interaction time, leaving behind the pure biodiesel. The single-pathway travel is suggested as the process of soap removal from biodiesel utilizing the ELM-DES/AC system. Figure 2.14 illustrates how the fatty acid salt molecules are

removed from the biodiesel phase and transported into the silicon oil-containing membrane phase. The fatty acid salt molecules are then transported via the membrane phase into the membrane/internal interfaces. In this configuration, the stripping agents of DES and AC eliminate the fatty acid salts from the membrane phase through a complex formation, while the AC contaminants by adsorption.

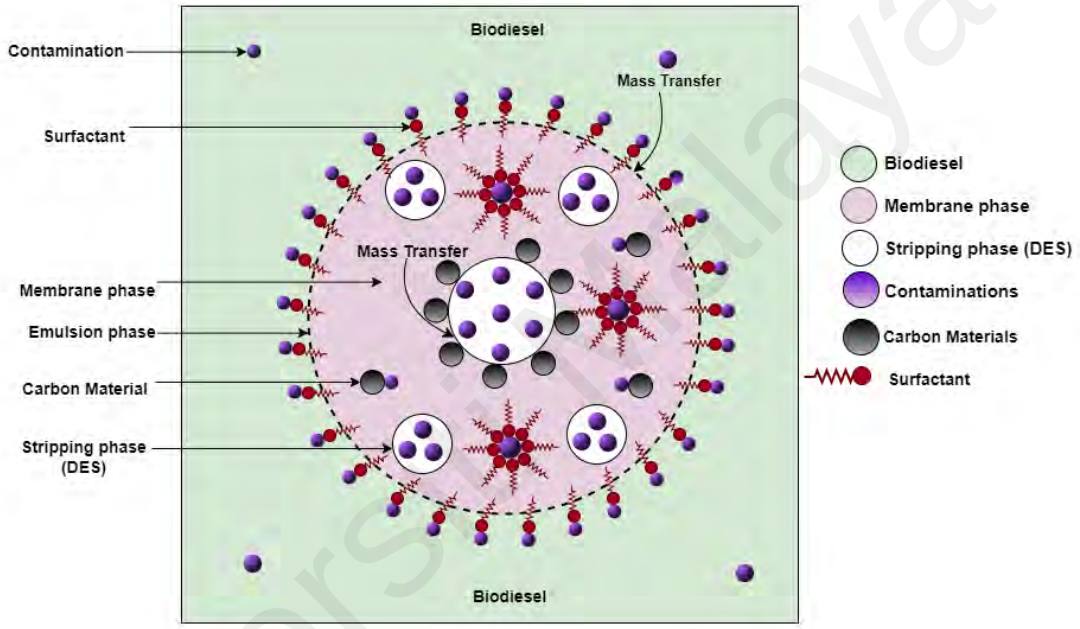

Figure 2.14: Suggested mechanism of contaminants elimination using DES/ELM technique.

A different investigation was reported to describe the kinetics and mass transfer of solute in the ELM technique. The suggested mathematical model for contaminants extraction from crude oil is based on the following conditions:

Steady state transport mechanism.

The phases of the ELMS are immiscible.

One directional first order transport model.

The reaction on the membrane-internal interface is one directional.

The solute loss during the process is neglected.

The mathematical model of solute mass transfer in ELM is described by the Fick's law:

$$J = -\frac{V}{A_g}\frac{dC_t}{dt} \tag{2.22}$$

The A_g (Eq. 2.22) is described by the following Eq.:

$$-\frac{A_g}{V_g} = \frac{S_g}{V_T} \rightarrow A_g = V_g\frac{\pi D_g^2}{\frac{1}{6}\pi D_g^3} = V_g\frac{6}{D_g} \tag{2.23}$$

Where J (mol/cm ^{2}) is the solute flux, V (cm^3) is the feed phase volume, dC_t/dt ($mol/cm^3.s$) is the solute concentration gradient, V_T (cm^3) is the total emulsion volume, S_g (cm^2) is the surface area of the droplet, V_g (cm^3) is the droplet volume, and D_g (cm) is the droplet size.

Eq. (2.24) is derived by substituting Eq. (2.23) into Eq. (2.22):

$$J = -\frac{V}{V_g}\frac{D_g}{6}\frac{dC_t}{dt} = k\,C_t \tag{2.24}$$

Eq. (2.25) can be obtained by rearranging Eq. (2.24) as follows:

$$J = -\frac{V}{V_g}\frac{D_g}{6}\frac{dC_t}{dt} = k\,C_t \tag{2.25}$$

The integration of Eq. (2.6) at the initial conditions (0 → t and Co → Ct) yields Eq. (2.26)–- (2.28):

$$-k\frac{V_g}{V}\frac{6}{D_g}\int_0^t dt = \int_{C_0}^{C_t}\ln C_t \tag{2.26}$$

$$-k\frac{V_g}{V}\frac{6}{D_g}t = \ln\frac{C_t}{C_o} \tag{2.27}$$

$$\frac{C_t}{C_o} = e^{-(k\frac{V_g}{V}\frac{6}{D_g})t} \tag{2.28}$$

Where Co is the initial concentration of solute, Ct is the concentration of solute at any time t (s), and k is the mass transfer constant.

The overall mass transfer coefficient in the ELM system is expressed by Eq. (2.29):

$$\frac{1}{K_o} = \frac{1}{K_M} + \frac{1}{K_F} \quad (2.29)$$

Where, K_o: overall mass transfer coefficient (m/s),

K_M : mass transfer coefficient of the external phase (m/s)

K_F : the interfacial reaction rate constant (in m/s).

Skelland and Le''s Eq. (Kohli et al., 2019) estimates the mass transfer coefficient of the external phase:

$$\frac{K_M}{\sqrt{ND}} = 2.932 \times 10^{-7} \left(\frac{V_s+V_m}{V_s+V_m+V_f}\right)\left(\frac{d_i}{d_t}\right)^{0.584} Re^{1.371} \quad (2.30)$$

Where, $V_s, V_m,$ and V_f represents the relative volumes of the external phase, membrane phase, and internal phase. D represents the diffusion coefficient of a contaminant in the membrane layer, and N is the mixing speed.

Eq. (2.31) is obtained by comparing it with Eq. (2.27) to determine the K_F as follows:

$$\ln\frac{C_t}{C_o} = -AK_F\, t \quad (2.31)$$

where A is the emulsion's specific area.

The interplay of these coefficients highlights the intricate interrelationships within the system and highlights the significance of the ELM phase'' characteristics in dictating the overall mass transfer rate.

2.4. Limitations, Advantages, and Disadvantages of Biodiesel Refining Methods

The refinement of crude biodiesel is essential for the production of high-quality biodiesel fuel that can be efficiently utilized in diesel engines. Different techniques have been developed to purify crude biodiesel, with varying levels of success and limitations. For instance, water washing, although effective for the removal of impurities, generates a significant volume of wastewater and requires substantial amounts of energy (Atadashi

et al., 2011b). The negative aspects associated with the water-washing technique have led to the use of water-free techniques. However, these approaches face obstacles such as adsorbent regeneration of waste due to inadequate knowledge of chemical processing (Atadashi, 2015). Several aspects must be considered with regard to the selection of the ion exchange resin, such as the structural properties, stability, exchangeability, type of resin, and resin strength. While ion exchangers have shown encouraging findings in the removal of pollutants, their performance in the removal of methanol is still inadequate (Atadashi et al., 2011b). Furthermore, the high cost of ion exchange processes poses a considerable challenge. Due to the challenges in these traditional techniques, the use of membrane techniques for biodiesel refinement has increased. Among these methods, the membrane technique appears to be an advanced choice for biodiesel purification since it retains the unreacted triglycerides (Shuit et al., 2012). Furthermore, the advancement of membrane techniques in biodiesel purification enhances the kinetics of the biodiesel refining techniques and the membrane procedure is shown to improve the physicochemical properties of biodiesel (Saleh et al., 2011). Furthermore, the high cost of membrane manufacturing, low stability, membrane fouling, membrane swelling when exposed to organic solvents and the loss of energy resulting from vacuum conditions in these methods must be considered.

Supercritical biodiesel purification techniques have several benefits, including catalyst-free processing, flexible feedstock and simplicity of use (Khursheed et al., n.d.). They possess certain disadvantages though, such as the strong reaction conditions that could lower the quality and yield of biodiesel (Mandari & Devarai, 2021). It is imperative that these constraints -such as high energy (high temperature and high pressure) requirements and economic implications must be addressed for biodiesel production before utilizing this technology (Mandari & Devarai, 2021).

MBRs play a crucial role in biodiesel purification and refinery processes, but they also possess certain limitations. While they offer efficient separation and purification (Garg et al., 2023), MBRs require large energy consumption for operation, while membrane fouling could reduce the performance over time (Garg et al., 2023; Govindaraju et al., 2021). Additionally, the initial investment and maintenance costs can be significant, and the limited flux affects the overall productivity (Garg et al., 2023; Govindaraju et al., 2021). Proper system design and management expertise are essential for successful biodiesel production and refinery (Hafeez et al., 2020).

ELM and BLM can be used in a single extraction and stripping processes with a high capacity of separation and high selectivity at a lower cost. Such techniques eliminate the contaminants for example the glycerol (Dai et al., 2016). These techniques show a significant potential for contaminant removal due to the high mass transfer area and smaller amount of solvents and in the absence of water. Furthermore, although the ELM processes have produced biodiesel with desirable physicochemical properties, challenges include emulsion instability, membrane ruptures, process complexity, and the limitation of applications that demand high- or low-temperature settings due to the stability of the emulsions (Zaulkiflee et al., 2022). More studies are needed to investigate the emulsion stability, break-down of emulsion, emulsification time and the correct selection of the stripping phase during the refining process. These aspects require more effort and consideration in the area of biodiesel refining. Thus, Table 2.7 compares the purification technique'' advantages and disadvantages.

The quality of biodiesel is a crucial factor in industrial production and application, emphasizing the need for continued development of refining techniques to achieve highly refined biodiesel. The benefits of producing high-quality biodiesel require less blockages in the fuel injectors, improved exhaust emissions and better lubricant properties.

Furthermore, the absence of soap, catalyst and glycerol reduces corrosion and elastomeric seal failures, resulting in high engine performance and decreased engine oil degradation.

Table 2.7: Advantages and disadvantages of different purification techniques.

Techniques		Advantages	Disadvantages	References
Equilibrium based				
Distillation		- Can be performed in a single-column -High-quality products with low impurity levels.	-Sophisticated operation control. -More expensive than the other methods.	Dunn, 2011
Supercritical Extraction		-The reaction is completed rapidly. -More environmentally friendly. -It involves a much simpler purification of products than a catalytic reaction.	-Pressures between 35 and 60 mPa and temperatures between 525 and 675 K are required for the reaction. - Required high energy related to requirements of high pressure and high temperature. -Low conversion when biodiesel is produced enzymatically using supercritical CO_2.	Demirbas, 2005, 2009; Demirbaş, 2002; Kusdiana & Saka, 2004; Madras et al., 2004; Mandari & Devarai, 2021

Techniques		Advantages	Disadvantages	References
Solvent Extraction	Water washing	-Requires cheap equipment. -Simple and effective technique for biodiesel purification. -Successful technique for removal of soap and catalyst residual. -Effective technique for removal of alcohol and glycerol. -Running cost is less than the affinity-based separation process. -Possibility of using acidic water for biodiesel purification.	-Required a lot of water. -Required using of deionized water. -High energy consumed -The possibility of formation of FFA by hydrolysis of ester due to presence of water. -Produced a high amount of wastewater. -Increase the cost of drying -Formation of stable emulsion due to presence of soap that can decrease the quality and yield of biodiesel. -Need long time due to the multiple processes such as multiple washing steps, separation of water from biodiesel, and drying of biodiesel. -Environmental and economic drawbacks. -The purification is not successful with biodiesel from calcium-based catalyst transesterification because it could result in stable calcium soaps.	Bateni et al., 2019; Caetano et al., 2019; Demirbas, 2008; Stojković et al., 2014

Techniques		Advantages	Disadvantages	References
	Organic Solvents	-FFAs, soap, and free glycerol are among the contaminants that can be eliminated from biodiesel more easily with the use of organic solvents. -Increase the effectiveness of the purifying process by eliminating undesirable components.	-Usually followed by demineralized water addition to remove the soap and catalyst. -High costs related to wastewater treatment -High energy and equipment costs, associated with the required residual water evaporation after washing. - Sometimes followed by a filtration process to remove the residual catalyst. -The possible toxicity and endurance of organic solvents make them potentially hazardous to the ecosystem.	Atadashi et al., 2011b; Mousavi et al., 2022
	Deep Eutectic Solvents	-Environmentally friendly systems. -An effective and inexpensive method. -Using non-toxic and biodegradable solvents.	-There is a high cost associated with using shakers to increase purification rates.	Abedet al., 2023

Techniques		Advantages	Disadvantages	References
Affinity based Adsorption and Ion Exchange		-Easier than equilibrium-based separation techniques. -low energy consumed. -Minimize the time of the process. -Impossible water in biodiesel. -Reduction of wastewater. -Applicable in continuous mode. -Ion exchange and magnesium silicate are effective for soap removal. -less equipment space from equilibrium-based separation techniques. -The waste of Magnesol can be added to animal food or utilized as fertilizer. -Less waste disposal -When comparing dry washing methods to wet washing methods, the resulting biodiesel has a better purity.	-Need extra pumps and columns. -not effective for methanol removal. -Purification of biodiesel from glycerol before using ion exchange resin. -Purified biodiesel might not meet the ASTM D6751 and EN 14214 specifications. -Regeneration of spent adsorbents and a limited understanding of substances' chemistry are challenges of these techniques. -Structural proprieties, exchange capacity, stability, and resin strength should be considered when utilizing the ion exchange technique. -Required to activate the substrate.	Atadashi, Aroua, & Aziz, 2011; Atadashi, 2015; Berrios & Skelton, 2008; Stojković et al., 2014

Techniques		Advantages	Disadvantages	References
Membrane based Supported liquid membrane		-Generated less waste, reduced effluent quantity -Less energy consumption -Compared to wet washing methods, dry washing techniques have produced biodiesel with a better level of purity.	-High cost of synthesis of the membrane. -Energy losses associated with the use of vacuum pumps. -Impurities have the ability to foul or plug membranes over time, decreasing their effectiveness. -Frequent cleaning and maintenance are required due to fouling, which raises operating expenses. -The total sustainability of the biodiesel synthesis process can be impacted by energy use.	Atadashi et al., 2011b; Bertram et al., 2009; Garg et al., 2023
Bulk liquid membrane		-One system that handles both the extraction and stripping stages. -Can recycle the membrane and stripping phases. -One advantage of BLM is that it is low-cost and easy to use. -High selectivity, and high efficiency. -Potentially combine the utilisation of the BLM system with low-cost, ecologically friendly solvents like DESs.	-Diffusion rates can be quite slow, especially in viscous membrane systems or low permeability systems. -Overall efficacy may be impacted by this delayed transmission, which may lead to longer processing duration and reduced yield. -The efficacy and stability of BLM can be impacted by the limitations of temperatures.	Hayyan et al., 2022

Techniques		Advantages	Disadvantages	References
Emulsion liquid membrane		-ELM water-less technology. -Less number and amount of solvents. -Can replace the organic solvents by green solvents. -Can recycle the membrane and stripping phases. -Employs smaller stripping phase than the feed phase volumes, which lowers solvent consumption. - High surface area improved High mass transfer rates of solute. -Less operation time. -Can include the porous materials to enhance efficiency and stability. - Providing flexible operation. -Reducing the path of diffusion between phases and lower membrane thickness. -Utilizes multiple forces, such as solubility, electrostatic charge, -Lower costs (40% cheaper than solvent extraction)	- ELM evaluation discloses drawbacks such as emulsion stability. -Limitation of applications that demand high- or low-temperature settings because the stability of the emulsions is challenged.	Azarang et al., 2019; Kumar et al., 2019a; Kumbasar, 2010; Zaulkiflee et al., 2022

Techniques		Advantages	Disadvantages	References
Reaction based Reactive distillation		-The smaller size of the reactor compared with the traditional reactor. -reduces downstream separation steps and energy demand. -Small reaction time of 10–15 min. -less amount of alcohol approximately 3.5:1 mol/mol	-More complex to operate. -Reactive distillation has not yet been used commercially in biodiesel refineries since it is typically more complicated to run. -In the case of slow reactions that need extended contact time, which leads to use a large column size.	He et al., 2005, 2007; Müller, 2019
Membrane bioreactor		-Yielding high-purity biodiesel. -High catalytic activity and stability. -Stability and resistance to chemicals in comparison to polymeric membranes. -Corresponds to the benefits of distillation in terms of preserving biodiesel quality.	-Require energy for operation. -The energy-intensive nature of membrane processes can impact overall process sustainability. -The initial maintenance costs can be significant. -Membrane fouling can reduce performance over time. - Insufficient flow impacts overall productivity.	Baroutian et al., 2011; Dubé et al., 2007; Garg et al., 2023; Govindaraju et al., 2021; Hafeez et al., 2020

2.5. Research Gap and Novelty in Biodiesel Purification Methods

This study addresses a critical gap in biodiesel purification by introducing a novel emulsion liquid membrane (ELM) system for soap removal, a technique not previously explored in the literature. Conventional methods for biodiesel purification, such as water washing, are resource-intensive and generate significant wastewater, posing environmental and operational challenges. This study proposes an innovative solution by integrating activated carbon and deep eutectic solvents (DES) into the ELM system, eliminating the need for water-based washing while enhancing purification efficiency.

The novelty of this approach lies in its synergistic use of activated carbon and DES within the ELM framework. Activated carbon, with its high surface area and strong adsorption capacity, targets the physical removal of soap molecules, while DES offers chemical selectivity through its tunable properties, effectively solubilizing and extracting soap contaminants. This dual-action mechanism within the ELM system not only improves soap removal efficiency but also provides a sustainable, waste-free alternative to traditional methods. By addressing the limitations of existing purification techniques and introducing a new application of ELM technology, this study pioneers a unique strategy in biodiesel refinement. The integration of advanced materials and innovative processing techniques establishes a significant advancement in the field, paving the way for more sustainable and efficient biodiesel purification processes.

CHAPTER 3: PALM RACEME AS A PROMISING BIOMASS PRECURSOR FOR ACTIVATED CARBON TO PROMOTE LIPASE ACTIVITY WITH THE AID OF DEEP EUTECTIC SOLVENTS

3.1. Introduction

This chapter concerns the role of activated carbon (AC) from palm raceme as a support material for the enhancement of lipase-catalyzed reactions in an aqueous solution, with deep eutectic solvent (DES) as a co-solvent. The effects of carbonization temperature, impregnation ratio, and carbonization time on lipase activity were studied. The activities of Amano lipase from *Burkholderia cepacia* (AML) and lipase from the *porcine pancreas* (PPL) were used to investigate the optimum conditions for AC preparation. Additionally, the effect of incubation temperature and water content as well as kinetic study were optimized to assess the biocompatibility of AC with DES. Moreover, the morphology of AC including surface area, pore characterization, and scanning electron microscopy (SEM) were observed. The results of this chapter were published in the Journal of Molecules (Abed et al., 2022).

3.2. Literature Review

Palm biomass, such as empty fruit bunches, mesocarp fiber, palm kernel shells, fronds, and trunks are under-utilized in industry. They are disposed of haphazardly by open burning or land-filling (Bakar & Anandarajah, 2015). It should, instead, be turned into activated carbon (AC), which is useful for various applications (Dias et al., 2007; Sud et al., 2008; Rashidi & Yusup, 2019).

In industrial-scale applications, activated carbon has been used to immobilize enzymes. Rao et al., (2020) discovered the functionality of invertase hydrolyses on charcoal

adsorption in the production of enzyme nanoparticles. Enzyme-supporting particle complexes have been studied to determine how the shape, size, and structure of enzymes and supporting material change (Arsalan & Younus, 2018). The key characteristics of AC are its high porosity, its adsorption capability, and its unique surface area, which make it a suitable sorbent for the removal of various compounds (Atkinson & Rood, 2012; K. Yang et al., 2010; Hu & Srinivasan, 1999). Suitable carbon support material for enzyme immobilization can minimize diffusion limitations required for efficient bio-catalyzed reactions (Rao et al., 2020). However, the high cost of commercially available AC makes it unsuitable for large-scale operations (Danish & Ahmad, 2018). As a result, low-cost, naturally occurring supporting materials are of interest. Locally available supporting materials with low cost and excellent properties of immobilization have been given much attention in recent years. Tobacco stem, coconut husk, *Albizia lebbeck*, cotton stalk, and pineapple have been thermally activated with KOH and K_2CO_3 activators, yielding activated carbons with a high micropore content (Baysal et al., 2018; Hu & Srinivasan, 1999).

Recently, solvents such as deep eutectic solvents (DESs) have emerged, which serve as promising dual support materials for the immobilization of enzyme. The scientific and industrial communities have recently been captivated by new developments in novel deep eutectic solvents (DESs). A hydrogen bond acceptor (HBA), such as phosphonium or ammonium salt, and a hydrogen bond donor (HBD), such as ethylene glycol, urea, or glycerol, can readily be used for the preparation of DESs (Juneidi et al., 2015; Hayyan et al., 2013). A stable product mixture and a solid network of hydrogen bonds, which offer additional characteristics, show the eutectic merits of the prepared DESs (Yadav & Pandey, 2014; Abbott et al., 2011). Adaptive freezing point, viscosity, improved solvation power and freezing point, and high thermal stability are among the physicochemical properties of DESs which are useful in industrial applications (Hayyan et al., 2021). DESs

also possess other merits, particularly because of their low cost and easily prepared precursor materials, resulting in cheap mixtures which operate differently (Yadav & Pandey, 2014). Furthermore, DES storage is low-maintenance and does not require any additional purification steps. DESs can be formulated for a particular application due to their adaptive physicochemical characteristics (Hayyan et al., 2017). Several research studies have been conducted on DESs and their applicability in several research fields, including chemical reactions and the manufacturing of pharmaceuticals (Liu et al., 2022). Applications also include biofuel development (Hayyan et al., 2021; Hayyan et al., 2017), carbon nanomaterials functionalization (Abed et al., 2022; Cooper et al., 2004), extraction of aromatic compounds from aliphatic mixture (Rodriguez et al., 2015; Hou et al., 2015), porous materials synthesis (Cooper et al., 2004), and biomass processing (Elgharbawy et al., 2020).

Enzymes are excellent for high-performance analysis and can be employed to facilitate environmentally friendly and cost-effective research as natural biocatalysts (P. Reis et al., 2009). Enzymes are also biodegradable and safe, and microbes may produce enormous amounts of them. Despite the benefits, Liu & Dong, (2020) claim that the poor stability and reusability of free enzymes greatly restricts their ability to catalyze reactions. Therefore, different diffusion restrictions imposed by substrate and its product for efficient catalyzed reactions could be overcome by immobilizing enzymes onto the support (Seenuvasan et al., 2020). In fact, lipases can only become active when exposed to support material (Elias et al., 2019).

The supporting materials and solvents such as AC and DESs serve as a significant dual support material for the immobilization of enzymes. AC and DESs have advantages and merits for balancing important influences in boosting biocatalyst performance. Considering the excellent compatibility of AC and DES towards enzymes, the objectives of this chapter are: (1) to examine the influence of conditions used in preparing activated

carbon on the activity of immobilized lipases of porcine pancreas (PPL) and Amano lipase (AML); (2) to determine the effects of AC and DESs on the enzymatic activity of lipase; (3) to discuss and determine the kinetics parameters of the hydrolysis of p-nitrophenyl palmitate by immobilized lipases at optimum reaction temperature and water content in DESs.

3.3. Materials and Methods

3.3.1. Chemical and Biochemical Materials

Palm racemes were utilized as a starting raw material to produce the activated carbon. Palm raceme samples were collected from a variety found in the west of the Baghdad area of Iraq. To remove dust and impurities, the raceme was washed several times in purified water before drying at 100 °C and 24 h, being crushed with a knife's Mill, and being sieved. For the preparation, a portion with an average particle size of 5 mm was chosen. Palm raceme was chemically activated with sodium hydroxide and hydrochloric acid (Poch SA Company, Poland). In addition to sodium deoxycholate (purity 97%), isopropanol, and Arabic gum, Sigma-Aldrich provided the standards and substrate for the lipase assay: p-nitrophenol (*p*NP) and p-nitrophenyl palmitate (*p*NPP). Lipases from the porcine pancreas (PPL) (100 to 500 units, mg^{-1} protein) and Amano lipase PS originated from *Burkholderia cepacia* (AML) (30 units, mg^{-1} protein) and were acquired from Sigma-Aldrich. HmbG Chemicals and MERCK (Hamburg, Germany) provided additional analytical-grade chemicals.

3.3.2. Preparation of AC

Different impregnation ratios (the ratio of activator to dried palm raceme weight) were used to combine 10 g of dried palm raceme with 100 mL of NaOH solution. The concentration of NaOH depends on the impregnation ratio (IR), where 100 mL of distilled

water was added to dry NaOH. The impregnation mass ratios of NaOH to biomass (palm raceme) used in this study were 0.5, 1.0, 1.5, 2.0, and 2.5. The mixtures were then gently heated for half an hour at 80 °C during mixing and then kept for 24 h at room temperature. The treated samples were then dried in an oven (Model IH-100, England) at 100 °C until totally dry and kept in a desiccator. A cylindrical stainless-steel reactor was used to carbonize dried impregnated samples. In an electric furnace, the reactor was heated at a continuous rate of 10 °C min^{-1} and kept (during 0.5–2.5 h) at carbonization temperatures (400–800 °C). The samples were removed from the furnace and allowed to cool at the end of the activation process. The samples were then immersed in a 0.01 M HCl solution for 10 min, resulting in 10 mL. g^{-1} as a liquid to solid ratio. The mixtures were placed overnight at room temperature and washed several times with distilled water before the filtrate pH reached 6.5–7. The samples were dried at 100 °C for 24 h afterward. The impacts of impregnation ratio (0.5–2.5, NaOH/biomass, w/w), activation temperature (400–800 °C), and activation time (0.5–2.5 h) of activated carbon on lipase activity were investigated to optimize the preparation conditions of carbon activated with NaOH. Table 3.1 lists the experimental runs and conditions for preparing AC using NaOH activation. Finally, the samples were placed in tightly sealed bottles for further analysis.

Table 3.1: Factorial design of experimental runs and conditions of activation of carbon with NaOH.

No.	Sample	Activation Temperature /ºC	Impregnation ratio (NaOH/biomass)/(g/g)	Activation Time/ min
1	A 1	400	1.5	90
2	A 2	500	1.5	90
3	A 3	600	1.5	90
4	A 4	700	1.5	90
5	A 5	800	1.5	90
6	A 6	600	0.5	90
7	A 7	600	1.0	90
8	A 8	600	2.0	30
9	A 9	600	2.5	90
10	A 10	600	1.5	30
11	A 11	600	1.5	60
12	A 12	600	1.5	120
13	A 13	600	1.5	150

3.3.3. Preparation of DESs

The DES was prepared from alanine (89.1 g) and NaOH (40 g), which were mixed for two hours at 350 rpm at 85 °C until the DESs appeared to be in the homogeneous phase. The prepared DESs were stored in a regulated moisture state for future use.

3.3.4. Immobilization of Lipases

AML, and PPL were immobilized on 0.1 g of activated carbon that was treated at different conditions, namely A1 to A13. The lipase solution (0.5 mg/mL) was incubated with 0.1 g of AC sample for 2 h at 350 rpm in a thermomixer (BIOBASE), and the activity was then assessed using the lipase assay as illustrated in Section 3.3.5.

3.3.5. Assay for Lipase Activity

A colorimetric method was used to assess the activity of the lipase enzyme in aqueous solutions. To measure lipase activity, the *p*NP which was liberated due to the hydrolysis of *p*NPP was chosen as a standard approach for assessment. Substrate solution A

contained 7 mg of *p*NPP dissolved in 4 mL isopropanol. Solution B contained 0.07 g of Arabic gum and 140 mg of sodium deoxycholate in 65 mL of sodium phosphate buffer (pH 8.00) with 0.35 mL of Triton-X-100 loaded to eliminate turbidity. The final solution was always prepared instantly by mixing solutions A+B. The lipase solution was prepared by dissolving 5 mg of each enzyme in 10 mL of buffer solution (pH 8.00). The reaction was begun by the addition 0.3 mL of lipase, or lipase/DES to 0.1 g of AC, followed by the addition of 0.7 mL of the newly formulated solution. The same amount of the solid lipase was dissolved when preparing the lipase solution in DES and for the purpose of immobilization.

Using a water bath heated to 40 °C, all tubes were incubated for 15 min before the reaction was terminated with a 0.3 mL solution of acetone/ethanol (1:1). A MultiskanTM GO microplate spectrophotometer was used to measure the absorbance of p-nitrophenol (*p*NP) at 410 nm. Each assay was performed three times. At 410 nm, the absorbance of *p*NP was determined to calculate the molar extension coefficient (Є) from the *p*NP calibration curve (Eq. (3.1)). A unit of enzyme activity is described as the enzyme quantity that releases *p*NP (µmol/min/min) = unit/mL. The DES absorbance without an enzyme was deducted from the actual data for value adjustment.

$$\text{Lipase Activity } \left(\frac{\text{U}}{\text{mL}}\right) = \frac{\text{µmol of pNP realease} \times \text{Total reaction volume}}{\text{volume used in spectrophotometer} \times \text{enzyme volume}} \times \frac{1}{\text{reaction time (min)}}\text{ty U/mL= µmol of pNP realease} \times \text{Total reaction volume/volume used in spectrophotometer} \times \text{enzyme volume} \times 1/\text{reaction time (min)} \quad (3.1)$$

The relative activity of lipase was calculated based on Eq. (3.2):

$$\text{Relative Activity\%} = \frac{\text{Residual activity (Final}-\text{Initial)U/mL}}{\text{Initial Activity U/mL}} \times 100\text{vity\%= Residual activity (Final-Initial)U/mL/Initial Activity U/mL} \times 100 \quad (3.2)$$

where Initial is the activity of lipase before treatment (the control), Final is the value of the lipase activity after treatment, and Residual activity of the enzyme is the difference between the final value after treatment and before the treatment (control).

3.3.6. Screening of Lipases Activities with Different Activated Carbon

With the thirteen AC samples mentioned in Table 3.1, two types of lipases, PPL and AML, were screened. In a 2-mL centrifuge tube, the buffer was combined with 1 mL of the free lipase or AC/lipase samples. In the control samples, lipase solution that was prepared in phosphate buffer was used with a 1:1 ratio (1 mL of enzyme at 0.5 mg/mL in 1 mL of buffer), while for the DES/lipase samples, a 1:1 ratio was used with 1 mL enzyme solution against 1 mL DES. All samples were vortexed before proceeding with the following steps. All samples were labeled from A1 to A13 and then accordingly loaded with 0.1 g of AC. The solutions were incubated for 2 h at 350 rpm in a ther-momixer (BIOBASE). The supernatant was collected after centrifuging for 2 min (8000 rpm). The supernatant samples were then subjected to lipase activity determination as described in Section 3.5.

3.3.7. Statistical Analyses

Data were expressed as mean ± standard deviation of triplicate analyses. Analysis of variance (ANOVA) was conducted using GraphPad Prism version 9.0.0 to determine the significant difference between the means at a 95% confidence level ($p < 0.05$).

3.3.8. Morphology of Activated Carbon

The surface characteristics of AC were tested by N_2 adsorption–desorption isotherms at 77 K under varied relative pressure levels. The surface area of the selected AC was determined by the Brunauer Emmett and Teller (BET) surface area analysis using a fully automated gas sorption system (Micromeritics ASAP2020,Plus 2.00) as described by

(Liu & Dong, 2020). The BET method was used to calculate the surface area, and the t-plot method was used to calculate the volumes of the micropores and mesopores. Scanning electron microscopy (SEM) was also utilized to identify the surface morphology of AC.

3.4. Results and Discussions

3.4.1. Effect of Activated Carbon on Lipase Activity

3.4.1.1. Screening of Lipase Immobilization in Different AC

Figures 3.1 and 3.2 present the relative activity of AML and PPL after the immobilization on AC, after incubating all samples for 2 h before conducting the lipase assay. PPL and AML controls (CTRL) were added for comparison (CTRL is the free forms of the enzymes PPL and AML in phosphate buffer). However, we observe that AML was not enhanced by the immobilization on AC, though the activity was maintained around 80%. However, the highest red shade was observed in A1 and A2.

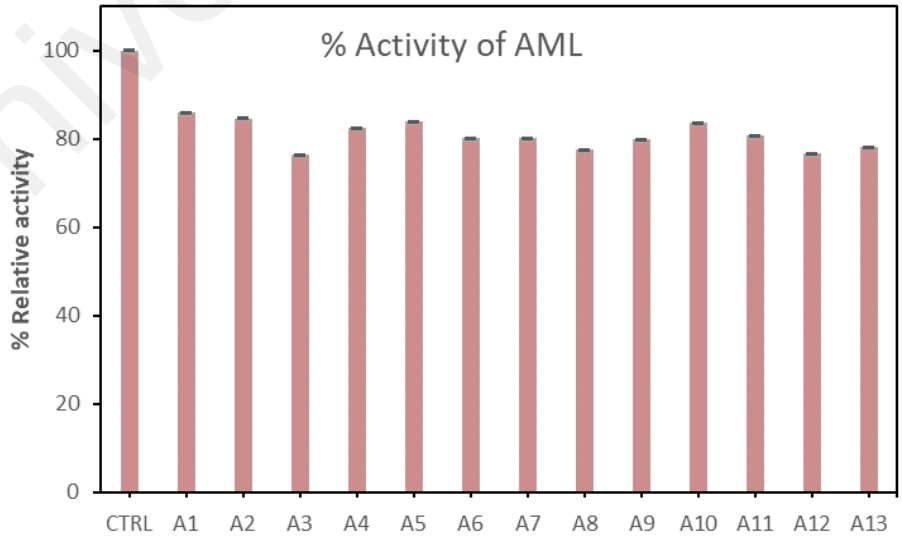

Figure 3.1: Relative activity of Amano lipase (AML) after immobilization on activated carbon samples from A1 to A13.

Figure 3.2 shows the effect of 13 types of AC on porcine lipase. It can be seen that A1 was recorded to have the highest activity. It also shows that the enzyme was immobilized successfully by activated carbon. The pores and active sites on the activated carbon enhanced the immobilization of enzymes in the micro- and mesopores. Furthermore, the lipase molecules are bound on the surface of the supporter after immobilization (Putra et al., 2022).

To confirm this, we have conducted a one-way ANOVA analysis to evaluate the statistical differences. R-squared revealed a good fit of the data with a significant difference among the mean values.

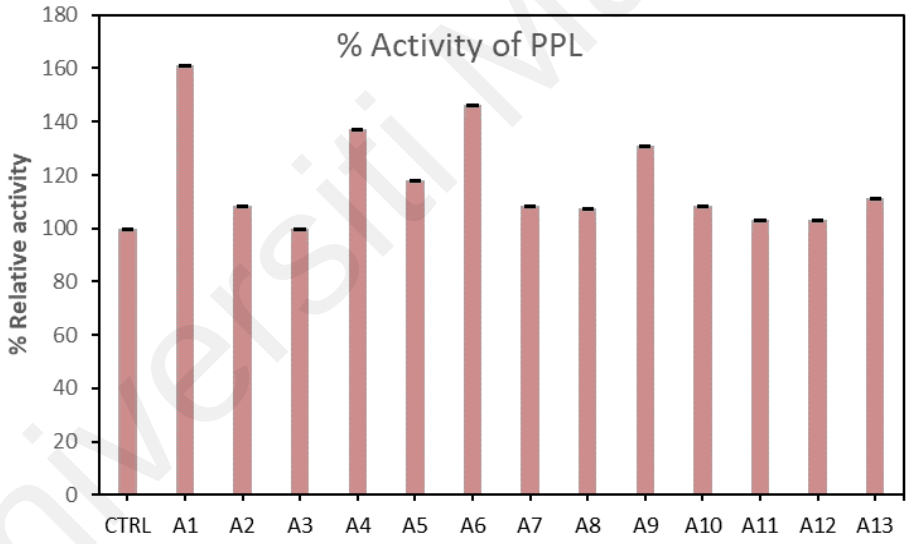

Figure 3.2: Relative activity of the Porcine enzyme (PPL) after the immobilization on activated carbon samples, from A1 to A13.

3.4.1.2. Carbonization Temperature Effect

The surface morphology, surface area, and pore size of AC were all affected by activation time and temperature. The relative activity of two types of lipases immobilized on activated carbon prepared at various temperatures is reported in Figure 3.3. The

carbonization temperature for all samples of AC was in the range of 400–800 °C. The enzymatic activity without AC was taken as 100% (control samples). Subsequently, Figure 3.3 illustrated that AML showed no improvement in enzymatic activity when immobilized on AC, while porcine lipase PPL showed more interaction with AC. As shown in Figure 3.3, the carbonization temperature of AC at 400 °C resulted in the highest activity for the porcine lipase. It is also worth noting that, at 700 °C, the results improved slightly. However, from a saving energy point of view, a low temperature is recommended. Therefore, 400 °C was selected as the best carbonization temperature to prepare AC in the enzymatic reaction.

A high temperature will affect the surface of the AC and may enhance the porosity of AC, and this lipase enzyme will not be bound or supported for a further reaction such as hydrolysis. For instance, Tsai W. (1994) investigated the influence of temperature on the adsorption of chlorinated volatile organic compounds, claiming that, when the temperature was raised from 283 to 313 K with a 440 mg L^{-1} intake, the absorption of methylene chloride on AC was decreased by 60% (Tsai, 1994). This supports our argument for lower lipase adsorption on the AC carbonized at a high temperature above 500 °C.

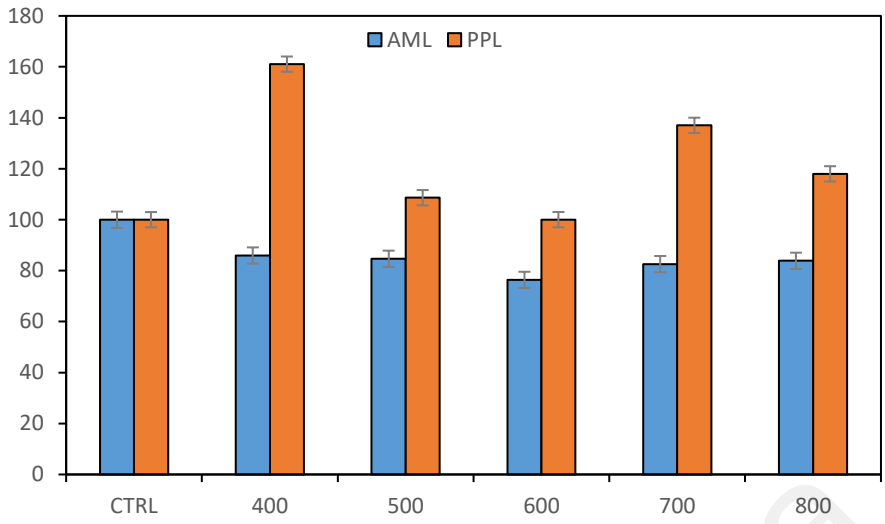

Figure 3.3: Effect of carbonization temperature of samples A1–A5 on the relative activity of two types of im-mobilized lipase, Amano lipase (AML) and porcine lipase (PPL), against the free lipases.

3.4.1.3. Effect of Impregnation Ratio

The impregnation ratio is one of the main factors which influence the formation of porosity and the development of the surface area in activated carbon. Figure 3.4 shows the impregnation ratio of an activator such as NaOH to biomass (palm raceme). At a carbonization temperature of 600 °C and a carbonization time of 90 min, the impregnation ratio (IR) effect on the immobilization of lipases was investigated. At different impregnation ratios, porcine lipase (immobilized PPL) activity was enhanced compared to AML.

The impact of the activation on the ratio of raw material on the Brunner Emmet and Teller (BET) surface area, and total pore volume, was more pronounced at 400 °C. At low activation temperatures, the activator to biomass ratio substantially affected the BET surface area, micropore volume, and micropore surface area (Danish & Ahmad, 2018). Furthermore, PPL activity was recorded at its highest at a 0.5 impregnation ratio (A10). When the impregnation ratio is higher, more Na molecules diffuse into the pores, making the holes bigger and creating large pores (Islam et al., 2017), and this is not suitable for

enzyme immobilizing and may affect the reaction negatively. Thus, the activation mechanism plays a crucial role in pore growth by increasing the impregnation ratio, resulting in a sustained increase in the BET surface area and pore volume (Rashidi & Yusup, 2019).

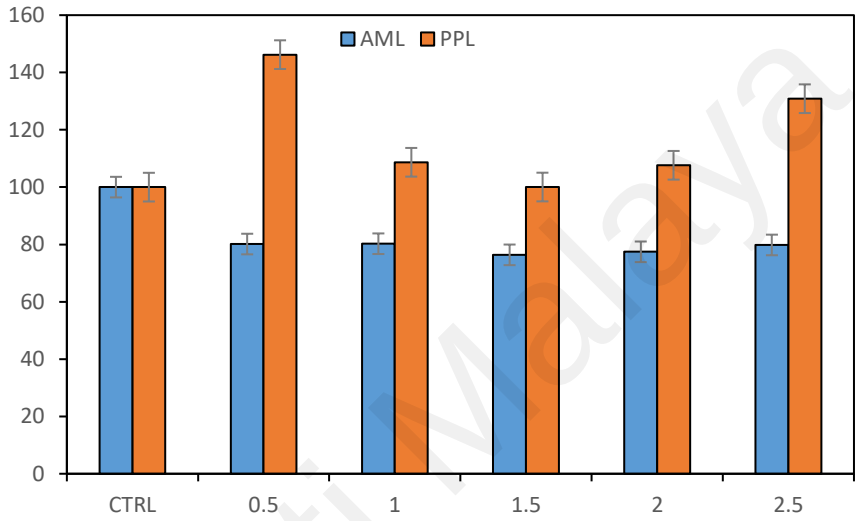

Figure 3.4: Effect of impregnation ratio (samples A3 and A6–A9) on relative activity for two types of immobilized lipases, Amano lipase (AML) and porcine lipase (PPL), compared to the free enzyme (CTRL).

3.4.1.4. Effect of Carbonization Time

Surface morphology, surface area, and pore size are all affected by carbonization time. Figure 3.5 shows the impact of carbonization time of AC on the immobilized lipase's activity. The carbonization time for all AC samples was about 30–150 min. For the enzymatic activity of lipase, at a constant activation temperature, the influence of changing the activation time was detected. Without AC, enzyme activity was 100%. Following that, Figure 3.5 showed that AML recorded no enhancement in the enzymatic activity (85%), while PPL interacted with AC more effectively, providing greater and more stable adsorption with AC; this is mainly due to evaporation of volatile materials

from the pores and surface of AC (Heidarinejad et al., 2020). At the same time, new pores and active sites formed on the surface of the carbon, which can contribute to lipase immobilization. The following conditions were optimal for preparing AC for PPL lipase immobilization: an impregnation ratio of 0.5 (NaOH/palm raceme, (g/g)) and an activation temperature of 400 °C for 150 min.

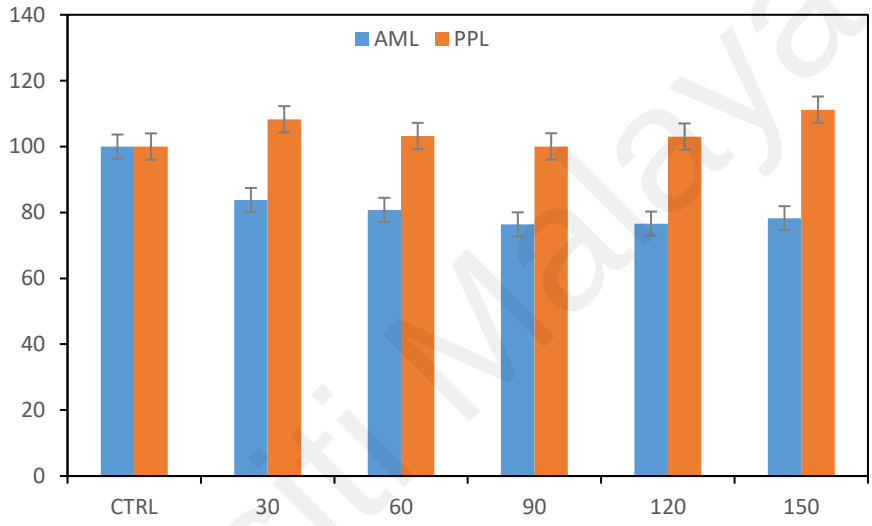

Figure 3.5: Impact of carbonization time on the relative activity of two types of immobilized lipase, Amano enzyme (AML) and porcine enzyme (PPL), against the free lipases (carbonization Temperature 600 °C and impregnation ratio 1.5).

3.4.2. AC and DESs Effect on the Activity of Lipases

3.4.2.1. Effect of Reaction Temperature

Further research into the impact of temperature on the immobilized enzyme activity was carried out. The findings revealed a typical enzyme activity pattern, with the ideal reaction temperatures ranging from 40 to 80 °C for each lipase. Figure 3.6 depicts the behaviors of lipase at different incubation temperatures. The phosphate buffer medium was the main medium for the enzyme reaction. The findings indicate a positive tendency of changing the optimal temperatures for the reactions for two hours, from 40 °C to 80

°C. The optimum temperatures for AC/DES/Enzyme and AC/Lipase enzyme were 60 and 40 °C, respectively. A significant relative activity (290%) was achieved by incubating the lipase with AC/DES.

As the reaction temperature was raised, enzyme activity gradually increased until it reached a certain point (around 60 °C). However, the reaction rate slowed significantly due to protein denaturation at higher temperatures (Elgharbawy et al., 2018). At high temperatures, the heat-induced disruption of non-covalent bonds triggered the partial unfolding of the enzyme. Further, because most known enzymes are proteins, they are protected from dehydration by water molecule layers which are bound to the surface of the protein. This hydrating layer, or at least a fraction of it, is a necessary component of the structure of the protein which is to serve as an enzyme (Ballesteros et al., 1998). Raising the temperature or adding organic solvents could significantly change the protein composition, leading to denaturation. As a result of many water molecules being withdrawn from the protein's hydrating layer, exposing the enzyme to elevated temperature, the enzyme is inactivated. This is apparent because the enzyme's relative activity hit 290.20% even at 70 °C when DES and AC were added as the necessary water layer required for the enzymatic activity, which is preserved due to the protein's adsorption on AC and AC/DES complex. AC-DES exhibited good stability at an elevated temperature, as the DES was acting as additional coating and protecting the enzyme from denaturing. For instance, the experimental results indicated that lipase incubation in slightly hydrated alanine [5% (v/v)] led to the highest level of residual activity, implying interfacial activation (Shehata et al., 2020). Furthermore, several researchers have reported that glycerol-containing DESs promote lipase activity (Tan & Dou, 2020; Elgharbawy et al., 2018).

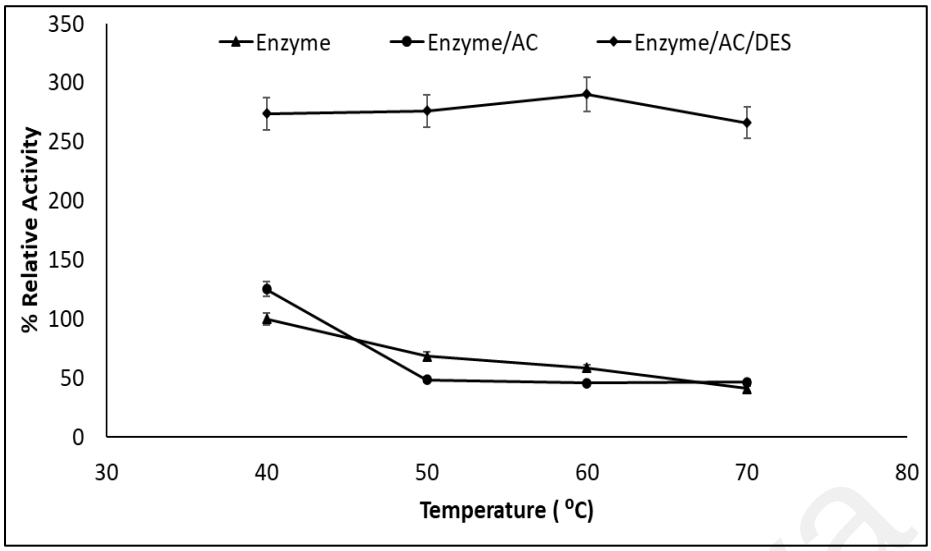

Figure 3.6: Immobilized and free Lipase activities at various incubation temperatures (2 h incubation time and 1:1 DES molar ratio).

3.4.2.2. Impact of Water Content

The fundamental factor which distinguishes molecular behavior in different media is the effect of water hydration between the enzyme and the bulk solvent (Fogarty & Laage, 2014). The reaction was carried out in the DES as a medium without changing the water content of the DES in the previous section (Section 3.4.2.1). However, according to previous studies, water is needed both for the three-dimensional arrangement of enzymes and the stabilization of protein (Durand et al., 2013). Water content in the range of 20–80% was investigated. Figure 3.7 shows the effect of water content on the immobilized lipase. DES improved the relative enzymatic activity up to 3–4-fold in the range of 20–80% water content. Nevertheless, introducing the DES/AC complex to the reaction media improved the relative activity up to 2–4-fold in the range of 20–40%. Overall, increasing the water content of DES slightly increased the relative activity after 40%.

Experimental observations confirmed the trend of DES activity after an hour of incubation. DES, without any ratio of water added, can enhance the enzymatic activity to a certain level. However, introducing water at a certain ratio to any enzymatic reaction

such as a hydrolysis reaction may contribute to the catalytic enhancement (Elgharbawy et al., 2018). Previous work (Huang et al., 2014) has also confirmed that the DES itself, rather than its fragmented components, influenced the enzyme's catalytic properties. It is proposed that the DES solubilized in an aqueous solution still exists, persisting as an intact cation-anion–HBD complex, and this is mainly due to the strong ionic contacts between the cation and the anion, and hydrogen-bond interactions between the anion and the HBD. Furthermore, in a molecular simulation study, the addition of water to alanine resulted in a significant increase in backbone mobility and a decrease in the compactness of lipase structures, which became more obvious for the open conformation, at 373 K, and high water levels (Shehata et al., 2020). Overall, their findings suggest that alanine-based DES could be a promising solvent, particularly for the application of lipase at high temperatures. While increasing the water content of alanine slightly increased the backbone flexibility, hydrated DES, especially at low levels (concentration of DES 30 wt.%), still exhibited thermo-stabilizing properties.

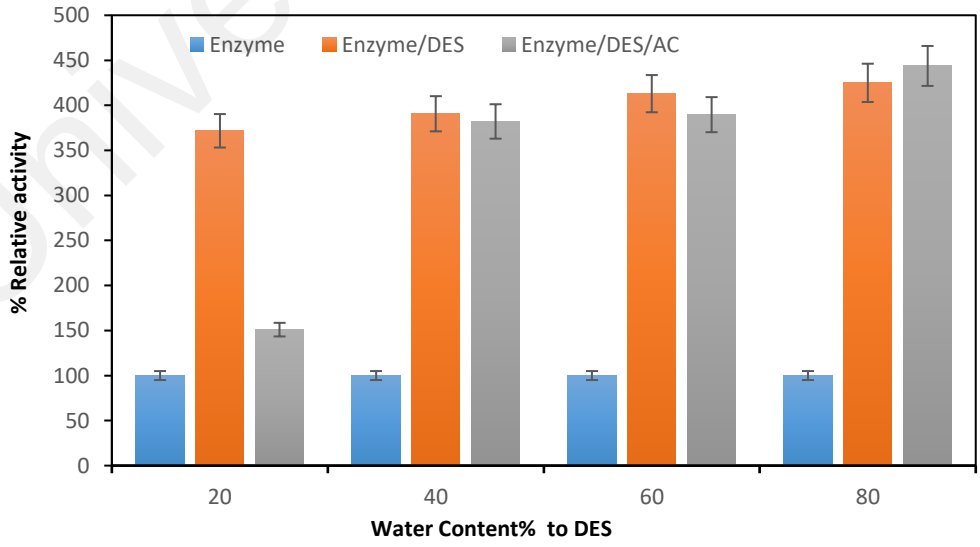

Figure 3.7: Activity of immobilized and free porcine pancreas lipase (PPL) at different concentrations of aqueous DES (1:1 NaOH: Alanine)

3.4.2.3. Kinetics Study

Further experiments were carried out to observe how AC with DES affected the kinetic parameters as contrasted to the buffer medium (control sample). Table 3.3 summarizes the findings. Measurements of enzyme activity with different concentrations of the substrates were used to evaluate the K_m and V_{max} values of the reaction of the hydrolysis of *p*NPP. The non-linear Michaelis–Menten curve was used to determine the parameters with which to express enzyme kinetics.

The kinetic parameters were determined based on the optimum water content value and the optimum temperature for porcine lipase. Kinetic parameters were computed at different concentrations of the substrate (*p*NPP), with the parameters being 2.5, 2.0, 1.5, and 1.0 mM. The kinetic parameters, maximum velocity (V_{max}), and Michaelis–Menten constant (K_m) were obtained after plotting the kinetic curve with a hyperbolic equation using the software GraphPad Prism. The catalytic measures of the turnover number (k_{cat}) and catalytic efficiency (K_{cat}/K_m) were computed, as the amount of enzyme used was known, see Figure 3.8.

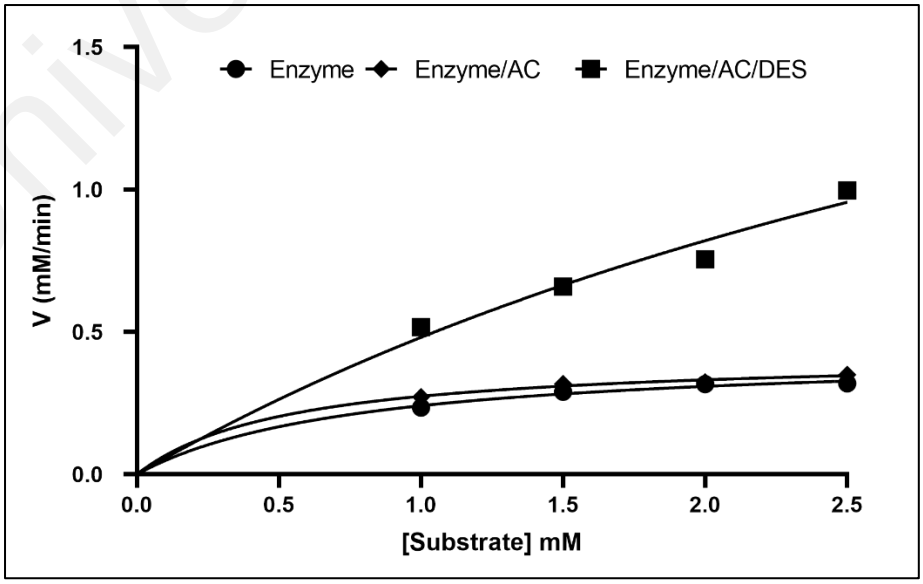

Figure 3.8: Non-linear kinetic curve (Michaelis–Menten equation) for PPL: free enzyme (control), enzyme with AC, and enzyme with AC/DES.

The kinetic parameters V_{max} of the porcine enzyme (PPL) and porcine enzyme immobilized on AC in DES as a medium were also estimated at 0.43 and 2.80 mM min^{-1}, and the K_m was calculated as 0.78 and 4.79 mM, respectively. The KM for the immobilized porcine lipase on AC was 4.5-fold lower than the porcine lipase in phosphate buffer (free enzyme). This indicates that the immobilization of PPL on AC increases the affinity of porcine lipase towards the substrate, which may be due to minor changes caused by electrostatic, hydrogen bonding, or the adsorption of PPL on the AC surface. Moreover, the V_{max} value for immobilized porcine lipase in DES medium was higher than that for free porcine lipase, and the activity significantly increased. The results agree with those obtained by Elgharbawy et al.(2020) using dendrimers nanomaterials for lipase activation.

A study by Ramani et al. (2012) dealt with mesoporous activated carbon (MAC) sur-face functioning, employing ethylene-amine and glutaraldehyde for strong acidic lipase (AL) immobilization on the MAC. AL has been made by employing lipid waste and fermentation by *Pseudomonas gessardii*. This study shows that the KM value of the immobilized lipase (0.21 mM) was lower compared to the free lipase before immobilization (0.66 mM) (Ramani et al., 2012). These results agree with our findings. In addition, two different techniques were employed by Soni et al. to immobilize *Burkholderia cepacia* lipase treated with surface carbon nanofibers, adsorption and covalent immobilization (Soni et al., 2018). They calculated the kinetic parameters and found that K_m was 2.07 mM and V_{max} was 1.73 mmol min^{-1} g^{-1} for the free lipase. In contrast, the values recorded for immobilized lipase were 0.15 mM and 1.77 mmol min^{-1} g^{-1}, respectively (Soni et al., 2018). In comparison to the results obtained in our study, the data are analogous since the activated carbon did not alter the V_{max}. However, the presence of the DES increased the value of activity significantly.

The overall efficiency calculation revealed that the catalytic activity of immobilized PPL with AC is two and four times higher than both pure PPL and PPL immobilized with AC in DES medium. This shows the promising capacity of the activated carbon in the enzymatic performance, although the velocity of the reaction was higher in the DES medium. However, the findings could be slightly different if other types of DESs were to be used in the study. It is to be noted that the study aimed not to investigate the effect of DESs, but rather to find the interaction of lipases with activated carbon and DESs.

Table 3.2: Kinetic parameters of immobilized and free porcine lipase (PPL) in various reaction media using pNPP at different concentrations.

Medium	K_m (mM)	V_{max} (mM min^{-1})	K_{cat} (min^{-1})	K_{cat}/K_m (min mM^{-1})
Enzyme only	0.78 ± 0.03	0.43 ± 0.03	4.01 ± 0.03	5.14 ± 0.01
Enzyme/AC	0.17 ± 0.02	0.42 ± 0.03	3.71 ± 0.02	21.82 ± 0.03
Enzyme/DES/AC	4.79 ± 0.03	2.80 ± 0.02	49.07 ± 0.01	10.24 ± 0.03

3.4.3. Morphology of A C

The surface area and pore characterization of AC was measured. Figure 3.9 shows the N_2 adsorption–desorption isotherm for AC, and the result showed that the micropore volumes are 0.047 cm^3/g, and the surface area was 117.447 m^2/g. This is conducive to provide more active sites for the lipase immobilization. The micropore volume structure was also confirmed by the fact that the produced AC had a micropore volume of 0.047 cm^3/g, which is suitable for lipase adsorption. Islam et al. (2017) found that AC from rattan hydrochar had an average pore width of 3.55, confirming the trend of NaOH activation to form mesoporous carbon. It was hypothesized that increasing the activator-to-hydrochar ratio would increase the activator's etching depth on the hydrochar surface, converting more micropores to mesopores.

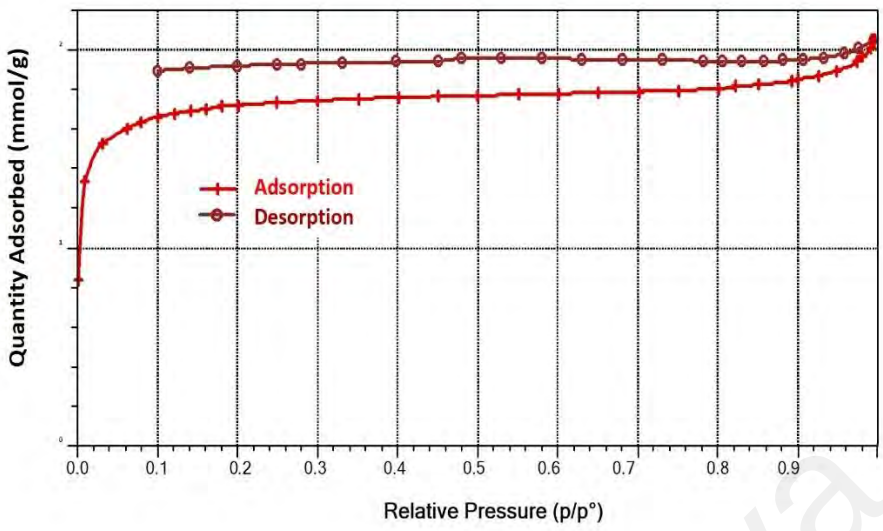

Figure 3.9: Adsorption–desorption isotherm curves of AC from palm raceme.

The surface morphology of activated carbon was observed under scanning electron microscopy (SEM). The morphology of the activated carbon surface 1.00k magnified is shown in Figure 3.10.

The surface of activated carbon development and uniformity were both enhanced by NaOH activation. The formation of a well-organized pore structure was accomplished. The shape, size, and structural changes in enzymes and supporters are frequently determined by identifying and characterizing the supporter (Arsalan & Younus, 2018). The good mechanical properties and the large surface area can hold enough enzymes with minimum diffusion (Mohamad et al., 2015).

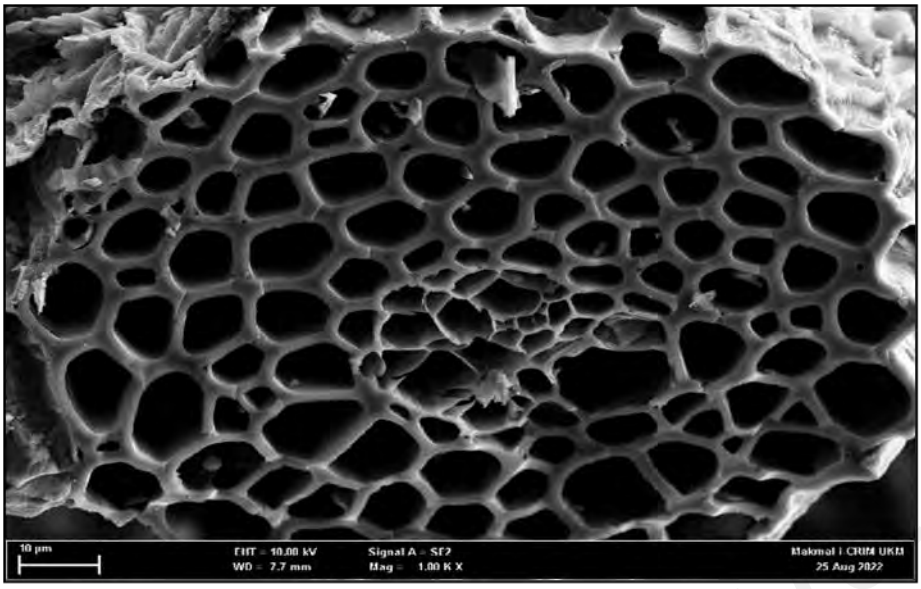

Figure 3.10: SEM image (at 10 µm scale) of prepared activated carbon at 1000X magnification.

Hydrochar's C-O-C and C-C bonds are broken during the activator's dehydration effect, leading to the formation of AC porosity. As a result of this reduction process, the sodium hydroxide (NaOH) is transformed into sodium metal, sodium carbonate (Na_2O_3), and hydrogen gas (H_2), as demonstrated by Eq. (3.3)

$$6NaOH + 2C \xrightarrow{\Delta} 2Na + 3H_2 + 2Na_2CO_3 \quad (3.3)$$

The breakdown of Na_2CO_3 into Na, CO, and CO_2 results in additional activation when N_2 gas is present, and the temperature is high. As a result, more Na molecules diffuse in the pores, widening the holes and forming new pores (Islam et al., 2017).

3.5. Conclusions

In this study, AC prepared from palm raceme was successfully utilized for the immobilization of AML and PPL. Alanine-based DES was used for the first time as a co-solvent for the enhancement of enzymatic activity. The results showed that AC can significantly increase the enzymatic activity of PPL, performing better than AML. Different samples (13 in total) of AC were treated under different conditions and defined

as A1–A13. In order to select the optimum treatment conditions, these samples were used for enzymatic immobilization and for enzymatic activity enhancement. Under optimum treatment conditions of impregnation mass ratio of 0.5, 150 min, and carbonization temperature of 400 °C, the highest relative enzymatic activity was 162.5% for PPL. Different operating parameters such as incubation temperature and water contents were optimized for the selected AC with/without the aid of DES. Immobilized PPL on AC/DES medium at 60 °C optimum incubation temperature achieved 290.2% of relative enzymatic activity. The relative enzymatic activity was improved up to three-to-four-fold in the range of 20–40% water content. Furthermore, kinetics data revealed that the catalytic activity of immobilized PPL with AC was two and four times higher, respectively, than both neat PPL and PPL immobilized with AC/DES medium. These findings and conclusions are evidence that the immobilization method using AC and DES is an ideal choice for potential implementation, with specific use for biotechnology applications.

CHAPTER 4: LACTIC ACID-BASED DEEP EUTECTIC SOLVENTS AND ACTIVATED CARBON FOR SOAP REMOVAL FROM CRUDE BIODIESEL

4.1. Introduction

This chapter aims to provide a comprehensive examination of the properties and potential uses of DESs, as well as the removal of soap from crude biodiesel. The physical properties of deep eutectic solvents (DESs) such as density, viscosity, conductivity, melting point and thermogravimetric analysis (TGA) prepared from tetramethylammonium chloride (TMAC) and lactic acid (LA) were investigated at temperatures from 303.15 K to 373.15 K. Three adjustable parameter correlations such as the Vogel-Fulcher-Tamman (VFT), Arrhenius and Litovitz models were used in the viscosity experiments. In addition, DESs and activated carbon (AC) were employed for the removal of soap from biodiesel as an alternative to traditional water-based washing operations. Moreover, the DESs molar ratio, DESs to biodiesel volume ratio, stirring speed, and extraction time were optimized. The utilization of AC and DES can be considered as a new route for the downstream processing of crude biodiesel and could replace water as the washing agent. The results of this chapter were published in the Journal of Biomass Conversion and Biorefinery, (Abed et al., 2023).

4.2. Literature Review

Ionic liquids (ILs) are compounds consisting of organic cations and inorganic anions which possess exceptional qualities such as low melting points (less than 100 °C) at ambient pressure and temperature, broad liquid phase range, non-flammable, high thermal stability and an exceptionally low vapor pressure (Hu et al., 2004; Sun et al., 1998). In recent years, there has been a remarkable growth in the study of ILs. Some of

the potential uses of ILs are as replacements for organic solvents in chemical processes (Hayyan et al., 2010; Wasserscheid & Welton, 2007; Harper & Kobrak, 2006; Visser et al., 2002). This is due to the very low vapor pressure of ILs without the presence of volatile molecules, which have attracted huge interest in green chemistry and engineering (Visser et al., 2002). Thus ILs could also be used in a variety of applications (Hayyan et al., 2010).

Green solvent research has piqued the interest of chemists, while the utilization of deep eutectic solvents (DESs) in chemical processes has increased dramatically. DESs have shown potential as substitutes to traditional solvents used in various processes, with improved sustainability and performance. Subsequently, DESs fully conforms to the principles of green chemistry as they are easy to synthesize from readily available raw materials and is environmentally sustainable, thus making it a viable option as green solvents for the removal of impurities from biodiesel. Generally, DES are also recognized as molten salts and are viable equivalents to traditional ILs (Hayyan et al., 2013; Hayyan et al., 2012). While ILs are valuable commodities in the fine chemical market, their utilizations in the nutrition and therapeutic industry are limited due to the toxicity, low purity and high costs (Morrison et al., 2009). DESs are composed of different anions (Smith et al., 2014) and are prepared from charge delocalization via the formation of an eutectic mixture with lower melting point than ILs, i.e. by the combination of a hydrogen bond acceptor (HBA) with a hydrogen bond donor (HBD) (Hayyan et al., 2013). DESs possess unique combination of properties that make them versatile solvents for a wide range of applications. Furthermore, with the utilization of quaternary ammonium salts, DESs offers a wider range of benefits over ILs, such as lower production costs, facile synthesis and high biocompatibility (Hayyan, et al., 2013). Moreover, the widespread utilization of synthetic ILs in the pharmaceutical and food-related applications is restricted by the toxicity of certain ingredients, as reported by previous studies (Zhao et

al., 2007; Docherty & Kulpa Jr, 2005). The toxicity of ILs presents a significant obstacle in their applications. In contrast, DESs which are considered as alternatives to ILs due to their lower toxicity effects have been utilized in the removal of environmental toxins (Yang et al., 2013; Li et al., 2008), fuel purification (Cheung et al., 2013; Abbott et al., 2007), organic extraction, organic reactions (Imperato et al., 2005), enzyme reactions (Abed et al., 2022), material surface chemistry (Abed et al., 2022b) and electrochemical processes (El Ttaib, 2011). The utilization of DESs in the field of separation is a growing area of interest, due to their numerous advantages such as the ease of preparation, lower cost, biodegradability and lower toxicity. These unique attributes of DESs offer highly attractive options for various separation applications. This work aims to provide a comprehensive examination of these properties and the potential uses of DESs, as well as addressing the need for further research in this area.

Biodiesel is an ecologically friendly and clean fuel alternative that is of interest to the bioenergy sector due to the high demands of sustainable energy generation (Hayyan et al., 2021). The transesterification of animal fats or vegetable oils catalyzed by NaOH or KOH is mostly utilized in the synthesis of biodiesel (Borges & Díaz, 2012). The advantage of this method is that it produces high yields of methyl esters in mild circumstances which requires shorter time for product formation (Sharma et al., 2011). Despite the various type of catalysts available in the transesterification reaction, the presence of unwanted byproducts such as soap and glycerides render the entire process ineffective. Soap is the most significant pollutant in biodiesel, thus must be removed to avoid instrumental breakdown and filter clogging. Tai-Shung (2007) reported that the purification process accounts for a significant portion, around 60-80% of the total cost of biodiesel production. The traditional methods of purification, such as the use of separators and evaporators, are ineffective in eliminating contaminants such as soap, free glycerol, traces of the catalyst, alcohol, water, metals and glycerides. To meet the ASTM D 6751

(Astm, 2012) and EN 14214 (EN, 2003) international standards, it is necessary to thoroughly verify and eliminate these contaminants from biodiesel. Furthermore, the washing step in the purification process requires large water consumption, where the volume of water needed for purification is ten times of the volume of biodiesel (Karaosmanoğlu et al., 1996). This not only increases the costs for purification, but also releases large quantities of wastewater (Veljković et al., 2015). Thus the decontamination of biodiesel is a critical phase that must be constantly improved to meet the international standards. One such alternative to the traditional water-based washing is the use of green solvents such as DESs. These solvents are not only environmentally friendly but are also more cost-effective compared to the traditional solvents. This work investigates the potential uses of DESs as a replacement for water in the removal of soap from biodiesel.

The density, viscosity, eutectic point, conductivity and thermogravimetric analysis (TGA) are important physicochemical properties that define the use of a DES for a particular application (Visser et al., 2002). Thus, substantial efforts have been focused on the physicochemical characterization of DESs. A novel study on the physical characteristics of fructose and glucose-based DESs prepared by the combination of choline chloride with monosaccharides such as D-glucose anhydrous was recently published (Hayyan et al., 2012). Glycerol (GL) and ethylene glycol (EG) were the HBD used to study the physical properties of choline chloride (ChCl), N,N-diethylenethanolammonium chloride (DAC), methyltriphenylphosphonium bromide (MTPB) and benzyltriphenylphosphonium chloride (BTPC)-based DESs (Hayyan et al., 2015). Leron et. al (2012) studied the densities and refractive indexes of DESs and their aqueous mixtures prepared from mixing choline chloride with ethylene glycol or glycerol.

This chapter investigates the influence of salt and HBD mole ratios on the various physicochemical properties. The outcomes of this research emphasize the physicochemical properties of DESs as prospective solvents. The physical properties of

these novel classes of DESs assist in the exploration of related applications, as well as the purification of chemical processes utilizing these DESs. This study is a continuation of our efforts to utilize DESs in green and sustainable applications in biodiesel research. The physical parameters such as density, viscosity and electrical conductivity were measured as a function of temperature.

4.3. Materials and Methods

4.3.1. Chemicals

Tetramethylammonium chloride (TMAC), hydrochloric acid (HCl), and acetone for synthesis were procured from Merck, while potassium hydroxide and bromophenol blue were supplied by Sigma-Aldrich. Lactic acid (LA purity 99%) was supplied by Johchem Sdn. Bhd. (Malaysia), methanol (MeOl) was supplied by Chemiz Sdn. Bhd. (Malaysia), while refined palm oil was supplied by local mill in Selangor, Malaysia. The activated carbon (AC) used in this study was prepared from palm raceme, reported elsewhere (Abed et al., 2022).

4.3.2. Preparation of DES

Although there have been some subsequent modifications in the DESs synthesis processes, the majority of DESs were prepared using the method reported by Abbott et al. (Abbott et al., 2003). The DES was synthesized by mixing tetramethylammonium chloride (TMAC) with LA as the HBD at 1:1, 1:2, 1:3 and 1:4 molar ratios. TMAC was dried before use in the preparation of DES. In this investigation, both the salt and the HBD were mixed in a jacketed cup with a motorized stirrer. The synthetic process produced a homogeneous and colorless liquid via mixing for 3 hours at 70°C. In addition, the moisture content of the DES samples was carefully regulated at ambient pressure, and the samples were stored in a desiccator to prevent moisture absorption.

4.3.3. Production of Biodiesel

Biodiesel is produced through a process known as transesterification. This process involves the reaction of vegetable oils or animal fats with primary alcohols such as methanol or ethanol using an acid or base catalyst. Refined palm oil (RPO) was selected for the production of biodiesel using potassium hydroxide (KOH) as the catalyst. Methanol and potassium hydroxide were mixed to produce the potassium methoxide mixture. The RPO was then mixed with 1%wt/v KOH in a 2.5 L reactor at a molar ratio of 1:10 (oil to methanol) thus providing excess methanol for the reaction (Arenas et al., 2021). The mixture was stirred for an hour at 500 rpm and 60 °C using a hotplate magnetic stirrer, followed by centrifugation for 10-20 minutes at 2500 rpm to separate the biodiesel from glycerol. The crude biodiesel was centrifuged and boiled for 15 minutes at 70–80 °C to eliminate the remaining methanol.

4.3.4. Physical Properties Measurements for DESs

Thermogravimetric analysis (TGA) and differential scanning calorimeter (DSC) were used to measure the thermal properties and the eutectic points. TGA was performed in nitrogen atmosphere using a Mettler Toledo TGA instrument to determine the thermal stability of the DES at various ratios. The onset of the decomposition temperature was investigated at a temperature range of 30 °C – 400 °C, a heating rate of 10 C/min and a nitrogen flow rate of 20 mL/min. Due to the hygroscopic property of the DES, every sample was heated at 378.2 K (105.05 °C) before each measurement to eliminate any moisture-related fluctuations in the decomposition curves (Navarro et al., 2013).

The freezing point temperatures of (TMAC and LA based) DESs mixtures at different molar ratios were determined using a differential scanning calorimeter (DSC) (Perkin Elmer DSC 8000). The measurement was carried out under liquid N_2 cooling system. Samples were hermetically sealed in aluminum pans, was heated from -70 °C to 170 °C

and then cooled from 170 °C -70 °C at a rate of 10 °C/min followed by heating to 170 °C with the same heating rate in 20 ml/min of N_2 gas.

After processing, all samples were maintained in well preserved vials, and only freshly prepared samples were used in the evaluation to minimize any structural changes and humidity effects from the environment that may affect the physicochemical properties of the DES. All physical properties were investigated over a temperature range of 303.15–373.15 K in this study. A rotating viscometer (Anton Paar Rheolab QC) was used to measure the viscosity of the DESs. A surrounding water circulator (Techne-TempetteTE-8A) with a temperature range of 30–80 °C was utilized to control the temperature. A KRUSS (K100M) tensiometer was set to a temperature range of 30–85 °C and regulated by a surrounding water circulator to assess the density. The ionic conductivities of the DESs were measured at various temperatures using a Eutech Cyberscan Con 11 hand-held conductivity meter. A temperature-controlled water bath was employed to control the differential temperature. The conductivities of several KCl solutions were used to determine the accuracy of the conductivity meter. Table 4.1 shows the uncertainties in the experimental measurement for each physical property.

Table 4.1: Experimental uncertainties in measurements.

Property	**Estimated uncertainties**
Density	±0.0001 g cm^{-3}
Viscosity (relative)	3-5 % of measured value
Conductivity	1.05S. cm^{-1}

4.3.5. Soap Removal from Biodiesel Using DESs

Screening studies were employed in the liquid-liquid steps to determine the best DESs molar ratio for the extraction of soap from BD. The synthesized DES was combined with 0.03 g of AC and 100 ml biodiesel in a conical flask. The extraction was performed by

filling the conical flask halfway with DES and biodiesel. In each measurement, different DES to biodiesel ratios were used by increasing the amount of biodiesel while keeping the DES constant. Four alternative DES: biodiesel volume ratios (1:1, 1:2, 1:3 and 1:4) were investigated with the increase in the volume of biodiesel. The orbital shaking (50-250 rpm) and duration (2-10 minutes) were used in the extraction trials to homogenize the biodiesel /DES mixture. Following the extraction process, the mixture was left to phase-separate before measuring the soap content. The separation of DES from biodiesel is achieved through a combination of its hydrophobic nature and the polarity differences between DES and biodiesel. This allows for the efficient separation of the two components. Upon achieving a homogeneous mixture of the DES and biodiesel, the mixture was centrifuged to separate the DES from the biodiesel, and finally allowed to settle. The centrifugation and settling processes effectively separate the two phases, with the DES phase settling at the bottom due to the higher density. The lighter biodiesel phase was collected from the top. This process ensures the effective removal of the DES from the biodiesel product. The extraction duration, DES: biodiesel volume ratio and stirring speed were investigated as the soap removal parameters.

4.3.6. Analytical Methods

The AOCS Technique Cc 1795 titration method was used to measure the amount of soap in the biodiesel before and after each trial (Mamtani et al., 2021). 100 ml of acetone and 0.0005 L of bromophenol blue were mixed to prepare a solution for the soap detection method. The soap detection method was then employed by mixing 0.05 L of analytical solution with 40 g of biodiesel sample. The mixture was then titrated with 0.01 M HCl until a yellow color was observed as the endpoint of the titration. The volume of HCl is represented by A milliliter in Eq. 4.1. Eq. 4.1 was used to calculate the soap concentration (ppm) in the BD, which was then compared to the ASTM D6751 and EN 14214 standards.

A total of three parallel titrations were performed to ensure the reliability of the results. The initial soap content was 781.567 ppm.

$$\text{Soap (ppm)} = \frac{\text{A mL} \times 0.01\ \text{M} \times 304400}{40\ \text{g}} \quad (4.1)$$

4.4. Results and Discussions

4.4.1. Physical properties of DES

This study examined the physical properties (TGA, freezing point, density, viscosity and conductivity) of TMAC-based LA as the HBD for the synthesis of DESs for the removal of soap from biodiesel. The DESs prepared in this study are novel and their physical properties are still unknown. Hence, the physical properties were reported before the liquid-liquid extraction process and this is mainly to assist the evaluation of the kinetics and mechanism of the extraction process. Researchers have investigated DESs and their ability to remove contaminants such as glycerol from biodiesel (Abbott et al., 2007). These DESs were employed as the extractant solvent in the elimination of soap residues from biodiesel. The temperature range was between 303.15 and 373.15 K in this investigation.

4.4.1.1. Thermal Stability

Several physical parameters of DESs were investigated and published in different temperature ranges, as such information is critical for future studies and applications. Figure 4.1 represents the dynamic TGA curves with a heating rate of 10 °C /min for four ratios of DESs. The highest temperature where the DESs are in the liquid state without decomposition or the stable temperature range of the DESs as solvents, is determined from the onset of the decomposition temperature (Florindo et al., 2014).

The molar ratio 1:1 shows that the complete decomposition of the DES occurs between 45 - 346 °C, which also shows that the first decomposition stage accounts for the 72.226%

weight loss at an onset temperature of 223.34 °C, while a 39.92% weight loss occurs at 295.06 °C in the second decomposition stage. The complete decomposition of the DES occurs between 43 and 374 °C at a molar ratio of 1:2, but still decomposes at constant weight loss of 1.5-0.9% at a temperature range of 374-682 °C. This also shows that the first stage of decomposition accounts for the 64.569% weight loss at an onset temperature of 225.28 °C. A 26.011% weight loss occurs at 280.75 °C in the second decomposition range. A molar ratio of 1:3 shows a complete decomposition of the DES between 42 -427 °C, but still decomposes at a constant weight loss of 1.5-1.1% at a temperature range of 427-793 °C. The first stage of decomposition accounts for the 52.883% weight loss at an onset temperature of 232.04 °C, while a 15.714% weight loss is observed at 293.37 °C in the second decomposition range.

The results in Figure 4.1 confirm that an increase in the HBD ratio causes a significant increase in the decomposition rate constant. The increase in the decomposition rate constant is due to the concentration and pH of the DES. The increase in the LA ratio lowers the pH, thus causing a significant increase in the rate of decomposition and these results are in accordance with those of Hall et al. (1949). Therefore, it is best to use HBD with lower volatility and better thermal stability to produce DESs with higher stability (Delgado-Mellado et al., 2018). This work shows the importance of TGA analysis in the determination of the most suitable temperature range for DES applications, therefore new solvents could be formulated in an industrial scale.

The freezing temperatures of the DES prepared from TMAC and LA as a function of molar ratio are presented in Figure 4.2. The DESs ratios are presented at a freezing temperature of around 23 °C, which confirms that these DESs are supramolecular complexes in a liquid state over a wide temperature range. From Figure 4.2, the lowest freezing point was formed at a 1:4 molar ratio.

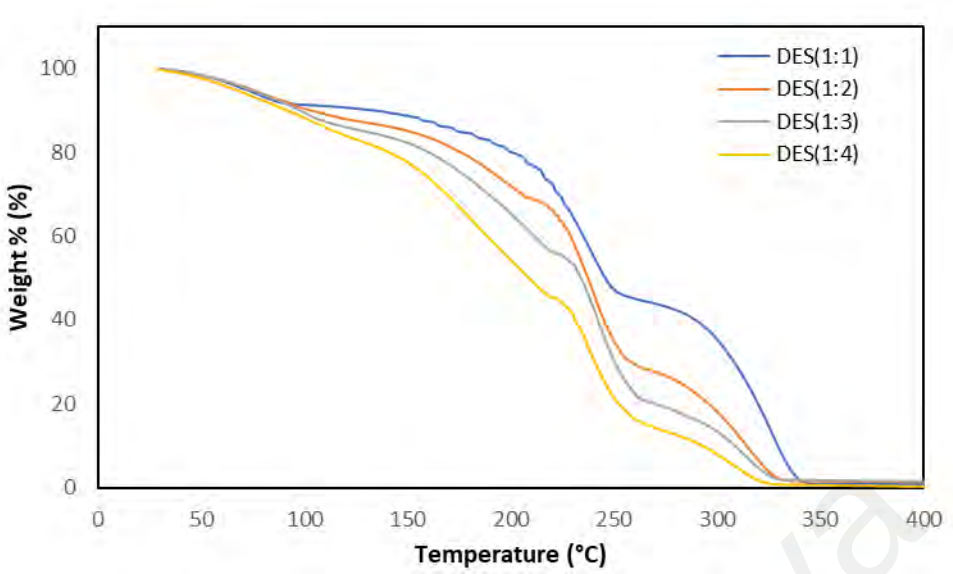

Figure 4.1: Dynamic TGA curves of DES at different molar ratio with a heating rate of 10 °C ·min^{-1}.

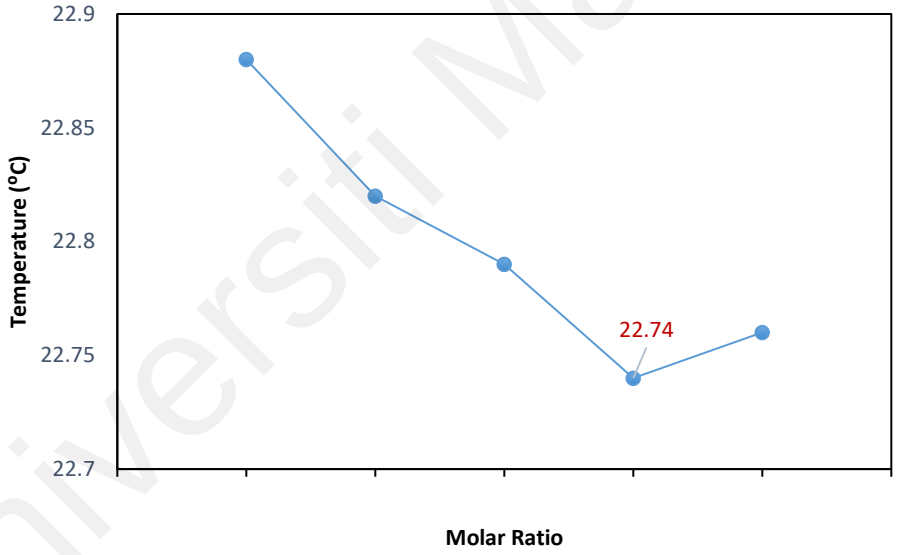

Figure 4.2: Freezing temperatures of DES as a function of molar ratio with a heating rate of 10 °C ·min^{-1}.

4.4.1.2. Density

Density is a physical characteristic that is used to determine the nature of the components in the environment, as well as in numerous industrial applications. The effect of temperature on the density of various DES ratios was investigated. Figure 4.3 shows the effect of temperature and the molar ratio on the density of the prepared DESs. The

experimental density results for the DES samples as a function of temperature are illustrated in Figure 4.3(a), while Figure 4.3(b) presents the experimental density versus the DES molar ratio. The density of the DESs decrease with the increase in temperature due to the enhanced thermal energy of the DES molecules, resulting in higher mobility and lower density as shown in Figure 4.3(a). The density decreases linearly with the temperature for the DES samples with R^2 values close to unity. The linear equation (Eq. 4.2) represents the correlation of density with temperature.

$$\text{Density } (\rho) = \alpha + \beta T \qquad (4.2)$$

where T is the temperature in Kelvin, while α and β are constants (curve fit parameters), are shown in Table 4.2.

Table 4.2: Fitting parameters of Eq. (2) for lactic acid-based DES.

DES Molar Ratio	α	β	R^2
1:1	1.2691	-0.0006	0.9998
1:2	1.3143	-0.0006	0.9994
1:3	1.3364	-0.0006	0.9997
1:4	1.3575	-0.0007	0.9996
LA	1.474	-0.0009	0.9979

The density of DES increases with the HBD component in the DES mixture at constant temperature. The density increases with the increase of the heavier component (LA). The trend of density vs. DES molar ratio (Figure 4.3b) is continuous over the temperature range and is due to the rise in mass produced by a higher HBD %. The densities of various DES proportions are lower than their HBD (LA) over the whole temperature range.

As seen in Figure 4.3, the DES density varies from a maximum of 1.1322 g cm^{-3} at room temperature to a minimum of 1.08552 g cm^{-3} at 373.15 K. The highest density of the DES is 1.1430 g cm^{-3} at ambient temperature at a molar ratio of 1:4, while the lowest density

is 1.09407 g cm^{-3} at 373.15 K. The density was the lowest in the DES with a molar ratio of 1:1, with a highest density value of 1.0904 g cm^{-3} at 313.15 K and a minimum of 1.05652 g cm^{-3} at 373.15 K. The experimental results of the density of the DESs are in good agreement with the results of Zubeir et.al (2016) and are close to those observed by Deng et.al for the DESs prepared from tetraethylammonium bromide and Levulinic acid (Deng et al., 2016).

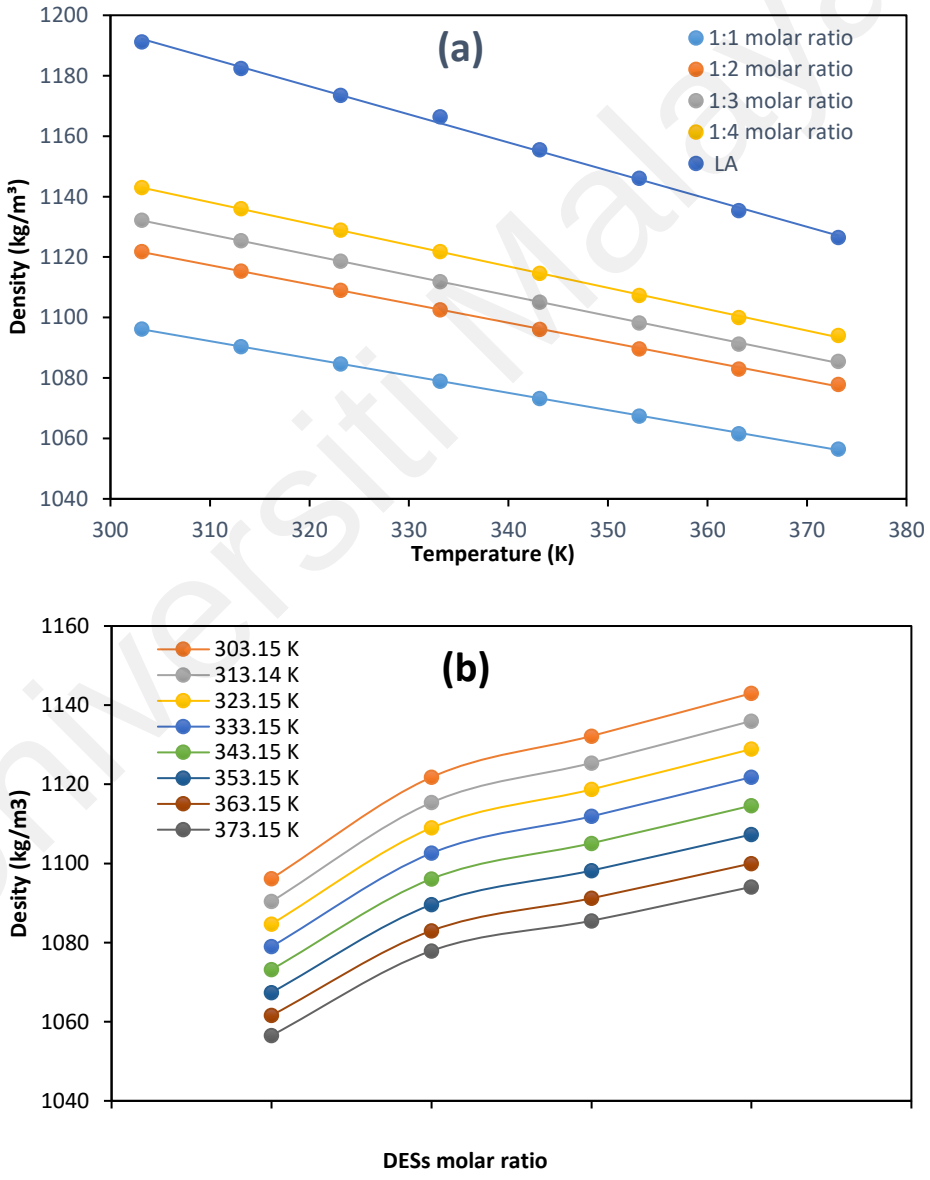

Figure 4.3: (a) Plot of density of lactic acid-based DESs as a function of temperature, (b) Plot of densities vs. DESs molar ratio at different temperature ranges.

Viscosity represents the solvent's non-fluidity and opposition towards liquid flow. It is also important to investigate the temperature effects on the viscosity of DESs to determine the amount of energy needed for the most suitable applications.

4.4.1.3. Viscosity

The viscosity of the various DES ratios as a function of temperature is depicted in Figure 4.4. The viscosity results of the DES samples as a function of temperature are plotted in Figure 4.4(a), while Figure 4.4(b) presents the experimental viscosity versus the DES molar ratio. The viscosity of the DESs at room temperature are greater than those of LA with the following order: 1:1> 1:2> 1:3> 1:4. At a given temperature, the viscosity of DES decreases with the concentration of HBD in the DES mixture. The viscosity increases with the higher fraction of the heavier component. The trend of the viscosity vs. DES molar ratio is consistent across the investigated range and correlates with the mass loss from the increase in the HBD percentage. These DESs are IL analogues since they are liquids at or below 100 °C and are almost similar in their physical properties with ILs, while being less expensive, has easier synthetic procedures and are in high purity. It is well known that the viscosity of a solvent is dependent on the free volume and the presence of voids of acceptable sizes which allows for the free flow of solvent molecules and ions (Schoettl et al., 2014; Klossek et al., 2013).

As a result, the DES components (HBA and HBD) (Zhang et al., 2012), as well as the sizes of the DES cation and anion, have significant influences on the viscosity. Temperature is one of the most critical factors that influences the viscosity. Figure 4.4(a) shows that the viscosity decreases exponentially with the temperature (Ghatee et al., 2010). The temperature effects are described by the hole hypothesis, which determines the movement of species into the mixture when a eutectic mixture is heated (Ghatee et al., 2010). The rise in the thermal energy causes the molecules to spread out and move at random (Hayyan et al., 2012), resulting in a larger free volume that allows for the free

movement of the molecules, thus lowering the viscosity. Figure 4.4(a) shows that the dynamic viscosity decreases at all temperature ranges. The viscosity also decreases with the increase of the molar ratio of DES (Figure 4.4b) and decreases with the increase in temperature, similar to the behavior of dynamic viscosity with temperature.

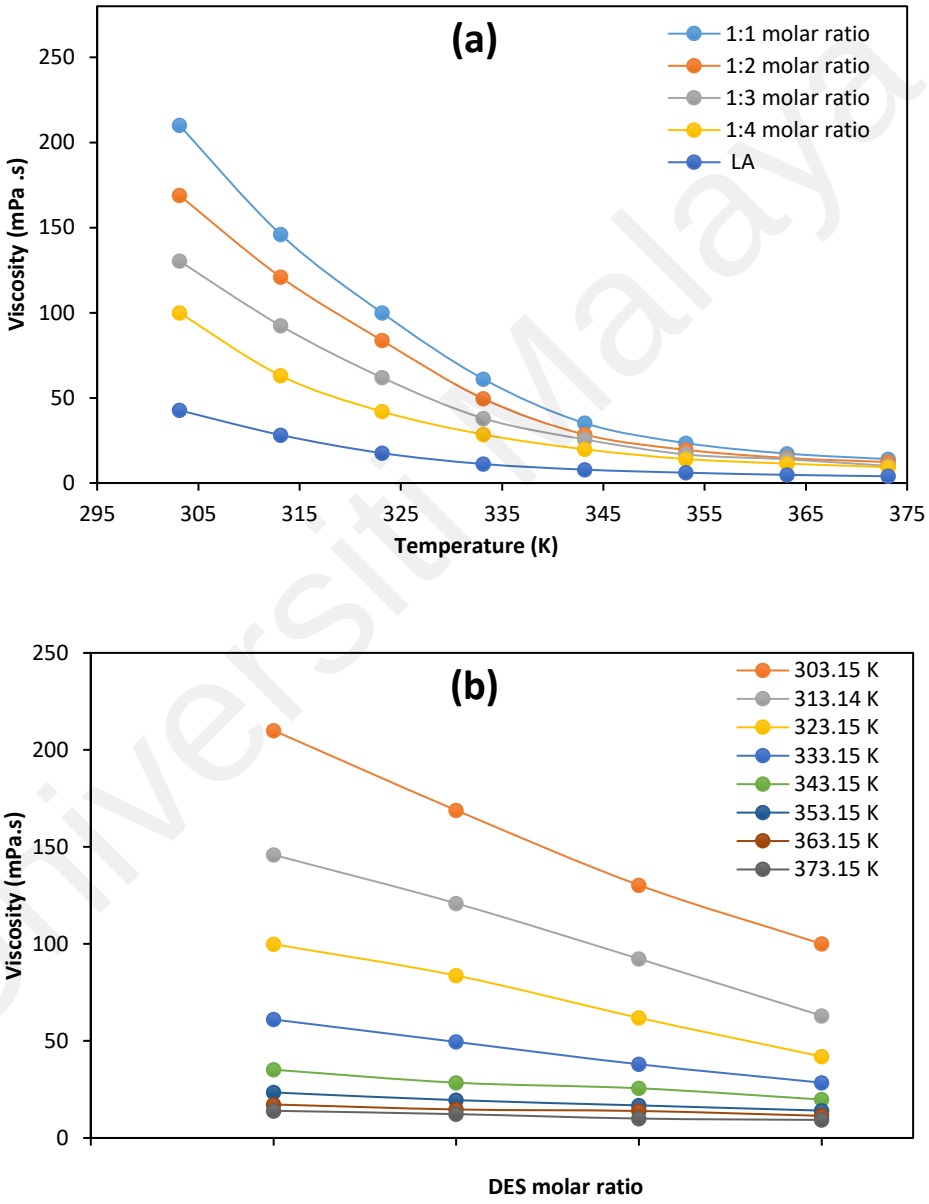

Figure 4.4: (a)Viscosities (μ) of lactic acid based-DES at a different molar ratio as a function of temperature; (b) Plot of viscosities vs. DESs molar ratio with different temperatures.

The Arrhenius model Eq. (4.3) can be used to explain the viscosity-temperature behavior:

$$\text{Viscosity } (\mu) = \mu_0 e^{[-\frac{E_\mu}{RT}]} \tag{4.3}$$

$$\ln \mu = \ln \mu_0 - \frac{E_\mu}{RT} \tag{4.4}$$

where μ_0 is the pre-exponential factor, E_μ is the activation energy, R is the gas constant and T is the temperature in Kelvin.

The Arrhenius equation explains the behavior of the viscosity as a function of temperature, which shows an exponential decrease. However, this equation is inaccurate for molecules which behave as small point charges. In this regard, other models such as the Vogel-Fulcher-Tamman (VFT) and Litovitz models provide a more accurate description. The VFT model which describes this behavior is as follows:

$$\mu = A \times \exp\left(\frac{B}{T - T_a}\right) \tag{4.5}$$

where A, B and Ta are adjustable parameters. The other equation which describes this behavior is the Litovitz equation:

$$\mu = A \times \exp\left(\frac{B}{RT^3}\right) \tag{4.6}$$

where A and B are the adjustable parameters in the Litovitz model.

The fitting of the adjustable parameters from the experimental data and the predicted models are presented in Table 4.3 and Figure 4.5.

Table 4.3: Adjustable parameters of the correlations: Litovitz, Arrhenius, and VFT models.

DES Molar ratio	Litovitz model		Arrhenius model*		VFT model	
	A	B	A	B	A	B
1:1	0.5778	1.718×10^{8}	6×10^{-5}	-4621.2	0.000262	3649.7
1:2	0.541	1.648×10^{8}	7×10^{-5}	-4493.7	0.000303	3549
1:3	0.5615	1.562×10^{8}	1×10^{-4}	-4247.9	0.000475	3355
1:4	0.5758	1.443×10^{8}	2×10^{-4}	-3952.9	0.000804	3123.5

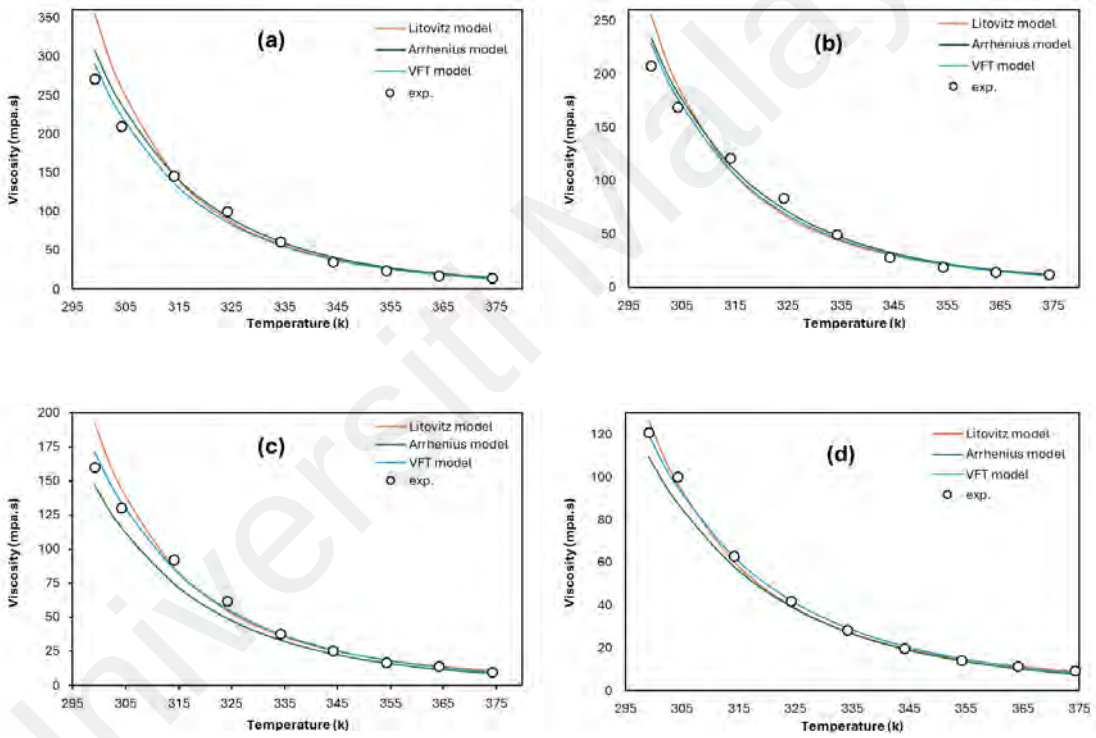

Figure 4.5: Viscosity(μ) of pure DES at different molar ratios as a function of temperature. (a) 1:1 molar ratio, (b) 1:2 molar ratio (c) 1:3 molar ratio, and (d) 1:4 molar ratio.

The data is fitted using different models: Litoviz, Arrhenius, and Voguel-Fulcher-Tamman. The $\mathbf{E_{\mu}}$ values estimated for the binary mixtures varies from -4621.2 Pa. L. mol $^{-1}$ (1:1 molar ratio) to -3952.9 Pa. L. mol $^{-1}$ (1:4 molar ratio) and reflect the abovementioned viscosity models. The higher $\mathbf{E_{\mu}}$ value represents stronger fluid

interactions where the ions have lower mobility. The DESs with the lowest TMAC: LA molar ratio (1:4) possesses the highest activation energy. Based on the comparison of the fitted models in Figure 4.5, the VFT model shows the closets fitting of the viscosity results.

4.4.1.4. Conductivity

The solution conductivity (S m^{-1}) depends on the concentration of ions and the interactions between the ions i.e. higher conductivity indicates higher concentration of ionic species moving rapidly in the solution. The ionic conductivity is an important parameter in the electroplating, semiconductor, petroleum, and iron and steel industries. The conductivity of the prepared DESs was tested as a function of temperature as shown in Figure 4.6. The ionic conductivities of the prepared DESs increase with the temperature. The extremely viscous DESs exhibit lower conductivity values, demonstrating that the conductivity variation and viscosity variation are reciprocal to each other, for the simple reason that the solvent's ionic conductivity is determined by the mobility level of the ionic species.

Pure LA possesses ionic conductivities ranging from 0.45 to 11.97 mS cm^{-1} within the investigated temperature range, whereas the DESs possess conductivities in the order of 40. This is expected as the HBAs used in this investigation is TMAC, which consists of the chloride and halide ions with higher conductivities. The conductivity behavior of the tested DESs at this temperature range is comparable to the viscosity and it is described by the following Arrhenius equation Eq. (4.7) (Vila et al., 2006):

$$\text{Conductivity (S)} = S_0 e^{\left[-\frac{E_S}{RT}\right]} \tag{4.7}$$

$$\ln S = \ln S_0 - \frac{E_S}{RT} \tag{4.8}$$

where; S: conductivity (mS. cm^{-1}), S_0: pre-exponential factor and Es: ionic conduction activation energy (collected in Table 4.4).

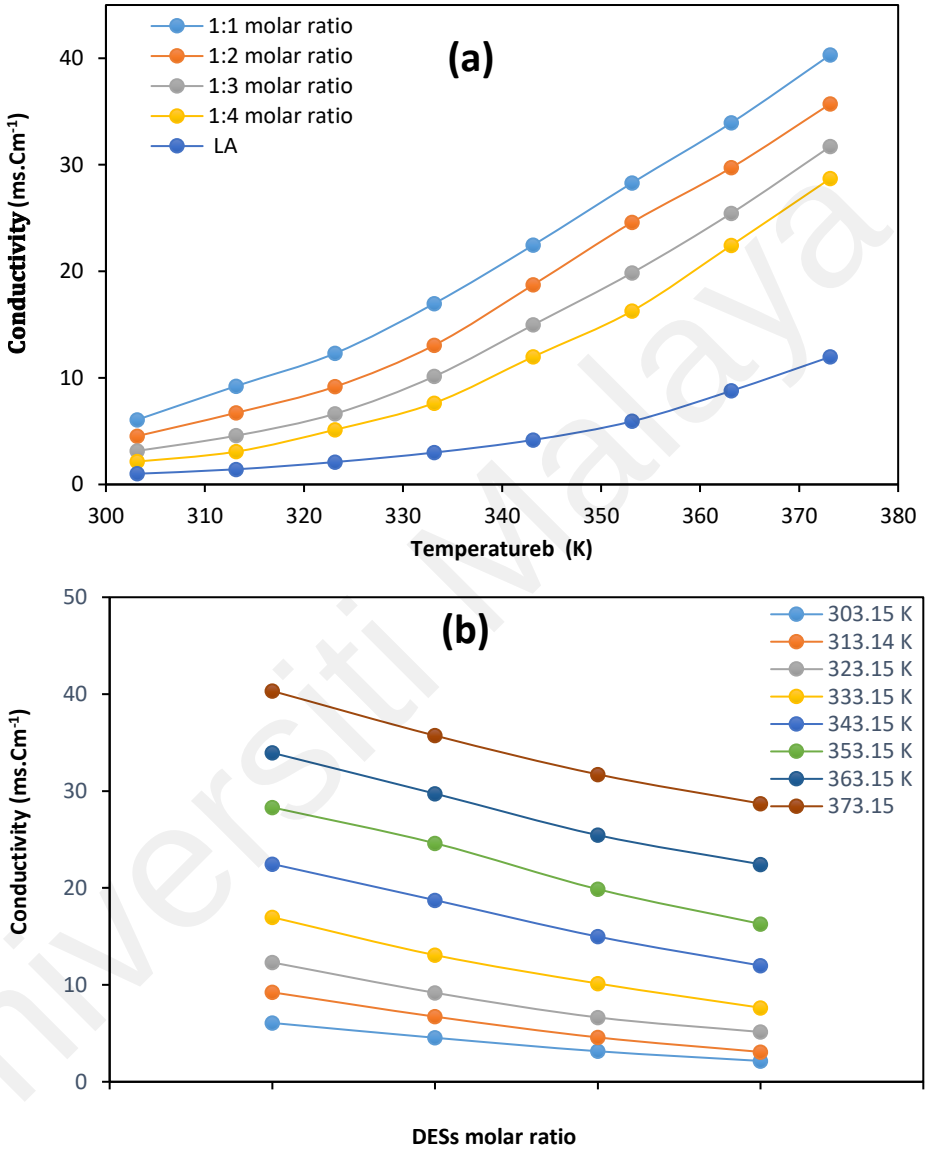

Figure 4.6: a) Conductivity (mS cm^{-1}) of lactic acid-based DESs at different molar ratios as a function of temperature; (b) Plot of conductivity vs. DESs molar ratio at different temperatures.

Table 4.3: Regression value parameters of Eq. (8) for DES at different molar ratio

DES molar ratio	$\frac{S_0}{S \cdot cm^{-1}}$	$\frac{E_S}{Pa \cdot L \cdot mol^{-1}}$	R^2
1:1	768.3495	29772.43	0.982
1:2	1525.755	32299.06	0.9898
1:3	1542.631	33051.48	0.998
1:4	4751.638	36909.17	0.9978

4.4.2. Soap Removal from Biodiesel Using DESs

4.4.2.1. Production of Biodiesel

NaOH and CH_3OH were selected for the preparation of the biodiesel due of their high capacity for the conversion of triglycerides into fatty acid methyl ester (Ali & Tay, 2013). The 10:1 oil to methanol ratio was selected as it gave the fastest production of the biodiesel (Hayyan, et al., 2021; Foon et al., 2004). The average initial soap level was 781.567 ppm even though the biodiesel was prepared from refined palm oil. This is higher than the international standards which recommend a soap concentration of less than 41 ppm (Díaz-Ballote et al., 2020; Gross et al., 2016).

4.4.2.2. Screening of DESs molar ratio for soap removal

This study investigates the use of TMAC-based lactic acid as the HBD in the synthesis of DESs for the removal of soap from biodiesel. The details of the synthesized DESs are listed in section 4.2.2. Researchers have experimented on different molar ratios of DESs and their ability to remove contaminants, such as glycerol from biodiesel (Hayyan et al., 2022; Abbott et al., 2007). These DESs are employed as green solvents for the elimination of soap content from the biodiesel as a preliminary approach.

Liquid-liquid extraction was used to determine the optimal DESs molar ratio for the soap extraction from biodiesel. Four distinct HBA: HBD molar ratios (1:1, 1:2, 1:3 and 1:4)

were studied by changing the quantity of HBD. The extraction experiments were carried out using an orbital shaker to homogenize the mixture at 150 rpm for six minutes. The mixture was allowed to phase-separate after the liquid-liquid extraction process, before the soap concentration in the biodiesel samples were determined. Figure 7 shows the effect of the DES molar ratio on the removal of soap in the presence and absence of AC, where the increase in the DES molar ratio decreases the soap content. The purification of biodiesel using pure DES was below the standard limits for a 1:4 DES molar ratio (Figure 4.7), while purification using the AC+DES shows better soap removal, where the DESs with 1:2, 1:3 and 1:4 molar ratios show lower standard limits. This is due to the presence of AC with large surface area. Furthermore, the oxygen groups on the AC surface facilitates the removal of impurities such as soap, mono and diglycerides, glycerol and free fatty acid (FFA) molecules found in the biodiesel during production (Fadhil et al., 2016). Consequently, the purification of biodiesel in the presence of AC produced better results (Fadhil et al., 2016). These results revealed that the increase in the molar ratio from 1:1 to 1:4 lowers the soap level from 93.66 ppm to 23.42 ppm. This could be due to an increase in the quantity of LA in the DES, which results in a larger amount of HBD to enhance the biodiesel purification. The concentration polarization between biodiesel and DES contact surface could be prevented due to the soap dispersion to a higher molar ratio (large quantity of HBD) of DES during the extraction process. Increasing the molar ratio to 1:3 or 1:4 has a significant influence on the soap removal capabilities, owing to the extractant's huge contact area between the HBD and biodiesel and the steep driving force between the biodiesel and DES phases to maintain a high extraction efficiency. The optimal DES molar ratio for the extraction of soap from biodiesel according to the ASTM D6751 standard is 1:4. The introduction of AC improved the soap removal efficiency from the biodiesel and decreased the amount of HBD needed to achieve the soap concentration below the ASTM D6751 standard. Thus the 1:4 molar ratio of DES was

selected for future research, in the utilization of a liquid-liquid extraction method for the removal of soap molecules.

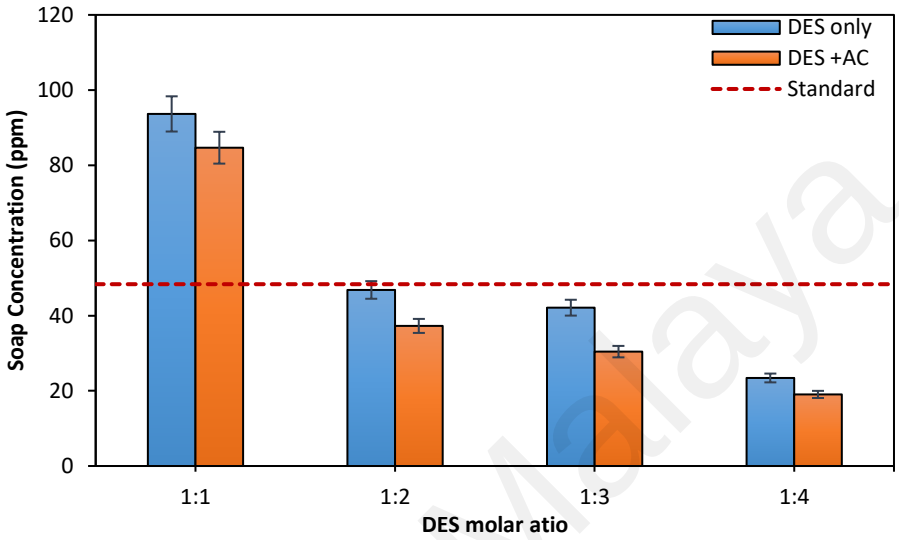

Figure 4.7: Soap content in the biodiesel after the extraction process at different molar ratios (1:1 DES to biodiesel volume ratio, and 6 min extraction time, dashed line: standard)

4.4.2.3. Optimization of soap removal from crude biodiesel

In this study, DES and AC were used in a liquid-liquid extraction technique for the removal of soap from biodiesel. The soap separation via a liquid-liquid removal system had an effect on the duration of the extraction process. This is because the soap molecules require a certain contact time to diffuse from the biodiesel phase into the DES phase. Figure 4.8 depicts the effect of extraction time on the decrease of the soap concentration using DES as the extractant. When the extraction duration is increased from 2 to 8 minutes, the final soap content decreases from 84.5 ppm to 19.36 ppm. At 10 minutes, the soap content reaches 0 ppm (no soap content was detected), indicating the effectiveness of the DES and AC for the removal of soap from biodiesel. The 6-minute extraction time is also the first time where the soap concentration decreases below the

standard limit of 40.3 ppm. The addition of 0.03 g of AC into the DES decreases the reaction time to 4 minutes and enhances the extraction efficiency. The AC possesses rough surface and high porosity, thus the high surface area leads to stronger interactions between the functional groups of the soap molecules and the surface of AC. It is well known that the adsorbate and the adsorbent surface interact either physically or chemically via the physisorption and chemisorption process, respectively (Fadhil & Abdulahad, 2014). In addition, the oxygen groups on the surface of AC play an important role in the adsorption of the soap molecules. These results reveal that the soap concentration could meet the international standards within 6 minutes and 4 minutes of extraction time using pure DES and DES in the presence of AC, respectively.

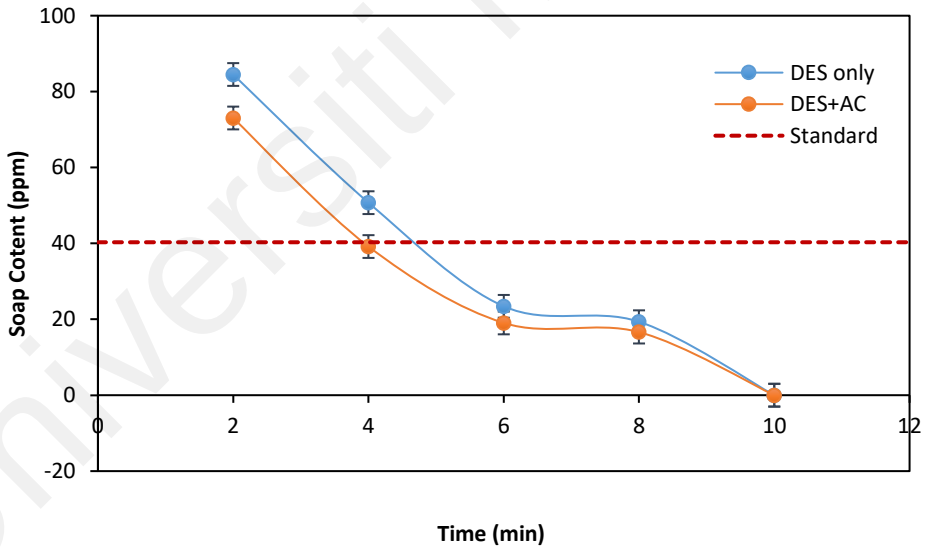

Figure 4.8: Soap content in the biodiesel after the liquid extraction process at different extraction time (1:1 DES to biodiesel volume ratio, 1:4 DES molar ratio, 150 rpm stirring speed, dashed line: standard).

Figure 4.9 shows the effect of the DES: biodiesel volume ratio in the presence and absence of AC, on the soap content in biodiesel after the extraction process. The increase in the DES: biodiesel volume ratio from 1:1 to 1:2 increases the soap content from 23.42

ppm to 101.3 ppm. This could be due to the increased amount of biodiesel in the system, resulting in a lower volume of DES for the removal of soap in the biodiesel. The concentration polarization between the biodiesel and DES contact surface during the extraction process could be avoided if the soap molecules are distributed to a larger amount of DES under stirring. This is also consistent with the findings of Ma et al. (2020), who found that the increase in the amount of extractant improves the extraction efficiency. Nonetheless, the increase in the biodiesel ratio to 1:3 or 1:4 is even less effective towards the soap removal capability, owing to the extractant's smaller contact area between the DES and biodiesel, and also to the lower driving force (soap concentration gradient) between the biodiesel and DES phases. The presence of AC resulted in better soap removal capability compared to those purified by using pure DES. This is due to the presence of numerous oxygen functional groups on the surface of the AC, which play a crucial role in the purification process (Fadhil et al., 2012). The purification of biodiesel in the presence of the AC adsorbent produced better results. Thus, the DES:biodiesel ratio of 1:1 is capable of extracting soap from biodiesel producing a low soap content which complying to the ASTM D6751 standards. When the soap molecules form hydrogen bonding with the LA, it becomes soluble in the LA based DESs. This could be due to the high solubility of the soap molecules in water, where water does not react with the DES to obstruct the soap removal (Shahbaz et al., 2010). On the other hand, the introduction of a minute amount of water decreases the viscosity of DES, thus enhancing the solvation capabilities (Ma et al., 2018).

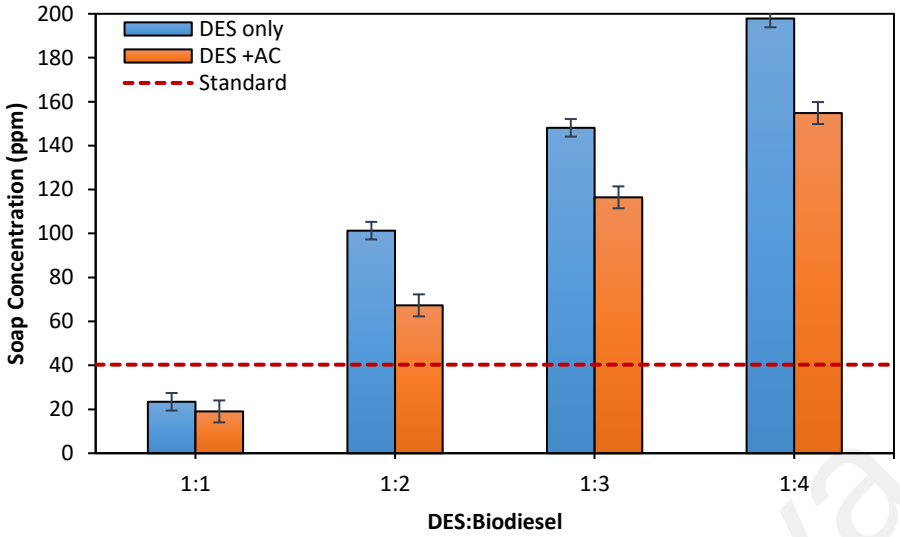

Figure 4.9: Soap concentration in the biodiesel in the presence and absence of AC after the liquid-liquid extraction process at different DES: biodiesel volume ratio.

Figure 4.10 depicts the effect of the stirring speed during the extraction process for the removal of soap in the presence and absence of AC. These results show that the increase in the stirring speed from 130 rpm to 170 rpm using pure DES and DES+AC during the extracting process, decreases the final soap content from 287.49 ppm to 23.42 ppm and from 265.21 ppm to 17.04, respectively, which meets the ASTM D6751 standard. Generally, stirring enhances the mass transport between the different phases during the extraction process (Cunico et al., 2020). Thus the increase in the stirring speed improves the mixing of the different phases due to the increased hydrodynamics and lower DES viscosity during the extraction process (Chang, 2016). This also helps to avoid soap concentration polarization on the biodiesel -DES interface, resulting in the larger driving force (highest soap concentration gradient) between the phases for enhanced mass transport of the soap molecules (Hayyan et al., 2022). However, the increase in the stirring speed had no significant effect on the final soap concentration, with the final soap concentrations of 16.91 ppm-23.42 ppm and 15.93 ppm-17.04 ppm using pure DES and DES+AC, respectively, where equilibrium was reached after a 6-minute extraction interval. However, the liquid-liquid extraction process failed at higher mixing speeds

greater than 250 rpm due to the entrainment of the extractant, which suggesting that the liquid-liquid extraction system possesses hydrodynamic instability. To meet the standard requirements, an extractant stirring speed of 150 rpm was selected as the optimum speed in a liquid-liquid extraction process for the removal of soap from biodiesel. The reuse of the DES and AC from the soap content after the liquid-liquid extraction process is highly recommended as a future investigation.

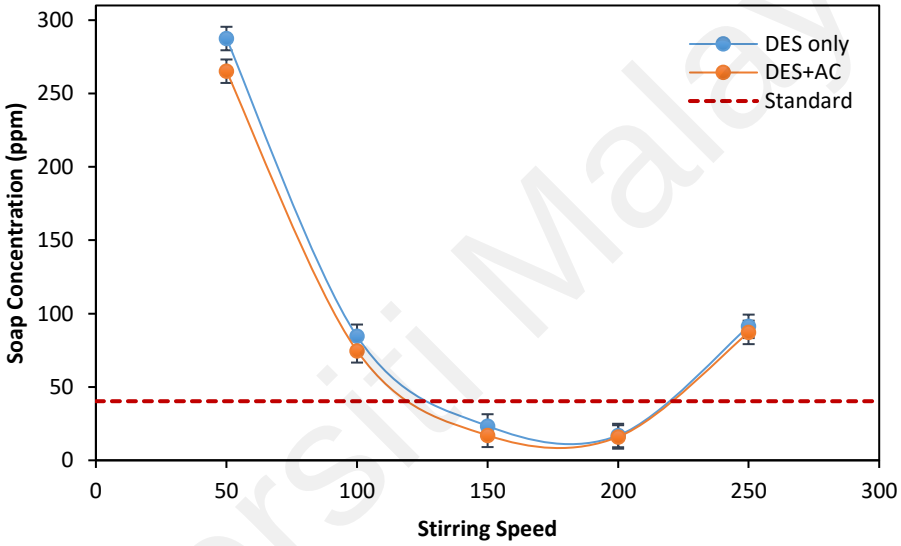

Figure 4.10: Soap content in the biodiesel after the extraction process at different stirring speed (1:1 DES to biodiesel volume ratio, 1:4 DES molar ratio, and 6 min extraction time, dashed line: standard limits)

4.5. Conclusions

In conclusion, the measurements of melting point, TGA, density, viscosity and conductivity were conducted for DESs at various molar ratios and temperatures. These results reveal that the lowest freezing point is at a 1:4 molar ratio, and the density of the DESs decrease linearly with temperature. The VFT model shows the closest dependence of viscosity on the temperature. From the application of DES in soap removal from

biodiesel, the soap content decreases from 781.567 ppm to 23.24 ppm under optimum conditions (1:4 DES molar ratio, 6 min, 150 rpm and 1:1 DES: biodiesel volume ratio). Furthermore, the addition of 0.03 gm of activated carbon (AC) into the DES mixture improves the soap removal compared to the pure DES, while also providing economic benefits by decreasing the energy usage and shortening the extraction time. These findings provide valuable information for the soap removal from crude biodiesel using DESs as a natural extraction media and AC as a novel adsorbent. This technique could replace typical purification technologies that uses water and it could decrease the generation of wastewater during the purification of crude biodiesel.

CHAPTER 5: INTEGRATION OF DEEP EUTECTIC SOLVENT AND ACTIVATED CARBON IN EMULSION LIQUID MEMBRANE SYSTEM FOR SOAP REMOVAL FROM CRUDE BIODIESEL

5.1. Introduction

The present chapter investigated the incorporation of deep eutectic solvent (DES) and activated carbon (AC) in the emulsion liquid membrane (ELM) process on soap removal from biodiesel. As far as our concern, there is no report on the use of DES and AC in ELM technique in related field yet. The DES in this study was applied as stripping phase, and it was synthesized from tetramethylammonium chloride (TMAC) and lactic acid (LA). Upon identifying the best DES molar ratio as the stripping phase, the synergistic effect given by DES and AC in ELM was investigated and compared. Furthermore, the effect of different operating conditions such as the DES: biodiesel ratio, surfactant concentration, mixing speed, extraction time and weight percent of AC on the performance of the system was also investigated. Lastly, the kinetics of process was evaluated and the transport mechanisms of soap in the DES-based ELM/AC system were postulated. This method offers a viable alternative to the conventional water-based purification process. It demonstrates the effective purification of crude biodiesel without the use of a large amount of water/washing agent in comparison to conventional water washing, thereby offering a more sustainable solution for the purification of biodiesel. The results of this chapter were published in the journal of Colloids and Surfaces A: Physicochemical and Engineering Aspects (Abed et al., 2023).

5.2. Literature Review

The rapid growth of energy demand over the past few decades has led to the seeking of renewable energy sources to replace fossil fuels. Fossil fuels which consist of 88% of the world's energy consumption are mostly derived from non-renewable sources. The negative effects of fossil fuels towards on the environment are beginning to take effect (Thangaraj et al., 2019). In contrast, biofuels derived from vegetable oils or animal fats could are the best option to replace fossil fuels. Among the biofuels, biodiesels are the most widespread compared to biogas and bio-alcohols as they are, renewable, low cost, non-toxic, environmentally friendly, biodegradable, and possess good emission profile upon combustion)Hayyan et al., 2021; Jahirul et al., 2013(.

The transesterification of animal fats or vegetable oils catalyzed by NaOH or KOH is the most utilized process in the synthesis of biodiesel (Borges & Díaz, 2012). The advantage of this method is that it produces high yields of methyl esters in mild circumstances which requires shorter time for product formation (Sharma et al., 2011). However, regardless of the type of catalyst, byproducts such as soap and glycerides during the transesterification reaction render the whole process worthless. This caused biodiesel to be less competitive compared to fuel diesel is due to the more complex and expensive downstream purification required (Šalić et al., 2020). Tai-Shung (2007) reported that the purification process accounts around 60–80% of the total cost of biodiesel. For example, a separator is used to separate the glycerol biodiesel, and then an evaporator is used to eliminate the methanol. Even after these procedures, biodiesel is unsuitable to be used in engines due to the presence of other impurities such as soap, free glycerol, traces of the catalyst, alcohol, water, metals and glycerides. Before the utilization of biodiesel as a fuel, the content of these contaminants should verified according to the ASTM D 6751(Astm, 2012) and EN 14214 (EN 14214, 2003) standards and eliminated entirely if possible.

Soap is the most prevalent pollutant in biodiesel, thus must be removed to avoid instrumental breakdown and filter clogging. Traditionally, soap and trace amounts of glycerin are eliminated by rinsing the biodiesel in water, where the soap is transferred into the water phase and be removed when the water is separated from the biodiesel. However, the use of water for the removal of soap by simple washing possesses numerous challenges (Wall et al., 2011). The large amount of water consumed during the washing step is one of the main problems in biodiesel purification (Atadashi, Aroua, & Aziz, 2011). The volume ratio of water to biodiesel used in the purification process is 10:1 to meet international standards (Karaosmanoğlu et al., 1996). This technique imposes additional purification costs due to the large quantity of wastewater released (Veljković et al., 2015). Besides that, water washing prolongs the processing time due to the extra requirements for drying, multiple washing, and separation of water from biodiesel (Wall et al., 2011). Several alternative "waterless" purification procedures have been developed, such as ion exchange resins and solid adsorbents (Wall et al., 2011), micro and ultrafiltration membrane technology (Alves et al., 2013) and liquid-liquid extraction (Abed et al., 2023). Nevertheless, it is to be noted the methods showed several drawbacks such as consuming a lot of water, producing wastewater that needs treatment, poisoning the biodiesel with water that needs extra treatment, high cost associated with ion exchange possesses, high pressure to operate the pumps and using shakers to improve mass transfer, etc.

Liquid-liquid extraction is one of the purification methods that can be used to purify biodiesel. As an alternatively, environmentally friendly solvents such as ionic liquids and especially cheaper alternatives such as deep eutectic solvents (DESs) could be used in the purification process (Ho et al., 2015; Hayyan et al., 2010). These DESs are considered environmentally friendly due to their low toxicity and are highly biodegradable. Subsequently, DESs also conform to the principles of green chemistry, thus are excellent

option for the removal of impurities from biodiesel. This is due to the facile preparation of DESs from readily available raw materials and are environmentally friendly, making them a viable and eco-friendly alternative solvent. Therefore, they are an excellent option as alternative to replace the conventional solvents for the removal of impurities from biodiesel. DESs could be produced by mixing together solid organic salts with a hydrogen bond donor (HBD) (Hayyan et al., 2021; Abbott et al., 2004; Abbott et al., 2003). DESs have been used effectively to purify biodiesel (Ho et al., 2015; Hayyan et al., 2010; Abbott et al., 2006; Abbott et al., 2004), using batch liquid-liquid extraction techniques with shakers to improve mass transfer.

Other than from the view of environmentally friendly solvent, the liquid-liquid extraction operations could also be improved by an emulsion liquid membrane (ELM) process for a more cost-effective purification. This new technology, utilizes multiple forces, such as solubility, electrostatic charge, hydrophobicity, and molecular size for separation (Azarang et al., 2019; Abed, 2014a). Thes mechanisms could improve the separation process by reducing the length of the diffusion channel between the phases. The ELM technique has several advantages such as higher surface area, lower membrane thickness, higher solute transfer rate (Davoodi-Nasab et al., 2018), continuous and flexible operation, single extraction and stripping operation (Abed & Al-Hemiri, 2015; Al-Hemiri et al., 2012), smaller internal phase volume than the feed phase, solvent recyclability etc., which has attracted considerable attention from several diverse fields towards the ELM techniques (Chakraborty & Bart, 2006), including biodiesel refinery (Hayyan et al., 2022). In addition, its reported that the presence solid particles in the emulsion phase could enhance the stability and strength between the globules in the emulsion phase and prevent the globules from collision and coalescence (Al-Obaidi et al., 2021; Lin et al., 2015). This leads to an idea that activated carbon (AC) can be utilized as one of the ELM components to strengthen the ELM stability. Besides preventing coalescence, AC also

possesses rough and high surface area with numerous void spaces. This could further lead to stronger interactions between the oxygen functional groups in the soap molecules and the surface of the AC, thereby, improving the soap removal via chemisorption or physisorption process.

5.3. Materials and Methods

5.3.1. Materials

Tetramethylammonium chloride (TMAC), acetone, span 20, and hydrochloric acid were procured from Merk. Potassium hydroxide and bromophenol blue were procured from Sigma-Aldrich. Lactic acid (99% purity) and silicon oil (viscosity of 350 cP, specific gravity of 1.04, and density of 1.04 g/mL) were procured from John Kollin Chemicals, while methanol was obtained from Chemiz Sdn. Bhd. Refined palm oil was acquired from a local mill located in Selangor, Malaysia. Finally, activated carbon (AC) used in this study was prepared from palm raceme, as previously reported (Abed et al., 2022).

5.3.2. Preparation of DES

Although there have been some subsequent modifications in the synthetic process of DESs, the majority of DESs were prepared using the approach by Abbott et al. (Abbott et al., 2003). A digital analytical balance (N92, A&D company, limited) was used in the weight measurements in our study. Four DES were synthesized by mixing tetramethylammonium chloride (TMAC) with lactic acid (LA). Table 5.1 shows four mixtures of HBD and HBA at different molar ratios are employed in this study in the preparation of the DES samples. TMAC was dried before use in the preparation of DES. The HBA and the HBD were mixed in a jacketed cup with a motorized stirrer. The mixing duration and temperature were reduced to a minimum of 3 hours and 70 °C, respectively, during the synthesis of the homogenous colorless liquid. Due to hygroscopic nature of

DES, water content was determined using a coulometric Karl-Fischer titrator (C30, Mettler Toledo) and found to be in the range of 30-80 ppm. In addition, the moisture content was carefully controlled by drying the synthesized DESs at 70 °C overnight prior to storage in the desiccator.

Table 5.1: Acronyms and compositions for the DESs under consideration

Abbreviation	HBA	HBD	Molar ratio	Mass ratio (g:g)
DES1	TMAC	LA	1:1	20:16.44
DES2	TMAC	LA	1:2	20:32.87
DES3	TMAC	LA	1:3	20:49.31
DES4	TMAC	LA	1:4	20:65.75

5.3.3. Production of Biodiesel

Refined palm oil (RPO) from plant sources was selected as the biodiesel using potassium hydroxide as the catalyst. Methanol (MeOH) and potassium hydroxide were mixed to produce potassium methoxide. The RPO was then mixed with 1%wt/v KOH in a reaction flask at a molar ratio of 1:10 (oil to methanol) with an excess of methanol for the reaction (Arenas et al., 2021; Abbott et al., 2007a). A hotplate magnetic stirrer was used to stir the mixture for an hour at 500 rpm and 60 °C. The mixture was centrifuged for 10 minutes at 2500 rpm to separate the biodiesel from the glycerol. The biodiesel was centrifuged and then boiled for 15 minutes at 70–80 °C to eliminate the remaining methanol.

5.3.4. Preparation of ELM

The ELM system formulation involves three main steps i.e. the formation of the emulsion membrane; mass transport of soap from the source phase (biodiesel) to the stripping phase (DES) via the DES-based ELM system; and separation of phases through separating funnel. To create the emulsion membrane phase, a mixture of 0.15 wt.% of Span-20 and

10 ml of silicon oil was homogenized along with 0.3 wt.% of AC under 10000 rpm for a duration of 3 minutes. On the other hand, the DES–oil emulsions were synthesized by mixing 10 mL of DES with the emulsion membrane phase and homogenizing for 3 min at 10000 rpm. Then, the purification methods were carried out by pouring the emulsions into 30 mL of biodiesel phase containing 765 ppm soap and then mixed for 10 min at 300 rpm by a mechanical mixer. The system was mixed to disperse and forming emulsions as shown in Figure 5.1. Finally, the emulsion mixture was poured into a separating funnel forming three layers, namely: purified biodiesel as the top layer; DES as the lower layer; and silicon oil as the middle layer. The samples were separated through a separating funnel and the soap content was evaluated using the AOCS Technique Cc 1795 titration method (AOCS, 2017). Eq. 5.1 was used to estimate the soap concentration (ppm) in biodiesel, which was then compared to the ASTM D6751 and EN 14214 standards.

$$\text{Soap content (ppm)} = \frac{\text{A} \times \text{N} \times 304400}{\text{B}} \quad (5.1)$$

Where A and N are the volume (ml) and normality of the titrated HCl respectively; while B is biodiesel weight (g). The extraction efficiency of soap from biodiesel was calculated by using Eq. 5.2.

$$\text{Extraction efficincy (\%E)} = \frac{C_o - C_t}{C_o} \times 100 \quad (5.2)$$

Where C_o and C_t are the initial and final soap concentrations (ppm), respectively.

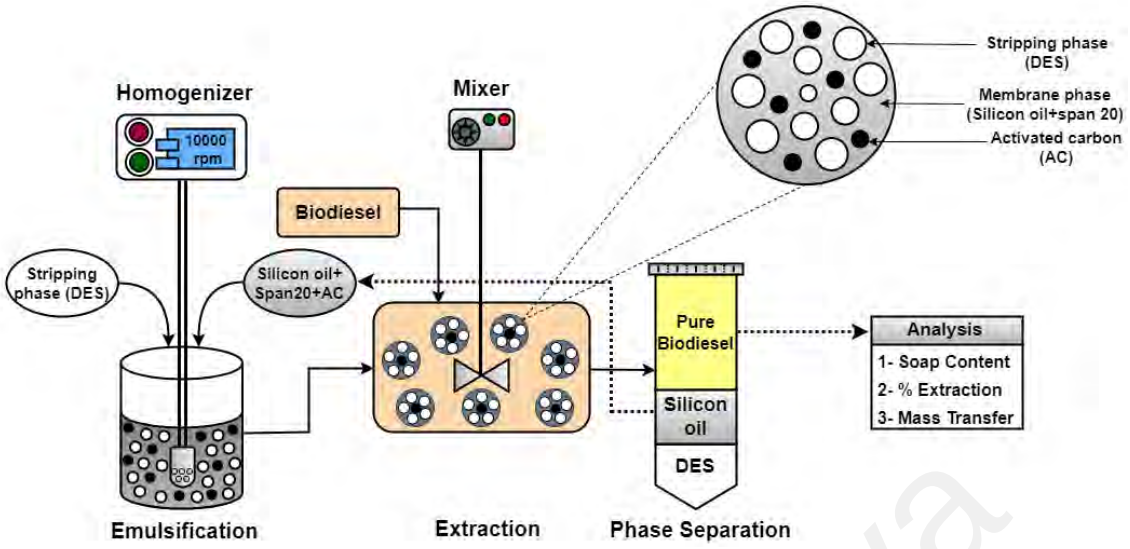

Figure 5.1: Schematic representation of DES-based ELM/AC system.

5.4. Results and Discussions

5.4.1. Screening Experiments

5.4.1.1. The Impact of Molar Ratio of DESs

The soap content in biodiesel after the screening process of four DESs at different molar ratios as the stripping phase in the ELM technique is presented in Figure 5.2. The DES was used in this investigation as the stripping phase. The DES molar ratio of 1:4 was the only molar ratio which produced a soap concentration that conforms to the ASTM D6751 standard. The soap content was reduced from an initial concentration of 765 ppm to 18.26 ppm at constant process conditions with a DES to biodiesel ratio of 1:3, 1.5 wt.% surfactant, 0.3 wt.% of AC, 300 rpm stirring 6 min, which confirms the high soap removal efficiency from the biodiesel. Thus, the DES molar ratio of 1:4 was selected for further optimization for soap removal from biodiesel.

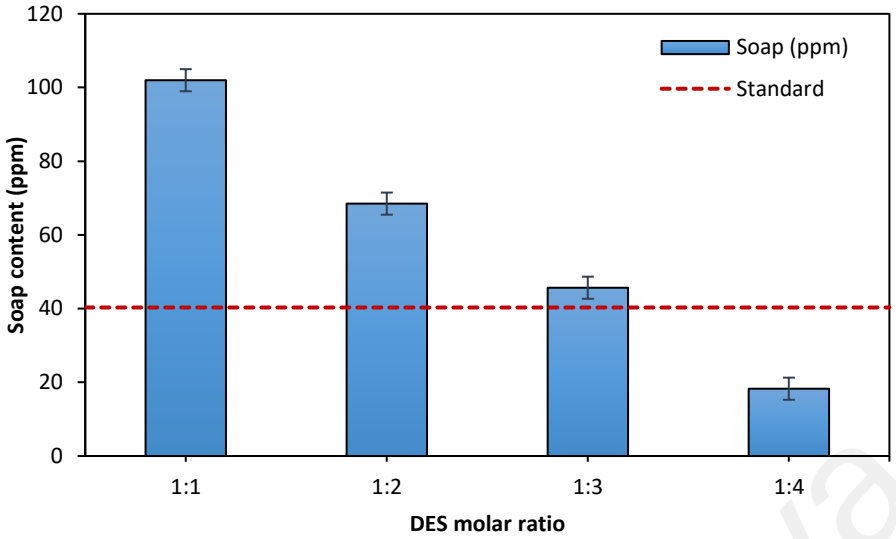

Figure 5.2: Screening of different DES molar ratio for soap removal from biodiesel using ELM technique (initial soap concentration of 765 ppm, DES to biodiesel ratio of 1:3, 1.5 wt.% surfactant, 0.3 wt.% of AC, 300 rpm stirring 6 min, dashed line: international standard).

5.4.1.2. Comparative Study of Synergistic Separation Techniques

Glycerol and biodiesel were separated using a separation funnel after the formation of biodiesel. The biodiesel was collected and analyzed for the soap content before and after the purification process. In this study, three separation processes were performed, which were the adsorption of soap using AC, DES-based ELM and DES-based ELM with the presence of AC (DES-based ELM/AC). Figure 5.3 presents the soap content before and after the purification processes.

In the adsorption process, the soap content was reduced from 765 ppm (initial concentration) to 322.6 ppm for 30 ml of biodiesel at constant operating parameters of 0.3 wt.% of AC and 300 rpm stirring speed for 6 min. The soap content was reduced due to the presence of active sites such as the oxygen functional groups on the AC surface which could interact with the potassium species in the soap (Ayoob & Fadhil, 2020; Baroutian et al., 2011).

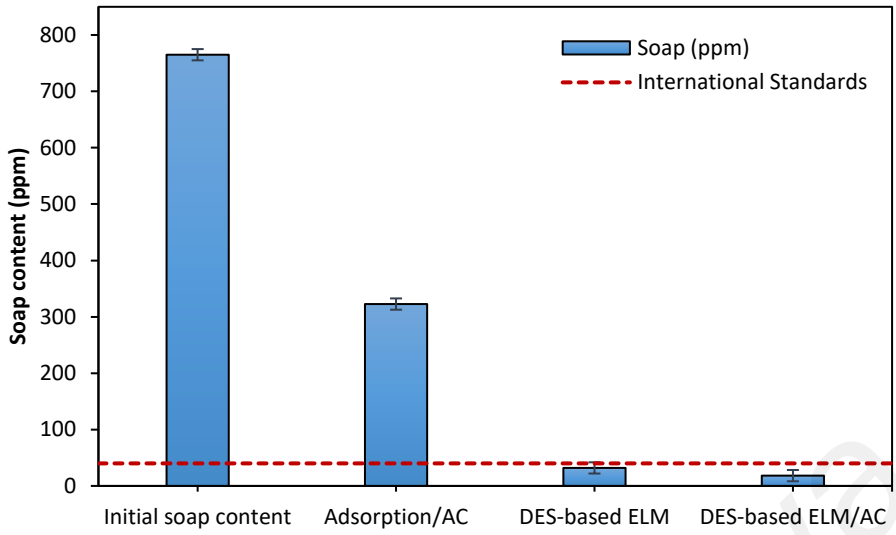

Figure 5.3: Soap content in biodiesel using different purification techniques (DES to biodiesel ratio of 1:3, 1.5 wt.% surfactant, 0.3 wt.% of AC, 300 rpm stirring 6 min, dashed line: international standard).

In the next experiments, DES-based ELM and DES-based ELM/AC were carried out at DES to biodiesel ratio of 1:3, 1.5 wt.% surfactant, 300 rpm stirring speed at 6 min in the presence of 0.3 wt.% of AC (for DES-based ELM/AC only). Figure 5.3 shows that the DES-based ELM possesses higher purification efficiency (95.82%) than the adsorption method (57.82), where most of the soap was removed from the biodiesel. Nevertheless, it was found that a minimum soap content was achieved after the purification using the DES-based ELM/AC (97.61% extraction efficiency). By introducing AC into the ELM system, the solid AC particles adsorb onto the surface of the internal phase droplets (DES), forming a bridge to prevent the integration of droplets (Alitabar-Ferozjah & Rahbar-Kelishami, 2022). As consequence the extraction efficiency of ELM was enhanced.

5.4.2. Effect of DES: biodiesel Ratio

The impact of the DES to biodiesel volume ratio on the soap content and extraction efficiency of biodiesel using the ELM technique is presented in Figure 5.4. The DES to

biodiesel ratio was examined from 1:1 to 1:5 volume ratio to determine the optimum impact of the DES to biodiesel ratio that maximizes the extraction efficiency, while other operating parameters of 1.5 wt.% surfactant concentration, 0.3 wt.% of AC and 300 rpm stirring speed for a 6-minute duration were kept constant. The perfect phase ratio provides stable emulsion globule formation where the soap was subsequently diffused and encapsulated in the DES globules.

Figure 5.4 shows that the extraction efficiency could be reduced by decreasing the volume ratio of DES to biodiesel. This could be due to the increase in external phase (biodiesel) in the ELM system which does not provide sufficient amount of DES in the emulsion phase for the soap removal from biodiesel. Nevertheless, all investigated ratios were able to retain the amount of soap to meet the ASTM D6751 standard. The emulsion stability and the extraction efficiency simultaneously decrease with the increase in the volume of the external phase (Ye et al., 2017). The HBD in DES (stripping agent) was the primary driving force in the purification technique and enhanced in the removal of soap from the membrane phase (Rosly et al., 2019).

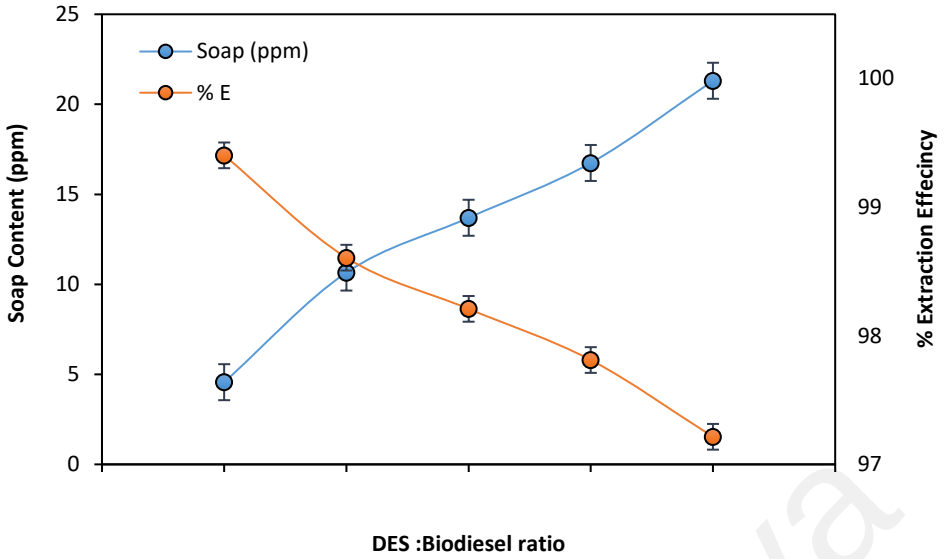

Figure 5.4: Effect of the DES: biodiesel volume ratio on the soap concentration and extraction efficiency of biodiesel using the ELM technology, at 1.5 wt.% of surfactant concentration, 0.3 wt.% of AC and 300 rpm stirring speed for a 6-minute extraction time.

5.4.3. Effect of Surfactant Concentration

The impact of surfactant concentration on the soap removal and extraction efficiency in biodiesel is presented in Figure 5.5. Other process conditions such as the DES to biodiesel ratio of 1:3, 0.3 wt.% of AC, 300 rpm stirring speed for 6 min extraction time were held constant, whereas the concentration of surfactant was varied from 0.5 to 2.5 wt% to investigate the optimum surfactant concentration that could reduce the soap content to the minimum. The results showed that the use of 0.5 wt.% of span 20 decreased the soap content m 765 ppm to 60.88 ppm. Thus span 20 is decreases the surface tension of silicone oil as well as facilitating the mass transport of soap through the silicon film to the DES. As shown in Figure 5.5, the minimum soap content was achieved at 2 wt.% of span 20 in the membrane phase. The surface tension of the membrane was decreased when the concentration of span 20 increased from 0.5 wt.% to 2.0 wt.% (Tahmasebizadeh et al., 2021). This causes the dispersion of the emulsion globules with the formation of fine bubbles, increasing the contact area between the DES and external phases. However, the

excessive presence of span 20 increases the viscosity of the membrane (Reis & Carvalho, 2004) which resulted in large emulsion droplets (Khan et al., 2021).

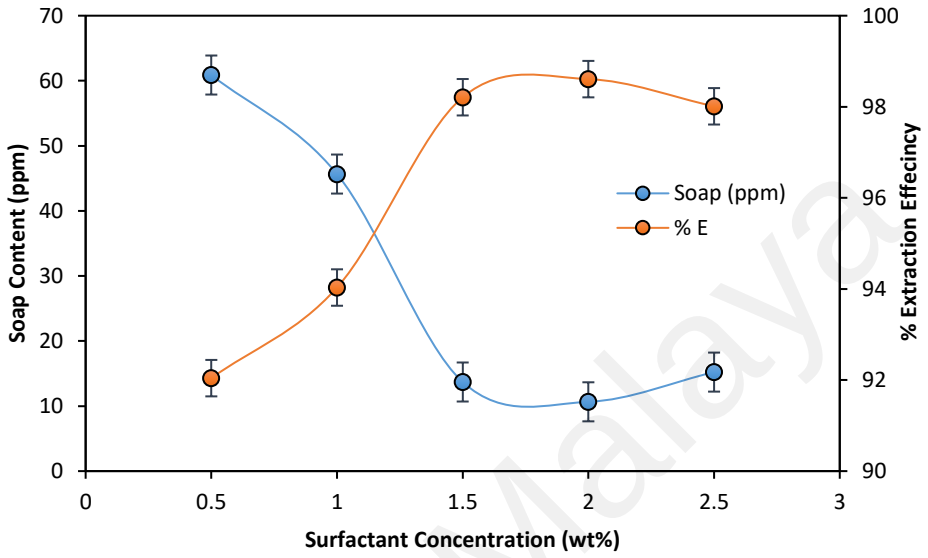

Figure 5.5: Impact of span-20 concentration on soap removal and extraction efficiency of biodiesel using the ELM technology, (DES to biodiesel ratio of 1:3, 0.3 wt.% of AC, 300 rpm stirring speed for 6 min duration of reaction).

5.4.4. Effect of Extraction Time

The effect of the extraction duration on the extraction efficiency and soap content in biodiesel is shown in Figure 5.6. Figure 5.6 shows that the soap content decreases and the extraction efficiency was enhanced with the increase in the purification process duration. After 2 minutes, the soap concentration decreases from 765 ppm (initial soap concentration) to 129.37 ppm, which is due to the longer contact time between the soap molecules in the biodiesel phase and the emulsion phase with the increase in the extraction time. After 6 minutes of extraction time, the soap concentration decreases below of the international standard limits with an extraction efficiency of 98.21%. It was found that 6 minutes of extraction time was sufficient to meet the international standards for soap content and extraction efficiency. These results agree with the results in the

literature (Ye et al., 2017). In fact, several studies (Kankekar et al., 2010; Matsumiya et al., 2004; Kulkarni et al., 2002) have reported that the emulsion breakage increases with the contact time more than the optimum duration. This is due to the membrane swelling which causes the degradation of the emulsion at longer contact time.

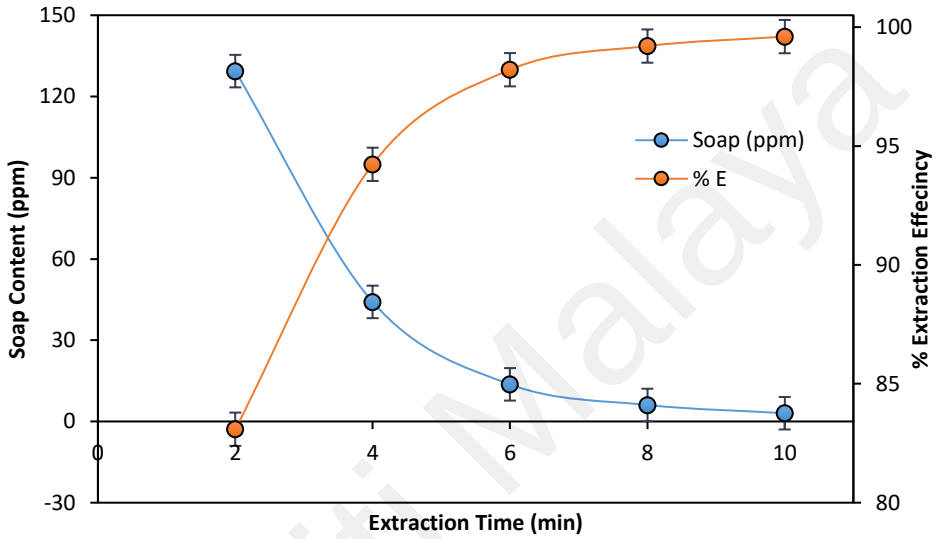

Figure 5.6: Impact of extraction time on the soap removal and extraction efficiency of biodiesel using the ELM technology, (DES to biodiesel ratio of 1:3, 1.5 wt. span 20, 0.3 wt.% of AC and 300 rpm stirring speed).

5.4.5. Effect of Mixing Speed

The effect of the mixing speed on the extraction efficiency and soap content in biodiesel is shown in Figure 5.7. Figure 5.7 shows that the soap concentration decreases and the extraction efficiency increases when the stirring speed is increased from 100 to 400 rpm. With the increase in the mixing speed, the impact of the shear forces on the emulsion droplets increases which decreases the globule sizes to become smaller. This further increase the available contact area for mass transfer increases which enhances the performance of the purification process (Alitabar-Ferozjah & Rahbar-Kelishami, 2022). However, the soap extraction rate was found to decrease with the increase in the stirring

rate to more than 400 rpm due to the instability of the emulsion droplets resulting in greater leakage of the internal phase (Dâas & Hamdaoui, 2010). According to other researchers, the extraction technique of ELMs is controlled by the external surface area of the globules compared to the internal phase surface area of the globules (Alitabar-Ferozjah & Rahbar-Kelishami, 2022; Ahmad et al., 2011; Reis & Carvalho, 2004). Thus, the mass transport area is also enhanced which increases the extraction efficiency is increased with the increase in the mixing speed. In addition, it is increasingly challenging to disperse the emulsion under sustained contact due to increased viscosity of the system as the mixing speed is raised during the purification process (Ahmad et al., 2021; Goyal et al., 2011).

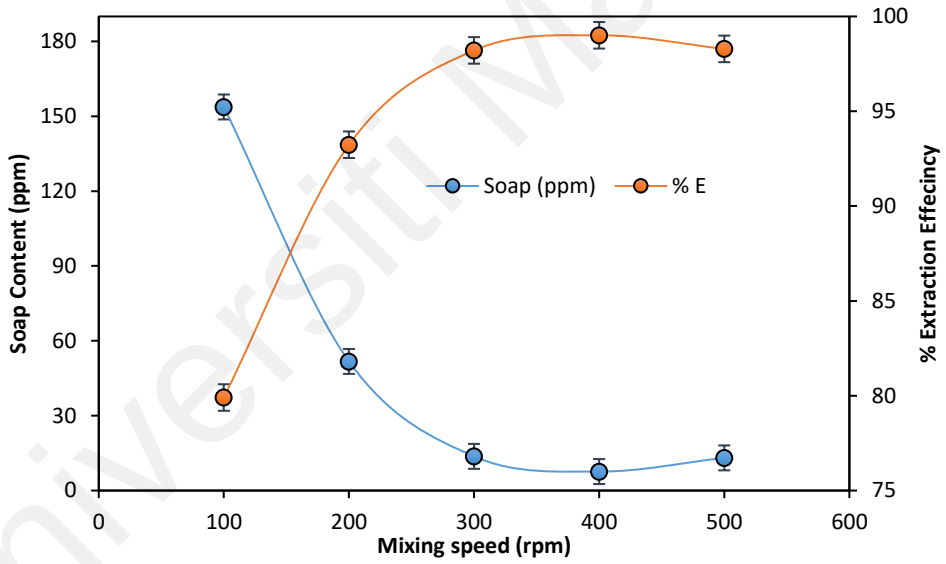

Figure 5.7: Impact of mixing speed on the soap removal and extraction efficiency of biodiesel using the ELM technology, (DES to biodiesel ratio of 1:3, 0.3 wt.% of AC and 1.5 wt.% span 20 for 6 min duration of reaction)

5.4.6. Effect of AC Dosage

The effect of the amount of AC on the soap removal and extraction efficiency in biodiesel is presented in Figure 5.8. Other process conditions such as DES to biodiesel ratio of 1:3, 1.5 wt.% of span 20, 300 rpm stirring speed and 6 min duration were held constant, while

the amount of AC was varied from 0.1 to 0.5 wt.% to investigate the optimum amount of AC required to for achieving minimum soap content. Figure 5.8 shows the increase in the extraction efficiency with the amount of AC, as more active sites (oxygen functional groups) are available for the purification process (Ayoob & Fadhil, 2020). The presence of solid AC particles in the emulsion phase improve the stability and strength between the emulsion globules, preventing the collision or coalescence of the globules (Al-Obaidi et al., 2021; Lin et al., 2015). In addition, the potassium species in soap could also interact strongly with the functional groups on the AC surface (Baroutian et al., 2011). The highest removal efficiency of soap to meet international standards was achieved at 0.3 wt.% of AC. However, a slight decrease in the soap removal occurs when the amount of AC exceeds 0.3 wt.%. Furthermore, the utilization of AC is considered beneficial for the refinement of unpurified biodiesel from pollutants (such as soap) that were formed during the synthesis (Fadhil & Saeed, 2016).

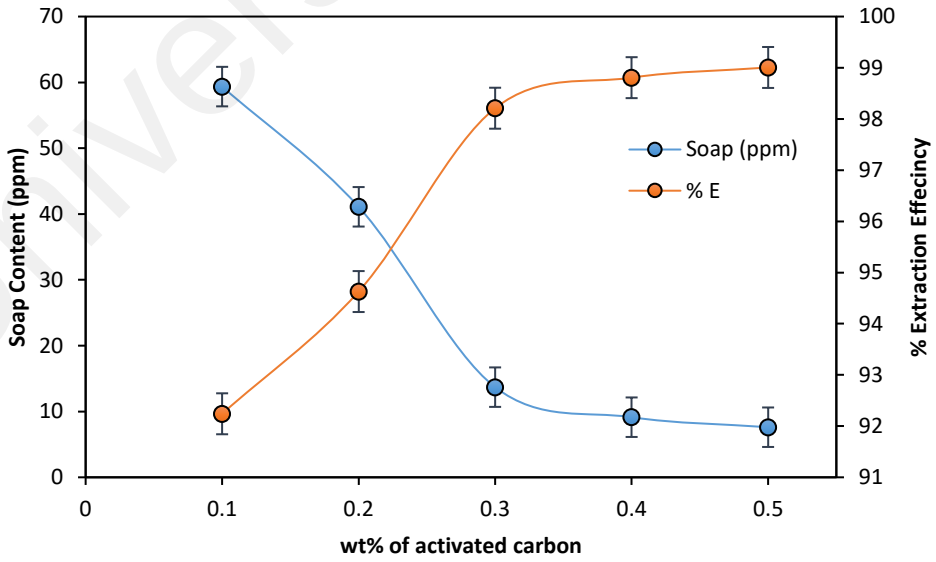

Figure 5.8: Impact of adding AC on the soap removal and extraction efficiency of biodiesel using the ELM technology, (DES to biodiesel ratio of 1:3, 300 rpm and 1.5 wt.% span 20 for 6 min duration of reaction).

5.4.7. Kinetic and Mass Transfer Modelling

The effect of kinetics and mass transfer were studied for the soap removal via the ELM technique at optimum conditions. The optimum conditions from our previous investigations were: 1:4 DES molar ratio,1:1 DES: biodiesel volume ratio, 2wt.% surfactant, 0.5 wt. of AC and 400 rpm mixing speed. The model presented in this study assumes that the phases and interfaces are immiscible, the stripping reaction of soap at the interface is irreversible, the loss of soap in the feed phase equals to the soap content in the membrane and stripping phases, and the loss of soap in the system is negligible. Fick's first law states that diffusion is the rate-limiting step in the mass transfer of soap in the ELM as described by the following Eq.:

$$J_{Soap} = -\frac{V}{A_g}\frac{dC_t}{dt} \tag{5.3}$$

where J_{Soap} (mol/cm^2.S) , V (cm^3), A_g (cm^2), and dC_t dt (mol/cm^3.S) are molar flux of soap, the volume of solution, the emulsion globules' surface area, and the change of soap content with time. A_g can be calculated as follows:

$$-\frac{A_g}{V_T} = \frac{S_g}{V_g} \rightarrow A_g = V_T\frac{\pi D_g^2}{\frac{1}{6}\pi D_g^3} = V\frac{6}{D_g} \tag{5.4}$$

Here, V_T (cm^3), S_g (cm^2),V_g (cm^3), and D_g, are the total emulsion globules' volume, the globule's surface area, the globule's volume, and the average globule size, respectively. This expression is obtained after rearranging the equations:

$$J_{Soap} = -\frac{V}{A_d}\frac{D_g}{6}\frac{dC_t}{dt} \tag{5.5}$$

Multiplying both sides of the Eq. by $\frac{1}{C_t}$:

$$\frac{J_{Soap}}{C_t} = -\frac{V_T}{A_g}\frac{D_g}{6}\frac{dC_t}{C_t dt} \tag{5.6}$$

$$-k\frac{V_d}{V}\frac{6}{D_g}dt = d\left(\frac{C_t}{C_t}\right) \tag{5.7}$$

$$-k\frac{V_g}{V_T}\frac{6}{D_g}dt = d\ \ln C_t \tag{5.8}$$

With the integration of the previous Eq. (5.8) at boundary conditions: $\text{time}; 0 \rightarrow t$ and $C_t;\ C_o \rightarrow C_t$:

$$-k\frac{V_g}{V_T}\frac{6}{D_g}\int_0^t dt = d\int_{C_0}^{C_t} \ln C_t \tag{5.9}$$

$$-k\frac{V_g}{V_T}\frac{6}{D_g}t = \ln\frac{C_t}{C_o} \tag{5.10}$$

Reaaranging Eq. (5.10):

$$\ln\frac{C_t}{C_o} = -k\frac{V_g}{V_T}\frac{6}{D_g}t \tag{5.11}$$

$$k = \frac{\ln\frac{C_t}{C_o}}{t}\frac{V_T}{V_g}\frac{D_g}{6} \tag{5.12}$$

$$\frac{C_t}{C_o} = e^{-(k\frac{V_g}{V_T}\frac{6}{D_g})t} \tag{5.13}$$

Where C_o and C_t are the initial soap content and the soap content at time t and k is the mass transfer rate (m. S^{-1}).

With the substitution of $\frac{V_g}{V_T}\frac{6}{D_g} = a$; then Eq. (5.13) is as follows:

$$\frac{C_t}{C_o} = e^{-K_a t} \tag{5.14}$$

Where K_a is the volumetric mass transfer coefficient (S^{-1}), which can be calculated from Figure 5.9. In the test runs via ELM extraction, the soap content in the biodiesel phase was measured as a function of time. Hence, the soap content was calculated using Eq. (5.1). Thus the quantity (C/C_o) on the left of Eq. (5.14) was obtained. The relationship between (C/C_o) and time produces an exponential curve with a slope of ka. Figure 5.9 shows the exponential plot of (C/C_o) as a function of time. The figure indicates that the model fits the experimental data reasonably well. From the fitting of the experimental

results, Ka for soap removal from biodiesel via the ELM technique was calculated as 0.627 (1/sec).

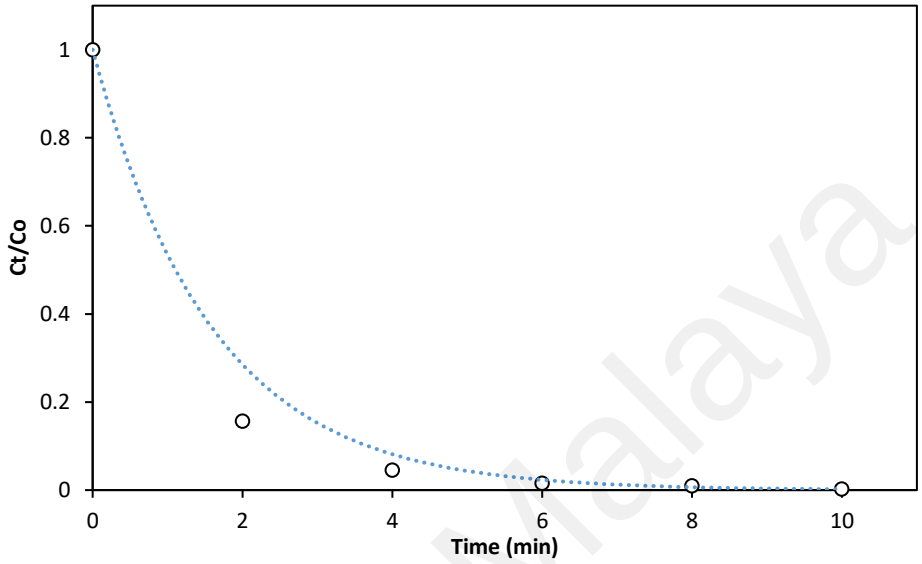

Figure 5.9: Soap concentration profile vs time (t) using an emulsion liquid membrane technique with a 765-ppm initial soap content (1:4 DES molar ratio, 1:1 DES: biodiesel volume ratio, 2 wt.% surfactant, 0.5 wt%. of AC, at 400 rpm mixing speed).

5.4.8. Transport Mechanism of Soap Removal

The mechanism of soap removal is based on the hydrophilic and hydrophobic nature of the soap molecules. Soap molecules are composed of a hydrophobic tail (nonpolar tail) and a hydrophilic head (polar head) as shown in Figure 5.10. The hydrophobic tail is a long nonpolar chain of carbon and hydrogen atoms, while the hydrophilic head consists of the polarized carboxylate or sulfonate anionic groups (Collings & Hird, 2017). The arrangement of these two components forms a structure which interacts with both water and oils, allowing the soap to effectively remove dirt and grime from any surfaces.

The mechanism of soap removal from biodiesel using DES-based ELM/AC system is postulated to be one-way transport. Figure 5.10 shows that the soap molecules are

extracted from the biodiesel via transporting into the membrane phase that comprise of silicon oil and span 20. This followed by transport of the soap molecules through the membrane phase and reach the membrane/stripping interface and membrane/AC interface. The DES and AC act as the stripping agent in this system and soap is removed from the membrane phase by adsorption and complex formation.

The highly porous AC material is capable of adsorbing polar and non-polar compounds (Li et al., 2002). In the emulsion phase, AC which provides large surface area and is effective in the removal of the nonpolar soap molecules from the membrane phase by attraction and entrapment of the soap molecules due to the functional groups and physicochemical properties of the surface. On the other hand, the HBD in DESs provides a polar environment that enhances the solubility of the soap molecules and bonds with the soap molecules to decrease the mobility of soap, and thus, removing the soap from the membrane phase. The synergistic effect of AC and DESs provides a broader range of soap molecules to be removed from the biodiesel, resulting in a more effective and efficient soap removal process.

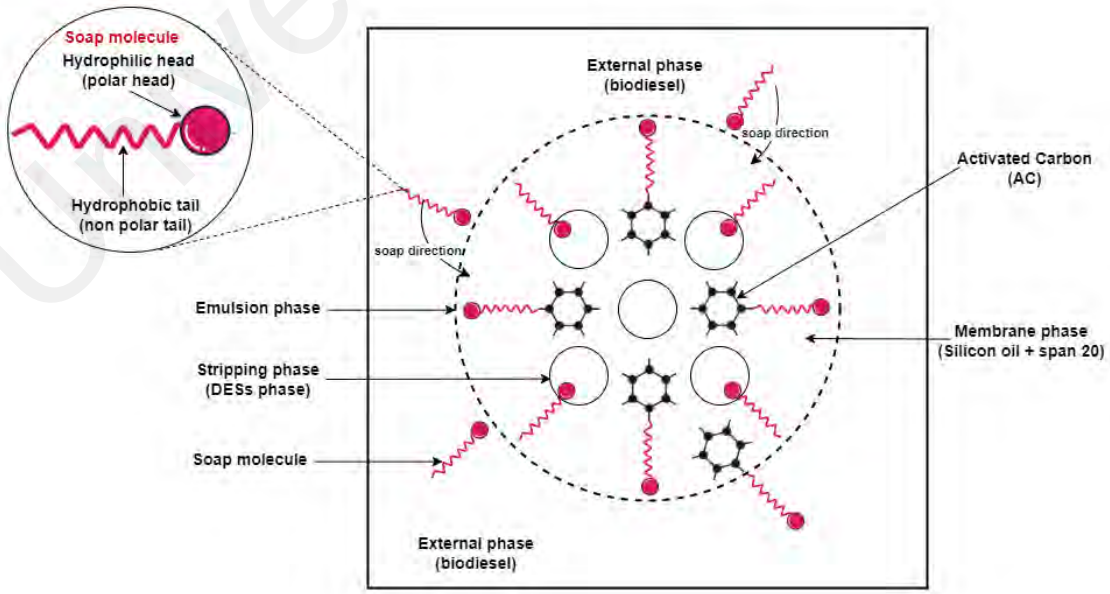

Figure 5.10: Postulated the transport mechanism of soap removal via DES-based ELM/AC.

5.4.9. Comparison between traditional technique and ELM technique

The main objective of biodiesel refinery is to ensure the production of high-purity biodiesel fuel that meets the international standards and can be utilized in biodiesel engines. The processing of crude biodiesel have significantly contributed to achieving high-quality products. However, these methods have certain challenges or limitations. For example, water washing generates a large amount of wastewater and consumes a considerable amount of energy (Atadashi, Aroua, Aziz, et al., 2011a). The drawbacks associated with the water washing method leads to the application of the waterless methods. However, these methods also possess challenges such as spent of adsorbent regeneration and a limited understanding of the chemistry (Atadashi, 2015). When choosing an appropriate ion exchange resin, various factors must be taken into account such as the structural characteristics, stability, exchange capacity, type and resin strength. While ion exchangers exhibited promising results in removing contaminants, their effectiveness in methanol removal is unsatisfactory. Moreover, the high cost associated with ion exchange possesses a significant challenge. The difficulties encountered in these traditional methods have promoted the utilization of membrane technology for biodiesel refining. Among these techniques, the membrane technology appears as a suitable option for biodiesel purification, as it retains unreacted triglycerides (Shuit et al., 2012). Additionally, the development of membrane technology in biodiesel purification further advances the dynamics of the biodiesel refining process. Although the membrane process has demonstrated positive impacts on the physicochemical properties of biodiesel (Saleh et al., 2011), more research efforts are needed to investigate the fouling patterns in biodiesel membrane refining techniques. In addition, attention should be given to the high cost of synthesis of the membrane and the energy losses associated with the use of vacuum pumps in membrane techniques. These aspects require more effort and exploration within the field of biodiesel refining (Atadashi, 2015).

Table 5.2 shows the performance comparison of different techniques for soap removal from biodiesel. It can be deduced that the DES-based ELM/AC system in this study shows comparable efficiency whereby it can remove the soap content from 765 ppm to as low as 1.52 ppm and meet the international standards. While the purification of biodiesel is well documented, we propose a novel approach that holds significant potential in improving the efficiency and effectiveness of the purification process in comparison to other LLE and ELM treatment methods. Besides that, in comparison to water washing, the DES-based ELM/AC technique not only is a waterless process, but also do not require large amount of membrane and stripping phase to a chive low soap content. This also suggested that thus, our work on developing an efficient and effective DES-based ELM/AC system for purifying biodiesel, can be further extended to the removal of various contaminants such as soap, glycerol, etc to enhance its overall quality and meet international standards.

Table 5.2: Comparison of different techniques for soap removal from biodiesel

Purification methods	Type of solvent	Initial soap (ppm)	Soap content (ppm)	Conditions	Reference
Water washing	water	1240	211	1240 of initial soap, 30 min, 60 ^{O}C, and 200 rpm	Berrios & Skelton, 2008
Acidic water washing	Hot acidic water	1670.05	158.12	2% H3PO4, constant stirring and washing 3 times at 55 ^{O}C	Faccini et al., 2011
Liquid-liquid extraction	DES	150	39	DES: biodiesel ratio of 3:1, extractant stirring speed of 170 rpm, and extraction time of 40 min.	Hayyan et al., 2022

Purification methods	Type of solvent	Initial soap (ppm)	Soap content (ppm)	Conditions	Reference
Liquid-liquid extraction (DES/AC)	DES	765	12.6	150 rpm, 1:1 of DES to biodiesel volume ratio and 0.3 g AC	Abed et al., 2023
Dry washing -adsorption	-	1670.05	61	1% mgnisol and 2% silica	Faccini et al., 2011
Waterless using ion exchange	-	1240	101	80 g of Purolite (particle size: 600µm), flowrate of 0.25 l/h for 2 h at 22 ^{O}C	Berrios & Skelton, 2008
Waterless using magisol	-	1240	340	100% (w/w) magnisol (particle size: 600µm) and 60 ^{O}C for 30 min	Berrios & Skelton, 2008
Ultrafiltration membrane	-	2600	1300	0.22 µm, 4 bar and final flux of 120 $kg.h^{-1}.m^{-2}$	Alves et al., 2013
DES-based ELM/AC	DES/silicon oil	765	1.87	DES to biodiesel ratio of 1:1, 1:4 DES molar ratio 2 wt.% of surfactant, 0.5 wt.% of AC, 400 rpm stirring and 10 min	Our study
DES-based ELM	DES/silicon oil	765	31.96	DES to biodiesel ratio of 1:3, 1.5 wt.% surfactant, 300 rpm stirring and 6 min	Our study

5.5. Conclusions

The use of DES and AC in ELM technique for the separation of soap from biodiesel was investigated using silicon oil and span 20 membrane phase. DES-based ELM/AC system showed superior removal efficiency at 97.61% in comparison to AC adsorption (57.82%)

and DES-based ELM (95.82). This suggested that the DES-based ELM/AC system provided a synergistic effect between AC and DES in the striping process to enhance soap removal via providing additional surface functional groups for the adsorption and the improved solubility of both polar and non-polar groups in the soap molecules in membrane and stripping phases. Highest removal efficiency of 99.75%, which is equivalent to 1.87 ppm soap content in the biodiesel, was achievable 2 wt.% of the surfactant, 0.5 wt.% of AC, 1:4 DES molar ratio as stripping phase, 1:1 DES: biodiesel ratio, 4000 rpm mixing speed and 6 min extraction time. The transport of soap in this system followed first order kinetic model with a rate constant of 0.6 min^{-1}. Overall, the DES-based ELM/AC technique is promising purification method for the effective removal of soap content from crude biodiesel. In comparison to conventional water washing, this technique does not consume water, and does not required high volume of membrane phase and stripping phase to achieve low soap concentration. Therefore, this technique has shown significant potential for further investigation for the purification of biodiesel, specifically from the view of the removal of other impurities from biodiesel such as glycerol to meet the international standards.

CHAPTER 6: EMULSION LIQUID MEMBRANE PERTRACTION OF SOAP FROM CRUDE BIODIESEL USING ACTIVATED CARBON AND GLYCOL-BASED DEEP EUTECTIC SOLVENTS

6.1. Introduction

Soap removal from crude biodiesel is considered as one of the most challenging processes in biorefinery. To the best of our understanding, DES-AC-ELM investigations on the removal of soap from crude biodiesel have yet to be reported. Besides that, there are no reports on the COSMO-RS investigations for the elimination of soap from crude biodiesel. In this chapter, a new technique incorporating activated carbon (AC) in an emulsion liquid membrane (ELM) system based on deep eutectic solvents (DES-AC-ELM) was utilized for soap removal. These DESs were prepared from two salts, namely tetramethylammonium chloride (TMAC) and choline chloride (ChCl), with different hydrogen bond donors (HBDs) such as ethylene glycol (EG), diethylene glycol (DEG) and triethylene glycol (TEG). COSMO-RS modelling was performed in the evaluation of activity coefficient and capacity at infinite dilution of DESs. In addition, the σ-profile and σ-potential were used to investigate the interaction between the soap molecules and each phase. Moreover, the impact of various process parameters on the soap removal such as the salt: HBD ratio, DES: biodiesel ratio, span-20 concentration, mixing speed, extraction time, and dosage of AC were evaluated. Furthermore, a kinetic model on the transport of soap from biodiesel through the DES-AC-ELM system was developed. Thus, the soap removal mechanisms from biodiesel to the DES-AC-ELM system was postulated based on these results. The results of this chapter were published in the Journal of Cleaner Production (Abed et al., 2024).

6.2. Literature Review

Biodiesel has emerged as a promising renewable energy source due to its potential to replace conventional fossil fuels. Transesterification, a widely-used process, produces biodiesel by combining plant oils or animal fats with an alkali catalyst and alcohols (Borges & Díaz, 2012). However, the resulting raw biodiesel contains impurities such as glycerine and soap, which must be removed to meet the fuel specification standards (Saleh et al., 2010). The presence of soap in particular, is a significant obstacle for the production of biodiesel as it reduces the bio-oil yield and complicates the final product's isolation and refinement (Atadashi et al., 2011b). The presence of soap molecules also increases the viscosity, forming hydrogels and emulsions, which hinders the separation of glycerol (Ferella et al., 2010).

To address these problems, conventional techniques such as equilibrium, affinity, membrane and reaction-based processes, have been explored to remove impurities from biodiesel. Among these techniques, membrane-based processes have shown promise due to their simplicity and high efficiency. The use of liquid membranes as selective separation barriers has increased in recent years (Kumar et al., 2019; Abed, 2014). The use of liquid membrane facilitates the extraction process due to the membrane's strong affinity towards specific solutes, which offers several benefits such as high selectivity, separation efficiency, enrichment efficiency, minimal product contamination, cost-effectiveness, mitigation of phase separation phenomenon, ease of scaling for commercial purposes, and decreased presence of organic phases compared to the traditional solvent extraction processes (Kumar et al., 2018). The emulsion liquid membrane (ELM) processes, in particular, offer a larger contact surface area in relation to the volume and greater selectivity for removing impurities with smaller volumes of the organic solvents (Davoodi-Nasab et al., 2018). However, the stability of ELM is critical for achieving high extraction efficiency.

DESs are recently utilized in membrane techniques and possess unique properties compared to the traditional solvents, such as high heat capacity, high stability with lower viscosity and lower toxicity (Mbous et al., 2017;Hayyan et al., 2022). DESs are relatively inexpensive and require simple synthetic procedures due to their optimal processing parameters, making them a viable option for future large-scale commercialization. Few types of DESs could remove glycerol from biodiesel products, for example, the quaternary ammonium salt-based DES (Abbott et al., 2007;Hayyan et al., 2010). DESs have been effectively utilized in the purification of biodiesel via several processes such as the liquid-liquid extraction (Abed et al., 2023) and bulk liquid membrane techniques (Hayyan, et al., 2022). However, the abovementioned techniques require additional stripping process and possess slower mass transfer rate, respectively, compared to the emulsion liquid membrane technique. In addition, the selection of the most appropriate DES for a specific task is challenging due to the large number of options available. To overcome this problem, Conductor-like Screening Model for Real Solvents (COSMO-RS) could simulate the thermodynamic characteristics of the liquid mixture/fluid, providing reliable and robust data for unknown regions using only molecular structure information as the input. To the best of our understanding, DES-AC-ELM investigations on the removal of soap from crude biodiesel have yet to be reported. Besides that, there are no reports on the COSMO-RS investigations for the elimination of soap from crude biodiesel.

6.3. Experimental and Methods

6.3.1. Materials

Tetramethylammonium chloride (TMAC), choline chloride (ChCl), hydrochloric acid and acetone were acquired from Merck (Malaysia). Bromophenol blue, span-20 (surfactant) and potassium hydroxide (KOH) were obtained from Sigma-Aldrich (US).

Triethylene glycol (TEG, 99%) was obtained from Fluka (Germany), while methanol and silicon oil were acquired from Chemiz (Malaysia). The refined palm oil was obtained from a local Malaysian mill. Lastly, the AC used in the investigation was prepared from biomass of palm raceme.

6.3.2. Screening using COSMO-RS

Six types DESs were investigated for their ability towards soap removal from biodiesel using the COSMO-RS approach. COSMO-SAC, as another alternative, may incorporate advancements with parameters for dispersion forces. Nonetheless, despite some limitations in thermodynamic consistency, COSMO-RS has robust predictive capabilities, making it suitable for screening and evaluating the solubility of soap molecules in various DESs. Two categories of salts, namely the tetramethylammonium chloride (TMAC) and choline chloride (ChCl), were used in conjunction with three distinct hydrogen bond donors (HBDs), namely: ethylene glycol (EG), diethylene glycol (DEG) and triethylene glycol (TEG). The DESs and their abbreviations are presented in Table 6.1. The compatibility of TMAC and ChCl with different HBDs such as EG, DEG and TEG, together with their dissolution of contaminants in biodiesel (Zhang et al., 2012) make them strong candidates as the stripping phase in the ELM system. The ability of these DESs towards the purification of contaminated biodiesel using liquid-liquid extraction techniques (Shahbaz et al., 2011a) also makes them suitable for an ELM system. Moreover, the immiscibility of DESs (internal phase) with the other phases of ELM, such as silicon oil (membrane phase) and biodiesel (external phase) make them a strong candidate for the formation of a stable emulsion. The Density Functional Theory (DFT) BP86 level and triple-zeta valence potential (TZVP) basis set were used to optimize the geometry of each species involved in the DESs, including the DES constituents and the soap. Subsequently, a single-point calculation was performed to

create the COSMO files that were used in the COSMO-RS simulations. The BP86 def2-TZVP basis set and the FINE grid matching tetrahedron cavity were employed in the single-point calculations to create identical COSMO surface segments for the COSMO-RS calculations. The graphical user interface enables the TURBOMOLE version of quantum chemistry software, TMoleX version 4.0 to carry out single point calculations as well as geometry optimization.

Table 6.1: List of the DES that have been chosen for screening in COSMO-RS.

DES	HBA	HBD	Molar ratio
DES1	TMAC	EG	1:2
DES2	TMAC	DEG	1:2
DES3	TMAC	TEG	1:2
DES4	ChCl	EG	1:2
DES5	ChCl	DEG	1:2
DES6	ChCl	TEG	1:2

The generated COSMO files were then used to predict the activity coefficient of soap in each DES ($\gamma\infty$) at infinite dilution via the COSMO-RS calculations. These values were subsequently used to estimate the capacity of soap in the DESs ($C\infty$) at infinite dilution, as expressed in Eq. (6.1) and Eq. (6.2):

$$\text{Activity coefficient } (\gamma\infty) = e^{\frac{(\mu-\mu_0)}{RT}} \quad (6.1)$$

where μ is the chemical potential of the solvent and μ_0 is the chemical potential of the pure compounds.

$$\text{Capacity } (C\infty) = \left(\frac{1}{\gamma\infty}\right)_{\text{DES phase}} \quad (6.2)$$

The values of $C\infty$ and $\gamma\infty$ were then used to identify suitable DESs as a stripping phase in the ELM system. All COSMO-RS results were conducted using COSMO thermX (19.0.5) software package.

6.3.3. Preparation of DESs

Choline chloride (ChCl) and tetramethylammonium chloride (TMAC) were mixed with three different HBDs in specific ratios according to predetermined compositions, as shown in Table 6.1. All chemicals were dried under a vacuum before being used in the synthesis of the DESs. Subsequently, the DESs with specific compositions were formed by stirring the mixture in a vessel at 70 °C for an hour, on a magnetic hotplate stirrer at 200 rpm, until a homogenous and transparent liquid was achieved. Then, the synthesized DESs were directly utilized in the ELM process. This step was crucial to achieve fresh DESs as the stripping phase for soap removal from biodiesel. The moisture content of the DES was determined using Karl-Fischer titration method.

6.3.4. Production of Biodiesel

The study utilizes refined palm oil as the vegetable oil and KOH as the catalyst to produce biodiesel. The reaction was initiated by mixing the palm oil with 1 wt% KOH catalyst in a conical flask, with a 1:10 volume ratio of the oil to methanol, to ensure an excess of methanol in the reaction (Foon et al., 2004). Stirring of the mixture was accomplished at 500 rpm and 60 °C for an hour. Upon completion of the reaction, the biodiesel product was separated from the glycerol by-product via centrifugation at 2500 rpm for 10 minutes. The biodiesel was then heated at 75 °C for 15 minutes to eliminate the methanol remnants.

6.3.5. Preparation of ELM

The ELM technique consists three major steps: the production of emulsion droplets, utilization of the emulsions for the extraction of solutes from the feed phase to the stripping phase, and phase separation through gravitational settling (Chaouchi & Hamdaoui, 2014). To form the ELM phase, a mixture of surfactant/silicon oil was homogenized along with AC (membrane phase) at 5000 rpm for 3 minutes. The DES/O emulsions (deep eutectic solvent/silicon oil) were subsequently produced by

homogenizing the stripping phase (DES) with the membrane phase for 5 minutes at 10000 rpm. The extraction procedure was performed by mixing the ELM into biodiesel comprising of 765 ppm of soap at 300 rpm with a mixing duration of 10 minutes. The emulsion blend was dispersed in the biodiesel and form biodiesel/silicon oil/DES emulsions as shown in Figure 6.1. After the extraction process, the biodiesel/silicon oil/DES emulsion mixture was transferred into a separation funnel and allowed to separate into three distinct layers. The purified biodiesel is present as the top phase, silicon oil as the middle phase, while the DES as the bottom phase. A newly prepared emulsion was used before performing each experiment. After the separation of the phases, the AOCS titration method (Cc 1795) was utilized to assess the soap content in the biodiesel samples (AOCS, 2017).

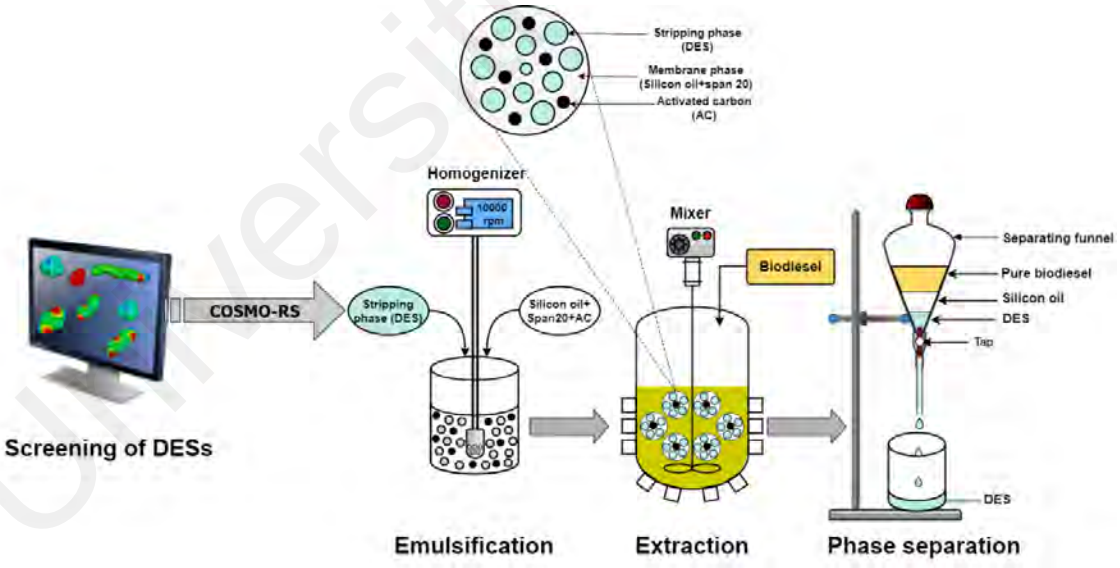

Figure 6.1: DES-based ELM/AC system schematic illustration for soap removal.

6.3.6. Soap Detection Method by Titration Analysis

The AOCS Method (Cc 17–95) was used to determine the soap content in crude biodiesel (AOCS, 2017). Initially, the crude biodiesel was mixed with an acetone solution in a conical flask. Then, a bromophenol blue indicator was added to the mixture, which turns

blue due to the presence of excess alkali of the sample as the soap molecules. Next, dilute hydrochloric acid was gradually added into the mixture until the blue colour changed into yellow. The amount of the HCl solution consumed was recorded, and the soap concentration was calculated based on the volume and concentration of the acid solution and the weight of the biodiesel. This method provides a measurement of the soap content in crude biodiesel. Eq. 6.3 was employed to estimate the soap content (in parts per million) in biodiesel, which was then compared to the international standards.

$$\text{Soap content (ppm)} = \frac{\text{N} \times \text{V} \times 304400}{\text{W}} \quad (6.3)$$

where N and V represent the normality and the volume (mL) of hydrochloric acid, respectively, while W denotes the weight (g) of biodiesel. The evaluation of soap extraction efficiency from biodiesel was calculated using Eq. (6.4):

$$\text{Extraction efficincy (\%E)} = \frac{C_o - C_t}{C_o} \times 100 \quad (6.4)$$

where C_o represents the initial soap concentration (ppm), while C_t represents the final soap content (ppm).

6.4. Results and Discussions

6.4.1. Simulation of Soap Molecules

The sigma (σ) surface of soap was generated using COSMO-RS. The chemical structure of the soap molecules and the 3-D structures are depicted in Figure 6.2. The sigma profile provides valuable information on the distribution of charge, polarity and hydrogen bonding of the soap molecules. In general, the soap molecules' surface is neutral, as illustrated by the green shade in Figure 6. 2b, while the red shade illustrates the electronegativity and the blue shade represents partial electro-positivity (Khan et al., 2020).

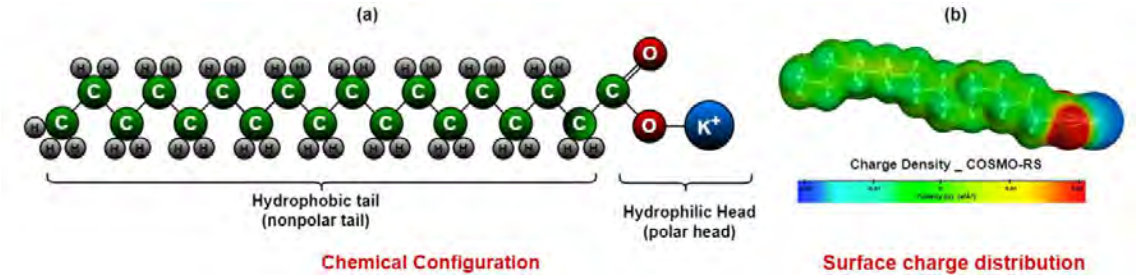

Figure 6.2: (a) Chemical configuration; (b) σ surface charge distribution of the soap molecules investigated in this study (Electrostatic potential: Red – negative; Green – neutral; Blue - positive).

The σ-profile is a reliable assistive tool to identify the charge density of a molecular surface and qualitatively evaluate its intermolecular interactions with other molecules. The HBD molecules have $\sigma < -0.0085$ e/Å^2, while non-polar molecules have σ values ranging from −0.0085 to 0.0085 e/Å^2, and the HBA molecules have $\sigma > 0.0085$ e/Å^2(Lotfi et al., 2017). As shown in Figure 6.3a, the soap molecules are highly non-polarized, as evidenced by a sharp peak at the non-polar region represented by the green surface in Figure 6.2b. The soap molecules consist of a long, nonpolar hydrocarbon hydrophobic tail and a polarized carboxylate or sulfonate anionic hydrophilic head. These molecules are either the HBDs or HBAs and have a good affinity towards the non-polar solvents.

The sigma-potential (μ(σ)) is an indicator of the chemical structure of the soap molecule and its attraction towards a distinct DESs. Higher negative value of μ(σ) indicates stronger attractive interactions between molecules. In the context of soap and DES interactions, this suggests that the soap molecules are more likely to be solubilized by the DES due to favorable electrostatic and van der Waals interactions. In contrast, a higher positive value of μ(σ) indicates repulsive interactions. This would indicate that the soap molecules are less likely to interact favorably with the DES, thus the lower solubility. Figure 6.3b shows the highest negative μ(σ) value for the soap, indicating a strong interaction with the non-

polar groups. This finding is consistent with the σ-profile results, where the soap molecule is substantially non-polarized (Rezaei Motlagh et al., 2020; Lotfi et al., 2017).

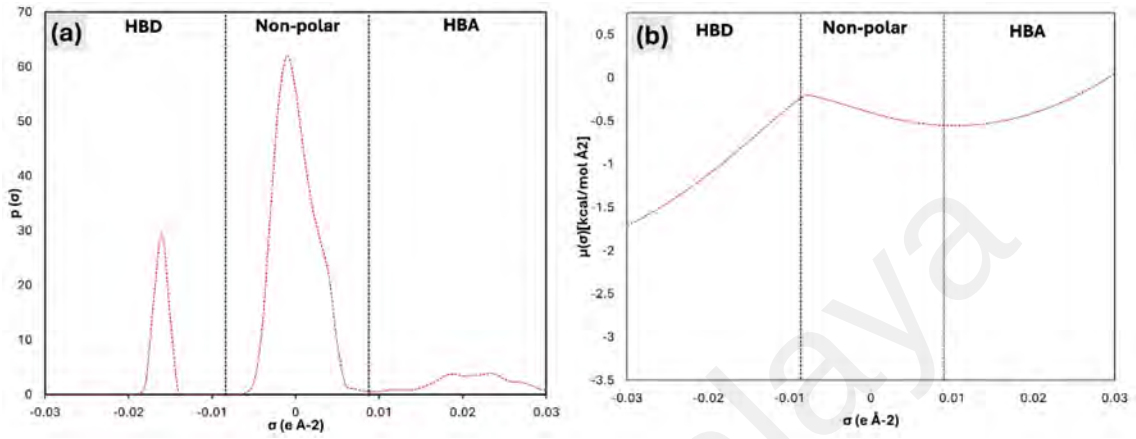

Figure 6.3: Distribution of predicted σ profile (a) and σ potential (b) of soap utilizing the COSMO-RS model.

6.4.2. Screening Using COSMO-RS

COSMO-RS was used in the screening of six different DESs with varying polarities to determine their soap-dissolving capacity, which was determined by calculating the reciprocal activity coefficient. Figure 6.4 shows the activity coefficient and the soap capacity for the screened DESs. The soap capacity was ranked in the descending order of: DES3 (31502.4) > DES2 (6891.6) > DES6 (6641.9) > DES1 (1735) > DES5 (1711.4) > DES4 (500.4). In general, the increase in the carbon chain length of the HBD in the DES increases its dissolution of the substance (Xu et al., 2022). This is due to the presence of longer carbon chains which provides more hydrophobic interactions which increases the solubility of the non-polar substances such as soap molecules (Khanian-Najaf-Abadi et al., 2022). In this study, DES3, which consists of TMAC and TEG, possesses the highest capacity, with TEG possessing a longer carbon chain length than the EG or DEG used in the other DESs. This suggests that the increase in the carbon chain length of the HBD

from EG to DEG and TEG significantly increases the DES capacity towards soap dissolution. In contrast, there are potential disadvantages associated with longer carbon chains, such as lower surface tension, larger viscosity leading to lower mass transport, slightly higher decomposition temperature (Chen et al., 2017), and lower ion mobility (Chen et al., 2017; Cotroneo-Figueroa et al., 2022). In addition, the density of the DES decreases with temperature and depends on the chain length of the HBD (Cotroneo-Figueroa et al., 2022). Nevertheless, other factors such as the DES polarity also play important roles in soap dissolution. The DESs with higher polarities attract more soap molecules and thereby increase the solubility, regardless of the length of the HBD carbon chains (Pandey et al., 2014). Therefore, a balanced approach that considers both the HBD carbon chain length and the polarity of the DES is necessary to optimize its soap dissolution capacity.

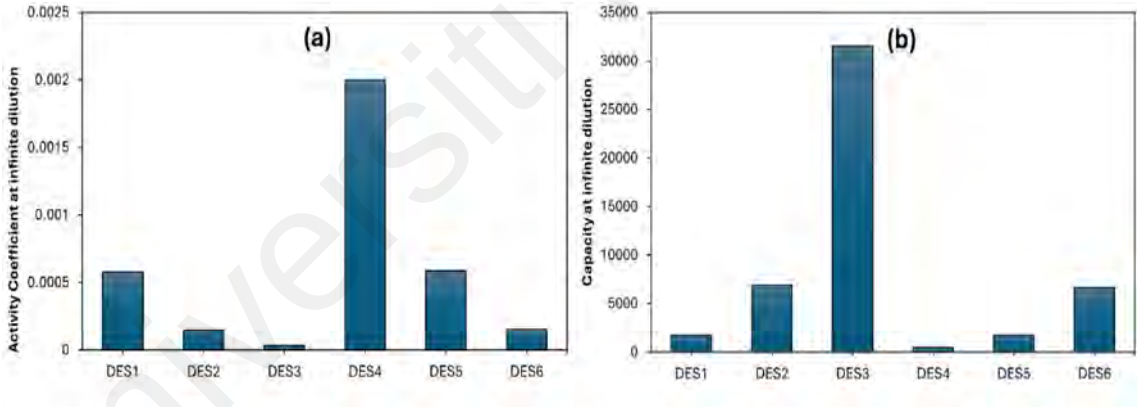

Figure 6.4: Assessment of DESs screening, accompanied by two key aspects: (a) the activity coefficient calculation and (b) capacity evaluation of soap within the context of DESs.

6.4.3. Molecular Interaction Between Soap and DES-AC-ELM System Phases

The interaction between the soap molecules in each phase of the ELM system can be studied by the analysis of σ-profile and σ-potential. The σ-profile is a depiction of the distribution of the molecular surface charge density in the form of a histogram. On the

other hand, the σ-potential measures the propensity of a component in a mixture to interact with the other component.

Figures 6.5 and 6.6 display the σ-profiles and σ-potential of biodiesel, soap, silicon oil, span 20 and various types of DESs that are described in Table 6.1. The interaction between the soap molecules and the compounds of the system was investigated to understand the mechanism of soap molecules extraction/stripping through the ELM process. This involves the presence of intermolecular forces among the various species in the three phases: dissolution of soap in biodiesel (external or feed phase), soap with silicon oil and span20 (membrane phase), and soap with DES (internal or stripping phase). In this study, the selected soap, which is specifically potassium stearate, exhibits favourable interaction in all three regions, namely the HBD, HBA and non-polar region. These interactions are evident from the σ-profile (dominant peaks) and σ-potential (negative μ values) curves. The non-polar interaction arises due to the non-polar nature of the stearate alkyl chain, while the HBD and HBA interactions resulting from the electropositive effect of the potassium cation and the HBA nature of the carboxylate anion (COOH), respectively. The major peak (σ = -0.06 e/Å^2) of the soap in the HBA region corresponds to the potassium cation (K^+), which is strongly attracted to other molecules displaying peaks in the HBA region. Consequently, DES3 and DES6 are expected to exhibit higher soap solubility due to their more prominent peaks in the HBA region compared to other DESs. In addition, the soap molecule also displays a broad peak in the HBA region, which corresponds to the negative surface charge densities of the stearate anion and being attracted to molecules with high peaks in the HBD region. In this context, all DESs exhibit similar curves, with DES5 and DES6 showing larger peak areas in the HBD region. Therefore, to further assist the evaluation of intermolecular interactions between the soap and other species, the σ-potential of each molecules were gathered. The σ-potential curve of soap shows negative values in all regions, indicating the presence of

attraction forces with the other compounds. Soap is slightly soluble in biodiesel (methyl ester) as evidenced by the higher μ values of biodiesel in the HBD region compared to the soap molecules. Additionally, biodiesel displays repulsive behaviour in the HBA region, indicating lower solubility of soap in the biodiesel.

Soap is expected to possess a higher degree of interaction with the HBD compounds, as indicated by the lower μ values observed in the HBD region. Eventually, when the membrane phase is introduced, strong hydrogen bonding forms between the soap and span-20 molecules due to the compromised negative μ values observed in the HBD (soap) and HBA (span-20) regions. These interactions suggest that the dissolved soap in biodiesel will ultimately migrate from the external feed phase into the membrane phase.

Similar to the soap molecules in the internal stripping phase, DES exhibits high negative μ values in all three regions which have positive μ values in the HBA region. This indicates the universal polarity of the DES to interact with both the polar and non-polar compounds. The μ values of the soap and DES in the three regions demonstrate the affinity of DES towards the soap molecules, thus effectively stripping the soap molecules from the membrane phase into the internal phase. Klamt (Klamt, 2005) provided a detailed explanation of the interactions between the molecules with regards to the COSMO-RS σ-profile and σ-potential, which accounts for the performance of DES. The screening charge density range of ± 0.0085 e/Å^2 is considered to be too non-polar for the molecular surface to engage in hydrogen bonding (Salleh et al., 2017). A greater percentage of the σ-profile within the HBA and HBD area indicates a stronger HBA or HBD characteristics of the compound.

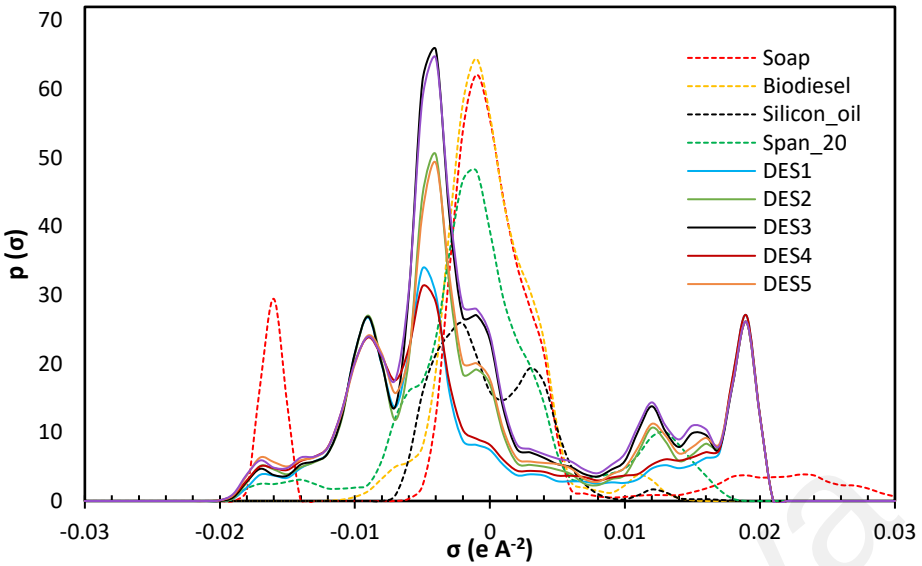

Figure 6.5: Energies of local surface interactions between σ-profiles of soap and ELM phases.

The soap molecule's sigma profile indicates that a significant portion of the molecule is non-polar, consistent with the presence of a conjugated tail region comprising of long carbon chains. The carboxylate group functionalities comprise of a relatively minor component, resulting in low HBD groups but a stronger HBA ability. Consequently, the soap molecules are expected to be more soluble in less polar DESs containing the HBD groups. The DESs also display sigma profiles that are primarily found in the non-polar regions, indicating comparable polarity of the soap molecules.

In the analysis of COSMO-RS, the σ-potential is used to determine the attraction of a component towards the other components in a mixture. The σ-potential plot provides insight on the molecular interactions, with a higher negative value indicating increased interaction between the molecules while the more positive value indicates a repulsive behaviour. The hydrogen bonding threshold is represented by the horizontal axis, with an increase in negative and positive regions representing stronger molecular interactions with the HBDs and HBAs, respectively. Similar to the σ-profile plot, the hydrogen bond threshold divides the σ-potential plot into three different areas. The σ-potential of soap,

as illustrated in Figure6, indicates that the solvents with effective HBD groups are more likely to provide greater solvation of the soap molecules.

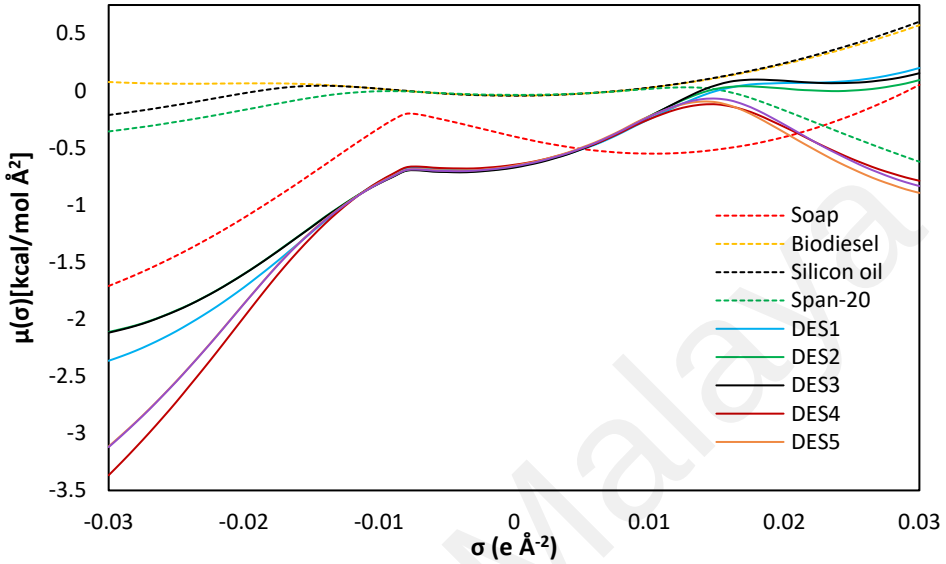

Figure 6.6: Energies of local surface interactions between σ-potential of soap and ELM phases.

Additionally, this indicates the universal polarity of DES to interact with both the polar and non-polar compounds. The complementing μ values of soap (fatty acid salts) and DESs in the three regions demonstrate the high affinity of DESs towards the soap molecules, thus effectively extracting fatty acid salts from the membrane phase. To maximize the efficiency of DESs in soap extraction, the DESs must possess a high negative value in the HBA area, emphasizing the complementary interactions. In contrast, the least negative value in the HBD area is due to the lower affinity towards the HBD molecules, thereby lowering the self-attachment between the HBA and HBD functional groups for the effective solvation of the soap molecules.

6.4.4. Experimental Validation

The screening in Section 6.3.2 yields noteworthy findings with regards to the effectiveness of DESs in soap removal from crude biodiesel. Specifically, DESs based on triethylene glycol demonstrate superior results for both types of salts (ChCl and TMAC). As a result, the investigation focuses on the utilization of these DESs and TEG as the novel stripping phases in the ELM system, for effective soap elimination from biodiesel. DES3 and DES6 were synthesized experimentally and the water content for the DESs were 39.859 and 43.172 mg/g, respectively.

6.4.4.1. Effect of DES molar ratio

The effect of salt: HBD or DES molar ratio for DES3 and DES6 on the removal of soap is shown in Figure 6.7. In general, the results show that the increase in the molar ratio for TEG in the DES increases the soap extraction efficiency, regardless of the types of salt used. With regards to the soap content, the molar ratios of 1:3 and 1:4 for DES3, and molar ratio of 1:4 for DES6 conforms to the international standards. This is evidenced by the soap concentration which was decreased from 765 ppm to 15.22 and 33.48 ppm, using DES3 and DES6, respectively. With regards to the types of DES, DES3 shows higher removal efficiency than DES6, with a lower soap content of 15.22 ppm compared to DES6 (34.49 ppm) at a molar ratio of 1:4. In fact, a comparable soap content of 32.97 ppm is achieved by DES3 even at relatively lower molar ratio of 1:3. The difference in the soap content between the DES molar ratios (1:3 and 1:4) has indicates the critical role of the DES composition in the efficacy of soap removal. The properties of DESs such as density, viscosity, conductivity and solubility are highly dependent on the molar ratio of HBD and HBA (Abed et al., 2023) which eventually affects the mas transfer process. This emphasizes the importance of the composition of DES in order to achieve the best interactions and effective soap removal. The observed variations highlight the impact of

mass transfer, kinetic, density, viscosity, solubility and molecular structure on the interactions between the soap and DES, offering important information for the development of an efficient soap removal system. Therefore, the molar ratio of 1:4 for both types of DESs was selected for further optimization of the extraction process.

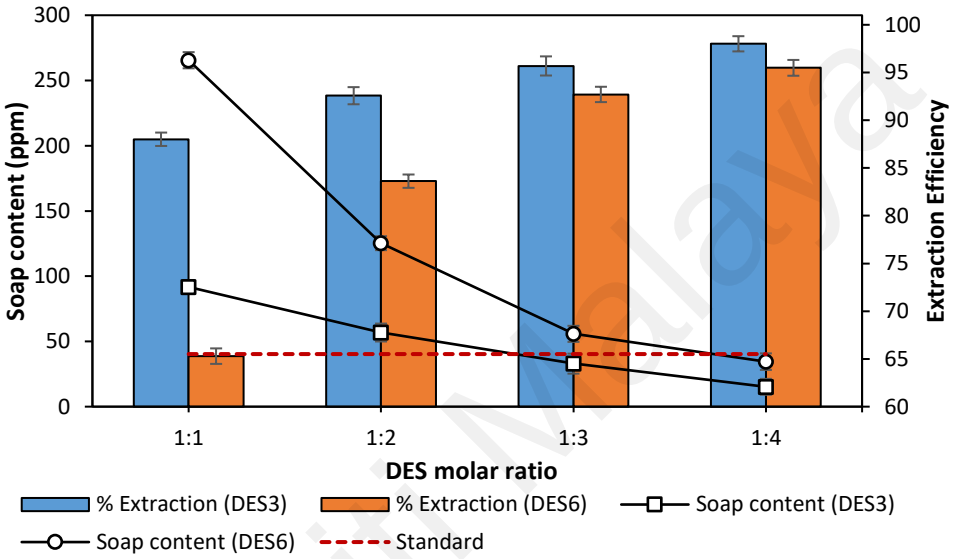

Figure 6.7: Effect of the salt:HBD molar ratio on the removal efficiency and soap concentration via the DES-AC-ELM technology; the experimental conditions are as follows 1:3 DES to biodiesel ratio, 1.5 wt.% of surfactant, 1.5 treatment ratio, 0.3 wt.% dosage of activated carbon and stirring at 300 rpm, with an extraction time of 6 minutes.

6.4.4.2. Effect of DES to biodiesel ratio

Figure 6.8 shows the extraction efficiency and the soap content at different DES to biodiesel volume ratio. The DESs have a high attraction towards the soap molecules through hydrogen bonding and dipole-dipole attraction, due to the polarity of DESs with the presence of the hydroxyl and carboxyl groups in both the soap and DESs.

The results indicated that DES3 and DES6 were able to decrease the soap content to below the international standard limit, with removal efficiencies of above 99.4% and 97.82%, respectively. It can be concluded that all TMAC: TEG constituents of the DESs were successful in reducing the soap concentration to below the limit established by the

international standards, as demonstrated in Figure 8. Both efficiency and stability of the emulsion decrease with the increase in the volume of the feed phase (Ye et al., 2017). The purification method relies heavily on the presence of HBD (high-affinity bonding) in DES, which facilitates the elimination of the soap from the membrane layer (Rosly et al., 2019).

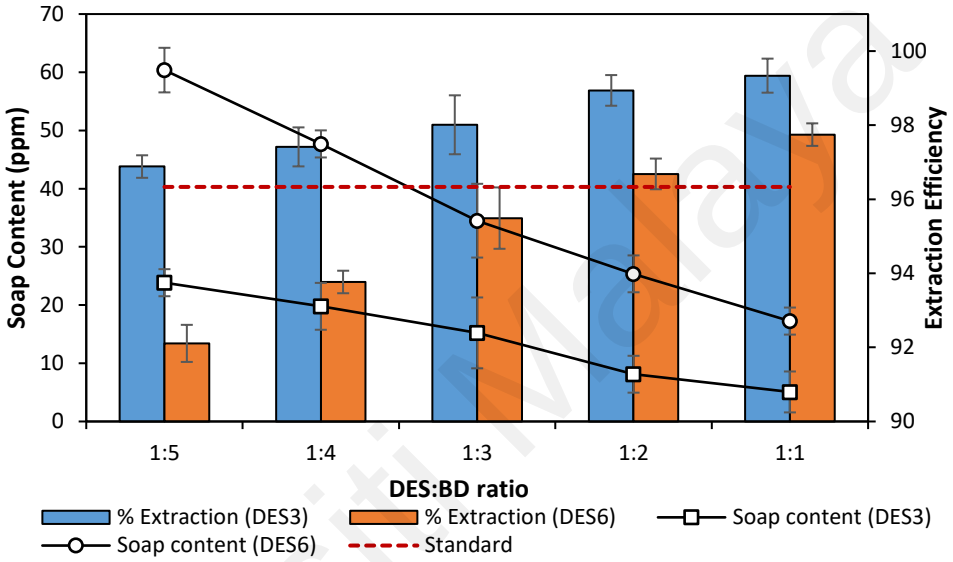

Figure 6.8: Effect of the DES:biodiesel ratio on the efficiency and soap concentration via the DES-AC-ELM technology; the experimental conditions are as follows: 1.5 wt% of surfactant, 1.5 treatment ratio, 0.3 wt% dosage of AC, and a mixing of 300 rpm, with a fixed extraction time of 6 minutes.

6.4.4.3. Effect Of Span-20 Concentration

The effect of surfactant content on the soap elimination from the biodiesel is presented in Figure 6. 9. The results show that the increase of span 20 concentration from 0.5 wt.% to 2.0 wt.% have led to substantial reduction in the soap content for both DESs. This confirms that the surfactant reduces the surface tension (Bera et al., 2013) of the membrane phase and facilitates the transportation of fatty acid salt via the membrane film into the DES stripping phase. The lowest soap concentration was obtained at 2 wt.% of surfactant concentration in the membrane layer for both DESs, owing to the decrease in the membrane surface tension upon increasing the span-20 concentration ranging from

0.5 - 2.0 wt.% (Tahmasebizadeh et al., 2021). In addition, DES3 produces a maximum extraction efficiency of 98.6% as the stripping agent. This effect is attributed to the formation of fine bubbles and dispersion of emulsion globules, thereby enhancing the contact area between the stripping and feed layers. However, it is noteworthy that a decrease in the extraction efficiency was observed when the span-20 concentration was further increased to 2.5 wt.%. Similar trends were also reported, whereby the optimum surfactant concentration was reported to be 4%-7%, depending on the types of surfactant used (Mortaheb et al., 2008; Rosly et al., 2020; Sabry et al., 2007). This could be due to the fact that the presence of excessively high surfactant concentration increased the viscosity (Reis & Carvalho, 2004; Rosly et al., 2020; Sabry et al., 2007) as well as the thickness of the emulsion membrane phase (Mortaheb et al., 2008) , with the formation of large emulsion droplets (Khan et al., 2021). These can further caused higher mass transfer resistance between the feed phase and the membrane phase, thereby decreasing the extraction efficiency. The selection of Span-20 was based on its good emulsification features, which led to the formation of a stable emulsion (Zaulkiflee et al., 2022) that was necessary and efficient for soap elimination. The Span-20 hydrophobic tail and hydrophilic head makes it a valuable stabilizer at the interface between the stripping and feed phases of the liquid membrane phase (Hejazifar et al., 2020). Moreover, the environmentally friendly features of span-20 supported our objective of developing an eco-friendly technique for soap removal.

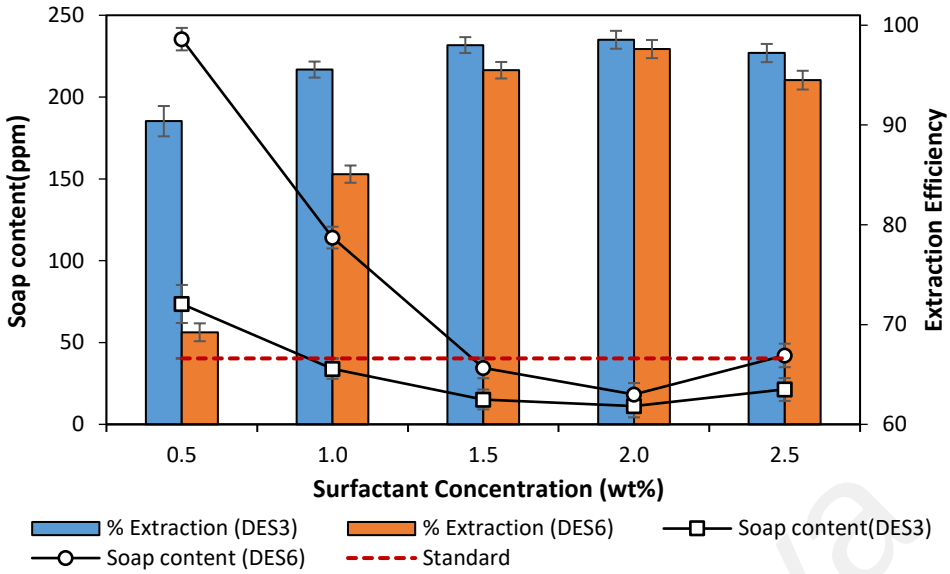

Figure 6.9: Effect of surfactant on the soap content and extraction efficiency via DES-AC-ELM technique; the experimental conditions are as follows 1:3 DES: biodiesel ratio, 1.5 treatment ratio, 0.3 wt% dosage of AC, and a mixing speed of 300 rpm, with a fixed extraction time of 6 minutes.

6.4.4.4. Effect of Extraction Time

The effect of contact time on the soap removal was investigated in a range of 2 to 10 minutes, as presented in Figure 6.10. It was found that the increase in the extraction time from 2 to 10 minutes resulted in higher soap extraction rates for both the ELM processes that utilized DES3 and DES6 as the stripping agent. The comparison between DES3 and DES6 revealed that DES3 possesses smaller mass transfer resistance and could achieve a higher soap removal efficiency of 99.8%. Notably, it was found that 4 and 6 minutes of extraction duration using DES3 and DES6, respectively, are sufficient to meet international standards. An extraction time of 10 minutes was able achieve the lowest soap content. These are in accordance with previous reports (Ye et al., 2017). Nevertheless, it is noteworthy that an extended contact duration could reduce the extraction efficiency, as emulsion breakdown increases at prolonged duration as a result of the membrane swelling (Kulkarni et al., 2002, Matsumiya et al., 2004, Kankekar et al., 2010).

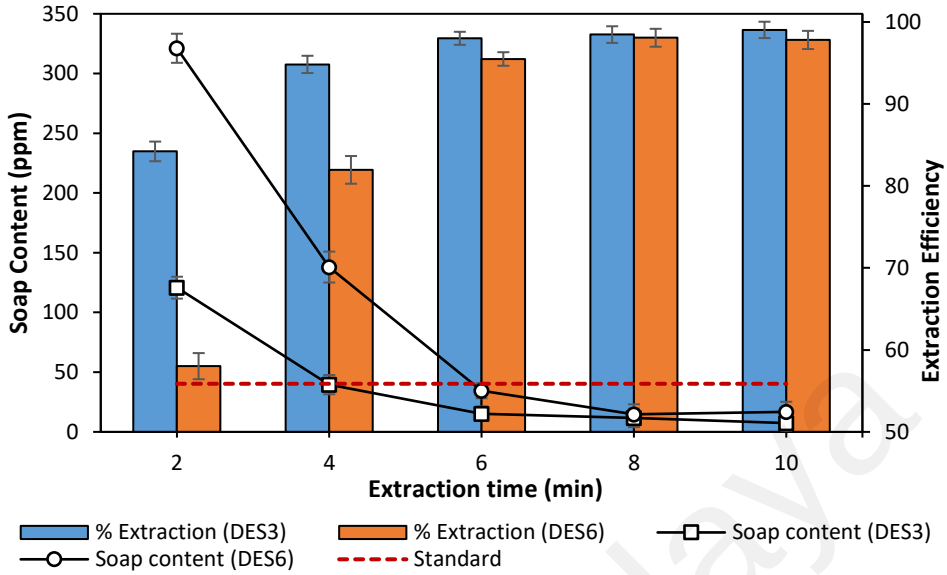

Figure 6.10: Effect of duration on both the soap content and efficiency via the DES-AC-ELM technique; the experimental conditions are as follows: 1.5 wt% of surfactant, 1:3 DES: biodiesel ratio, 1.5 treatment ratio and a 0.3 wt% dosage of AC, under a mixing speed of 300 rpm.

6.4.4.5. Effect of Mixing Speed

Figure 6.11 illustrates the effect of agitation speed on the fatty acid salt elimination in a range of 100 rpm to 500 rpm. The increase in the speed from 100 rpm to 400 rpm leads to better soap removal up to a minimum concentration. This is due to the increase in the agitation speed which could provide better force for effective extraction via the increase in volumetric mass transfer coefficient and interfacial area of mass transfer between the external phase and the membrane phase. Several studies also suggest that the ELMs separation method is mainly based on the external surface area of the droplets, as opposed to the internal phase surface area of the droplets (Reis and Carvalho, 2004;Alitabar-Ferozjah and Rahbar-Kelishami, 2022;Ahmad et al., 2011). As a result, increase in the agitation speed enhances the mass transport area and ultimately the extraction efficiency. Nevertheless, it is noteworthy that the further increase in the agitation speed from 400rpm onwards decreased the soap removal, which could be mainly due to the rupture of

emulsion globules due to hydrodynamic shear force at higher speeds (Kankekar et al., 2010). Additionally, the raised viscosity during the purification process makes it challenging to disperse emulsion with sustained contact as the mixing speed is increased (Goyal et al., 2011;Ahmad et al., 2021). In this study, it was observed that at 300 rpm, both ELMs using DES3 and DES6 show a decrease in the soap content meeting the international standards as demonstrated in Figure 6.11.

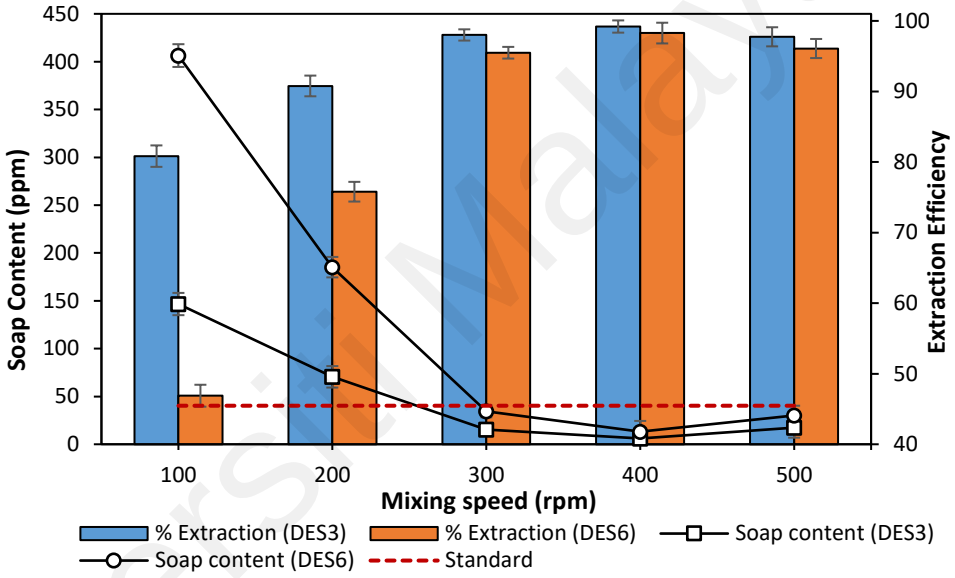

Figure 6.11: Effect of stirring speed on soap content and extraction efficiency via the DES-AC-ELM technique; the experimental conditions are as follows: 1.5 wt% of surfactant, 1:3 DES: biodiesel ratio, 1.5 treatment ratio, and 0.3 wt% dosage of AC, with a fixed extraction time of 6 minutes.

6.4.4.6. Effect of Treatment Ratio

The treatment ratio effect is the effect of the volume of the biodiesel to the emulsion phase (membrane and stripping phases). It plays a crucial role in the extraction process as the analyte content of the external phase directly affects the extraction rate. The optimal treatment ratio ensures effective interaction between the soap molecules and the emulsion globules. A range of treatment ratios from 0.5 to 2.5 was investigated in this study. Figure

6.12 shows that the increase in the treatment ratio increases the soap content, indicating a lower removal. When the volume of the external feed phase is low, there will be a sufficient amount DES in the emulsion phase as the main driving force behind the purification process which facilitates the fatty acid salts removal from the membrane phase (Rosly et al., 2019). Most of the extracted soap (solute) accumulate in the internal phase (DES) and do not diffuse into the external phase (Mohammed et al., 2018). Conversely, at a high treatment ratio, the amount of DES is insufficient for the removal of a larger amount of soap molecules from silicon oil (membrane phase), thereby resulting in a higher soap concentration in the external phase after the experiment. In this study, all the treatment ratios are found to the meet international standards when DES3 was used as the stripping agent. In contrast, the treatment ratios of 2 and 2.5 are insufficient to meet the international standards when DES6 is used in the removal of the soap molecules, as shown in Figure 6.12. The optimal treatment ratio is identified as 0.5 in this study.

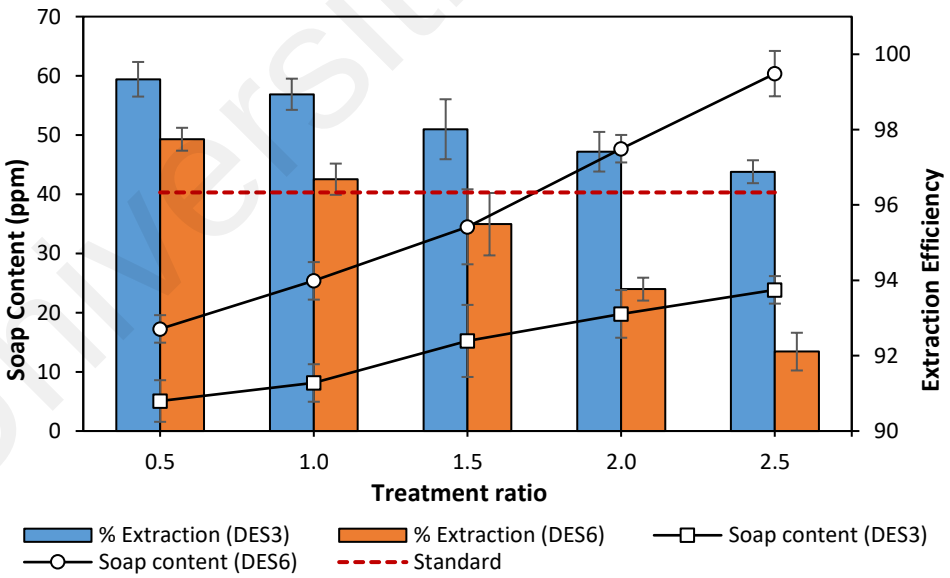

Figure 6.12: Effect of treatment ratio on both soap and efficiency via the DES-AC-ELM technology; the experimental conditions are as follows: 1.5 wt% of surfactant, 1:3 DES: biodiesel ratio, 0.3 wt% dosage of AC, and 300 rpm of mixing speed with a fixed extraction time of 6 minutes.

6.4.4.7. Effect of AC dosage

Figure 6.13 shows the effect of activated carbon in the stripping phase on the soap elimination from biodiesel. The presence of AC from 0.1 to 0.5 wt.% increases the extraction of soap molecules because of the presence of more active sites for the stripping purification process (Ayoob and Fadhil, 2020). In this study, an AC dosage of >0.1 wt.%, conforms to the international standards when DES3 was used as the stripping phase, while a dosage of >0.2 wt.% was needed to meet the international standards when DES6 was used as the stripping phase**.** The presence of nanocarbons such as AC enhances the strength between the emulsion droplets and stability, limiting their collision or coalescence (Al-Obaidi et al., 2021; Lin et al., 2015). The analysis of AC showed that the average pore size diameter is 2.3637 nm, and the surface area was 173.8369 m^2/g. This provides more active sites and functional groups for contaminant removal. Moreover, the AC, as a good porous medium adsorbs non-polar and polar impurities (Li et al., 2002). AC effectively removes the nonpolar impurities from the membrane layer by attracting and entrapping them via the surface functional groups due to the high surface area and porosity (Abed et al., 2023). In addition, the potassium ion in the salt of fatty acid reacts with the chemical functional groups of the AC (Baroutian et al., 2011). Besides, AC is effective in discoloration and adsorption the fine molecules in downstream processing (Hunsom & Autthanit, 2013; Manosak et al., 2011). In this study, highest soap extraction efficiency is achieved at 0.5 wt% dosage of AC using the DES3 and DES6 as the stripping phase, resulting in 99.4% and 98.4% removal efficiency, respectively.

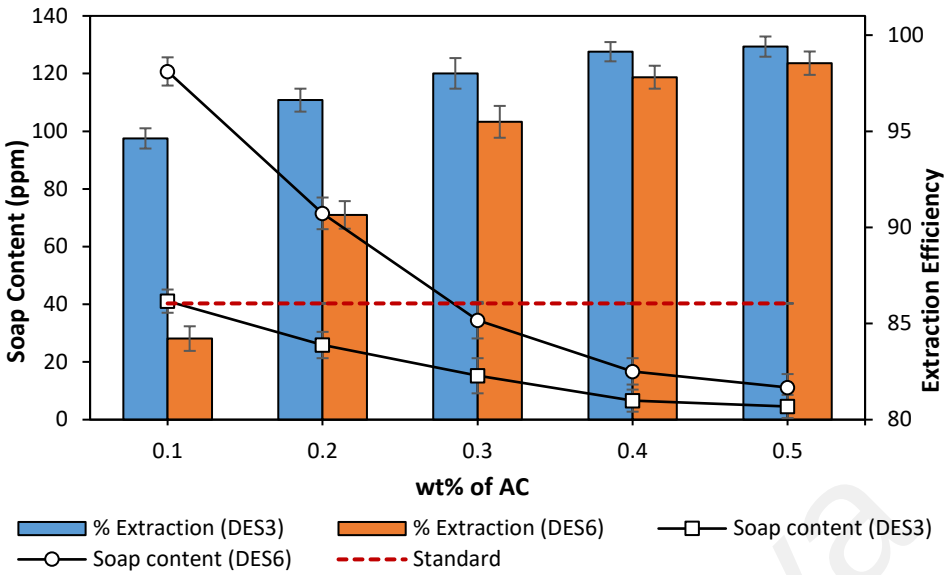

Figure 6.13: Impact of AC dosage on both the soap concentration and efficiency via DES-AC-ELM technique; the experimental conditions are as follows: 1.5 wt% of surfactant, 1:3 DES: biodiesel ratio, 1.5 treatment ratio, and 300 rpm of mixing speed with a fixed extraction time of 6 minutes.

6.4.5. Kinetic and Mass Transfer Modelling

The soap removal mechanisms using this process were further investigated by analysing the mass transfer kinetics based on the optimal conditions. A model was created according to the following presumptions: i) the soap diffusion was in a steady state, ii) the external layer, membrane layer, and internal layer are immiscible with each other, iii) the soap transfer occurs in the membrane layer and is assumed as a first-order one-directional process, iv) the soap stripping between the membrane phase and stripping phase is considered as an irreversible reaction, v) the lost of soap during the extraction is negligible, and vi) to simplify and facilitate the current model, AC was not taken into consideration.

The soap mass transfer in the DES-AC-ELM is derived according to Fick's equation, as expressed by Eq. (6.5) (Abed et al., 2023):

$$J_{Soap} = -\frac{V}{A_g}\frac{dC_t}{dt} \quad (6.5)$$

where J_{soap} represents the soap flux ($\frac{mol}{cm^2 .S}$), V represents the external phase volume (cm^3), A_g represents the surface area of the emulsion droplets (cm^2), and dC_t/dt represents the soap concentration gradient ($\frac{mol}{cm^3 .S}$).

The value of A_g was estimated using Eq. (6.6).

$$-\frac{A_g}{V_g} = \frac{S_g}{V_T} \rightarrow A_g = V_g \frac{\pi D_g^2}{\frac{1}{6}\pi D_g^3} = V_g \frac{6}{D_g} \tag{6.6}$$

where, V_T, S_g,V_g, and D_g, are the total emulsion globules' volume (cm^3), the globule's surface area (cm^2), the globule's volume (cm^3) and the average globule size (cm), respectively. Eq. (6.5) is further derived from the substitution of Eq. (6.6) into Eq. (6.5), while considering assumption 3 that the soap mass transport in DES-AC-ELM follows a first-order kinetic model.

$$J_{Soap} = -\frac{V_T}{V_g}\frac{D_g}{6}\frac{dC_t}{dt} = k\, C_t \tag{6.7}$$

By reorganizing, Eq. (6.7) can be expressed as Eq. (6.8).

$$-k\frac{V_g}{V_T}\frac{6}{D_g}dt = \left(\frac{d\, C_t}{C_t}\right) \tag{6.8}$$

Eq. (6.9) is obtained from the integration of Eq. (6.8) with respect to time and with the applications of the boundary conditions of time from 0 to t and concentration from C_o to C_t.

$$-k\frac{V_g}{V_T}\frac{6}{D_g}t = \ln\frac{C_t}{C_o} \tag{6.9}$$

Finally, rearranging terms, we arrive at Eq. (6.9)

$$\ln\frac{C_t}{C_o} = -k\frac{V_g}{V_T}\frac{6}{D_g}t \tag{6.10}$$

$$k = \frac{\ln\frac{C_t}{C_o}}{t}\frac{V_T}{V_g}\frac{D_g}{6} \tag{6.11}$$

$$\frac{C_t}{C_o} = e^{-(k\frac{V_g}{V_T}\frac{6}{D_g})t} \quad (6.12)$$

To simplify the Eq., we substitute the term $k\frac{V_g}{V_T}\frac{6}{D_g}$ with the variable 'K_a'. This leads to Eq. (6.13), where the reaction rate constant (K_a) is introduced.

$$\frac{C_t}{C_o} = e^{-K_a t} \quad (6.13)$$

Using the above-mentioiend Eq. (6.13), the mass transfer coefficient was calculated. The value of Ka can be obtained by fitting the experimental data into Eq. (6.12). The results of the curve fitting process are displayed in Figure 6.14, which shows that the model fits closely to the experimental data. Table 6.2 presents the reaction rate constants, sum square errors (SSE), and R^2 values for DES3 and DES6.

The R^2 values of the ELMs that incorporate DES3 and DES6 as the stripping agents are 0.9989 and 0.9993, respectively, indicating a good fit. Moreover, the SSE of the results are 0.000837 and 0.000518 for DES3 and DES6, respectively. The calculated Ka values for DES3 and DES6 are 0.904 and 0.448 min^{-1}, respectively. Overall, these findings suggest that the model is an accurate representation of the experimental data.

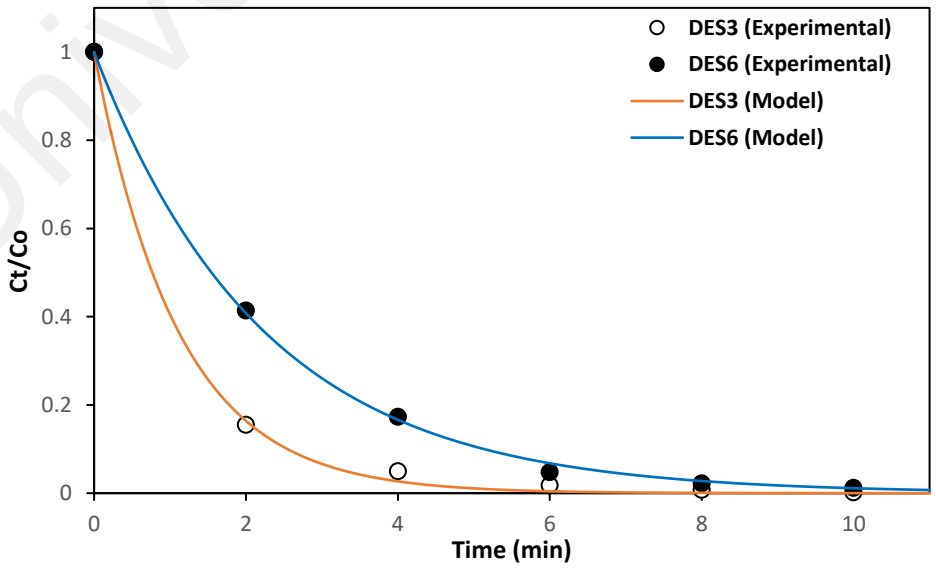

Figure 6.14: Soap concentration profiles over time (t) for (a) DES3 and (b) DES6 using the DES-AC-ELM technique. The initial concentration of soap was 765 ppm,

with a 1:4 HBA:HBD ratio, 1:1 DES:biodiesel ratio, 2 wt.% of surfactant, 0. 5 wt.% dosage of AC, 2.5 treatment ratio, and 400 rpm mixing speed.

Table 6. 2: Values of the reaction rate constants (K_a), and (SSE) values in the DES3-AC-ELM.

System	K_a (min^{-1})	SSE	R^2
DES3-AC-ELM	0.904	0.000837	0.9989
DES6-AC-ELM	0.448	0.000518	0.9993

6.4.6. Soap Removal Mechanism Through DES-AC-ELM Technique

The process of soap removal from a medium is obtained using the hydrophobic and hydrophilic characteristics of the soap molecules. The hydrophobic tail and hydrophilic head in the soap molecules allow the interaction of soap with both water and oils, effectively removing grime from surfaces.

In the DES-AC-ELM process, the soap molecules are transported from the feed biodiesel layer to the membrane layer (silicon oil and span 20) via an interaction mechanism. Then, the soap molecules are stripped from the membrane layer by the stripping phase that consists of DES and AC via the complexation and adsorption processes, respectively.

The removal mechanism is depicted in Figure 6.15. Soap is slightly soluble in biodiesel as evidenced by COSMO-RS σ-potential analysis. When the membrane phase is introduced, effective hydrogen bonding between the soap and span 20 is represented by the compromised negative μ values observed in the soap and span 20 from the COSMO-RS analysis. The AC, which is a good porous medium, is able to adsorb non-polar and polar impurities (Li et al., 2002). AC has a high surface area due to the high porosity, therefore during the emulsion layer, AC effectively removes the nonpolar impurities from the membrane layer by attracting and entrapping them via the surface functional groups

(Abed et al., 2023). In contrast, the HBD forms a polar medium that improves the soap solubility and form bonds between the soap and DES. The synergistic impact of DESs and AC broadens the range of fatty acid salt molecules that can be eliminated from the crude biodiesel that significantly enhance the extraction efficiency.

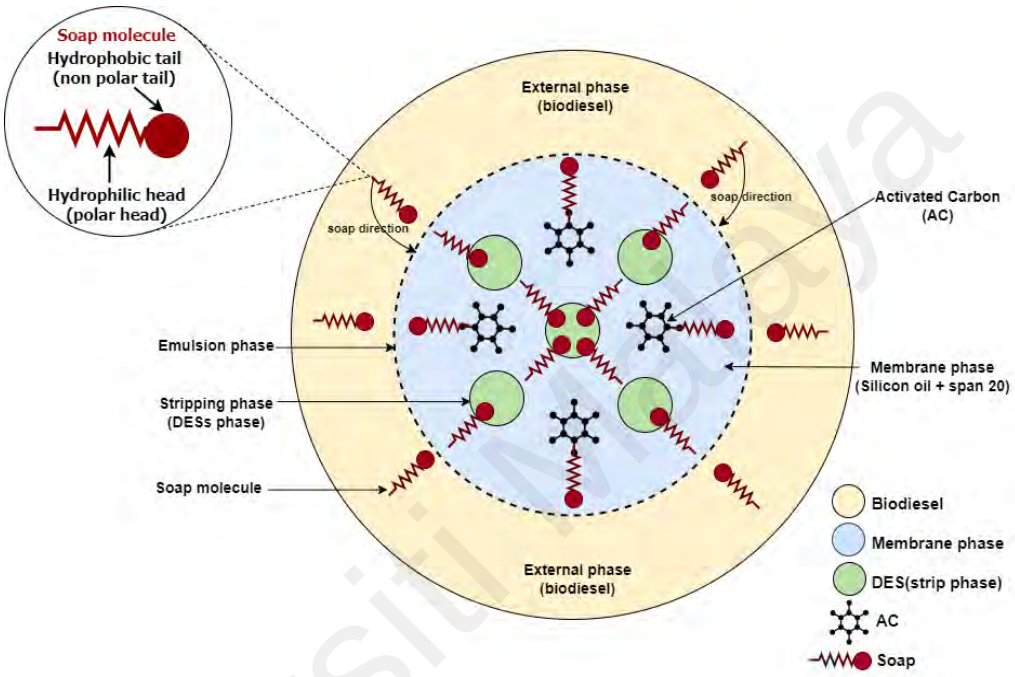

Figure 6.15: Proposed the soap transport mechanism via DES-based ELM/AC

6.5. Conclusion

A new purification technique for soap elimination from biodiesel using the ELM technique by utilizing TMAC and choline chloride-based DESs (DES3 and DES 6) as the stripping phase was evaluated. COSMO-RS was utilized in the screening of three TMAC-based DESs and three ChCl-based DESs with different HBD on the basis of capacity and activity coefficient at infinite dilution. The results showed that DES3 and DES 6 gave the highest capacity as solvents for soap removal. This was confirmed experimentally from the investigation on the ability of the screened DES as the stripping agent in the ELM process with the following optimized parameters: DES molar ratio of 1:4, DES: biodiesel ratio of 1:1 volume ratio, surfactant concerntration of 2 wt.%, extraction duration of 10

minutes, mixing speed of 400 rpm, treatment ratio of 0.5 volume ratio and AC dosage of 0.5 wt.%. At the optimal conditions, the maximum removal efficiency was 99.1% (6.856 ppm) for DES3 and 97.5% (18.773 ppm) for DES6, from the initial soap content of 765 ppm. The transport mechanisms in the ELM adhere to a first-order kinetic mass transfer process, with the kinetic rate constants of 0.64 and 0.463 min^{-1} for DES3 and DES6, respectively.

CHAPTER 7: NATURAL EUTECTIC SOLVENTS AND GRAPHENE INTEGRATED WITHIN EMULSION LIQUID MEMBRANE SYSTEM FOR SODIUM REMOVAL FROM CRUDE BIODIESEL

7.1. Introduction

Generally, sodium ions generated from catalyst residuals during biodiesel production are one of the major challenging contaminations in the biodiesel industry. To the best of our knowledge, there are no reported studies on sodium removal using an emulsion liquid membrane (ELM). Therefore, this chapter reports a new technique for sodium ion elimination from biodiesel using a green emulsion liquid membrane (GELM) system based on natural deep eutectic solvents (NADESs) and graphene. The DES consists of choline chloride with glycerol and lactic acid, and tetramethylammonium chloride with glycerol and lactic acid. Additionally, kinetic and mechanism studies were investigated using computational tools such as COSMO-RS. COSMO-RS was used to compute the intermolecular interaction of sodium with hydrogen bond acceptors and donors of the NADES. Moreover, the stability, the molar ratio of DES, treatment ratio, span 80 concentration, extraction duration, mixing speed, and the presence of graphene were optimized for extraction efficiency. Furthermore, the kinetics and mass transfer of sodium ions during the ELM system were studied. The results of this chapter were published in the Journal of Colloids and Surfaces A: Physicochemical and Engineering Aspects (Abed et al., 2024).

7.2. Literature Review

Alternative renewable energy sources are gaining importance due to the rising worldwide energy demand, urgent environmental and global warming issues, and depletion of fossil

fuel reserves. Therefore, there is an urgent need for clean fuels on a global scale (Atadashi, Aroua, & Aziz, 2011). Biodiesel is an appealing alternative fuel that is derived from a range of plant oils and animal fats. In addition of being biodegradable and renewable, the combustion of biodiesel occurs without significantly raising the atmospheric CO_2 levels making it a competitive alternative to diesel which is derived from fossil fuels (Sakthivel et al., 2018; Zhang et al., 2023).

Alkali catalysts such as NaOH and KOH, are the most widely used catalysts in the transesterification reaction for biodiesel synthesis (Dias et al., 2008; Takase et al., 2023; Vishal et al., 2020). Alkali catalyst shows several distinct benefits where the transesterification process can be carried out at 60 °C (Hazrat et al., 2023), ambient pressure, and produce large amounts of fatty acid methyl esters (FAME) that approaches 98% in a short time (Nisar et al., 2021). However, alkali catalysts also demonstrate hygroscopic characteristics as well as the creation of soap compounds during the transesterification process (Mandari & Devarai, 2021). Alkali metal is an impurity in biodiesel that forms deposits in the fuel injection system's components. These deposits decrease the engine performance due to contamination of the emission control system and clogging of the engine filter (Xue et al., 2011). As a result, it is crucial to remove the alkali metals from biodiesel after the transesterification reaction to < 5 mg/kg according to international standards.

Manufactured biodiesel normally comprises of several undesirable products such as unreacted materials, free glycerol, water, leftover catalysts, and soap (Maheshwari et al., 2022). As a result, many crucial steps are required for the purification of biodiesel to remove these impurities before it can be used as an eco-friendly alternative fuel source. Generally, there are three main techniques for biodiesel purification, which are: (i) membrane separation, (ii) dry washing, and (iii) wet washing (Ahmad et al., 2023; Catarino et al., 2020). However, dry and wet washing processes have several

disadvantages, such as higher purification costs, increased production times, the formation of liquid effluents harmful to the environment, and significant product losses via formation in the water phase. In contrast, membrane-based processes have shown promise due to their flexibility and high efficiency (Saleh et al., 2011). While it is successful, it can increase production costs and reduce process throughput. In comparison, liquid membrane is an alternative membrane process that can be applied at relatively lower capital cost. In general, there are three liquid membrane configurations, which are the bulk liquid membrane, supported liquid membrane and emulsion liquid membrane (ELM). The use of liquid membranes as selective separation barriers has shown some potential in recent years, due to their affinity for specific impurities (Abed et al., 2023; Kumar et al., 2019b). The ELM technique was used for the removal of antibiotics (Sharma et al., 2023), heavy metals (Khadivi & Javanbakht, 2020), dyes (Wu et al., 2024), and contaminants from biodiesel (Abed et al., 2023).

Recently, deep eutectic solvents (DESs) are introduced as a component in liquid membrane technique, either as the membrane phase or stripping phase (Abed et al., 2023; Hayyan et al. , 2022). DES possesses unique characteristics compared to traditional solvents, such as low toxicity, high stability, high heating capacity and low viscosity (Abed et al., 2023; Hayyan et al., 2022). DESs have enormous prospects for application as “green” solvents for industrial processes in the future. Quaternary ammonium salt-based DES have been utilized to eliminate glycerol (Abbott et al., 2007; Hayyan et al., 2010) and soap (Abed et al., 2023) from biodiesel. However, the selection of the most appropriate DES for the elimination of impurities in biodiesel is challenging due to the high number of DESs available via the combinations of different types of HBD and HBA. To resolve this issue, Conductor-like Screening Model for Real Solvents (COSMO-RS) could simulate the thermodynamic proprieties of the mixtures, giving solid and trustworthy data for uncharted areas by utilizing merely the chemical structure knowledge

as the input. In this chapter, COSMO-RS was used to investigate the selection of the most appropriate DES as the stripping phase in the DES-based ELM system for sodium removal from biodiesel. COSMO-RS was also used to verify the mechanism of sodium removal in the ELM phases. Additionally, the stability, the molar ratio of DES, treatment ratio, span 80 concentration, extraction duration, mixing speed, and the presence of graphene were optimized for extraction efficiency.

7.3. Materials and Methods

7.3.1. Materials

Choline chloride (ChCl), tetramethylammonium chloride, acetone, polysorbate 80, and hydrochloric acid (HCl), were sourced from Merk. Sodium hydroxide and bromophenol blue were obtained from Sigma-Aldrich (Malaysia). Lactic acid, Glycerol (Gly), and silicon oil were purchased from John Kollin Chemicals, while methanol was sourced from Chemiz. Lastly, Advance Chemical Supplier (ACS) provided graphene nanoplatelets (thickness of 2–10 nm).

7.3.2. Screening and simulation using COSMO-RS

COSMO-RS is a fast and practical approach in predicting the physicochemical characteristics and thermodynamic behaviors of mixtures. It is used in this work due to its robust capability to predict the thermodynamic properties and molecular interactions using only the chemical structure of the compounds involved. This makes it a valuable tool for identifying and optimizing suitable DESs for sodium ion extraction in the GELM system.

The prediction of mixture behaviors through COSMO-RS includes solvent characteristics, vapor-liquid equilibrium phase diagrams, liquid-liquid equilibrium phase diagrams, vapour pressures, activity coefficients, and molecular surface polarity

variations, etc. In this work, COSMO-RS was specifically used to evaluate the intermolecular interactions between DESs and sodium ions via the σ-profiles and σ-potentials. The choice was further justified by its success in accurately predicting the stripping efficiency of lactic acid-based NADES, which aligned with the experimental results. It should be mentioned that, in comparison to the experimental results, COSMO-RS investigations are generally been found to be primarily qualitative (Toumi et al., 2018). Nonetheless, several researchers have also indicated that it is quantitative to some extent (Diedenhofen and Klamt, 2010; Hadj-Kali et al., 2016).

In this chapter, four DESs were investigated using COSMO-RS simulation of sodium ions elimination from biodiesel. Tetramethylammonium chloride (TMAC) and choline chloride (ChCl), were used as the hydrogen bond acceptors (HBA) combined with two hydrogen bond donors (HBDs): lactic acid (LA) and glycerol (Gly). The charge distribution on the surface and 3D molecular structures of the HBAs and HBDs are shown in Figure 7.1. The graphical user interface enables the TURBOMOLE version of the quantum chemistry software, TMoleX version 4.0, to export each molecular geometry as the "COSMO" files. To produce the DES description sets, the COSMO-RS programme (COSMOThermX) was used for importing the COSMO files of the prepared HBAs and HBDs. The areas of the DES that are colored red, blue, and green represent the negative, positive, and non-polar in nature surfaces, respectively.

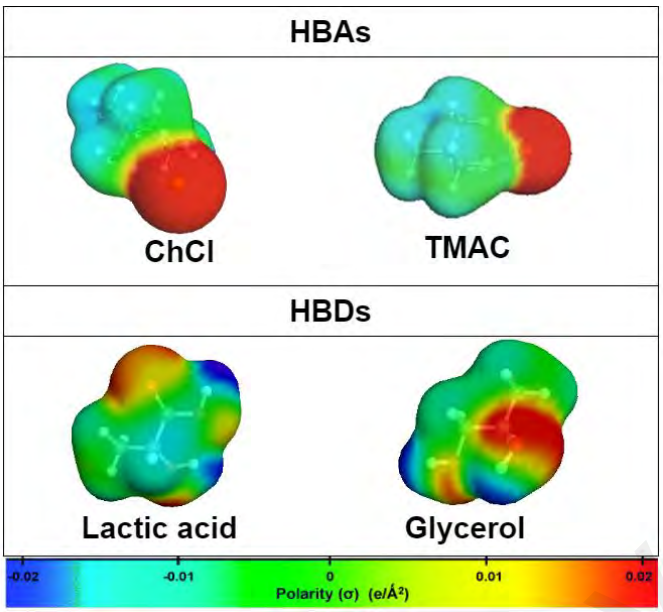

Figure 7.1: Charge densities and three-dimensional forms of the hydrogen bond donors and acceptors utilized in the present study; (Red represents negative, green as neutral and blue positive is the electrostatic potential).

The generated COSMO files were then used to predict the activity coefficient of sodium ions in each DES (γ∞) at infinite dilution via the COSMO-RS calculations. These values were subsequently used to estimate the capacity of sodium ions in the DESs (C∞) at infinite dilution, as expressed in Eq. (7.1) and Eq. (7.2):

$$\text{Activity coefficient } (\gamma\infty) = e^{\frac{(\mu-\mu_O)}{RT}} \tag{7.1}$$

where μ is the chemical potential of the solvent and μ_0 is the chemical potential of the pure compounds.

$$\text{Capacity } (C\infty) = \left(\frac{1}{\gamma\infty}\right)_{\text{DES phase}} \tag{7.2}$$

The values of C∞ and γ∞ were then used to identify the most suitable DESs as a stripping phase in the ELM system for sodium ion elimination. All COSMO-RS results were conducted using COSMO ThermX (19.0.5) software package.

7.3.3. Preparation of green stripping phase solvents

In this study, DESs were synthesized and used as a stripping agent in the ELM system. While some changes have been made recently on the DES synthesis procedure, the method established by Abott et al.'s (Abbott et al., 2003) was used to synthesize the majority of DESs. Choline chloride (ChCl) was combined with glycerol (Gly) and lactic acid (LA) to synthesize two NADESs, while tetramethylammonium chloride was combined with Gly and LA to synthesize the other two DESs. The abbreviations, HBA and HBD are listed in Table 7.1.

Table 7.1: The abbreviation of DESs, HBA and HBD

Abbreviation	HBA	HBD
NADES1	ChCl	LA
NADES2	ChCl	Gly
DES3	TMAC	LA
DES4	TMAC	Gly

7.3.4. Production of Biodiesel

Palm oil was provided from local mill situated in Selangor, Malaysia and it was selected as the raw material for the synthesis of biodiesel using sodium hydroxide as the catalyst. The transesterification reaction was carried out in a batch reactor using 350 g of palm oil. Firstly, homogeneous sodium methoxide was synthesized by dissolving sodium hydroxide (1% of oil) in methanol, followed by its addition to palm oil in the reactor at 60 °C. The experiment was conducted using a 1:10 molar ratio of oil to methanol and a mixing speed of 350 rpm for two hours (Abbott et al., 2007). Then, the mixture was placed into a separation funnel, and the bottom layer of the glycerol-rich phase was separated from the top layer (biodiesel). Finally, the biodiesel was subjected to centrifugation (for

10 min at 2500 rpm) and subsequently heated for 15 minutes at 75°C to remove the residual methanol (Hayyan et al., 2010).

7.3.5. Preparation of ELM

The surfactant (span 80) was mixed with silicon oil using a homogenizer, at 10000 rpm for 3 minutes to synthesize the membrane phase. Then, the ELM was established by homogenizing the NADES (stripping agent) with the membrane phase under 4000 rpm for a specific homogenization time. After that, the extraction of sodium residue from biodiesel was carried out via GELM-NADES system by contacting the ELM with biodiesel under stirring for 2-10 minutes. Dispersion promotes the production of globules by the ELM, where each globule was formed from droplets of the NADES encased in the membrane phase. After the extraction process, the mixture was transferred into a separation funnel for gravity phase separation. Three layers were formed after two hours of settling, where the stripping agent as the bottom layer, the external phase as the top layer, and the membrane phase as the middle layer. Finally, the sodium residue in the upper layer (external phase) was measured using inductively coupled plasma-optical emission (ICP-OES). From these results, the extraction efficiency of sodium ion can be calculated using Eq. (7.3):

$$\text{Extraction efficincy (\%E)} = \frac{C_o - C_t}{C_o} \times 100 \quad (7.3)$$

where C_o is the initial sodium ion concentration (ppm), and C_t is the final sodium concentration (ppm).

7.4. Results and Discussions

7.4.1. CCOSMO-RS Simulation and molecular interaction of sodium ions in ELM system

COSMO-RS was used in the screening of two NADES (DES1 and DES2) and two non-NADES (DES3 and DES4) with different polarities to determine their Na+-dissolving capacity. The DES polarity plays an important role in sodium ion dissolution. The DESs with higher polarities attract more sodium ions and thereby increase their solubility, regardless of the length of the HBD carbon chains (Pandey et al., 2014). Therefore, a balanced approach that considers both the HBD carbon chain length and the polarity of the DES is necessary to optimize its sodium ion dissolution capacity.

In order to understand the mechanism of sodium ion elimination through the ELM system, it is important to examine the interaction between the sodium ions in each phase of the system, which are the external phase (biodiesel), membrane phase (silicon oil and span 80) and stripping phase (NADES). Figure 2 shows that the selected sodium ions in this study, especially sodium stearate, exhibits favorable interaction in all three regions, namely the HBD, HBA and the non-polar region.

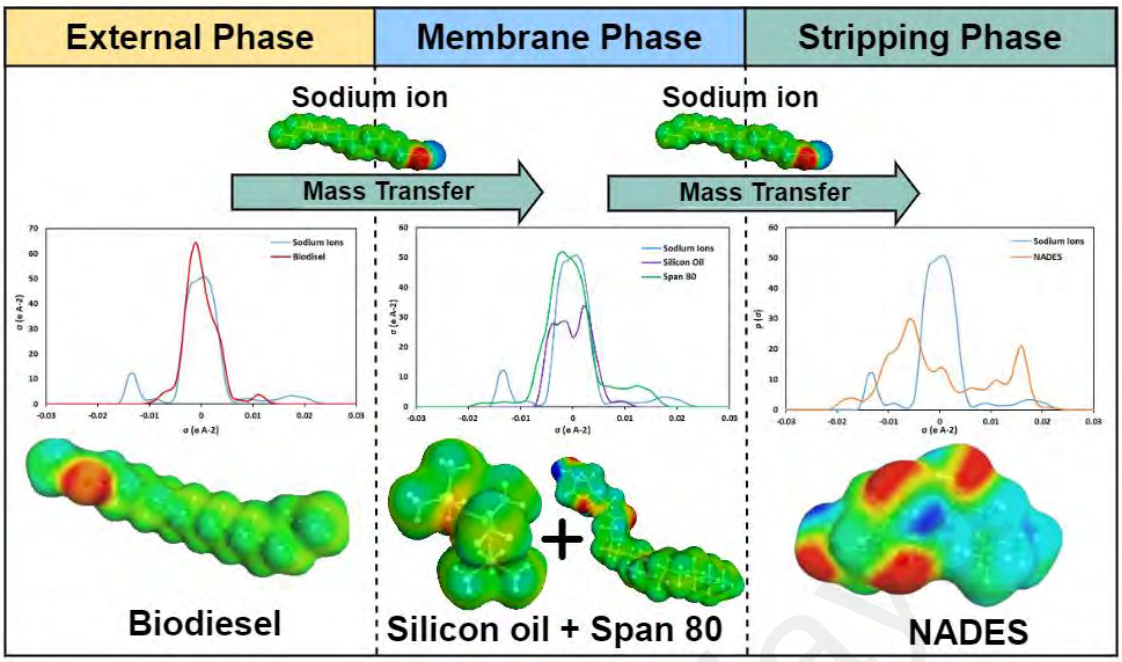

Figure 7.2: Mechanism of intermolecular forces present among the phases in the GELM-NADES system.

Figures 7.3 and Figure 7.4 display the σ-profiles and σ-potential of methyl ester (biodiesel), sodium ion, silicon oil, span 80 and the four DESs that are described in Table 7.1. These interactions are evident from the σ-profile (dominant peaks) and σ-potential (negative μ values) curves. The non-polar interaction arises due to the non-polar nature of alkyl chain of the stearate anion, while the hydrogen bond donor and acceptor interactions are due to the electropositive effect of the sodium cation and the hydrogen bond accepting nature of the carboxylate anion (COO-), respectively. The σ-potential curve of sodium ion shows negative values in all regions, which indicates strong attractive interactions with the surrounding compounds. This suggests that the sodium ions possess a high affinity for both the hydrogen bond regions, as well as non-polar regions in the DESs. Consequently, sodium ions are effectively dissolved and stabilized within the DESs, facilitating their removal from biodiesel. Sodium stearate or sodium ion exhibits lower solubility in methyl ester as evidenced by the higher μ values of biodiesel in the HBD region compared to sodium ion. Additionally, methyl ester displays repulsive

behavior in both the polar region, especially in the HBA region, indicating lower solubility of stearate in biodiesel. Sodium stearate is expected to have a higher degree of interaction with compounds that can form hydrogen bonds, as indicated by the lower μ values observed in the HBD region. Eventually, when the mixture of Span 80 and silicon oil is introduced, strong hydrogen bond formation between the sodium ion and Span-80 is due to the compromised negative μ values observed in the HBD (sodium stearate) and HBA (Span-80) regions. These interactions suggest that the dissolved sodium ions in biodiesel ultimately migrate to the membrane phase.

Similar to the internal phase, DES exhibits negative μ values in the HBD and HBA regions. This indicates the universal polarity of DES to interact with both the polar and non-polar compounds. The complementing μ values of sodium ions and DESs in the three regions demonstrate the high affinity of DES towards the sodium ions, thus effectively extracting sodium stearate from the membrane phase. By analyzing the DES σ-potential in Figure 7.4, it is suggested that the sodium ion-dissolving capacity is ranked in the descending order of DES3 ≈ NADES1 > NADES2 > DES4. It can be observed that NADES1 and DES3 are expected to extract more sodium stearate compared to the other DESs, as indicated by relatively lower μ values in the HBD and HBA regions. From an environmental viewpoint, NADES1 was selected as a striping phase in the next optimizations.

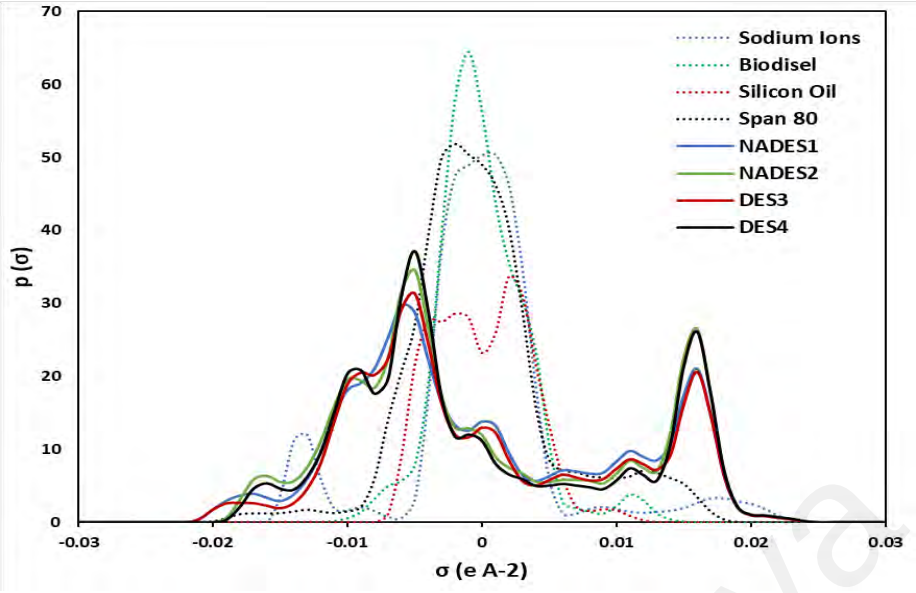

Figure 7.3: Energies of local surface interactions between σ-profiles of sodium ions and external, membrane and internal phases of GELM system.

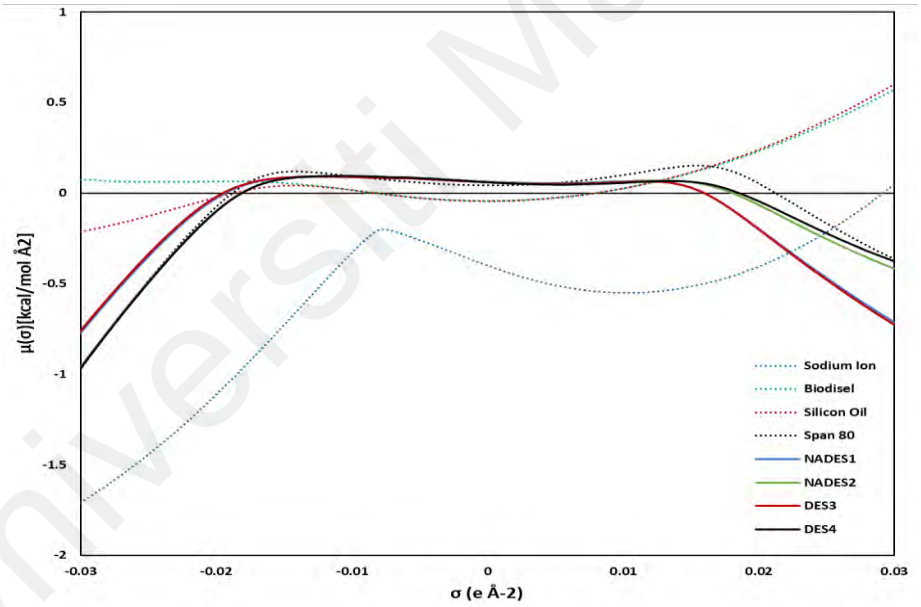

Figure 7.4: Energies of local surface interactions between σ-potential of sodium ions and external, membrane and internal phases of GELM system.

7.4.2. Experimental Validation

The COSMO-RS screening in Section 7.4.1 shows that (NADES1) lactic acid-based NADES (ChCl:LA) possesses better performance. Therefore, the research focuses on NADES1 as the innovative stripping phase in the ELM system. The experimental

synthesis of NADES1 was achieved at different molar ratio (Jablonský & Jančíková, 2023) with a water content of 40.821 mg/g.

7.4.2.1. Stability of ELM

The stability of GELM is an essential criterion in many applications, especially in the separation processes. It is affected by a number of conditions, primarily by the emulsification process, as well as the membrane components, viscosity, and the surface tension between the membrane phase and the internal phase. The emulsification process is highly dependent on the speed and time of emulsification, which are the most important factors that influence the stability of emulsion. In this study, the percentage of breakage, β, was considered to evaluate the emulsion stability of the system, which can be calculated using Eq. (7.4):

$$\beta = \frac{V_o - V_f}{V_o} \times 100 \quad (7.4)$$

where V_o and V_f represent the volumes of the emulsion before and after the extraction process, respectively.

The impact of emulsification speed on emulsion breakage is depicted in Figure 7.5. The emulsion breakage was found to significantly drop from 6.88 to 2% when the emulsification speed was increased from 1000 rpm to 4000 rpm. The mass transfer surface is subsequently extended as the emulsion droplet size decreases with increasing emulsification speed (Kumar et al., 2019a). It lowers the breakage ratio and increases the stability of the emulsion. Moreover, NADES droplets are distributed through the silicon oil phase as the emulsification speed increases. However, it is noteworthy that at very high emulsification speeds of > 4000 rpm, the breakage of emulsion increases, mainly due to coagulation phenomena (Liu et al., 2017). High emulsification speeds cause unstable emulsion due to the very small size of the droplets, which further weakens the surface tension to maintain the emulsion (Kahar et al., 2023).

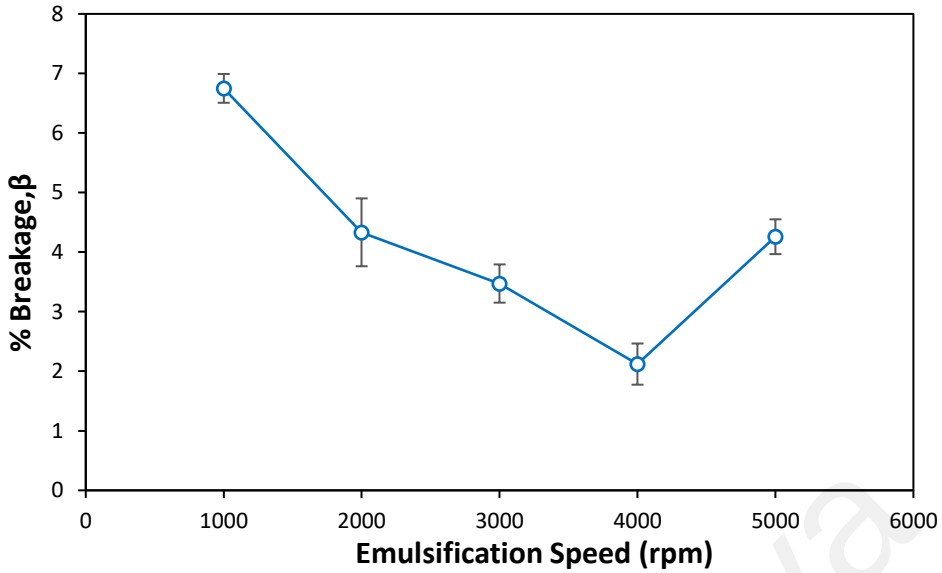

Figure 7.5: Effect of emulsification speed on the emulsion stability

Figure 7.6 depicts the effect of emulsification time on emulsion breakage. Figure 6 shows that the breakage significantly decreases from 10.33 to 3.06% when the emulsification time increases from 1 to 3 minutes. The increase in the emulsification duration allows sufficient time to produce a larger number of small droplets, which leads to a large surface area for mass transfer (Kumar et al., 2019a) and eventually longer time to coalesce. On the other hand, the prolonged emulsification time of > 3 minutes results in coagulation and high emulsion breakage (Zereshki et al., 2021). Based on the experimental results, the optimum emulsification speed and time were selected as 4000 rpm and 3 minutes for further investigation, as they gave the lowest emulsion breakage, i.e. highest emulsion stability.

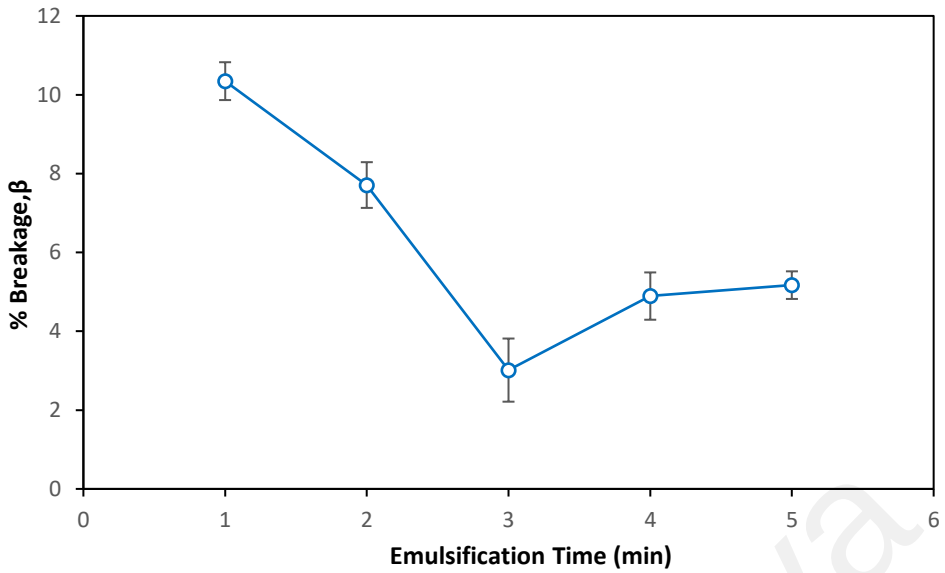

Figure 7.6: Effect of emulsification time on the emulsion stability

7.4.2.2. Effect of DES molar ratio

The effect of HBA: HBD molar ratio on the selected DES from Section 3.1 on the sodium ions elimination is presented in Figure 7.7. The figure shows that the use of molar ratios at1:4 and 1:5 for NADES1 successfully reduces the sodium ions content to values below the limit as specified by ASTM D6752 standard test. With the presence of NADES1 as the stripping phase, the sodium ions extraction efficiency becomes > 99 %. Furthermore, there was a positive association seen between the mole percentage of lactic acid in the eutectic mixture and the decrease in sodium ions concentration. The sodium ion removal efficiency increases with the NADES molar ratio due to an increase in the HBD mole fraction (Abed et al., 2023). Thus, the NADES molar ratio of 1:4 was selected for future optimizations, in the utilization of NADES as the stripping phase during the GELM process for sodium ion extraction.

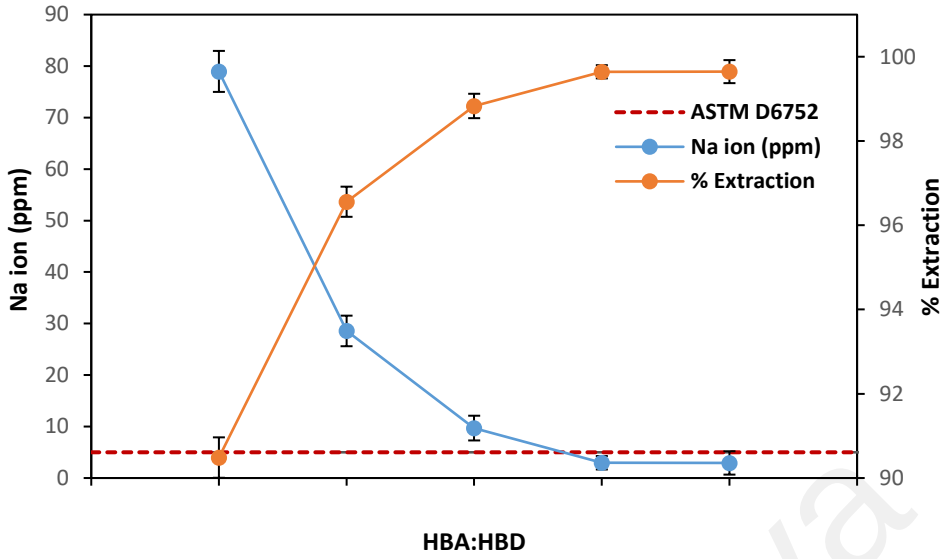

Figure 7.7: Impact of HBA:HBD molar ratio on both the extraction efficiency and sodium ion concentration via the NADES-GELM system; the experimental conditions are as follows 4 wt.% of surfactant, 0.5 treatment ratio, and speed of 300 rpm, with a fixed process duration of 5 minutes.

7.4.2.3. Effect of Treatment Ratio

The impact of biodiesel volume (external phase) to the emulsion phase (internal and membrane phases) is known as the treatment ratio. The treatment ratio is a critical criterion to be investigated since the removal rate is directly impacted by the sodium ions content in the external phase (biodiesel). This study looks into a range of treatment ratios from 0.5-2.5 ml/ml. Figure 7.8 shows that the treatment ratios of 0.5 mL/mL and 1 mL/mL are successful in bringing the sodium ion content below the ASTM D6751 and EN 14214 limits. The use of 0.5 mL/mL treatment ratio shows an extraction efficiency of more than 99.7 %. On the other hand, the treatment ratios above 1 mL/mL were unsuccessful in bringing the sodium ion concentration below the upper limit required by international criteria. Both of the extraction efficiency and emulsion stability decline with the rise in the external phase volume (Ye et al., 2017). With a smaller external phase volume, the amount of NADES in the emulsion phase is in abundance, which acts as the primary driving force for the removal of sodium ions from the membrane phase (Rosly et

al., 2019) to the stripping phase. The sodium ions accumulate in the receiving NADES phase rather than diffusing into the external phase (Mohammed et al., 2018). In contrast, a high treatment ratio causes the insufficient amount of NADES required for the removal of a large number of sodium ions from the membrane phase, which decreases the concentration gradient of sodium ions between the external phase and the membrane. This eventually reduces the sodium extraction rate and efficiency towards the membrane phase. The optimum treatment ratio was 0.5 in this investigation.

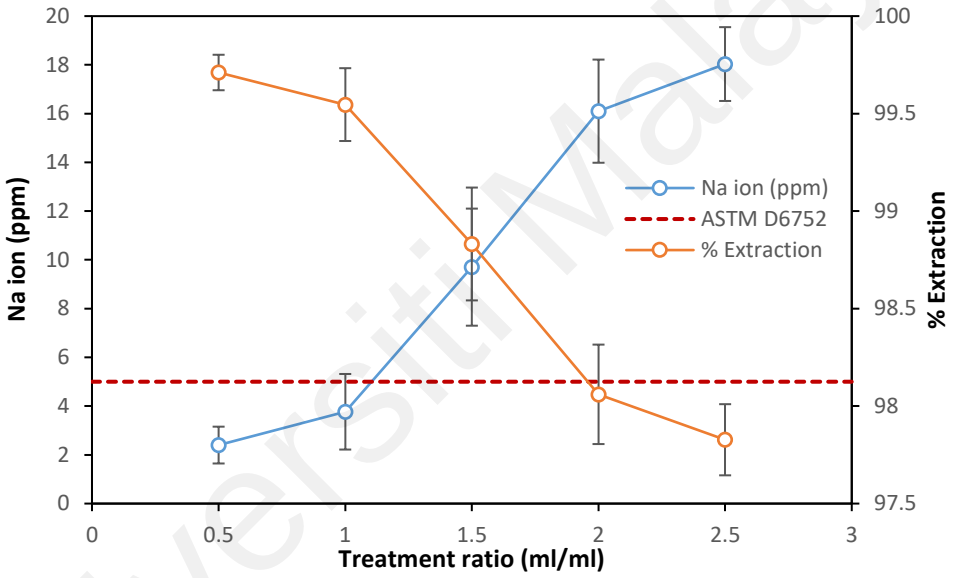

Figure 7.8: Impact of treatment ratio on both the extraction efficiency and sodium ion concentration via the NADES-GELM system; the experimental conditions are as follows 4 wt.% of surfactant, HBA:HBD of 1:4, and speed of 300 rpm, with a fixed process duration of 5 minutes.

7.4.2.4. Effect of surfactant concentration

Figure 7.9 shows the effect of surfactant concentration on sodium ion removal from biodiesel. This investigation was performed with a span 80 concentration in the range of 1-5 wt.%. The results showed that the stability of GELM and the extraction efficiency are significantly influenced by the span 80 concentration. The increase in span 80

concentration from 1-4 wt.% leads to a sharp reduction in the sodium ions content, indicating a high extraction efficiency. In fact, a maximum extraction efficiency of 99.5 % was achieved from 4 wt.% of span 80 concentration. A more stable system is established when the surfactant concentration increases due to the lower surface tension between the phases (Bera et al., 2013), resulting in the formation of smaller globules (Zereshki et al., 2018), which favour the dispersion of emulsion bubbles, thereby enhancing the contact area for mass transfer of the sodium ions (Sulaiman et al., 2021). In contrast, the emulsion is easily disrupted at low surfactant concentration as there is insufficient amount of emulsion to completely cover the striping phase (Zereshki et al., 2021).

In contrast, it is noteworthy that a noticeable drop in extraction efficiency was observed when the surfactant concentration was raised to 5 wt.%. This was in accordance with the results of Rosly et al. (Rosly et al., 2020), which is attributed to the production of large globules of emulsion (Khan et al., 2021) and the increase in the membrane phase thickness and viscosity (Rosly et al., 2020). This results in an increased mass transfer resistance between the phases, which further reduces the extraction efficiency. In this study, the optimum surfactant concentration achieved is 4 wt.%.

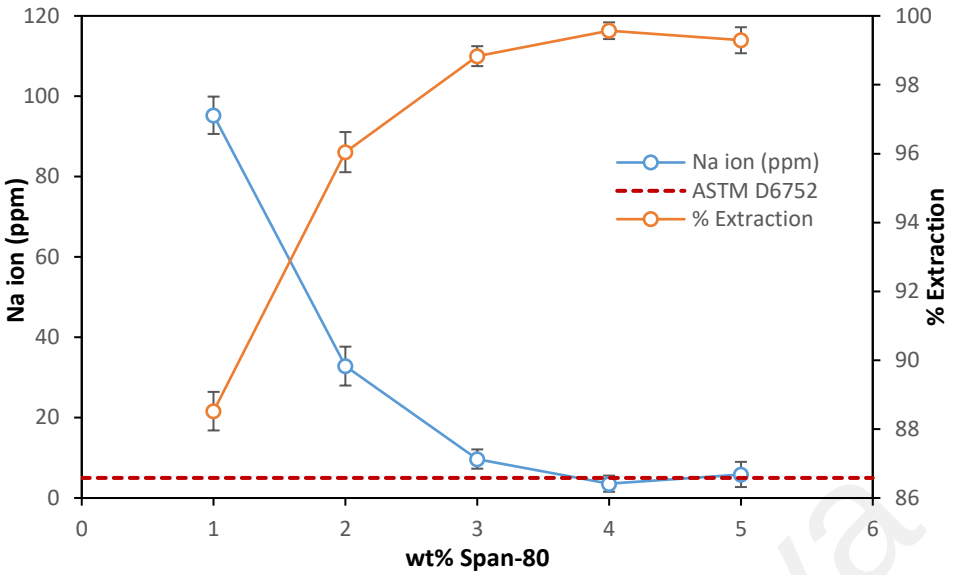

Figure 7.9: Effect of span 80 concentration on both the extraction efficiency and sodium ion concentration via the NADES-GELM system; the experimental conditions are as follows 1:4 of HBA:HBD molar ratio, 0.5 treatment ratio, and speed of 300 rpm, with a fixed process duration of 5 minutes.

7.4.2.5. Effect of extraction duration

The extraction duration, which is the contact time between the external phase (biodiesel) and the emulsion phase, was investigated in the range of 1 to 10 minutes Figure 7.10 shows that the extraction efficiency increases with the extraction duration. This is due to the presence of smaller emulsion globules and the homogeneous distribution of emulsion globules at prolonged extraction duration, where the maximum interfacial area is produced by this homogeneity, with improved mass transfer. In fact, the extraction rate becomes rapid, where the sodium ion concentration decreases from 830 ppm to 321.83 ppm in just 1 minute of extraction time. Additionally, the large number of emulsion globules and greater size of globules are due to the excessive brief mixing duration (Zaulkiflee et al., 2020). The sodium ions concentration decreases further to 3.5 ppm (extraction efficiency: 99.57%) when the extraction duration was extended from 1 to 7 minutes.

However, the sodium ions concentration increases slightly to 6.43-12.07 ppm with an increase in extraction duration to 8-10 minutes. The prolonged extraction duration causes the emulsion droplets to coalesce. This is consistent with the emulsion's increasing size at increased extraction duration. The formation of larger droplets results in the swelling of the membrane emulsion (Zaulkiflee et al., 2020). This observation is also in accordance with the work of Kulkarni and Mahajani (Kulkarni & Mahajani, 2002), Ooi et al. (Ooi et al., 2016) and Ahmad et al. (Ahmad et al., 2012) where emulsion instability was observed at extended extraction durations. As a result, the extraction duration of 7 minutes was selected as the optimum extraction duration for sodium ion removal from the biodiesel.

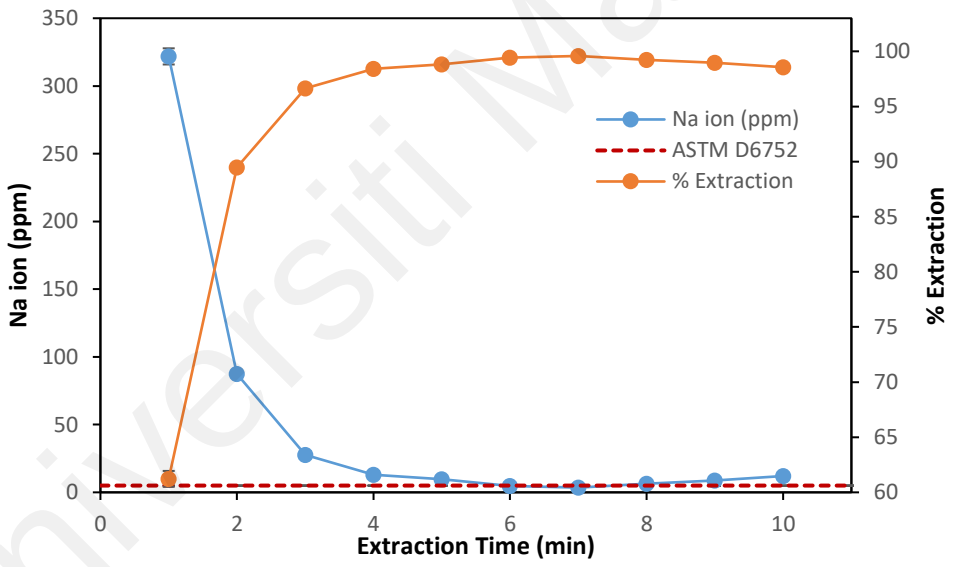

Figure 7.10: Impact of duration process on both the extraction efficiency and sodium ion concentration via the NADES-GELM system; the experimental conditions are as follows:1:4 HBA:HBD molar ratio, 4 wt.% of span80, 0.5 treatment ratio, and speed of 300 rpm.

7.4.2.6. Effect of mixing speed

Figure 7.11 illustrates the effect of mixing speed on sodium ion elimination at the range of 100-500 rpm. The increase of mixing speed from 100 rpm to 400 rpm improves the extraction efficiency. At low mixing speed, large droplets were generated as a result of

insufficient shear force to disperse the emulsion in the biodiesel (external phase) and this causes lower interfacial area for mass transfer (Kumbasar, 2008). Kumbasar (2008) and Othman et al. (Othman et al., 2016) also reported similar findings, where slow mixing speed results in poorly dispersed ELM droplets and the production of huge droplets in the emulsion. In contrast, when the mixing speed increases, the impeller applies more shear energy to the emulsion droplets, which forms finer membrane emulsion droplets with higher removal efficiency (Kumar et al., 2019a). In addition, the increase in the mixing speed also increases the wide dispersion of small emulsion globules, which improves the interfacial contact area between the external phase and the emulsion phase and allows for a high elimination of contaminants (Abbassian & Kargari, 2016). Nevertheless, it is noteworthy that the further increase in the mixing speed of > 400 rpm decreases sodium ion elimination, which is due to the excessive mixing which causes the thinning of the interfacial area of the emulsion droplets, which eventually leads to emulsion breakage (Zaulkiflee et al., 2020). The emulsion droplet size decreases with the mixing speed, where the mass transfer surface increases (Kumar et al., 2019a), with a lower breakage ratio and better emulsion stability. Unstable emulsions are due to the formation of very small size droplets at high speeds, which further results in weak surface tension to maintain the emulsions (Kahar et al., 2023). Thus, the optimum mixing speed of 400 rpm was selected in this study.

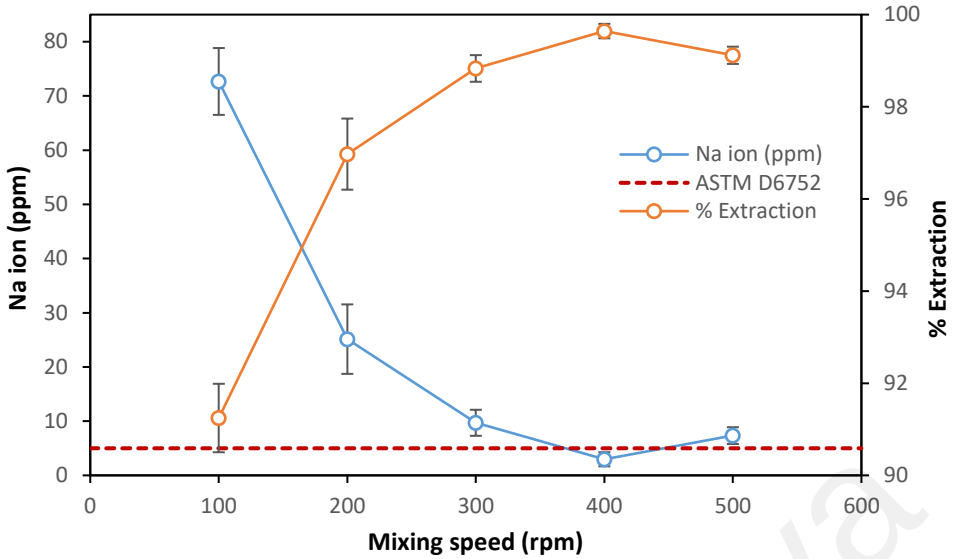

Figure 7.11: Impact of HBA:HBD molar ratio on both the extraction efficiency and sodium ion concentration via the NADES-GELM system; the experimental conditions are as follows: 1:4 HBA:HBD molar ratio, 4 wt.% of surfactant, 0.5 treatment ratio and fixed process duration of 6 minutes.

7.4.2.7. Effect of graphene presence

The effect of incorporating graphene into the GELM for enhanced sodium ions elimination was investigated by adding 0.3 g of graphene into the emulsion phase at the optimum conditions obtained from Section 3.2.2 – 3.2.6 (1:4 of HBA:HBD, 4 wt% of span 80, 7 minutes of extraction time, 400 rpm, and 0.5 treatment ratio). Figure 7.12 shows that the presence of graphene in the emulsion improves the extraction efficiency, as lower sodium ion concentration is observed in the biodiesel. The presence of graphene achieves international standards with an extraction duration of 4 minutes, whilst an extraction duration of 6 minutes was required in the absence of graphene. The presence of graphene not only provides more active sites for the extraction process (Ayoob & Fadhil, 2020), but also increases the strength and stability of the emulsion globules, which prevents their collision or coalescence (Al-Obaidi et al., 2021; Lin et al., 2015). Additionally, the metal ion (like sodium ion) in the salt of the fatty acid interacts with the functional group on the surface of graphene. (Baroutian et al., 2011). Furthermore, the

graphene and surfactant could also combine to form a three-dimensional lattice between the nanoparticles and globules to enhance the emulsion stability (Al-Ani et al., 2021). Additionally, the addition of nanoparticles also reduces the emulsion globules' size and interfacial tension (Cheraghian & Hendraningrat, 2016). This is observed in the microscopic images of the emulsion in Figure 7.13. In the presence of graphene, the GENM shows a larger number of emulsion droplets (Figure 7.13 a), and the aggregated nanographene particles are observed in Figures 7.13b and 7.13c. Figure 7.13d shows that the aggregated graphene is firmly affixed to the emulsion droplet margins. The emulsion globules are more homogeneous and smaller, which further improves the removal efficiency and prevents the Ostwald ripening process in the GELM system (Suliman et al., 2022).

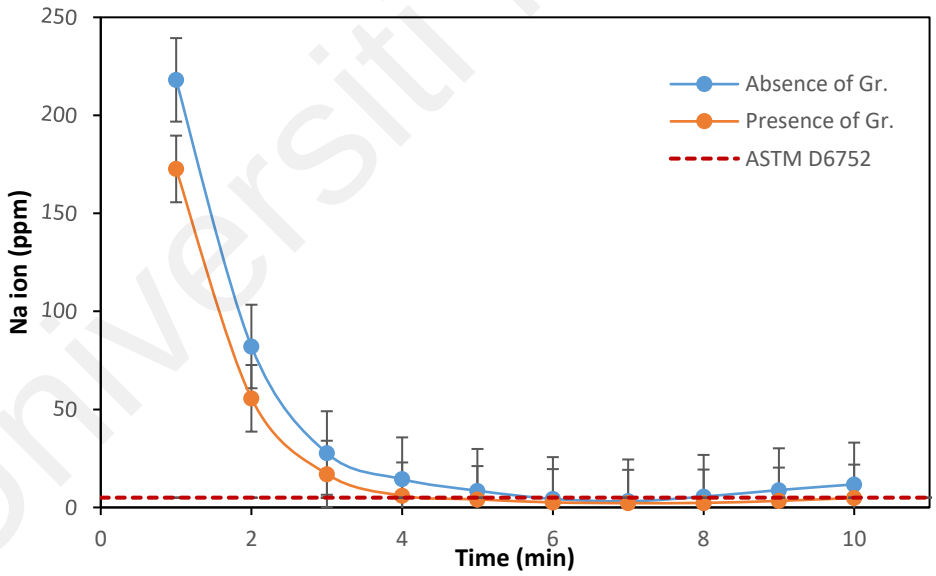

Figure 7.12: Effect of presence and absence of graphene nanoparticles in GELM system at the optimum conditions (1:4 of HBA:HBD, 4 wt% of span 80, 7 minutes of process duration, 400 rpm, and 0.5 treatment ratio)

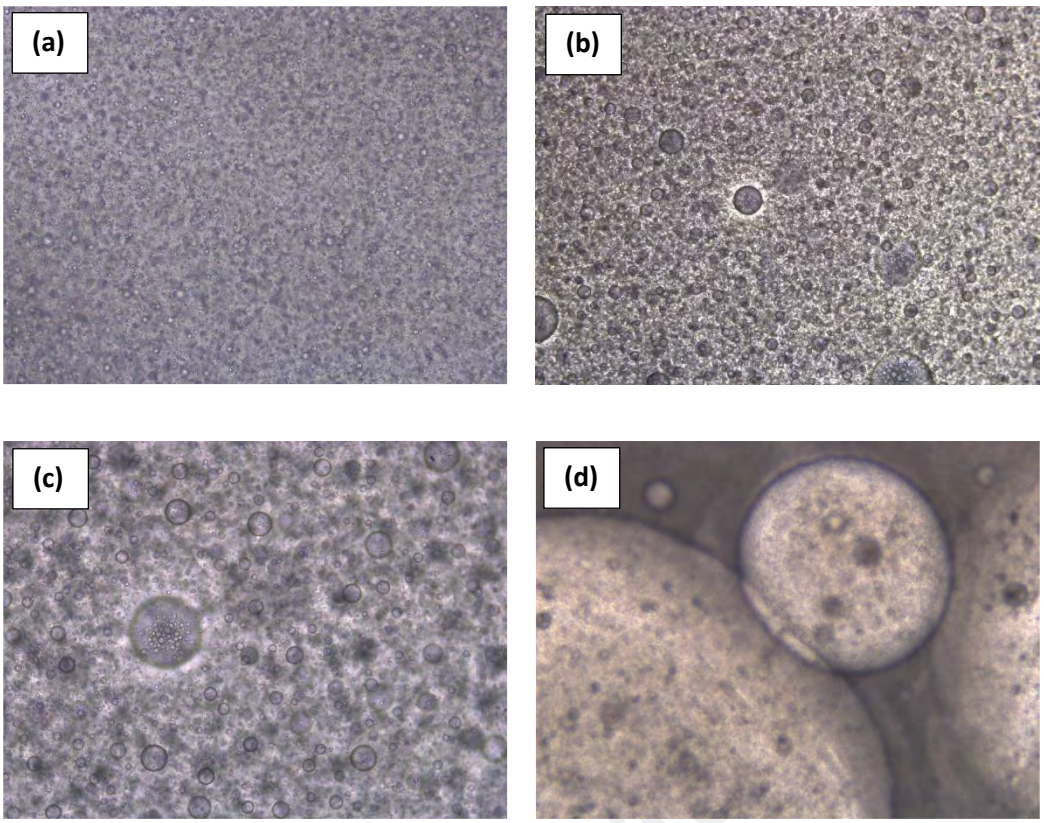

Figure 7.13: Microscopic images of emulsion in this study: (a) 4X (b) 10X (c) 20X and (d) 100X.

7.4.3. Mathematical modelling (Mass Transfer and Kinetic study)

7.4.3.1. Kinetic study

The sodium ion elimination from biodiesel using GELM was further investigated by the kinetics study and mass transfer coefficients using the optimum conditions. A mathematical model was fabricated based on these assumptions: i) the NADES layer, silicon oil layer, the biodiesel layer, are immiscible with each other, ii) the sodium ions transfer was in the steady state, iii) the sodium ion diffusion occurs in the silicon oil layer and is a 1^{st} -order one-directional process, iv) the sodium ion stripping between the silicon oil phase and the NADES phase is considered as an irreversible reaction and v) the amount of sodium ions lost during the process is neglected.

The sodium ions diffusion in the GELM-NADES is according to Fick's Law, as in Eq. (5):

$$J_{Na^+} = -\frac{V}{A_g}\frac{dC_t}{dt} \quad (7.5)$$

where J_{Na^+} represents the sodium ions flux ($\frac{mol}{cm^2 .S}$), V represents the biodiesel phase volume (cm^3), A_g represents the surface area of the emulsion droplets (cm^2), and dC_t/dt represents the sodium ion concentration gradient ($\frac{mol}{cm^3 .S}$).

The value of A_g was estimated using Eq. (7.6):

$$-\frac{A_g}{V_g} = \frac{S_g}{V_T} \rightarrow A_g = V_g \frac{\pi D_g^2}{\frac{1}{6}\pi D_g^3} = V_g \frac{6}{D_g} \quad (7.6)$$

where, V_T, S_g, V_g, and D_g, is the total emulsion droplets' volume (cm^3), the droplet's surface area (cm^2), the droplet's volume (cm^3) and the average droplet diameter (cm), respectively. Eq. (9) is derived from the substitution of Eq. (7.6) into Eq. (5), while considering assumption 3 that the sodium ion diffusion in GELM-NADES follows a 1st-order kinetic model.

$$J_{Na^+} = -\frac{V_T}{V_g}\frac{D_g}{6}\frac{dC_t}{dt} = k\,C_t \quad (7.7)$$

By reorganizing, Eq. (7.7) can be expressed as Eq. (7.8).

$$-k\frac{V_g}{V_T}\frac{6}{D_g}dt = \left(\frac{d\,C_t}{C_t}\right) \quad (7.8)$$

Eq. (7.9) is obtained from the integration of Eq. (7.8) with respect to time and with the applications of the boundary conditions of time from zero to t and concentration from C_o to C_t.

$$-k\frac{V_g}{V_T}\frac{6}{D_g}t = \ln\frac{C_t}{C_o} \quad (7.9)$$

Finally, rearranging terms, we arrive at Eq. (7.10)

$$\ln\frac{C_t}{C_o} = -k\frac{V_g}{V_T}\frac{6}{D_g}t \quad (7.10)$$

$$k = \frac{\ln\frac{C_t}{C_o}}{t}\frac{V_T}{V_g}\frac{D_g}{6} \quad (7.11)$$

$$\frac{C_t}{C_o} = e^{-(k\frac{V_g}{V_T}\frac{6}{D_g})t} \quad (7.12)$$

To simplify the Eq., we substitute the term $k\frac{V_g}{V_T}\frac{6}{D_g}$ is substituted with the expression "K_{obs}". This leads to Eq. (7.13), where the extraction rate constant, K_{obs} is introduced.

$$\frac{C_t}{C_o} = e^{-K_{obs}\,t} \quad (7.13)$$

$$\ln\frac{C_t}{C_o} = -K_{obs}\,t \quad (7.14)$$

The value of K_{obs} can be obtained by fitting the experimental data into Eq. (7.13). The results of the curve fitting process are shown in Figure 7.14, which shows that the model fits closely to the experimental data. The R^2 values of the GELMs that incorporate NADES as the stripping agents are 0.92, indicating a good fit. The calculated K_{obs} value is 0.647 (min^{-1}). Overall, these findings suggest that the model is an accurate representation of the experimental data.

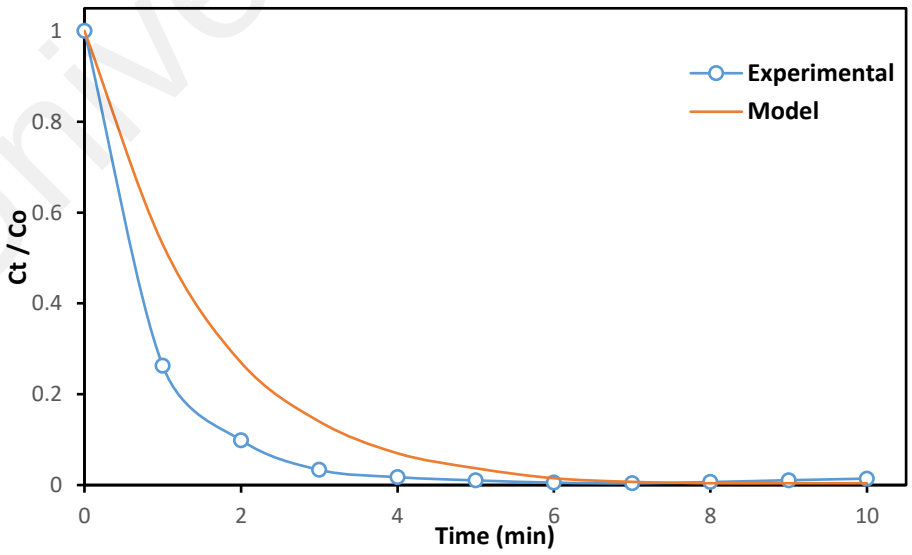

Figure 7.14: Sodium concentration profiles over time (t) for NADES1 using the GELM-NADES technique. The initial sodium content was 830 ppm, with a 1:4 HBA:HBD ratio, 4 wt.% of span 80, 0.5 treatment ratio, and 400 rpm mixing speed.

7.4.3.2. Evaluation of Overall Mass Transfer Coefficient

The overall mass transfer coefficient (K_o) in the GELM-NADES system is according to the following Eq., as expressed by Eq. (7.15):

$$\frac{1}{K_o} = \frac{1}{K_M} + \frac{1}{K_F} \tag{7.15}$$

$K_o$represent the overall mass transfer coefficient (m/s), K_M denotes the mass transfer coefficient of the external phase (m/s), and K_F signifies the interfacial reaction rate constant (in m/s).

The mass transfer coefficient of the external phase is estimated by the Eq. of Skelland and Lee (Kohli et al., 2019).

$$\frac{K_M}{\sqrt{ND}} = 2.932 \times 10^{-7} \left(\frac{V_s+V_m}{V_s+V_m+V_f}\right)\left(\frac{d_i}{d_t}\right)^{0.584} Re^{1.371} \tag{7.16}$$

Where, V_s, V_m, and V_f represent the volumes of the stripping phase, membrane phase and external phase, respectively. N represents the mixing speed of the system (400 rpm) while D represents the diffusion of sodium ions in the membrane phase. Furthermore, d_i and d_t represent the impeller's and the mixing tank's diameters, respectively. Eq. (7.17) is utilized to compute the Reynold factor for the system (Re) which is as follows:

$$Re = \frac{Nd_i^2\rho_C}{\mu_C} \tag{7.17}$$

In this Eq. (7.17), μ_C and ρ_C represent the continuous phase's viscosity and density, respectively. The resultant Re was found to be 2816.873.

The Wilke and Chang Eq. (Kohli et al., 2019) is used to calculate the diffusion coefficient (D) of the sodium ions in the membrane phase, which is represented by Eq. (7.18).

$$D_m = \frac{117.3 \times 10^{-18}.\ (\varphi M_W)^{0.5}\ .\ T}{\mu_m\ \vartheta_C^{0.6}} \tag{7.18}$$

Eq. (7.19) can be used to determine the interfacial reaction rate constant (K_F):

$$\ln \frac{C_t}{C_o} = -AK_F\, t \tag{7.19}$$

Eq. (7.19) makes it clear that K_F can be represented as follows by comparing Eq. (7.14) and (7.19).

$$K_F = \frac{K_{obs}}{A} \tag{7.20}$$

The emulsion's specific area, denoted by A, is determined using Eq. (7.21)

$$A = \frac{A_i}{V} = \frac{6\alpha}{d_{32}} \tag{7.21}$$

A_i is the interfacial area of the scattered droplets, V is the emulsion's unit volume, α is the volume percentage, and the volume surface mean diameter d_{32} is the droplet size, which can be calculated using the following Eq. (7.22) (Ahmad et al., 2011):

$$d_{32} = \frac{\sum n_i d_i^3}{\sum n_i d_i^2} = 6 \times \frac{V_T}{A_T} \tag{7.22}$$

In Eq. (7.22), n_i is the number of droplets characterized by a diameter di and V_T and A_T are the total volume and the area of the emulsion dispersed phase, respectively. The volume-surface mean diameter was calculated to be 1.8×10^{-6}.

Table 7.2 presents the values of the overall mass transfer coefficient (K_O), mass transfer coefficient of the external phase in the agitated reactor (K_M), and interfacial reaction rate constant (K_F). The reciprocal of the mass transfer coefficients of the external phase (K_M) and the interfacial reaction rate constant (K_F) have an impact on the overall mass transfer coefficient (K_o), according to the inverse relationship represented in Eq. (7.15). This suggests that there is a reciprocal relationship rather than only an additive influence between the phases during mass transfer. The interaction between these coefficients draws attention to the complex relationships present in the system and emphasizes the importance of the properties of the ELM phases in determining the total mass transfer rate.

Table 7.2: Values of the mass transfer coefficient of the external phase in agitated reactor (K_M), interfacial reaction rate constant (K_F) and overall mass transfer coefficient (K_O).

System	$K_F\ (m/s)$	$K_M\ (m/s)$	$K_O\ (m/s)$
GELM-NADES	5.392×10^{-9}	1.373×10^{-7}	5.188×10^{-9}

7.4.4. Mechanism of sodium removal from biodiesel using ELM technique

Sodium ion is often found in the form of a fatty acid salt in biodiesel. The mechanism of sodium ion removal from the biodiesel is based on the film theory between phases, hydrophobicity and hydrophilicity nature of the sodium ion complex. The mechanism present in the use of the GELM technique involves mechanical and chemical procedures. The membrane phase functions as a selective barrier that enables the diffusion of sodium ions from fatty acid methyl ester or FAME (external phase) to the receiving phase (NADES) while maintaining the biodiesel component. Based on the experimental results, the postulated transport mechanisms are presented in Figure 7.15.

Firstly, sodium ions are frequently present in FAME as the fatty acid salt molecule. The polar head of surfactant (span 80) in the membrane phase is highly favored by sodium ions in the fatty acid salt. Thus, the contact between the sodium ions and the surfactant facilitates the diffusion of sodium ions into the membrane phase. Then, the sodium ions are transported into the membrane phase by solubilization with the presence of surfactant in the membrane, which forms micelles around them. A hydrophobic environment with the presence of silicon oil is required to stabilize the micelles.

As the sodium ions are enclosed in the membrane phase's micelles, they start to permeate through the surfactant and silicon oil. Sodium ions migrate from the FAME phase into the membrane phase due to the differences in concentration. The characteristics of the

membrane phase and the micelles' attraction to the sodium ions are the main reasons for this migration and transportation phenomenon.

When the sodium ions reach the membrane/stripping interphase, they encounter nanographene and NADES. The sodium ions are stripped from the micelles in the NADES phase (Abed et al., 2023), while the remaining sodium ions are further adsorbed by the nanomaterials (L. Li et al., 2002) due to high surface area and adsorption capacity. Thus, the membrane phase is continuously regenerated and extracts more sodium ions from the external phase at any saturation during the process.

An efficient sodium ion removal from the biodiesel phase to the stripping phase via the GELM is dependent on the utilization of suitable components, including silicon oil, surfactant, graphene nanomaterials and NADES. The GELM technique makes it possible to effectively extract and remove sodium ions from the FAME in a targeted approach. The selective liquid membranes, mass transfer, and chemical affinity used in this process to remove the sodium ions is itself a unique technique.

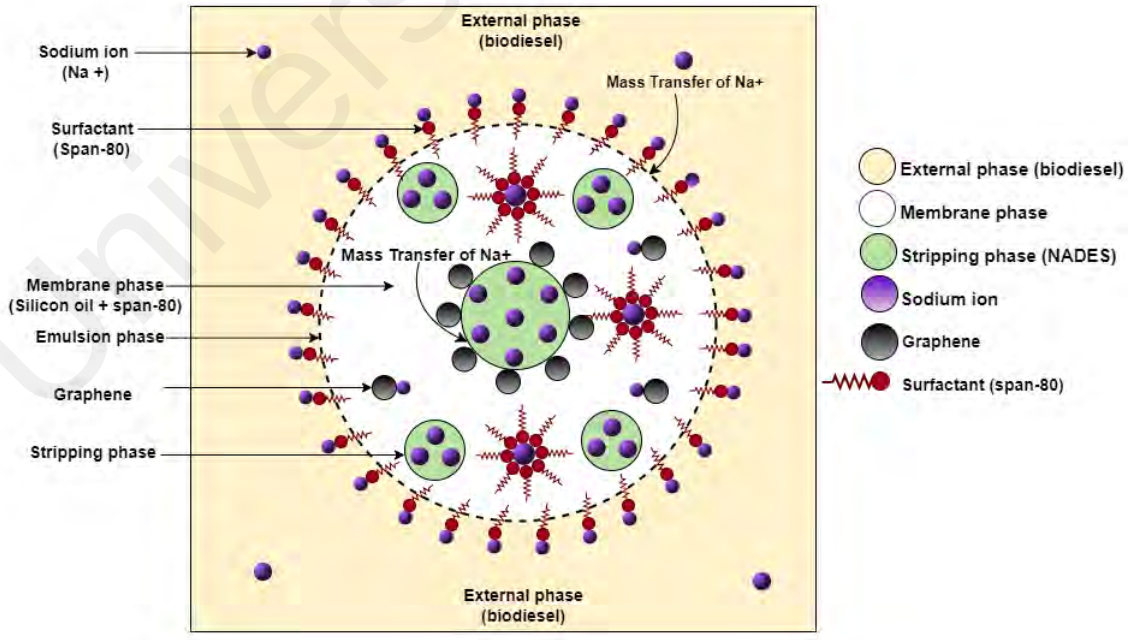

Figure 7.15: Proposed the sodium ions transport mechanism via GELM-NADES system.

7.4.5. Overview and Comparison of Biodiesel Purification Techniques

The production of high-quality products has been greatly aided by the processing of biodiesel in various techniques, though these techniques have certain drawbacks or difficulties. The water washing technique has several drawbacks, such as higher purification costs, longer production time, environmentally hazardous liquid effluent and equipment corrosion (Atadashi et al., 2011a).

The use of waterless techniques such as ion exchange resin and adsorption are prompted by the shortcomings of the water-washing approach. However, these techniques possess some drawbacks, such as limited chemical knowledge and the depletion and cost of adsorbent regeneration (Atadashi, 2015; Camilo et al., 2024). Considerations such as the cost, type, structure, strength, capacity, stability, etc, need to be assessed before selecting the most appropriate ion exchange resin (Abedet al., 2023).

The challenges faced by these conventional techniques have encouraged the application of membrane techniques in biodiesel refining. Membrane separation technology seems to be the preferred method in biodiesel purification as it preserves the unreacted triglycerides during the process (Shuit et al., 2012).The properties of biodiesel have been positively impacted by the membrane-based techniques (Saleh et al., 2011). The high cost of membrane construction, fouling of the membrane, and the energy losses related to the usage of vacuum pumps in the membrane separation techniques should also be taken into consideration. These drawbacks demand greater investigations and efforts (Atadashi, 2015).

Liquid membrane techniques have shown promise as highly selective separation barriers in the past few years (Kumar et al., 2019b). The use of ELM offers a variety of improved separation methods that maximize the purification process by utilizing the solubility, hydrophobicity, electrostatic charge, and molecule size (Azarang et al., 2019). ELM represents a significant breakthrough in purification technology with enhanced separation

efficiency by minimizing the diffusion path between the phases (K. M. Abed, Hayyan, Hizaddin, Hashim, et al., 2023). ELMs offer many benefits such as high extraction efficiency, high selectivity, lower product contamination, cost-effectiveness, absence of phase separation problems, ease of scaling for commercial purposes, and decrease of organic phases compared to the traditional methods (Kumar et al., 2018). Table 7.3 lists the performance comparisons of different techniques for the removal of contaminants from biodiesel.

The use of ELM integrated with DESs and graphene for the removal of sodium ions in biodiesel has been remarkable. This method offers the effective purification of crude biodiesel without the use of water or ion exchange resins, thereby offering a more sustainable solution for the purification of biodiesel.

The integration of DESs as liquid membranes in the ELM systems will surely open new frontiers in the biodiesel processing sector. In particular, this technology has demonstrated a great deal of opportunity for future research into the purification of biodiesel, particularly for the elimination of other contaminants such as glycerol, alcohol, water, etc. to conform to the international requirements.

Table 7.3: Comparative analysis of some of the various processes used to remove pollutants from biodiesel.

Purification Techniques	Extraction agent	Conditions	Contaminant	Remarks	References
Dry washing	Sulfuric acid–activated bentonite clay	Bentonite clay (200 mesh size), activated with 0.5 M H_2SO_4, stirring for 60 min at 60 °C	Free fatty acids and catalyst residue	Effective in biodiesel purification	Rameshaiah et al., 2024
Dry washing	Dowex HCR-S Cationic resin	The optimum conditions were a resin's pre-drying time of 4 hr, 50 min contact time, 6 wt.% of the resin, and 15 °C temperature.	Water	At the optimum conditions, 92.78 wt.% of the water in the biodiesel was eliminated.	Okumuş et al., 2019
Liquid-liquid extraction	DES based on aqueous glycerol and ammonium salt	DES: biodiesel molar ratio of 3:1, 170-rpm stirring speed, and 40-min extraction time.	Soap	The soap content complies with EN 14214 and ASTM D6751.	Hayyan et al., 2022
Liquid-liquid extraction	Lactic acid-based DES and activated carbon	DES: biodiesel volume ratio of 1:1, 6 minutes, 150 rpm stirring speed, and DES molar ratio of 1:4.	Soap	The soap concentration dropped from 781.567 to 23.24 ppm.	Abed et al., 2023

Purification Techniques	Extraction agent	Conditions	Contaminant	Remarks	References
Liquid-liquid extraction	DES based on based on choline chloride (ChCl) and methyltriphenylphosphonium bromide (MTPB) salts	DES: biodiesel of 0.75–3 molar ratio, 200 rpm of agitation for 1 hr and 2 hr settling.	Residual KOH	The removal efficiency of ChCl: glycerol and MTPB: glycerol was 98.59% and 97.57%, respectively.	Shahbaz et al., 2011a
Liquid-liquid extraction	DES based on ChCl and glycerine	Optimum DES:biodiesel molar ratio of 1:1 and a DES molar composition of 1:1.	Glycerol	Glycerol content fulfilled the EN 14214 and ASTM D 6751 standard.	Hayyan et al., 2010
Membrane-based microfiltration	Ceramic membrane	Kaolin and alumina were used as the membrane's material, with pressures of 0.25, 0.5 and 0.75 kg cm^{-2}.	Glycerol	At a pressure of 0.5 kg cm^{-2}, a glycerol rejection of 91%.	Kusumocahyo et al., 2024
DES-based ELM	Lactic acid-based DES and activated carbon	2 wt.% of the surfactant, 0.5 wt.% of AC, 1:4 DES molar ratio, 1:1 DES: biodiesel ratio, 400 rpm mixing speed, and 6 min extraction time.	Soap	The highest removal efficiency of 99.75%, which is equivalent to 1.87 ppm soap content was achieved	Abed et al., 2023

Purification Techniques	Extraction agent	Conditions	Contaminant	Remarks	References
NADES-based ELM	Lactic acid-based NADES and graphene	homogenization speed of 8000 rpm, homogenization time of 3 min, HBA: HBD molar ratio of 1:4, 3 wt.% of span 80, 10 minutes of extraction time, 400 rpm stirring speed, 0.3 g of graphene and 0.5 treatment ratio.	Sodium ion residual	The GELM-NADES technique can achieve a sodium ion extraction efficiency of 99.6% (3.17 ppm) with high stability.	Current study

7.5. Conclusion

A novel purification approach for sodium ion removal from biodiesel using the GELM technique incorporating NADES as the stripping phase was evaluated. Computational approaches were used to identify and select the most appropriate DES in this study. The removal of sodium ions from biodiesel is discussed in this article using COSMO-RS-based molecular interactions (σ-profiles and σ-potential) to demonstrate the capacity of DES for sodium ion extraction. COSMO-RS results showed that lactic acid-based NADES is the most effective stripping phase for sodium ion removal, and was validated by the experimental results. The ability of NADES as the stripping agent in the GELM-NADES process was proven, in which a high extraction efficiency can be achieved under the optimized parameters of HBA:HBD molar ratio of 1:4, span-80 concentration of 4 wt.%, process duration of 7 minutes, mixing speed of 400 rpm, and treatment ratio of 0.5. The incorporation of 0.3 g graphene into the GELM system further enhanced the extraction efficiency (99.6 %) and shortens the extraction duration from 6 minutes to 4 minutes that is required to meet the ASTM D6752 standard. At the optimal conditions, the sodium ions content in the biodiesel was reduced from 830 ppm to 3.17 ppm, which is well below the ASTM D6752 requirement. The transport mechanisms in the GELM-NADES adhere to a first-order mass transfer process, with an overall mass transfer coefficient K_O , mass transfer coefficient of the external phase in agitated reactor K_M , and interfacial reaction rate constant K_F of 5.188×10^{-9}88×10^-9,1.373×10^{-7} ,and 5.392×10^{-9} m/s, respectively. The use of ELM integrated with DESs and graphene offers an effective purification technique, thereby offering a remarkable and more sustainable solution for biodiesel industry. This technique surely opens up new frontiers in the biodiesel processing sector and demonstrate an advance purification method for meeting biodiesel international standards.

CHAPTER 8: CONCLUSION

This chapter provides a summary of research findings addressing each research question through the corresponding research objective. Afterwards, the significant of the study, and recommendations are provided.

8.1. Summary of Findings

In the following, the main research findings through this thesis are summarised in the order of each research objective:

- Activated carbon was prepared from palm raceme and lipase activity was utilized as an indicator to assess the optimal AC under different parameters. The parameters include carbonization temperature, impregnation ratio, and carbonization time, as well as the biocompatibility of AC and DES. The DES prepared from alanine/sodium hydroxide exhibited good biocompatibility with AC.
- A novel purification approach for soap removal from biodiesel using the ELM technique integrated with DES and carbon materials as the stripping phase was successfully evaluated.
- ELM results illustrated a superior soap removal efficiency of 1.87 ppm in comparison to liquid-liquid extraction results which was 23.23 ppm. The highest removal efficiency of 99.75% was achievable under 2 wt% of the surfactant, 0.5 wt% of AC, 1:4 TMAC: LA molar ratio, 1:1 DES: BD ratio, 4000 rpm mixing speed and 6 min extraction time.
- DESs prepared from TMAC: TEG and ChCl: TEG provided goog capability for soap removal when integrated with AC in ELM system under the the following

conditions: DES molar ratio of 1:4, DES: biodiesel ratio of 1:1 volume ratio, surfactant concentration of 2 wt.%, extraction duration of 10 min, mixing speed of 400 rpm, treatment ratio of 0.5 volume ratio and AC dosage of 0.5 wt.%. The maximum removal efficiency was 99.1% for TMAC: TEG and 97.5% for ChCl: TEG.

- LA-based DES as natural DES also highlighted high removal efficiency (99.6) under the following conditions: 2 wt.% of the surfactant, 0.3 g of graphene, 1:4 DES molar ratio as stripping phase, 1:1 DES: BD ratio, 400 rpm mixing speed, and 6 min extraction time.
- Also, this work highlights the potential of COSMO-RS in the prediction of the best candidate stripping phase as well as for the molecular interaction between soap and DESs. The soap exhibited favourable interactions in all three regions, namely hydrogen bond donor, hydrogen bond acceptor, and non-polar.
- The kinetics of the soap transport mechanism during the ELM system adheres to the first-order kinetic model. The overall mass transfer coefficient, mass transfer coefficient of the external phase in an agitated reactor, and the interfacial reaction rate constant of 5.188×10^{-9},1.373×10^{-7} , and 5.392×10^{-9} m/s, respectively.
- Overall, in this study, a novel ELM process has been developed through a unique integration of DESs and carbon materials as sustainable materials in downstream processing. Combining with the experimental data and the novel predictive investigation using COSMO-RS, this work is expected to have a high impact on biodiesel purification via ELM techniques in relevant industries.

8.2. Significance of Study

Emulsion liquid membrane (ELM) offers a viable alternative to the conventional water-based purification process. It demonstrates the effective purification of crude biodiesel without the use of a large amount of water/washing agent in comparison to conventional water washing, thereby offering a more sustainable solution for the purification of biodiesel. Moreover, the integration of deep eutectic solvents with carbon materials during the ELM technique illustrated a new cleaner, and simpler route for the purification of crude biodiesel.

Despite the successful purification of biodiesel with desirable physicochemical properties through ELM processes, challenges remain, including emulsion instability and limitations in applications requiring extreme temperatures due to emulsion stability. Further research is necessary to explore emulsion stability, breakdown, emulsification time, and the proper selection of the stripping phase during the refining process. These aspects warrant more attention in the field of biodiesel refining.

8.3. Recommendations and Future Works

Based on the results of the present work, the following recommendations for future work can be proposed:

- The investigation of other DES and possibly other DES families is recommended as only a limited number of DES were evaluated for this study.
- The investigation of other DES and possibly other DES families is recommended as only a limited number of DES were evaluated for this study.
- One concern in the ELM separation is the stability of the emulsion. Consequently, different homogenization speeds and time in the emulsion

formulation step should be investigated so as to achieve a stable emulsion with high flux.

- In this work, the soap was removed from biodiesel using the ELM system. The removal of other impurities such as glycerol, FFA, and catalyst traces from the contaminated biodiesel using the ELM system is recommended.
- The employment of other types of liquid membranes such as bulk liquid membranes and supported liquid membranes is also recommended for the purification of contaminated biodiesel.

REFERENCES

Abbassian, K., & Kargari, A. (2016). Effect of polymer addition to membrane phase to improve the stability of emulsion liquid membrane for phenol pertraction. *Desalination and Water Treatment*, *57*(7), 2942–2951.

Abbott, A. P., Barron, J. C., Frisch, G., Ryder, K. S., & Silva, A. F. (2011). The effect of additives on zinc electrodeposition from deep eutectic solvents. *Electrochimica Acta*, *56*(14), 5272–5279.

Abbott, A. P., Boothby, D., Capper, G., Davies, D. L., & Rasheed, R. K. (2004). Deep eutectic solvents formed between choline chloride and carboxylic acids: versatile alternatives to ionic liquids. *Journal of the American Chemical Society*, *126*(29), 9142–9147.

Abbott, A. P., Capper, G., Davies, D. L., Rasheed, R. K., & Tambyrajah, V. (2003). Novel solvent properties of choline chloride/urea mixtures. *Chemical Communications*, *1*, 70–71.

Abbott, A. P., Capper, G., & Gray, S. (2006). Design of improved deep eutectic solvents using hole theory. *Chemphyschem: A European Journal of Chemical Physics and Physical Chemistry*, *7*(4), 803–806.

Abbott, A. P., Capper, G., McKenzie, K. J., & Ryder, K. S. (2007). Electrodeposition of zinc–tin alloys from deep eutectic solvents based on choline chloride. *Journal of Electroanalytical Chemistry*, *599*(2), 288–294. https://doi.org/10.1016/j.jelechem.2006.04.024

Abbott, A. P., Cullis, P. M., Gibson, M. J., Harris, R. C., & Raven, E. (2007). Extraction of glycerol from biodiesel into a eutectic based ionic liquid. *Green Chemistry*, *9*(8), 868–872. https://doi.org/https://doi.org/10.1039/B702833D

Abed, K., Hayyan, A., Hizaddin, H. F., Hashim, M. A., & Basirun, W. J. (2022). Functionalized nanotubes. In *Graphene, Nanotubes and Quantum Dots-Based Nanotechnology* (pp. 421–444). Elsevier. https://doi.org/10.1016/b978-0-323-85457-3.00028-1

Abed, K. M. (2014). Kinetic of Alkaloids Extraction from Plant by Batch Pertraction in Rotating Discs Contactor. *Iraqi Journal of Chemical and Petroleum Engineering*, *15*(2), 75–84.

Abed, K. M., & Al-Hemiri, A. A. (2015). Separation of Alkaloids From Plants by Bulk Liquid Membrane Technique Using Rotating Discs Contactor. *Second Engineering Scientific Conference*, *8*(4), 785–793.

Abed, K. M., Hayyan, A., Elgharbawy, A. A. M., Hizaddin, H. F., Hashim, M. A., Hasan, H. A., Hamid, M. D., Zuki, F. M., Saleh, J., & Aldaihani, A. G. H. (2022). Palm Raceme as a Promising Biomass Precursor for Activated Carbon to Promote Lipase Activity with the Aid of Eutectic Solvents. *Molecules*, *27*(24), 8734.

Abed, K. M., Hayyan, A., Hizaddin, H. F., Basirun, W. J., & Hashim, M. A. (2023). Lactic acid-based deep eutectic solvents and activated carbon for soap removal from crude biodiesel. *Biomass Conversion and Biorefinery*, 1–14. https://doi.org/https://doi.org/10.1007/s13399-023-04310-w

Abed, K. M., Hayyan, A., Hizaddin, H. F., Hashim, M. A., Ng, Y.-S., Alanazi, Y. M., Saleh, J., Basirun, W. J., Gupta, B. Sen, & Salleh, M. Z. M. (2024). Natural Eutectic Solvents and Graphene Integrated within Emulsion Liquid Membrane System for Sodium Removal from Crude Biodiesel. *Colloids and Surfaces A: Physicochemical and Engineering Aspects*, 134666.

Abed, K. M., Hayyan, A., Hizaddin, H. F., Hashim, M. A., Ng, Y.-S., & Basirun, W. J. (2023). Integration of deep eutectic solvent and activated carbon in emulsion liquid

membrane system for soap removal from crude biodiesel. *Colloids and Surfaces A: Physicochemical and Engineering Aspects*, 131786.

Abed, K. M., Hayyan, A., Hizaddin, H. F., Hashim, M. A., Ng, Y.-S., Basirun, W. J., Alias, Y., & Salleh, M. Z. M. (2024). Emulsion Liquid Membrane Pertraction of Soap from Crude Biodiesel Using Activated Carbon and Glycol Based Deep Eutectic Solvents. *Journal of Cleaner Production*, 143404.

Ahmad, A. L., Kusumastuti, A., Derek, C. J. C., & Ooi, B. S. (2011). Emulsion liquid membrane for heavy metal removal: An overview on emulsion stabilization and destabilization. *Chemical Engineering Journal*, *171*(3), 870–882.

Ahmad, A. L., Kusumastuti, A., Derek, C. J. C., & Ooi, B. S. (2012). Emulsion liquid membrane for cadmium removal: Studies on emulsion diameter and stability. *Desalination*, *287*, 30–34.

Ahmad, A. L., Mohd Harun, M. H. Z., Akmal Jasni, M. K., & Zaulkiflee, N. D. (2021). Removal of ibuprofen at low concentration using a newly formulated emulsion liquid membrane. *Membranes*, *11*(10), 740.

Ahmad, M., Zafar, M., Bokhari, A., Akhtar, M. S., Alshgari, R. A., Karami, A. M., & Asif, S. (2023). Membrane reactor for production of biodiesel from nonedible seed oil of Trachyspermum ammi using heterogenous green nanocatalyst of manganese oxide. *Chemosphere*, *322*, 138078.

Akoh, C. C., Chang, S.-W., Lee, G.-C., & Shaw, J.-F. (2007). Enzymatic approach to biodiesel production. *Journal of Agricultural and Food Chemistry*, *55*(22), 8995–9005.

Al-Ani, F. H., Alsalhy, Q. F., & Al-Dahhan, M. (2021). Enhancing emulsion liquid membrane system (ELM) stability and performance for the extraction of phenol from wastewater using various nanoparticles. *Desalination Water Treat*, *210*, 180–

191.

Al-Hemiri, A. A., Abed, K. M., & Al-Shahwany, A. W. (2012). Extraction of Pelletierine from Punica granatum L.by Liquid Membrane Technique and Modelling. *Iraqi Journal of Chemical and Petroleum Engineering*.

Al-Humairi, S. T., Lee, J. G. M., Salihu, M., & Harvey, A. P. (2022). Biodiesel production through acid catalyst in situ reactive extraction of chlorella vulgaris foamate. *Energies*, *15*(12), 4482.

Al-Obaidi, Q., Alabdulmuhsin, M., Tolstik, A., Trautman, J. G., & Al-Dahhan, M. (2021). Removal of hydrocarbons of 4-nitrophenol by emulsion liquid membrane (ELM) using magnetic Fe2O3 nanoparticles and ionic liquid. *Journal of Water Process Engineering*, *39*, 101729.

Al-Shahwany, A. W., Al-Hemiri, A. A., & Abed, K. M. (2013). Comparative evaluation of alkaloids extraction methods from the root bark of Punica granatum Linn. *Advances in Bio Research*, *4*(1), 33–39. http://www.soeagra.com/abr/abrmarch2013/5.pdf

Ali, E. N., & Tay, C. I. (2013). Characterization of biodiesel produced from palm oil via base catalyzed transesterification. *Procedia Engineering*, *53*, 7–12. https://doi.org/10.1016/j.proeng.2013.02.002

Alitabar-Ferozjah, H., & Rahbar-Kelishami, A. (2022). Simultaneous effect of multi-walled carbon nanotube and Span85 on the extraction of Ibuprofen from aqueous solution using emulsion liquid membrane. *Journal of Molecular Liquids*, *365*, 120051.

Alnaief, M., Sandouqa, A., Altarawneh, I., Al-Shannag, M., Alkasrawi, M., & Al-hamamre, Z. (2020). Adsorption characteristics and potential of olive cake alkali residues for biodiesel purification. *Energies*, *14*(1), 16.

Alves, M. J., Cavalcanti, Í. V., de Resende, M. M., Cardoso, V. L., & Reis, M. H. (2016). Biodiesel dry purification with sugarcane bagasse. *Industrial Crops and Products*, *89*, 119–127.

Alves, M. J., Nascimento, S. M., Pereira, I. G., Martins, M. I., Cardoso, V. L., & Reis, M. (2013). Biodiesel purification using micro and ultrafiltration membranes. *Renewable Energy*, *58*, 15–20.

Amelio, A., Loise, L., Azhandeh, R., Darvishmanesh, S., Calabró, V., Degrève, J., Luis, P., & Van der Bruggen, B. (2016). Purification of biodiesel using a membrane contactor: Liquid–liquid extraction. *Fuel Processing Technology*, *142*, 352–360. https://doi.org/https://doi.org/10.1016/j.fuproc.2015.10.037

AOCS. (2017). The titrimetric method determines the alkalinity of the test sample as sodium oleate. In *Official Methods and Recommended Practices of the AOCS* (7th ed.).

Ardehali, B. A., Zaheri, P., & Yousefi, T. (2020). The effect of operational conditions on the stability and efficiency of an emulsion liquid membrane system for removal of uranium. *Progress in Nuclear Energy*, *130*, 103532.

Arenas, E., Villafán-Cáceres, S. M., Rodríguez-Mejía, Y., García-Loyola, J. A., Masera, O., & Sandoval, G. (2021). Biodiesel dry purification using unconventional bioadsorbents. *Processes*, *9*(2), 194.

Arsalan, A., & Younus, H. (2018). Enzymes and nanoparticles: Modulation of enzymatic activity via nanoparticles. *International Journal of Biological Macromolecules*, *118*, 1833–1847.

Astm, D. (2012). Standard specification for biodiesel fuel blend stock (B100) for middle distillate fuels. In *ASTM International, West Conshohocken*.

Atadashi, I. M. (2015). Purification of crude biodiesel using dry washing and membrane technologies. *Alexandria Engineering Journal*, *54*(4), 1265–1272.

Atadashi, I. M., Aroua, M. K., & Aziz, A. A. (2011). Biodiesel separation and purification: a review. *Renewable Energy*, *36*(2), 437–443.

Atadashi, I. M., Aroua, M. K., Aziz, A. R. A., & Sulaiman, N. M. N. (2011a). Membrane biodiesel production and refining technology: A critical review. *Renewable and Sustainable Energy Reviews*, *15*(9), 5051–5062.

Atadashi, I. M., Aroua, M. K., Aziz, A. R. A., & Sulaiman, N. M. N. (2011b). Refining technologies for the purification of crude biodiesel. *Applied Energy*, *88*(12), 4239–4251.

Atadashi, I. M., Aroua, M. K., Aziz, A. R. A., & Sulaiman, N. M. N. (2012). The effects of water on biodiesel production and refining technologies: A review. *Renewable and Sustainable Energy Reviews*, *16*(5), 3456–3470.

Atadashi, I. M., Aroua, M. K., Aziz, A. R. A., & Sulaiman, N. M. N. (2015). Crude biodiesel refining using membrane ultra-filtration process: An environmentally benign process. *Egyptian Journal of Petroleum*, *24*(4), 383–396.

Atkinson, J. D., & Rood, M. J. (2012). Preparing microporous carbon from solid organic salt precursors using in situ templating and a fixed-bed reactor. *Microporous and Mesoporous Materials*, *160*, 174–181.

Avagyan, A. B., Singh, B., Avagyan, A. B., & Singh, B. (2019). Biodiesel from plant oil and waste cooking oil. *Biodiesel: Feedstocks, Technologies, Economics and Barriers: Assessment of Environmental Impact in Producing and Using Chains*, 15–75.

Ayoob, A. K., & Fadhil, A. B. (2020). Valorization of waste tires in the synthesis of an

effective carbon based catalyst for biodiesel production from a mixture of non-edible oils. *Fuel*, *264*, 116754.

Azarang, A., Rahbar-Kelishami, A., Norouzbeigi, R., & Shayesteh, H. (2019). Modeling and optimization of pertraction performance of heavy metal ion from aqueous solutions using M2EHPA/D2EHPA: application of response surface methodology. *Environmental Technology & Innovation*, *15*, 100432.

Azhad, M. F. R., & Fathallah, A. Z. M. (2023). Analysis of silica gel desiccant application in fuel storage tanks model to reduce palm oil-based biodiesel degradation. *IOP Conference Series: Earth and Environmental Science*, *1203*(1), 12008.

Bačić, M., Ljubić, A., Gojun, M., Šalić, A., Tušek, A. J., & Zelić, B. (2021). Continuous Integrated Process of Biodiesel Production and Purification—The End of the Conventional Two-Stage Batch Process? *Energies*, *14*(2), 403.

Bakar, D. A., & Anandarajah, G. (2015). Sustainability of bioenergy in Malaysia with reference to palm oil biomass: adopting principles governing bioenergy policy in the UK. In H. H. Al-Kayiem, C. A. Brebbia, & S. S. Zubir (Eds.), *WIT Trans Ecol Environ* (Vol. 206). https://doi.org/10.2495/ESS140051

Balat, M., & Balat, H. (2010). Progress in biodiesel processing. *Applied Energy*, *87*(6), 1815–1835.

Ballesteros, A., Plou, F. J., Iborra, J. L., & Halling, P. J. (1998). Engineering stability of enzymes in systems with organic solvents. *Stability and Stabilization of Biocatalysts: Proceedings of an International Symposium Organized Under Auspices of the Working Party on Applied Biocatalysis of the European Federation of Biotechnology, the University of Cordoba, Spain, and the Spanish Soc*, *15*, 355.

Barabás, I., & Todoruţ, I.-A. (2011). Biodiesel quality, standards and properties. In *Biodiesel: Quality, emissions and by-products* (Vol. 2). InTech Pleasanton, CA,

USA.

Baroutian, S., Aroua, M. K., Raman, A. A. A., & Sulaiman, N. M. N. (2011). A packed bed membrane reactor for production of biodiesel using activated carbon supported catalyst. *Bioresource Technology*, *102*(2), 1095–1102.

Baroutian, S., Shahbaz, K., Mjalli, S. F., Alnashef, M. I., & Hashim, A. M. (2012). Adsorptive removal of residual catalyst from palm biodiesel: application of response surface methodology. *Hemijska Industrija*, *66*(3), 373–380.

Bateni, H., & Karimi, K. (2016). Biodiesel production from castor plant integrating ethanol production via a biorefinery approach. *Chemical Engineering Research and Design*, *107*, 4–12.

Bateni, H., Saraeian, A., Able, C., & Karimi, K. (2019). Biodiesel purification and upgrading technologies. *Biodiesel: From Production to Combustion*, 57–100.

Baysal, M., Bilge, K., Yılmaz, B., Papila, M., & Yürüm, Y. (2018). Preparation of high surface area activated carbon from waste-biomass of sunflower piths: Kinetics and equilibrium studies on the dye removal. *Journal of Environmental Chemical Engineering*, *6*(2), 1702–1713. https://doi.org/10.1016/j.jece.2018.02.020

Bera, A., Ojha, K., & Mandal, A. (2013). Synergistic effect of mixed surfactant systems on foam behavior and surface tension. *Journal of Surfactants and Detergents*, *16*, 621–630.

Berrios, M., Martín, M. A., Chica, A. F., & Martín, A. (2011). Purification of biodiesel from used cooking oils. *Applied Energy*, *88*(11), 3625–3631.

Berrios, M., Siles, J. A., Martín, M. A., & Martín, A. (2013). Ion exchange. In *Separation and Purification Technologies in Biorefineries* (pp. 149–165). Wiley Online Library.

Berrios, M., & Skelton, R. L. (2008). Comparison of purification methods for biodiesel. *Chemical Engineering Journal*, *144*(3), 459–465.

Bertram, B., Abrams, C., & Cooke, B. S. (2009). *Purification of biodiesel with adsorbent materials*. Google Patents.

Boog, J. H. F., Silveira, E. L. C., De Caland, L. B., & Tubino, M. (2011). Determining the residual alcohol in biodiesel through its flash point. *Fuel*, *90*(2), 905–907.

Borges, M. E., & Díaz, L. (2012). Recent developments on heterogeneous catalysts for biodiesel production by oil esterification and transesterification reactions: A review. *Renewable and Sustainable Energy Reviews*, *16*(5), 2839–2849.

Budžaki, S., Šalić, A., & Zelić, B. (2015). Enzyme-catalysed biodiesel production from edible and waste cooking oils. *Chemical and Biochemical Engineering Quarterly*, *29*(3), 329–333.

Burton, R. (2008). An overview of ASTM D6751: biodiesel standards and testing methods. *Alternative Fuels Consortium*.

Caetano, N. S., Ribeiro, V., Ribeiro, L., Baptista, A., & Monteiro, J. (2019). Biodiesel production systems: operation, process control and troubleshooting. *Biodiesel: From Production to Combustion*, 27–56.

Camilo, G. L., Queiroz, A., Ribeiro, A. E., Gomes, M. C. S., & Brito, P. (2024). Review of biodiesel production using various feedstocks and its purification through several methodologies, with a specific emphasis on dry washing. *Journal of Industrial and Engineering Chemistry*.

Cao, P., Dubé, M. A., & Tremblay, A. Y. (2008a). High-purity fatty acid methyl ester production from canola, soybean, palm, and yellow grease lipids by means of a membrane reactor. *Biomass and Bioenergy*, *32*(11), 1028–1036.

Cao, P., Dubé, M. A., & Tremblay, A. Y. (2008b). Methanol recycling in the production of biodiesel in a membrane reactor. *Fuel*, *87*(6), 825–833.

Carmona, M., Lech, A., de Lucas, A., Perez, A., & Rodriguez, J. F. (2009). Purification of glycerol/water solutions from biodiesel synthesis by ion exchange: sodium and chloride removal. Part II. *Journal of Chemical Technology & Biotechnology: International Research in Process, Environmental & Clean Technology*, *84*(8), 1130–1135.

Carmona, M., Valverde, J. L., Pérez, A., Warchol, J., & Rodriguez, J. F. (2009). Purification of glycerol/water solutions from biodiesel synthesis by ion exchange: sodium removal Part I. *Journal of Chemical Technology & Biotechnology: International Research in Process, Environmental & Clean Technology*, *84*(5), 738–744.

Casas, A., Ruiz, J. R., Ramos, M. J., & Pérez, A. (2010). Effects of triacetin on biodiesel quality. *Energy & Fuels*, *24*(8), 4481–4489.

Catarino, M., Ferreira, E., Soares Dias, A. P., & Gomes, J. (2020). Dry washing biodiesel purification using fumed silica sorbent. *Chemical Engineering Journal*, *386*, 123930. https://doi.org/https://doi.org/10.1016/j.cej.2019.123930

Chakraborty, M., & Bart, H.-J. (2006). Emulsion liquid membranes: Role of internal droplet size distribution on toluene/n-heptane separation. *Colloids and Surfaces A: Physicochemical and Engineering Aspects*, *272*(1–2), 15–21.

Chakraborty, M., Ivanova-Mitseva, P., & Bart, H. (2006). Selective Separation of Toluene from n-Heptane via Emulsion Liquid Membranes Containing Substituted Cyclodextrins as Carrier. *Separation Science and Technology*, *41*(16), 3539–3552.

Chang, S. H. (2016). Types of bulk liquid membrane and its membrane resistance in heavy metal removal and recovery from wastewater. *Desalination and Water*

Treatment, *57*(42), 19785–19793. https://doi.org/10.1080/19443994.2015.1102772

Chaouchi, S., & Hamdaoui, O. (2014). Extraction of priority pollutant 4-nitrophenol from water by emulsion liquid membrane: emulsion stability, effect of operational conditions and membrane reuse. *Journal of Dispersion Science and Technology*, *35*(9), 1278–1288.

Chaouchi, S., & Hamdaoui, O. (2016). Removal of 4-nitrophenol from water by emulsion liquid membrane. *Desalination and Water Treatment*, *57*(12), 5253–5257.

Chatzifragkou, A., & Papanikolaou, S. (2012). Effect of impurities in biodiesel-derived waste glycerol on the performance and feasibility of biotechnological processes. *Applied Microbiology and Biotechnology*, *95*, 13–27.

Chaves, E. S., dos Santos, E. J., Araujo, R. G. O., Oliveira, J. V., Frescura, V. L. A., & Curtius, A. J. (2010). Metals and phosphorus determination in vegetable seeds used in the production of biodiesel by ICP OES and ICP-MS. *Microchemical Journal*, *96*(1), 71–76.

Chaves, E. S., Saint'Pierre, T. D., Dos Santos, E. J., Tormen, L., Bascuñan, V. L. A. F., & Curtius, A. J. (2008). Determination of Na and K in biodiesel by flame atomic emission spectrometry and microemulsion sample preparation. *Journal of the Brazilian Chemical Society*, *19*, 856–861.

Chen, B., Wang, W., Liu, X., Xue, W., Ma, X., Chen, G., Yu, Q., & Li, R. (2012). Adsorption study of glycerol in biodiesel on the sulfonated adsorbent. *Industrial & Engineering Chemistry Research*, *51*(39), 12933–12939.

Chen, B., Wang, W., Ma, X., Wang, C., & Li, R. (2012). Adsorption Behaviors of Glycerol from Biodiesel on Sulfonated Polystyrene–Divinylbenzene Resins in Different Forms. *Energy & Fuels*, *26*(11), 7060–7067.

Chen, Z., Ludwig, M., Warr, G. G., & Atkin, R. (2017). Effect of cation alkyl chain length on surface forces and physical properties in deep eutectic solvents. *Journal of Colloid and Interface Science*, *494*, 373–379.

Cheraghian, G., & Hendraningrat, L. (2016). A review on applications of nanotechnology in the enhanced oil recovery part A: effects of nanoparticles on interfacial tension. *International Nano Letters*, *6*, 129–138.

Cheung, O., Bacsik, Z., Liu, Q., Mace, A., & Hedin, N. (2013). Adsorption kinetics for CO2 on highly selective zeolites NaKA and nano-NaKA. *Applied Energy*, *112*, 1326–1336. https://doi.org/https://doi.org/10.1016/j.apenergy.2013.01.017

Colinart, P., Delepine, S., Trouve, G., & Renon, H. (1984). Water transfer in emulsified liquid membrane processes. *Journal of Membrane Science*, *20*(2), 167–187.

Collings, P. J., & Hird, M. (2017). *Introduction to liquid crystals chemistry and physics*. Crc Press.

Cooper, E. R., Andrews, C. D., Wheatley, P. S., Webb, P. B., Wormald, P., & Morris, R. E. (2004). Ionic liquids and eutectic mixtures as solvent and template in synthesis of zeolite analogues. *Nature*, *430*(7003), 1012–1016.

Cotroneo-Figueroa, V. P., Gajardo-Parra, N. F., López-Porfiri, P., Leiva, Á., Gonzalez-Miquel, M., Garrido, J. M., & Canales, R. I. (2022). Hydrogen bond donor and alcohol chain length effect on the physicochemical properties of choline chloride based deep eutectic solvents mixed with alcohols. *Journal of Molecular Liquids*, *345*, 116986.

Cunico, L. P., Sun, M., Rui, Y., Ghirmai, S., Enekvist, M., Lundegard, S., Sandahl, M., & Turner, C. (2020). Enhanced distribution kinetics in liquid-liquid extraction by CO2-expanded solvents. *The Journal of Supercritical Fluids*, *163*, 104874. https://doi.org/10.1016/J.SUPFLU.2020.104874

Dâas, A., & Hamdaoui, O. (2010). Extraction of anionic dye from aqueous solutions by emulsion liquid membrane. *Journal of Hazardous Materials*, *178*(1–3), 973–981.

Dai, Y., Rozema, E., Verpoorte, R., & Choi, Y. H. (2016). Application of natural deep eutectic solvents to the extraction of anthocyanins from Catharanthus roseus with high extractability and stability replacing conventional organic solvents. *Journal of Chromatography A*, *1434*, 50–56.

Danish, M., & Ahmad, T. (2018). A review on utilization of wood biomass as a sustainable precursor for activated carbon production and application. *Renewable and Sustainable Energy Reviews*, *87*, 1–21.

Das, D., Juvekar, V. A., Roy, S. B., & Bhattacharya, R. (2014). Comparative studies on co-extraction of uranium (VI) and different mineral acid from aqueous feed solutions using TBP, TOPO and TOA. *Journal of Radioanalytical and Nuclear Chemistry*, *300*(1), 333–343.

Davoodi-Nasab, P., Rahbar-Kelishami, A., Safdari, J., & Abolghasemi, H. (2018). Selective separation and enrichment of neodymium and gadolinium by emulsion liquid membrane using a novel extractant CYANEX® 572. *Minerals Engineering*, *117*, 63–73.

de Amorim, F. R., Bof, C., Franco, M. B., da Silva, J. B. B., & Nascentes, C. C. (2006). Comparative study of conventional and multivariate methods for aluminum determination in soft drinks by graphite furnace atomic absorption spectrometry. *Microchemical Journal*, *82*(2), 168–173.

de Castro Vasques, É., Granhen Tavares, C. R., Itsuo Yamamoto, C., Rogério Mafra, M., & Igarashi-Mafra, L. (2013). Adsorption of glycerol, monoglycerides and diglycerides present in biodiesel produced from soybean oil. *Environmental Technology*, *34*(16), 2361–2369.

de Jesus, A., Silva, M. M., & Vale, M. G. R. (2008). The use of microemulsion for determination of sodium and potassium in biodiesel by flame atomic absorption spectrometry. *Talanta*, *74*(5), 1378–1384.

de Jesus, A., Zmozinski, A. V, Barbara, J. A., Vale, M. G. R., & Silva, M. M. (2010). Determination of calcium and magnesium in biodiesel by flame atomic absorption spectrometry using microemulsions as sample preparation. *Energy & Fuels*, *24*(3), 2109–2112.

de Oliveira, M. A. L., Balesteros, M. R., Faria, A. F., & Vaz, F. A. S. (2010). Determination of olive oil acidity. In *Olives and Olive Oil in Health and Disease Prevention* (pp. 545–552). Elsevier.

De Paola, M. G., Mazza, I., Paletta, R., Lopresto, C. G., & Calabrò, V. (2021). Small-scale biodiesel production plants—An overview. *Energies*, *14*(7), 1901.

Delgado-Mellado, N., Larriba, M., Navarro, P., Rigual, V., Ayuso, M., García, J., & Rodríguez, F. (2018). Thermal stability of choline chloride deep eutectic solvents by TGA/FTIR-ATR analysis. *Journal of Molecular Liquids*, *260*, 37–43.

Demirbas, A. (2005). Biodiesel production from vegetable oils via catalytic and non-catalytic supercritical methanol transesterification methods. *Progress in Energy and Combustion Science*, *31*(5–6), 466–487.

Demirbas, A. (2008). Biofuels. In A. Demirbas (Ed.), *Biodiesel : a realistic fuel alternative for diesel engines*. Springer London2008.

Demirbas, A. (2009). Progress and recent trends in biodiesel fuels. *Energy Conversion and Management*, *50*(1), 14–34.

Demirbaş, A. (2002). Biodiesel from vegetable oils via transesterification in supercritical methanol. *Energy Conversion and Management*, *43*(17), 2349–2356.

Deng, D., Jiang, Y., Liu, X., Zhang, Z., & Ai, N. (2016). Investigation of solubilities of carbon dioxide in five levulinic acid-based deep eutectic solvents and their thermodynamic properties. *The Journal of Chemical Thermodynamics*, *103*, 212–217.

Dias, J. M., Alvim-Ferraz, M. C. M., & Almeida, M. F. (2008). Comparison of the performance of different homogeneous alkali catalysts during transesterification of waste and virgin oils and evaluation of biodiesel quality. *Fuel*, *87*(17–18), 3572–3578.

Dias, J. M., Alvim-Ferraz, M. C. M., Almeida, M. F., Rivera-Utrilla, J., & Sánchez-Polo, M. (2007). Waste materials for activated carbon preparation and its use in aqueous-phase treatment: A review. In *Journal of Environmental Management* (Vol. 85, Issue 4, pp. 833–846). Academic Press. https://doi.org/10.1016/j.jenvman.2007.07.031

Dias, J. M., Santos, E., Santo, F., Carvalho, F., Alvim-Ferraz, M. C. M., & Almeida, M. F. (2014). Study of an ethylic biodiesel integrated process: Raw-materials, reaction optimization and purification methods. *Fuel Processing Technology*, *124*, 198–205.

Díaz-Ballote, L., Maldonado, L., Genesca, J., Hoil-Canul, E. R., & Vega-Lizama, T. (2020). Electrochemical impedance: A new alternative to assess the soap removal from biodiesel in the washing process. *Fuel*, *265*, 116880.

Diedenhofen, M., & Klamt, A. (2010). COSMO-RS as a tool for property prediction of IL mixtures—A review. *Fluid Phase Equilibria*, *294*(1–2), 31–38.

Docherty, K. M., & Kulpa Jr, C. F. (2005). Toxicity and antimicrobial activity of imidazolium and pyridinium ionic liquids. *Green Chemistry*, *7*(4), 185–189.

Doherty, M. F., Fidkowski, Z. T., Malone, M. F., & Taylor, R. (2008). Chapter 13. Distillation. *Perry's Chemical Engineers' Handbook, Edited by RH Perry and DW Green. New York: McGraw-Hill*.

Dubé, M. A., Tremblay, A. Y., & Liu, J. (2007). Biodiesel production using a membrane reactor. *Bioresource Technology*, *98*(3), 639–647.

Dunn, R. O. (2011). Improving the cold flow properties of biodiesel by fractionation. In T.-B. Ng (Ed.), *Soybean: Applications and Technology* (pp. 211–240). Intech. Croatia.

Durand, E., Lecomte, J., & Villeneuve, P. (2013). Deep eutectic solvents: Synthesis, application, and focus on lipase-catalyzed reactions. *European Journal of Lipid Science and Technology*, *115*(4), 379–385.

e Melo, V. M., Ferreira, G. F., & Fregolente, L. V. (2024). Sustainable catalysts for biodiesel production: The potential of CaO supported on sugarcane bagasse biochar. *Renewable and Sustainable Energy Reviews*, *189*, 114042.

El Ttaib, K. (2011). *The electrodeposition of composite materials using deep eutectic solvents*. University of Leicester.

Elgharbawy, A. A. M., Hayyan, M., Hayyan, A., Basirun, W. J., Salleh, H. M., & Mirghani, M. E. S. (2020). A grand avenue to integrate deep eutectic solvents into biomass processing. *Biomass and Bioenergy*, *137*, 105550.

Elgharbawy, A. A. M., Putra, S. S. S., Hayyan, M., Hayyan, A., Basirun, W. J., Mirghani, M. E. S., Majrashi, A. A., Nawawi, W. M. F. W., Alias, Y., & Salleh, H. M. (2020). Polyamidoamine dendrimers: Favorable polymeric nanomaterials for lipase activation. *Materials Today Communications*, *25*, 101492.

Elgharbawy, A., Hayyan, A., Hayyan, M., Rashid, S. N., Nor, M. R. M., Zulkifli, M. Y., Alias, Y., & Mirghani, M. E. S. (2018). Shedding light on lipase stability in natural deep eutectic solvents. *Chemical and Biochemical Engineering Quarterly*, *32*(3), 359–370. https://doi.org/https://doi.org/10.15255/CABEQ.2018.1335

Elias, N., Wahab, R. A., Chandren, S., Razak, F. I. A., & Jamalis, J. (2019). Effect of operative variables and kinetic study of butyl butyrate synthesis by Candida rugosa lipase activated by chitosan-reinforced nanocellulose derived from raw oil palm leaves. *Enzyme and Microbial Technology*, *130*, 109367.

EN. (2003). *The EN 14214 standard-specifications and test methods*.

EN 14214. (2003). *Fatty acid methyl esters (FAME) for diesel engines - Requirements and test methods*. European Committee for Standardization.

Erich, K. (1982). Separating processes. In *Handbook of Laboratory Distillation with an Introduction to Pilot Plant Distillation. Elsevier, New York, United State*.

Faccini, C. S., Cunha, M. E. da, Moraes, M. S. A., Krause, L. C., Manique, M. C., Rodrigues, M. R. A., Benvenutti, E. V, & Caramão, E. B. (2011). Dry washing in biodiesel purification: a comparative study of adsorbents. *Journal of the Brazilian Chemical Society*, *22*, 558–563.

Fadhil, A. B., & Abdulahad, W. S. (2014). Transesterification of mustard (Brassica nigra) seed oil with ethanol: Purification of the crude ethyl ester with activated carbon produced from de-oiled cake. *Energy Conversion and Management*, *77*, 495–503.

Fadhil, A. B., Aziz, A. M., & Altamer, M. H. (2016). Potassium acetate supported on activated carbon for transesterification of new non-edible oil, bitter almond oil. *Fuel*, *170*, 130–140.

Fadhil, A. B., & Dheyab, M. M. (2015). Purification of biodiesel fuels produced from spent frying oils over activated carbons. *Energy Sources, Part A: Recovery, Utilization, and Environmental Effects*, *37*(2), 149–155.

Fadhil, A. B., Dheyab, M. M., & Abdul-Qader, A.-Q. Y. (2012). Purification of biodiesel using activated carbons produced from spent tea waste. *Journal of the Association*

of Arab Universities for Basic and Applied Sciences, *11*(1), 45–49.

Fadhil, A. B., & Saeed, L. I. (2016). Sulfonated tea waste: A low-cost adsorbent for purification of biodiesel. *International Journal of Green Energy*, *13*(1), 110–118.

Falahati, H., & Tremblay, A. Y. (2012). The effect of flux and residence time in the production of biodiesel from various feedstocks using a membrane reactor. *Fuel*, *91*(1), 126–133.

Ferella, F., Di Celso, G. M., De Michelis, I., Stanisci, V., & Vegliò, F. (2010). Optimization of the transesterification reaction in biodiesel production. *Fuel*, *89*(1), 36–42.

Ficheux, M.-F., Bonakdar, L., Leal-Calderon, F., & Bibette, J. (1998). Some stability criteria for double emulsions. *Langmuir*, *14*(10), 2702–2706.

Florindo, C., Oliveira, F. S., Rebelo, L. P. N., Fernandes, A. M., & Marrucho, I. M. (2014). Insights into the synthesis and properties of deep eutectic solvents based on cholinium chloride and carboxylic acids. *ACS Sustainable Chemistry & Engineering*, *2*(10), 2416–2425.

Fogarty, A. C., & Laage, D. (2014). Water dynamics in protein hydration shells: the molecular origins of the dynamical perturbation. *The Journal of Physical Chemistry B*, *118*(28), 7715–7729.

Foon, C. S., May, C. Y., Ngan, M. A., & Hock, C. C. (2004). Kinetics Study on Transesterification of Palm Oil. *Journal of Oil Palm Research*, *16*(4), 19–29.

Franjo, M., Šalić, A., & Zelić, B. (2018). Microstructured devices for biodiesel production by transesterification. *Biomass Conversion and Biorefinery*, *8*(4), 1005–1020.

Freedman, B., Pryde, E. H., & Mounts, T. L. (1984). Variables affecting the yields of

fatty esters from transesterified vegetable oils. *Journal of the American Oil Chemists Society*, *61*(10), 1638–1643.

Garg, S., Behera, S., Ruiz, H. A., & Kumar, S. (2023). A review on opportunities and limitations of membrane bioreactor configuration in biofuel production. *Applied Biochemistry and Biotechnology*, *195*(9), 5497–5540.

Ghatee, M. H., Zare, M., Moosavi, F., & Zolghadr, A. R. (2010). Temperature-dependent density and viscosity of the ionic liquids 1-alkyl-3-methylimidazolium iodides: experiment and molecular dynamics simulation. *Journal of Chemical & Engineering Data*, *55*(9), 3084–3088.

Gomes, M. C. S., Arroyo, P. A., & Pereira, N. C. (2011). Biodiesel production from degummed soybean oil and glycerol removal using ceramic membrane. *Journal of Membrane Science*, *378*(1–2), 453–461.

Gomes, M. G., Santos, D. Q., de Morais, L. C., & Pasquini, D. (2015). Purification of biodiesel by dry washing, employing starch and cellulose as natural adsorbents. *Fuel*, *155*, 1–6.

Govindaraju, R., Chen, S.-S., Wang, L.-P., Chang, H.-M., & Pasawan, M. (2021). Significance of membrane applications for high-quality biodiesel and byproduct (glycerol) in biofuel industries. *Current Pollution Reports*, *7*, 128–145.

Goyal, R. K., Jayakumar, N. S., & Hashim, M. A. (2011). Chromium removal by emulsion liquid membrane using [BMIM]+[NTf2]− as stabilizer and TOMAC as extractant. *Desalination*, *278*(1–3), 50–56.

Gross, E. M., Williams, S. H., Williams, E., Dobberpuhl, D. A., & Fujita, J. (2016). Synthesis and characterization of biodiesel from used cooking oil: a problem-based green chemistry laboratory experiment. In *Green Chemistry Experiments in Undergraduate Laboratories* (pp. 71–92). ACS Publications.

Gunstone, F. (2009). *The chemistry of oils and fats: sources, composition, properties and uses*. John Wiley & Sons.

Hadj-Kali, M. K., Mulyono, S., Hizaddin, H. F., Wazeer, I., El-Blidi, L., Ali, E., Hashim, M. A., & AlNashef, I. M. (2016). Removal of thiophene from mixtures with n-heptane by selective extraction using deep eutectic solvents. *Industrial & Engineering Chemistry Research*, *55*(30), 8415–8423.

Hafeez, S., Al-Salem, S. M., Manos, G., & Constantinou, A. (2020). Fuel production using membrane reactors: a review. *Environmental Chemistry Letters*, *18*(5), 1477–1490.

Hall, G. A. (1949). The kinetics of the decomposition of malonic acid in aqueous solution. *Journal of the American Chemical Society*, *71*(8), 2691–2693.

Harper, J. B., & Kobrak, M. N. (2006). Understanding organic processes in ionic liquids: Achievements so far and challenges remaining. *Mini-Reviews in Organic Chemistry*, *3*(3), 253–269. https://doi.org/10.2174/157019306777935037

Hasabnis, A., & Mahajani, S. (2010). Entrainer-based reactive distillation for esterification of glycerol with acetic acid. *Industrial & Engineering Chemistry Research*, *49*(19), 9058–9067.

Haseeb, A., Masjuki, H. H., Ann, L. J., & Fazal, M. A. (2010). Corrosion characteristics of copper and leaded bronze in palm biodiesel. *Fuel Processing Technology*, *91*(3), 329–334.

Hayyan, A., Abed, K. M., Hizaddin, H. F., Yusoff, W. M. F. W., Ng, Y.-S., Junaidi, M. U. M., Saleh, J., Aljohani, A. S. M., Alhumaydhi, F. A., Abdulmonem, W. Al, Alkandari, K. H., Alajmi, F. D. H., Aldeehani, A. K., Basirun, W. J., Abidin, M. I. I. Z., & Al Abdulmonem, W. (2022). Application of natural deep eutectic solvents in bulk liquid membrane system for removal of free glycerol from crude fatty acid

methyl ester. *Colloids and Surfaces A: Physicochemical and Engineering Aspects*, *650*, 129449. https://doi.org/https://doi.org/10.1016/j.colsurfa.2022.129449

Hayyan, A., Abed, K. M., Hizaddin, H. F., Yusoff, W. M. F. W., Ng, Y.-S., Junaidi, M. U. M., Saleh, J., Aljohani, A. S. M., Alhumaydhi, F. A., & Al Abdulmonem, W. (2022). Application of natural deep eutectic solvents in bulk liquid membrane system for removal of free glycerol from crude fatty acid methyl ester. *Colloids and Surfaces A: Physicochemical and Engineering Aspects*, *650*, 129449.

Hayyan, A., Alam, M. Z., Mirghani, M. E. S., Kabbashi, N. A., Hakimi, N. I. N. M., Siran, Y. M., & Tahiruddin, S. (2010). Sludge palm oil as a renewable raw material for biodiesel production by two-step processes. *Bioresource Technology*, *101*(20), 7804–7811.

Hayyan, A., Hizaddin, H. F., Abed, K. M., Mjalli, F. S., Hashim, M. A., Abo-Hamad, A., Saleh, J., Aljohani, A. S. M., Alharbi, Y. M., Alhumaydhi, F. A., Ahmad, A. A., Yeow, A. T. H., Aldeehani, A. K., Alajmi, F. D. H., & Al Nashef, I. (2021). Encapsulated deep eutectic solvent for esterification of free fatty acid. *Biomass Conversion and Biorefinery 2021*, 1–11. https://doi.org/10.1007/S13399-021-01913-Z

Hayyan, A., Mjalli, F. S., Alnashef, I. M., Al-Wahaibi, T., Al-Wahaibi, Y. M., & Hashim, M. A. (2012). Fruit sugar-based deep eutectic solvents and their physical properties. *Thermochimica Acta*. https://doi.org/10.1016/j.tca.2012.04.030

Hayyan, A., Mjalli, F. S., Alnashef, I. M., Al-Wahaibi, Y. M., Al-Wahaibi, T., & Hashim, M. A. (2013). Glucose-based deep eutectic solvents: Physical properties. *Journal of Molecular Liquids*, *178*, 137–141. https://doi.org/10.1016/j.molliq.2012.11.025

Hayyan, A., Ng, Y.-S., Hadj-Kali, M. K., Junaidi, M. U. M., Ali, E., Aldeehani, A. K., Alkandari, K. H., Alajmi, F. D. H., Yeow, A. T. H., & Zulkifli, M. Y. (2022). Natural

and low-cost deep eutectic solvent for soap removal from crude biodiesel using low stirring extraction system. *Biomass Conversion and Biorefinery*, 1–9.

Hayyan, A., Rashid, S. N., Hayyan, M., Zulkifliy, M. Y., Hashim, M. A., & Osman, N. A. (2017). Synthesis of Novel Eutectic Catalyst for the Esterification of Crude Palm Oil Mixed with Sludge Palm Oil. *Journal of Oil Palm Research*, *29*(3), 373–379.

Hayyan, A., Yeow, A. T. H., Abed, K. M., Basirun, W. J., Kiat, L. B., Saleh, J., Han, G. W., Min, P. C., Aljohani, A. S. M., & Zulkifli, M. Y. (2021). The development of new homogenous and heterogeneous catalytic processes for the treatment of low grade palm oil. *Journal of Molecular Liquids*, *344*, 117574.

Hayyan, A., Yeow, A. T. H., Alkahli, N. A. M., Saleh, J., Aldeehani, A. K., Alkandari, K. H., Alajmi, F. D. H., Alias, Y., Junaidi, M. U. M., & Hashim, M. A. (2022). Application of acidic ionic liquids for the treatment of acidic low grade palm oil for biodiesel production. *Journal of Ionic Liquids*, *2*(1), 100023.

Hayyan, M., Aissaoui, T., Hashim, M. A., AlSaadi, M. A., & Hayyan, A. (2015). Triethylene glycol based deep eutectic solvents and their physical properties. *Journal of the Taiwan Institute of Chemical Engineers*, *50*, 24–30.

Hayyan, M., Hashim, M. A., Al-Saadi, M. A., Hayyan, A., AlNashef, I. M., & Mirghani, M. E. S. (2013). Assessment of cytotoxicity and toxicity for phosphonium-based deep eutectic solvents. *Chemosphere*, *93*(2), 455–459.

Hayyan, M., Hashim, M. A., Hayyan, A., Al-Saadi, M. A., AlNashef, I. M., Mirghani, M. E. S., & Saheed, O. K. (2013). Are deep eutectic solvents benign or toxic? *Chemosphere*, *90*(7), 2193–2195. https://doi.org/https://doi.org/10.1016/j.chemosphere.2012.11.004

Hayyan, M., Mjalli, F. S., Hashim, M. A., & AlNashef, I. M. (2010). A novel technique for separating glycerine from palm oil-based biodiesel using ionic liquids. *Fuel*

Processing Technology, *91*(1), 116–120. https://doi.org/https://doi.org/10.1016/j.fuproc.2009.09.002

Hazrat, M. A., Rasul, M. G., Khan, M. M. K., Ashwath, N., Fattah, I. M. R., Ong, H. C., & Mahlia, T. M. I. (2023). Biodiesel production from transesterification of Australian Brassica napus L. oil: Optimisation and reaction kinetic model development. *Environment, Development and Sustainability*, *25*(11), 12247–12272.

He, B. B., Singh, A. P., & Thompson, J. C. (2005). Experimental optimization of a continuous-flow reactive distillation reactor for biodiesel production. *Transactions of the ASAE*, *48*(6), 2237–2243.

He, B. B., Singh, A. P., & Thompson, J. C. (2007). Function and performance of a pre-reactor to a reactive distillation column for biodiesel production. *Transactions of the ASABE*, *50*(1), 123–128.

He, B., Shao, Y., Ren, Y., Li, J., & Cheng, Y. (2015). Continuous biodiesel production from acidic oil using a combination of cation-and anion-exchange resins. *Fuel Processing Technology*, *130*, 1–6.

He, H. Y., Guo, X., & Zhu, S. L. (2006). Comparison of membrane extraction with traditional extraction methods for biodiesel production. *Journal of the American Oil Chemists' Society*, *83*(5), 457–460.

Heidarinejad, Z., Dehghani, M. H., Heidari, M., Javedan, G., Ali, I., & Sillanpää, M. (2020). Methods for preparation and activation of activated carbon: a review. *Environmental Chemistry Letters*, *18*(2), 393–415.

Hejazifar, M., Lanaridi, O., & Bica-Schröder, K. (2020). Ionic liquid based microemulsions: A review. *Journal of Molecular Liquids*, *303*, 112264.

Ho, K. C., Shahbaz, K., Rashmi, W., Mjalli, F. S., Hashim, M. A., & Alnashef, I. M.

(2015). Removal of glycerol from palm oil-based biodiesel using new ionic liquids analogues. *Journal of Engineering Science and Technology*, *10*(1), 98–111.

Homan, T., Shahbaz, K., & Farid, M. M. (2017). Improving the production of propyl and butyl ester-based biodiesel by purification using deep eutectic solvents. *Separation and Purification Technology*, *174*, 570–576.

Hou, Y., Li, Z., Ren, S., & Wu, W. (2015). Separation of toluene from toluene/alkane mixtures with phosphonium salt based deep eutectic solvents. *Fuel Processing Technology*, *135*, 99–104.

Hu, Y., Wang, Z., Huang, X., & Chen, L. (2004). Physical and electrochemical properties of new binary room-temperature molten salt electrolyte based on LiBETI and acetamide. *Solid State Ionics*, *175*(1–4), 277–280.

Hu, Z., & Srinivasan, M. P. (1999). Preparation of high-surface-area activated carbons from coconut shell. *Microporous and Mesoporous Materials*, *27*(1), 11–18.

Huang, H., & Ramaswamy, S. (2013). Overview of biomass conversion processes and separation and purification technologies in biorefineries. In *Separation and purification technologies in biorefineries* (pp. 1–36). Wiley Online Library.

Huang, Z.-L., Wu, B.-P., Wen, Q., Yang, T.-X., & Yang, Z. (2014). Deep eutectic solvents can be viable enzyme activators and stabilizers. *Journal of Chemical Technology & Biotechnology*, *89*(12), 1975–1981. https://doi.org/https://doi.org/10.1002/jctb.4285

Hunsom, M., & Autthanit, C. (2013). Adsorptive purification of crude glycerol by sewage sludge-derived activated carbon prepared by chemical activation with H3PO4, K2CO3 and KOH. *Chemical Engineering Journal*, *229*, 334–343.

Imdad, S., & Dohare, R. K. (2022). A critical review on heavy metals removal using ionic

liquid membranes from the industrial wastewater. *Chemical Engineering and Processing-Process Intensification*, *173*, 108812.

Imperato, G., Eibler, E., Niedermaier, J., & König, B. (2005). Low-melting sugar–urea–salt mixtures as solvents for Diels–Alder reactions. *Chemical Communications*, *9*, 1170–1172.

Islam, M. A., Ahmed, M. J., Khanday, W. A., Asif, M., & Hameed, B. H. (2017). Mesoporous activated carbon prepared from NaOH activation of rattan (Lacosperma secundiflorum) hydrochar for methylene blue removal. *Ecotoxicology and Environmental Safety*, *138*, 279–285.

Jaber, R., Shirazi, M. M. A., Toufaily, J., Hamieh, A. T., Noureddin, A., Ghanavati, H., Ghaffari, A., Zenouzi, A., Karout, A., & Ismail, A. F. (2015). Biodiesel wash-water reuse using microfiltration: toward zero-discharge strategy for cleaner and economized biodiesel production. *Biofuel Research Journal*, *2*(1), 148–151.

Jablonský, M., & Jančíková, V. (2023). Comparison of the acidity of systems based on choline chloride and lactic acid. *Journal of Molecular Liquids*, *380*, 121731.

Jahirul, M. I., Brown, R. J., Senadeera, W., O'Hara, I. M., & Ristovski, Z. D. (2013). The use of artificial neural networks for identifying sustainable biodiesel feedstocks. *Energies*, *6*(8), 3764–3806.

Jan C. J. Bart, N. P. and S. C. (2010). *Biodiesel science and technology*. Woodhead publishing limited.

Jiao, H., Peng, W., Zhao, J., & Xu, C. (2013). Extraction performance of bisphenol A from aqueous solutions by emulsion liquid membrane using response surface methodology. *Desalination*, *313*, 36–43.

Juneidi, I., Hayyan, M., & Hashim, M. A. (2015). Evaluation of toxicity and

biodegradability for cholinium-based deep eutectic solvents. *RSC Advances*, *5*(102), 83636–83647.

Jusoh, N., Rosly, M. B., Othman, N., Rahman, H. A., Noah, N. F. M., & Sulaiman, R. N. R. (2020). Selective extraction and recovery of polyphenols from palm oil mill sterilization condensate using emulsion liquid membrane process. *Environmental Science and Pollution Research*, *27*(18), 23246–23257.

Kahar, I. N. S., Othman, N., Noah, N. F. M., Sofi, M. H. M., & Suliman, S. S. (2023). Emulsion liquid membrane as a greener approach for precious metals recovery from industrial wastewater–A short review. *Journal of Industrial and Engineering Chemistry*.

Kankekar, P. S., Wagh, S. J., & Mahajani, V. V. (2010). Process intensification in extraction by liquid emulsion membrane (LEM) process: A case study; enrichment of ruthenium from lean aqueous solution. *Chemical Engineering and Processing: Process Intensification*, *49*(4), 441–448.

Karaosmanoğlu, F., Cığızoğlu, K. B., Tüter, M., & Ertekin, S. (1996). Investigation of the refining step of biodiesel production. *Energy & Fuels*, *10*(4), 890–895.

Kargari, A. (2013). Simultaneous extraction and stripping of 4-chlorophenol from aqueous solutions by emulsion liquid membrane. *Desalination and Water Treatment*, *51*(10–12), 2275–2279.

Khadivi, M., & Javanbakht, V. (2020). Emulsion ionic liquid membrane using edible paraffin oil for lead removal from aqueous solutions. *Journal of Molecular Liquids*, *319*, 114137.

Khan, H. W., Reddy, A. V. B., Bustam, M. A., Goto, M., & Moniruzzaman, M. (2021). Development and optimization of ionic liquid-based emulsion liquid membrane process for efficient recovery of lactic acid from aqueous streams. *Biochemical*

Engineering Journal, *176*, 108216.

Khan, H. W., Reddy, A. V. B., Nasef, M. M. E., Bustam, M. A., Goto, M., & Moniruzzaman, M. (2020). Screening of ionic liquids for the extraction of biologically active compounds using emulsion liquid membrane: COSMO-RS prediction and experiments. *Journal of Molecular Liquids*, *309*, 113122.

Khanian-Najaf-Abadi, M., Ghobadian, B., Dehghani-Soufi, M., & Heydari, A. (2022). Determination of biodiesel yield and color after purification process using deep eutectic solvent (choline chloride: ethylene glycol). *Biomass Conversion and Biorefinery*, 1–13.

Khursheed, U., Mushtaq, A., & Qayyum, A. (n.d.). *Catalyst free supercritical fluid technology for sustainable biodiesel production: A review*.

Kiss, A. A. (2010). Separative reactors for integrated production of bioethanol and biodiesel. *Computers & Chemical Engineering*, *34*(5), 812–820.

Kiss, A. A., Dimian, A. C., & Rothenberg, G. (2008). Biodiesel by catalytic reactive distillation powered by metal oxides. *Energy & Fuels*, *22*(1), 598–604.

Kiss, A. A., Omota, F., Dimian, A. C., & Rothenberg, G. (2006). The heterogeneous advantage: biodiesel by catalytic reactive distillation. *Topics in Catalysis*, *40*, 141–150.

Klamt, A. (2005). *COSMO-RS: from quantum chemistry to fluid phase thermodynamics and drug design*. Elsevier.

Klossek, M. L., Touraud, D., & Kunz, W. (2013). Eco-solvents–cluster-formation, surfactantless microemulsions and facilitated hydrotropy. *Physical Chemistry Chemical Physics*, *15*(26), 10971–10977.

Kockmann, N. (2014). History of distillation. In *Distillation* (pp. 1–43). Elsevier.

Kogelnig, D., Stojanovic, A., Jirsa, F., Körner, W., Krachler, R., & Keppler, B. K. (2010). Transport and separation of iron (III) from nickel (II) with the ionic liquid trihexyl (tetradecyl) phosphonium chloride. *Separation and Purification Technology*, *72*(1), 56–60.

Kohli, H. P., Gupta, S., & Chakraborty, M. (2019). Stability and performance study of emulsion nanofluid membrane: A combined approach of adsorption and extraction of Ethylparaben. *Colloids and Surfaces A: Physicochemical and Engineering Aspects*, *579*, 123675.

Kolah, A. K., Lira, C. T., & Miller, D. J. (2013). Reactive distillation for the biorefinery. In *Separation and purification technologies in biorefineries* (pp. 439–465). Wiley Online Library.

Kucek, K. T., César-Oliveira, M. A. F., Wilhelm, H. M., & Ramos, L. P. (2007). Ethanolysis of refined soybean oil assisted by sodium and potassium hydroxides. *Journal of the American Oil Chemists' Society*, *84*(4), 385–392.

Kulkarni, P. S., & Mahajani, V. V. (2002). Application of liquid emulsion membrane (LEM) process for enrichment of molybdenum from aqueous solutions. *Journal of Membrane Science*, *201*(1–2), 123–135.

Kulkarni, P. S., Mukhopadhyay, S., Bellary, M. P., & Ghosh, S. K. (2002). Studies on membrane stability and recovery of uranium (VI) from aqueous solutions using a liquid emulsion membrane process. *Hydrometallurgy*, *64*(1), 49–58.

Kumar, A., Thakur, A., & Panesar, P. S. (2018). Lactic acid extraction using environmentally benign green emulsion ionic liquid membrane. *Journal of Cleaner Production*, *181*, 574–583.

Kumar, A., Thakur, A., & Panesar, P. S. (2019a). A review on emulsion liquid membrane (ELM) for the treatment of various industrial effluent streams. *Reviews in*

Environmental Science and Bio/Technology, *18*, 153–182.

Kumar, A., Thakur, A., & Panesar, P. S. (2019b). Recent developments on sustainable solvents for emulsion liquid membrane processes. *Journal of Cleaner Production*, *240*, 118250.

Kumbasar, R. A. (2008). Selective separation of chromium (VI) from acidic solutions containing various metal ions through emulsion liquid membrane using trioctylamine as extractant. *Separation and Purification Technology*, *64*(1), 56–62.

Kumbasar, R. A. (2010). Selective extraction of chromium (VI) from multicomponent acidic solutions by emulsion liquid membranes using tributhylphosphate as carrier. *Journal of Hazardous Materials*, *178*(1–3), 875–882.

Kusdiana, D., & Saka, S. (2004). Effects of water on biodiesel fuel production by supercritical methanol treatment. *Bioresource Technology*, *91*(3), 289–295.

Kusumocahyo, S. P., Az'zura, N. Z., Yusri, S., Sutanto, H., Meliyanti, M., Maryani, E., & Hernawan, H. (2024). Study on microfiltration of crude biodiesel using ceramic membrane. *AIP Conference Proceedings*, *3073*(1).

Leron, R. B., Soriano, A. N., & Li, M.-H. (2012). Densities and refractive indices of the deep eutectic solvents (choline chloride+ ethylene glycol or glycerol) and their aqueous mixtures at the temperature ranging from 298.15 to 333.15 K. *Journal of the Taiwan Institute of Chemical Engineers*, *43*(4), 551–557.

Li, L., Quinlivan, P. A., & Knappe, D. R. U. (2002). Effects of activated carbon surface chemistry and pore structure on the adsorption of organic contaminants from aqueous solution. *Carbon*, *40*(12), 2085–2100.

Li, N. N. (1968). Separating hydrocarbons with liquid membranes. US Patent 3410794. In *assigned to Exxon Research Engineering Co.*

Li, R., Liang, N., Ma, X., Chen, B., & Huang, F. (2018). Free glycerol removal from biodiesel using anion exchange resin as a new type of adsorbent. *Industrial & Engineering Chemistry Research*, *57*(50), 17226–17236.

Li, X., Hou, M., Han, B., Wang, X., & Zou, L. (2008). Solubility of CO2 in a choline chloride+ urea eutectic mixture. *Journal of Chemical & Engineering Data*, *53*(2), 548–550. https://doi.org/https://doi.org/10.1021/je700638u

Lin, Z., Yu, D., & Li, Y. (2015). Study on the magnetic ODSA-in-water Pickering emulsion stabilized by Fe3O4 nanoparticle. *Colloid and Polymer Science*, *293*(1), 125–134.

Liu, D.-M., & Dong, C. (2020). Recent advances in nano-carrier immobilized enzymes and their applications. *Process Biochemistry*, *92*, 464–475.

Liu, H., Zhang, Y., Huang, J., Liu, T., Xue, N., & Shi, Q. (2017). Optimization of vanadium (IV) extraction from stone coal leaching solution by emulsion liquid membrane using response surface methodology. *Chemical Engineering Research and Design*, *123*, 111–119.

Liu, Y., Wu, Y., Liu, J., Wang, W., Yang, Q., & Yang, G. (2022). Deep eutectic solvents: recent advances in fabrication approaches and pharmaceutical applications. *International Journal of Pharmaceutics*, 121811.

Lobo, F. A., Goveia, D., Oliveira, A. P., Romão, L. P. C., Fraceto, L. F., Dias Filho, N. L., & Rosa, A. H. (2011). Development of a method to determine Ni and Cd in biodiesel by graphite furnace atomic absorption spectrometry. *Fuel*, *90*(1), 142–146.

Lotfi, M., Moniruzzaman, M., Sivapragasam, M., Kandasamy, S., Mutalib, M. I. A., Alitheen, N. B., & Goto, M. (2017). Solubility of acyclovir in nontoxic and biodegradable ionic liquids: COSMO-RS prediction and experimental verification. *Journal of Molecular Liquids*, *243*, 124–131.

Ma, C., Laaksonen, A., Liu, C., Lu, X., & Ji, X. (2018). The peculiar effect of water on ionic liquids and deep eutectic solvents. *Chemical Society Reviews*, *47*(23), 8685–8720. https://doi.org/10.1039/C8CS00325D

Ma, F., Clements, L. D., & Hanna, M. A. (1998). The effects of catalyst, free fatty acids, and water on transesterification of beef tallow. *Transactions of the ASAE*, *41*(5), 1261.

Ma, F., & Hanna, M. A. (1999). Biodiesel production: a review. *Bioresource Technology*, *70*(1), 1–15.

Ma, S., Li, F., Liu, L., Liao, L., Chang, L., & Tan, Z. (2020). Deep-eutectic solvents simultaneously used as the phase-forming components and chiral selectors for enantioselective liquid-liquid extraction of tryptophan enantiomers. *Journal of Molecular Liquids*, *319*, 114106.

Madras, G., Kolluru, C., & Kumar, R. (2004). Synthesis of biodiesel in supercritical fluids. *Fuel*, *83*(14–15), 2029–2033.

Maheshwari, P., Haider, M. B., Yusuf, M., Klemeš, J. J., Bokhari, A., Beg, M., Al-Othman, A., Kumar, R., & Jaiswal, A. K. (2022). A review on latest trends in cleaner biodiesel production: Role of feedstock, production methods, and catalysts. *Journal of Cleaner Production*, *355*, 131588.

Mahfud, F. H., Melian-Cabrera, I., Manurung, R., & Heeres, H. J. (2007). Biomass to fuels: upgrading of flash pyrolysis oil by reactive distillation using a high boiling alcohol and acid catalysts. *Process Safety and Environmental Protection*, *85*(5), 466–472.

Mamtani, K., Shahbaz, K., & Farid, M. M. (2021). Deep eutectic solvents–Versatile chemicals in biodiesel production. *Fuel*, *295*, 120604.

Mandari, V., & Devarai, S. K. (2021). Biodiesel production using homogeneous, heterogeneous, and enzyme catalysts via transesterification and esterification reactions: A critical review. *BioEnergy Research*, *15*(2), 1–27. https://doi.org/10.1007/s12155-021-10333-w

Manique, M. C., Faccini, C. S., Onorevoli, B., Benvenutti, E. V., & Caramão, E. B. (2012). Rice husk ash as an adsorbent for purifying biodiesel from waste frying oil. *Fuel*, *92*(1), 56–61.

Manosak, R., Limpattayanate, S., & Hunsom, M. (2011). Sequential-refining of crude glycerol derived from waste used-oil methyl ester plant via a combined process of chemical and adsorption. *Fuel Processing Technology*, *92*(1), 92–99.

Mantell, C., Casas, L., Rodríguez, M., & de la Ossa, E. M. (2013). Supercritical fluid extraction. In *Separation and purification technologies in biorefineries* (pp. 79–100). Wiley Online Library.

Manuale, D. L., Mazzieri, V. M., Torres, G., Vera, C. R., & Yori, J. C. (2011). Non-catalytic biodiesel process with adsorption-based refining. *Fuel*, *90*(3), 1188–1196.

Mata, T. M., Cardoso, N., Ornelas, M., Neves, S., & Caetano, N. S. (2011). Evaluation of two purification methods of biodiesel from beef tallow, pork lard, and chicken fat. *Energy & Fuels*, *25*(10), 4756–4762.

Matsumiya, H., Kageyama, T., & Hiraide, M. (2004). Multielement preconcentration of trace heavy metals in seawater with an emulsion containing 8-quinolinol for graphite-furnace atomic absorption spectrometry. *Analytica Chimica Acta*, *507*(2), 205–209.

Mazzieri, V. A., Vera, C. R., & Yori, J. C. (2008). Adsorptive properties of silica gel for biodiesel refining. *Energy & Fuels*, *22*(6), 4281–4284.

Mbous, Y. P., Hayyan, M., Hayyan, A., Wong, W. F., Hashim, M. A., & Looi, C. Y. (2017). Applications of deep eutectic solvents in biotechnology and bioengineering—promises and challenges. *Biotechnology Advances*, *35*(2), 105–134.

McNutt, J., & Yang, J. (2017). Utilization of the residual glycerol from biodiesel production for renewable energy generation. *Renewable and Sustainable Energy Reviews*, *71*, 63–76.

Mis Solval, K., & Sathivel, S. (2012). Use of an Adsorption Process for Purification of Pollock-Oil-Based Biodiesel Comprises Methyl Esters. *Journal of the American Oil Chemists' Society*, *89*(9), 1713–1721.

Miyuranga, K. A. V., Arachchige, U. S. P. R., Jayasinghe, R. A., & Samarakoon, G. (2022). Purification of residual glycerol from biodiesel production as a value-added raw material for glycerolysis of free fatty acids in waste cooking oil. *Energies*, *15*(23), 8856.

Mohamad, N. R., Marzuki, N. H. C., Buang, N. A., Huyop, F., & Wahab, R. A. (2015). An overview of technologies for immobilization of enzymes and surface analysis techniques for immobilized enzymes. *Biotechnology & Biotechnological Equipment*, *29*(2), 205–220.

Mohammed, S. A. M., Zouli, N., & Al-Dahhan, M. (2018). Removal of phenolic compounds from synthesized produced water by emulsion liquid membrane stabilized by the combination of surfactant and ionic liquid. *Desalination and Water Treatment*, *110*, 168–179.

Morrison, H. G., Sun, C. C., & Neervannan, S. (2009). Characterization of thermal behavior of deep eutectic solvents and their potential as drug solubilization vehicles. *International Journal of Pharmaceutics*, *378*(1–2), 136–139.

Mortaheb, H. R., Amini, M. H., Sadeghian, F., Mokhtarani, B., & Daneshyar, H. (2008). Study on a new surfactant for removal of phenol from wastewater by emulsion liquid membrane. *Journal of Hazardous Materials*, *160*(2–3), 582–588.

Mousavi, H.-S., Rahimi, M., & Mohadesi, M. (2022). Purification of glycerol using organic solvent extraction in a microreactor. *Biomass Conversion and Biorefinery*, *12*(6), 2243–2251.

Müller, T. E. (2019). Biodiesel production systems: reactor technologies. *Biodiesel: From Production to Combustion*, 15–25.

Muniyappa, P. R., Brammer, S. C., & Noureddini, H. (1996). Improved conversion of plant oils and animal fats into biodiesel and co-product. *Bioresource Technology*, *56*(1), 19–24.

Na-Ranong, D., Laungthaleongpong, P., & Khambung, S. (2015). Removal of steryl glucosides in palm oil based biodiesel using magnesium silicate and bleaching earth. *Fuel*, *143*, 229–235.

Nabieyan, B., Kargari, A., Kaghazchi, T., Mahmoudian, A., & Soleimani, M. (2007). Bench-scale pertraction of iodine using a bulk liquid membrane system. *Desalination*, *214*(1–3), 167–176.

Nag, A. (2015). *Distillation & Hydrocarbon Processing Practices*. PennWell Books.

Navarro, P., Larriba, M., Rojo, E., Garcia, J., & Rodriguez, F. (2013). Thermal properties of cyano-based ionic liquids. *Journal of Chemical & Engineering Data*, *58*(8), 2187–2193.

Nezhadali, A., Mohammadi, R., Akbarpour, M., & Ebrahimi, J. (2016). Selective transport of Cu (II) ions from a mixture of Mn (II), Co (II), Ni (II), Cu (II), Zn (II), and Pb (II) cations through a bulk liquid membrane using benzyl bis

(thiosemicarbazone) as carrier. *Desalination and Water Treatment*, *57*(29), 13818–13828.

Ng, Y. S., Jayakumar, N. S., & Hashim, M. A. (2010). Performance evaluation of organic emulsion liquid membrane on phenol removal. *Journal of Hazardous Materials*, *184*(1–3), 255–260.

Nisar, S., Hanif, M. A., Rashid, U., Hanif, A., Akhtar, M. N., & Ngamcharussrivichai, C. (2021). Trends in widely used catalysts for fatty acid methyl esters (Fame) production: A review. *Catalysts*, *11*(9), 1085.

Okumuş, Z. Ç., Doğan, T. H., & Temur, H. (2019). Removal of water by using cationic resin during biodiesel purification. *Renewable Energy*, *143*, 47–51.

Ooi, Z. Y., Othman, N., & Mohamed Noah, N. F. (2016). Response surface optimization of kraft lignin recovery from pulping wastewater through emulsion liquid membrane process. *Desalination and Water Treatment*, *57*(17), 7823–7832.

Osorio-González, C. S., Gómez-Falcon, N., Sandoval-Salas, F., Saini, R., Brar, S. K., & Ramírez, A. A. (2020). Production of biodiesel from castor oil: A review. *Energies*, *13*(10), 2467.

Othman, N., Noah, N. F. M., Poh, K. W., & Yi, O. Z. (2016). High performance of chromium recovery from aqueous waste solution using mixture of palm-oil in emulsion liquid membrane. *Procedia Engineering*, *148*, 765–773.

Özgül-Yücel, S., & Türkay, S. (2003). Purification of FAME by rice hull ash adsorption. *Journal of the American Oil Chemists' Society*, *80*(4), 373–376.

Pandey, A., Rai, R., Pal, M., & Pandey, S. (2014). How polar are choline chloride-based deep eutectic solvents? *Physical Chemistry Chemical Physics*, *16*(4), 1559–1568.

Park, J.-Y., Kim, D.-K., Wang, Z.-M., Lee, J.-P., Park, S.-C., & Lee, J.-S. (2008).

Production of biodiesel from soapstock using an ion-exchange resin catalyst. *Korean Journal of Chemical Engineering*, *25*(6), 1350–1354.

Perera, M., Yan, J., Xu, L., Yang, M., & Yan, Y. (2022). Bioprocess development for biolubricant production using non-edible oils, agro-industrial byproducts and wastes. *Journal of Cleaner Production*, *357*, 131956.

Pirmoradi, M., & Ashrafizadeh, S. N. (2017). Removal of nitrate from water by bulk liquid membrane. *Desalination and Water Treatment*, *58*, 228–238.

Plata, V., Haagenson, D., Dağdelen, A., Wiesenborn, D., & Kafarov, V. (2015). Improvement of palm oil biodiesel filterability by adsorption methods. *Journal of the American Oil Chemists' Society*, *92*(6), 893–903.

Pohl, P., Vorapalawut, N., Bouyssiere, B., Carrier, H., & Lobinski, R. (2010). Direct multi-element analysis of crude oils and gas condensates by double-focusing sector field inductively coupled plasma mass spectrometry (ICP MS). *Journal of Analytical Atomic Spectrometry*, *25*(5), 704–709.

Praveena, V., Martin, L. J., Matijošius, J., Aloui, F., Pugazhendhi, A., & Varuvel, E. G. (2024). A systematic review on biofuel production and utilization from algae and waste feedstocks–a circular economy approach. *Renewable and Sustainable Energy Reviews*, *192*, 114178.

Predojević, Z. J. (2008). The production of biodiesel from waste frying oils: A comparison of different purification steps. *Fuel*, *87*(17–18), 3522–3528.

Putra, S. S. S., Basirun, W. J., Elgharbawy, A. A. M., Hayyan, A., Hayyan, M., & Mohammed, M. A. (2022). Nanocellulose and natural deep eutectic solvent as potential biocatalyst system toward enzyme immobilization. *Molecular Catalysis*, *528*, 112422.

Qiu, Z., Zhao, L., & Weatherley, L. (2010). Process intensification technologies in continuous biodiesel production. *Chemical Engineering and Processing: Process Intensification*, *49*(4), 323–330.

Ramani, K., Karthikeyan, S., Boopathy, R., Kennedy, L. J., Mandal, A. B., & Sekaran, G. (2012). Surface functionalized mesoporous activated carbon for the immobilization of acidic lipase and their application to hydrolysis of waste cooked oil: Isotherm and kinetic studies. *Process Biochemistry*, *47*(3), 435–445. https://doi.org/10.1016/j.procbio.2011.11.025

Rameshaiah, G. N., Kodi, R. K., Jyothi, B., Deepika, V., & Prasanna, K. T. (2024). Activated bentonite clay–based dry-wash purification of waste cooking oil biodiesel in comparison with a wet washing process. *Biomass Conversion and Biorefinery*, *14*(4), 5135–5147.

Ramos, M., Dias, A. P. S., Puna, J. F., Gomes, J., & Bordado, J. C. (2019). Biodiesel production processes and sustainable raw materials. *Energies*, *12*(23), 4408.

Rao, A., Sathiavelu, A., & Mythili, S. (2020). Mini review on nanoimmobilization of lipase and cellulase for biofuel production. *Biofuels*, *11*(2), 191–200.

Rashidi, N. A., & Yusup, S. (2019). Production of palm kernel shell-based activated carbon by direct physical activation for carbon dioxide adsorption. *Environmental Science and Pollution Research*, *26*(33), 33732–33746. https://doi.org/10.1007/s11356-018-1903-8

Reis, M. T. A., & Carvalho, J. M. R. (2004). Modelling of zinc extraction from sulphate solutions with bis (2-ethylhexyl) thiophosphoric acid by emulsion liquid membranes. *Journal of Membrane Science*, *237*(1–2), 97–107.

Reis, P., Holmberg, K., Watzke, H., Leser, M. E., & Miller, R. (2009). Lipases at interfaces: a review. *Advances in Colloid and Interface Science*, *147*, 237–250.

Rezaei Motlagh, S., Harun, R., Awang Biak, D. R., Hussain, S. A., Omar, R., & Elgharbawy, A. A. (2020). COSMO-RS based prediction for alpha-linolenic acid (ALA) extraction from microalgae biomass using room temperature ionic liquids (RTILs). *Marine Drugs*, *18*(2), 108.

Rodriguez, J. M. (2016). Effects of Raw Materials and Production Practices on Biodiesel Quality and Performance. In G. Montero & M. Stoytcheva (Eds.), *BIODIESEL–QUALITY, EMISSIONS AND BY-PRODUCTS* (Second, p. 63).

Rodriguez, N. E., & Martinello, M. A. (2021). Molecular distillation applied to the purification of biodiesel from ethanol and soybean oil. *Fuel*, *296*, 120597.

Rodriguez, N. R., Requejo, P. F., & Kroon, M. C. (2015). Aliphatic–aromatic separation using deep eutectic solvents as extracting agents. *Industrial & Engineering Chemistry Research*, *54*(45), 11404–11412.

Rosly, M. B., Jusoh, N., Othman, N., Rahman, H. A., Noah, N. F. M., & Sulaiman, R. N. R. (2019). Effect and optimization parameters of phenol removal in emulsion liquid membrane process via fractional-factorial design. *Chemical Engineering Research and Design*, *145*, 268–278.

Rosly, M. B., Jusoh, N., Othman, N., Rahman, H. A., Sulaiman, R. N. R., & Noah, N. F. M. (2020). Stability of emulsion liquid membrane using bifunctional diluent and blended nonionic surfactant for phenol removal. *Chemical Engineering and Processing-Process Intensification*, *148*, 107790.

Russbueldt, B. M. E., & Hoelderich, W. F. (2009). New sulfonic acid ion-exchange resins for the preesterification of different oils and fats with high content of free fatty acids. *Applied Catalysis A: General*, *362*(1–2), 47–57.

Sabry, R., Hafez, A., Khedr, M., & El-Hassanin, A. (2007). Removal of lead by an emulsion liquid membrane: Part I. *Desalination*, *212*(1–3), 165–175.

Sabudak, T., & Yildiz, M. (2010). Biodiesel production from waste frying oils and its quality control. *Waste Management*, *30*(5), 799–803.

Saifuddin, N., & Chua, K. H. (2004). *Production of ethyl ester (biodiesel) from used frying oils: Optimization transesterification process using microwave irradiation*.

Sakthivel, R., Ramesh, K., Purnachandran, R., & Mohamed Shameer, P. (2018). A review on the properties, performance and emission aspects of the third generation biodiesels. *Renewable and Sustainable Energy Reviews*, *82*, 2970–2992. https://doi.org/https://doi.org/10.1016/j.rser.2017.10.037

Saleh, J., Dube, M. A., & Tremblay, A. Y. (2010). Effect of soap, methanol, and water on glycerol particle size in biodiesel purification. *Energy & Fuels*, *24*(11), 6179–6186.

Saleh, J., Dubé, M. A., & Tremblay, A. Y. (2011). Separation of glycerol from FAME using ceramic membranes. *Fuel Processing Technology*, *92*(7), 1305–1310.

Saleh, J., Tremblay, A. Y., & Dubé, M. A. (2010). Glycerol removal from biodiesel using membrane separation technology. *Fuel*, *89*(9), 2260–2266.

Šalić, A., Tušek, A. J., Gojun, M., & Zelić, B. (2020). Biodiesel purification in microextractors: Choline chloride based deep eutectic solvents vs water. *Separation and Purification Technology*, *242*, 116783.

Salleh, Z., Wazeer, I., Mulyono, S., El-blidi, L., Hashim, M. A., & Hadj-Kali, M. K. (2017). Efficient removal of benzene from cyclohexane-benzene mixtures using deep eutectic solvents–COSMO-RS screening and experimental validation. *The Journal of Chemical Thermodynamics*, *104*, 33–44.

Schoettl, S., Marcus, J., Diat, O., Touraud, D., Kunz, W., Zemb, T., & Horinek, D. (2014). Emergence of surfactant-free micelles from ternary solutions. *Chemical Science*,

5(8), 2949–2954.

Seenuvasan, M., Kumar, K. S., Kumar, A., & Parthiban, R. (2020). Review on surface modification of nanocarriers to overcome diffusion limitations: An enzyme immobilization aspect. *Biochemical Engineering Journal*, *158*, 107574.

Shahbaz, K., Baroutian, S., Mjalli, F. S., Hashim, M. A., & AlNashef, I. M. (2012). Prediction of glycerol removal from biodiesel using ammonium and phosphunium based deep eutectic solvents using artificial intelligence techniques. *Chemometrics and Intelligent Laboratory Systems*, *118*, 193–199.

Shahbaz, K., Mjalli, F. S., Hashim, M. A., & Al Nashef, I. M. (2010). Using deep eutectic solvents for the removal of glycerol from palm oil-based biodiesel. *Journal of Applied Sciences*, *10*(24), 3349–3354. https://doi.org/10.3923/JAS.2010.3349.3354

Shahbaz, K., Mjalli, F. S., Hashim, M. A., & AlNashef, I. M. (2011a). Eutectic solvents for the removal of residual palm oil-based biodiesel catalyst. *Separation and Purification Technology*, *81*(2), 216–222.

Shahbaz, K., Mjalli, F. S., Hashim, M. A., & AlNashef, I. M. (2011b). Using Deep Eutectic Solvents Based on Methyl Triphenyl Phosphunium Bromide for the Removal of Glycerol from Palm-Oil-Based Biodiesel. *Energy & Fuels*, *25*(6), 2671–2678. https://doi.org/10.1021/ef2004943

Shahbaz, K., Mjalli, F. S., Hashim, M. A., & AlNashef, I. M. (2013). Elimination of All Free Glycerol and Reduction of Total Glycerol from Palm Oil-Based Biodiesel Using Non-Glycerol Based Deep Eutectic Solvents. *Http://Dx.Doi.Org/10.1080/01496395.2012.731124*, *48*(8), 1184–1193. https://doi.org/10.1080/01496395.2012.731124

Sharma, A., Kohli, H. P., & Chakraborty, M. (2023). Removal of diclofenac using Fe2O3 nanoparticles stabilised emulsion nanofluid membrane. *Materials Today:*

Proceedings.

Sharma, Y. C., Singh, B., & Korstad, J. (2011). Latest developments on application of heterogenous basic catalysts for an efficient and eco friendly synthesis of biodiesel: A review. *Fuel*, *90*(4), 1309–1324.

Shehata, M., Unlu, A., Sezerman, U., & Timucin, E. (2020). Lipase and Water in a Deep Eutectic Solvent: Molecular Dynamics and Experimental Studies of the Effects of Water-In-Deep Eutectic Solvents on Lipase Stability. *Journal of Physical Chemistry B*, *124*(40), 8801–8810. https://doi.org/10.1021/acs.jpcb.0c07041

Shibasaki-Kitakawa, N., Hiromori, K., Ihara, T., Nakashima, K., & Yonemoto, T. (2015). Production of high quality biodiesel from waste acid oil obtained during edible oil refining using ion-exchange resin catalysts. *Fuel*, *139*, 11–17.

Shibasaki-Kitakawa, N., Kanagawa, K., Nakashima, K., & Yonemoto, T. (2013). Simultaneous production of high quality biodiesel and glycerin from Jatropha oil using ion-exchange resins as catalysts and adsorbent. *Bioresource Technology*, *142*, 732–736.

Shibasaki-Kitakawa, N., Tsuji, T., Kubo, M., & Yonemoto, T. (2011). Biodiesel production from waste cooking oil using anion-exchange resin as both catalyst and adsorbent. *BioEnergy Research*, *4*(4), 287–293.

Shuit, S. H., Ong, Y. T., Lee, K. T., Subhash, B., & Tan, S. H. (2012). Membrane technology as a promising alternative in biodiesel production: a review. *Biotechnology Advances*, *30*(6), 1364–1380.

Silviana, S., Anggoro, D. D., Salsabila, C. A., & Aprilio, K. (2021). Utilization of geothermal waste as a silica adsorbent for biodiesel purification. *Korean Journal of Chemical Engineering*, *38*, 2091–2105.

Simasatitkul, L., Siricharnsakunchai, P., Patcharavorachot, Y., Assabumrungrat, S., & Arpornwichanop, A. (2011). Reactive distillation for biodiesel production from soybean oil. *Korean Journal of Chemical Engineering*, *28*(3), 649–655.

Singh, R., Mehta, R., & Kumar, V. (2011). Simultaneous removal of copper, nickel and zinc metal ions using bulk liquid membrane system. *Desalination*, *272*(1–3), 170–173.

Smith, E. L., Abbott, A. P., & Ryder, K. S. (2014). Deep eutectic solvents (DESs) and their applications. *Chemical Reviews*, *114*(21), 11060–11082.

Soni, S., Dwivedee, B. P., & Banerjee, U. C. (2018). Facile fabrication of a recyclable nanobiocatalyst: Immobilization of: Burkholderia cepacia lipase on carbon nanofibers for the kinetic resolution of a racemic atenolol intermediate. *RSC Advances*, *8*(49), 27763–27774. https://doi.org/10.1039/c8ra05463k

Soniya, M., & Muthuraman, G. (2015). Comparative study between liquid–liquid extraction and bulk liquid membrane for the removal and recovery of methylene blue from wastewater. *Journal of Industrial and Engineering Chemistry*, *30*, 266–273.

Soriano Jr, N. U., Venditti, R., & Argyropoulos, D. S. (2009). Biodiesel synthesis via homogeneous Lewis acid-catalyzed transesterification. *Fuel*, *88*(3), 560–565.

Squissato, A. L., Fernandes, D. M., Sousa, R. M. F., Cunha, R. R., Serqueira, D. S., Richter, E. M., Pasquini, D., & Munoz, R. A. A. (2015). Eucalyptus pulp as an adsorbent for biodiesel purification. *Cellulose*, *22*(2), 1263–1274.

Steytler, D. (1996). Supercritical fluid extraction and its application in the food industry. In *Separation Processes in the Food and Biotechnology Industries: Principles and Applications* (p. 17). Elsevier.

Stojković, I. J., Stamenković, O. S., Povrenović, D. S., & Veljković, V. B. (2014).

Purification technologies for crude biodiesel obtained by alkali-catalyzed transesterification. *Renewable and Sustainable Energy Reviews*, *32*, 1–15.

Sud, D., Mahajan, G., & Kaur, M. P. (2008). Agricultural waste material as potential adsorbent for sequestering heavy metal ions from aqueous solutions - A review. In *Bioresource Technology* (Vol. 99, Issue 14, pp. 6017–6027). Elsevier. https://doi.org/10.1016/j.biortech.2007.11.064

Sulaiman, R. N. R., Othman, N., Harith, N. H., Rahman, H. A., Jusoh, N., Noah, N. F. M., & Rosly, M. B. (2021). Phenol recovery using continuous emulsion liquid membrane (CELM) process. *Chemical Engineering Communications*, *208*(4), 483–499.

Suliman, S. S., Othman, N., Noah, N. F. M., & Johari, K. (2022). Stability of primary emulsion assisted with nanoparticle in emulsion liquid membrane process for zinc extraction. *Materials Today: Proceedings*, *65*, 3081–3092.

Suliman, S. S., Othman, N., Noah, N. F. M., Jusoh, N., & Sulaiman, R. N. R. (2021). Empirical Correlation of Emulsion Size Prediction for Zinc Extraction Using Flat Blade Impeller System in Emulsion Liquid Membrane Process. *Malaysian Journal of Fundamental and Applied Sciences*, *17*(6), 742–751.

Suliman, S. S., Othman, N., Noah, N. F. M., & Kahar, I. N. S. (2023). Extraction and enrichment of zinc from chloride media using emulsion liquid membrane: Emulsion stability and demulsification via heating-ultrasonic method. *Journal of Molecular Liquids*, *374*, 121261.

Sun, J., Forsyth, M., & Macfarlane, D. R. (1998). Room-temperature molten salts based on the quaternary ammonium ion. *The Journal of Physical Chemistry B*, *102*(44), 8858–8864.

Suppalakpanya, K., Ratanawilai, S. B., & Tongurai, C. (2010). Production of ethyl ester

from esterified crude palm oil by microwave with dry washing by bleaching earth. *Applied Energy*, *87*(7), 2356–2359.

Tabatabaei, M., Karimi, K., Horváth, I. S., & Kumar, R. (2015). *Recent trends in biodiesel production. 7*, 258–267. https://doi.org/10.18331/BRJ2015.2.3.4

Tahmasebizadeh, P., Javanshir, S., & Ahmadi, A. (2021). Zinc extraction from a bioleaching solution by emulsion liquid membrane technique. *Separation and Purification Technology*, *276*, 119394.

Tai-Shung, N. C. (2007). Development and purification of biodiesel. In *Separation and Purification Technology* (Vol. 20, pp. 377–381).

Takase, M., Bryant, I. M., Essandoh, P. K., & Amankwa, A. E. K. (2023). A comparative study on performance of KOH and 32% KOH/ZrO 2-7 catalysts for biodiesel via transesterification of waste Adansonia digitata oil. *Green Technologies and Sustainability*, *1*, 100004.

Tan, J. N., & Dou, Y. (2020). Deep eutectic solvents for biocatalytic transformations: focused lipase-catalyzed organic reactions. *Applied Microbiology and Biotechnology*, *104*(4), 1481–1496. https://doi.org/10.1007/s00253-019-10342-y

Thangaraj, B., Solomon, P. R., Muniyandi, B., Ranganathan, S., & Lin, L. (2019). Catalysis in biodiesel production—a review. *Clean Energy*, *3*(1), 2–23.

Tomasevic, A. V, & Siler-Marinkovic, S. S. (2003). Methanolysis of used frying oil. *Fuel Processing Technology*, *81*(1), 1–6.

Toumi, K.-H., Benguerba, Y., Erto, A., Dotto, G. L., Khalfaoui, M., Tiar, C., Nacef, S., & Amrane, A. (2018). Molecular modeling of cationic dyes adsorption on agricultural Algerian olive cake waste. *Journal of Molecular Liquids*, *264*, 127–133.

Tremblay, A. Y., Cao, P., & Dubé, M. A. (2008). Biodiesel production using ultralow

catalyst concentrations. *Energy & Fuels*, *22*(4), 2748–2755.

Tsai W. (1994). *Study of activated carbon adsorption and catalyst combustion of VOCs*. National Taiwan University, Taipei, Taiwan.

Vávra, A., Hájek, M., & Skopal, F. (2017). The removal of free fatty acids from methyl ester. *Renewable Energy*, *103*, 695–700.

Veljković, V. B., Banković-Ilić, I. B., & Stamenković, O. S. (2015). Purification of crude biodiesel obtained by heterogeneously-catalyzed transesterification. *Renewable and Sustainable Energy Reviews*, *49*, 500–516.

Venkatesan, S. (2013). Adsorption. In *Separation and Purification Technologies in Biorefineries* (pp. 101–148). John Wiley & Sons, Ltd. https://doi.org/10.1002/9781118493441.CH5

Vila, J., Ginés, P., Pico, J. M., Franjo, C., Jiménez, E., Varela, L. M., & Cabeza, O. (2006). Temperature dependence of the electrical conductivity in EMIM-based ionic liquids: evidence of Vogel–Tamman–Fulcher behavior. *Fluid Phase Equilibria*, *242*(2), 141–146.

Vishal, D., Dubey, S., Goyal, R., Dwivedi, G., Baredar, P., & Chhabra, M. (2020). Optimization of alkali-catalyzed transesterification of rubber oil for biodiesel production & its impact on engine performance. *Renewable Energy*, *158*, 167–180.

Visser, A. E., Swatloski, R. P., Reichert, W. M., Mayton, R., Sheff, S., Wierzbicki, A., Davis, J. H., & Rogers, R. D. (2002). Task-specific ionic liquids incorporating novel cations for the coordination and extraction of Hg2+ and Cd2+: synthesis, characterization, and extraction studies. *Environmental Science & Technology*, *36*(11), 2523–2529.

Wall, J. A., Van Gerpen, J. H., & Thompson, J. C. (2011). Soap and Glycerin Removal

from Biodiesel Using Waterless Processes. *Transactions of the ASABE*, *54*(2), 535–541. https://doi.org/10.13031/2013.36456

Wang, J., Ge, X., Wang, Z., & Jin, Y. (2001). Experimental studies on the catalytic distillation for hydrolysis of methyl acetate. *Chemical Engineering & Technology*, *24*(2), 155–159.

Wang, L., He, H., Xie, Z., Yang, J., & Zhu, S. (2007). Transesterification of the crude oil of rapeseed with NaOH in supercritical and subcritical methanol. *Fuel Processing Technology*, *88*(5), 477–481.

Wang, Y., Nie, J., Zhao, M., Ma, S., Kuang, L., Han, X., & Tang, S. (2010). Production of biodiesel from waste cooking oil via a two-step catalyzed process and molecular distillation. *Energy & Fuels*, *24*(3), 2104–2108.

Wang, Y., Ou, S., Liu, P., & Zhang, Z. (2007). Preparation of biodiesel from waste cooking oil via two-step catalyzed process. *Energy Conversion and Management*, *48*(1), 184–188.

Wang, Y., Wang, X., Liu, Y., Ou, S., Tan, Y., & Tang, S. (2009). Refining of biodiesel by ceramic membrane separation. *Fuel Processing Technology*, *90*(3), 422–427.

Wasserscheid, P., & Welton, T. (2007). Ionic Liquids in Synthesis. In P. Wasserscheid & T. Welton (Eds.), *Ionic Liquids in Synthesis: Second Edition* (Second Edi, Vol. 1). John Wiley. https://doi.org/10.1002/9783527621194

Wei, C.-Y., Huang, T.-C., Yu, Z.-R., Wang, B.-J., & Chen, H.-H. (2014). Fractionation for biodiesel purification using supercritical carbon dioxide. *Energies*, *7*(2), 824–833.

Wirawan, S. S., Solikhah, M. D., Setiapraja, H., & Sugiyono, A. (2024). Biodiesel implementation in Indonesia: Experiences and future perspectives. *Renewable and*

Sustainable Energy Reviews, *189*, 113911.

Wu, D., Pan, G., Wang, M., Yu, W., Wang, G.-G., & Zhang, J. (2024). Sustainable superwetting membrane for effective separation of oil–water emulsion and dye removal. *Separation and Purification Technology*, *343*, 127084.

Xu, D., Chow, J., Weber, C. C., Packer, M. A., Baroutian, S., & Shahbaz, K. (2022). Evaluation of deep eutectic solvents for the extraction of fucoxanthin from the alga Tisochrysis lutea–COSMO-RS screening and experimental validation. *Journal of Environmental Chemical Engineering*, *10*(5), 108370.

Xue, J., Grift, T. E., & Hansen, A. C. (2011). Effect of biodiesel on engine performances and emissions. *Renewable and Sustainable Energy Reviews*, *15*(2), 1098–1116.

Yadav, A., & Pandey, S. (2014). Densities and viscosities of (choline chloride+ urea) deep eutectic solvent and its aqueous mixtures in the temperature range 293.15 K to 363.15 K. *Journal of Chemical & Engineering Data*, *59*(7), 2221–2229.

Yang, D., Hou, M., Ning, H., Zhang, J., Ma, J., Yang, G., & Han, B. (2013). Efficient SO 2 absorption by renewable choline chloride–glycerol deep eutectic solvents. *Green Chemistry*, *15*(8), 2261–2265. https://doi.org/https://doi.org/10.1039/C3GC40815A

Yang, K., Peng, J., Srinivasakannan, C., Zhang, L., Xia, H., & Duan, X. (2010). Preparation of high surface area activated carbon from coconut shells using microwave heating. *Bioresource Technology*, *101*(15), 6163–6169.

Yang, L., Chen, X. Q., & Jiao, F. P. (2009). Extractive Resolution of racemic mandelic acid through a bulk liquid membrane containing binary chiral carrier. *Journal of the Brazilian Chemical Society*, *20*, 1493–1498.

Ye, C., Sun, Y., Pei, X., Sun, J., & Wu, Y. (2017). Mass transfer and equilibrium characteristics of defluorination from groundwater by emulsion liquid membrane.

Journal of Chemical Technology & Biotechnology, *92*(1), 76–82.

Yori, J. C., D'ippolito, S. A., Pieck, C. L., & Vera, C. R. (2007). Deglycerolization of biodiesel streams by adsorption over silica beds. *Energy & Fuels*, *21*(1), 347–353.

Zaulkiflee, N. D., Ahmad, A. L., Che Lah, N. F., & Shah Buddin, M. M. H. (2022). Removal of emerging contaminants by emulsion liquid membrane: perspective and challenges. *Environmental Science and Pollution Research*, *29*(9), 12997–13023.

Zaulkiflee, N. D., Ahmad, A. L., Sugumaran, J., & Lah, N. F. C. (2020). Stability study of emulsion liquid membrane via emulsion size and membrane breakage on acetaminophen removal from aqueous solution using TOA. *ACS Omega*, *5*(37), 23892–23897.

Zereshki, S., Daraei, P., & Shokri, A. (2018). Application of edible paraffin oil for cationic dye removal from water using emulsion liquid membrane. *Journal of Hazardous Materials*, *356*, 1–8.

Zereshki, S., Shokri, A., & Karimi, A. (2021). Application of a green emulsion liquid membrane for removing copper from contaminated aqueous solution: Extraction, stability, and breakage study using response surface methodology. *Journal of Molecular Liquids*, *325*, 115251.

Zhang, Q., Vigier, K. D. O., Royer, S., & Jerome, F. (2012). Deep eutectic solvents: syntheses, properties and applications. *Chemical Society Reviews*, *41*(21), 7108–7146.

Zhang, W., Wang, C., Luo, B., He, P., Li, L., & Wu, G. (2023). Biodiesel production by transesterification of waste cooking oil in the presence of graphitic carbon nitride supported molybdenum catalyst. *Fuel*, *332*, 126309.

Zhao, D., Liao, Y., & Zhang, Z. (2007). Toxicity of ionic liquids. *Clean–Soil, Air, Water*,

35(1), 42–48.

Zubeir, L. F., Held, C., Sadowski, G., & Kroon, M. C. (2016). PC-SAFT modeling of CO2 solubilities in deep eutectic solvents. *The Journal of Physical Chemistry B*, *120*(9), 2300–2310.